Numerical study of nonlinear McKendrick–von Foerster type equations

A thesis submitted to the
School of Mathematics and Statistics
University of Hyderabad

in partial fulfillment for the award of
Doctor of Philosophy
in Applied Mathematics

by

Joydev Halder

School of Mathematics and Statistics

UNIVERSITY OF HYDERABAD
P.O. – Central University, Gachibowli
Hyderabad - 500 046
Telangana
India

February 2023

DECLARATION

I, **Joydev Halder**, hereby declare that this thesis entitled "**Numerical study of nonlinear McKendrick–Von Foerster type equations**" submitted by me under the guidance and supervision of **Dr. Suman Kumar Tumuluri** is a bonafide research work. I also declare that it has not been submitted previously in part or in full to this University or any other University or Institution for the award of any degree or diploma.

Joydev Halder

Thesis Author: Joydev Halder
(Reg. No. 17MMPA01)

Date: 28/02/2023

CERTIFICATE

This is to certify that the thesis entitled "**Numerical study of nonlinear McKendrick–Von Foerster type equations**" by **Joydev Halder** bearing Reg. No. 17MMPA01 in partial fulfillment of the requirements for the award of Doctor of Philosophy in **Applied Mathematics** is a bonafide work carried out by him under my supervision and guidance.

This thesis is free from Plagiarism and has not been submitted previously in part or in full to this or any other University or Institution for the award of any degree or diploma.

Further, the student has the following publications and preprints before submission of the thesis for adjudication:

1. Joydev Halder, Suman Kumar Tumuluri, *A numerical scheme for a diffusion equation with nonlocal nonlinear boundary condition*, *Computational and Applied Mathematics*, Vol 42, No. 2, article number: 84, 2023.

2. Joydev Halder, Suman Kumar Tumuluri, *Numerical solution to a nonlinear McKendrick–Von Foerster equation with diffusion*, *Numerical Algorithms*, Vol 92, No. 2, pp 1007–1039, 2023.

3. Joydev Halder, Suman Kumar Tumuluri, *A survey of age–structured models in population dynamics*, *The Proceedings of Telangana Academy of Sciences*, Special Issue (Mathematical Sciences, Frontiers in Mathematics), Vol 1, No. 1, pp 156-168, 2020.

4. Joydev Halder, Suman Kumar Tumuluri, *A higher order numerical scheme to a nonlinear McKendrick–Von Foerster equation with singular mortality.* (communicated)

List of publications and preprints (not part of the thesis work):

1. Joydev Halder, Suman Kumar Tumuluri, *Decay estimates and blow up of solutions to a class of heat equations.* (communicated)

2. Joydev Halder, Bhargav Kumar Kakumani, Suman Kumar Tumuluri, *Existence of global solutions to a semilinear pseudo-parabolic equation.* (communicated)

Also made presentations in the following conference:

1. International Conference on Computational Partial Differential Equations and Applications (ICCPDEA-2022)
September 06–08, 2022, BML Munjal University, Haryana, India

2. International Conference on Applied Mathematics and Computational Sciences (ICAMCS-2022)
October 12–14, 2022, DIT University, Uttarakhand, India

Further, the student has passed the following courses towards fulfillment of coursework requirement for Ph.D.

Course Code	Course Name	Credit	Pass/Fail
AM 802	Advance PDE	5	Pass
AM 803	Analysis	5	Pass
AM 812	Mathematical Theory of Population Dynamics	5	Pass
AM 810	Research Methodology & Ethics	4	Pass

Thesis Supervisor:

T. Suman Kumar

Dr. Suman Kumar Tumuluri

Dr. T. SUMAN KUMAR
सह प्रोफ़ेसर / Associate Professor
गणित और सांख्यिकी संकाय
School of Mathematics & Statistics
हैदराबाद विश्वविद्यालय / University of Hyderabad
हैदराबाद / Hyderabad-500 046. तेलंगाना, T.S.

Dean of the School:

R. Radha

Prof. R. Radha 28/2/2023

संकाय-अध्यक्ष / DEAN
गणित और सांख्यिकी संकाय
School of Mathematics & Statistics
हैदराबाद विश्वविद्यालय/University of Hyderabad
हैदराबाद/Hyderabad-500 046. तेलंगाना, T.S.

ACKNOWLEDGEMENTS

I am grateful for the direct and indirect assistance of numerous individuals who have made my journey possible. I would like to express my appreciation to everyone who has supported me, and apologize to those whom I may have unintentionally overlooked.

Firstly, I would like to express my deepest gratitude to my advisor Dr. Suman Kumar Tumuluri for the continuous help, wise advise, unparalleled support and encouragements. The completion of this thesis would not have been possible without his constant guidance and support. He is always there for me and influence my life in so many ways for which I am deeply indebted to him. I consider myself fortunate to be one of his students.

I am very thankful to my doctoral committee members, Prof. B. Sri Padmavati and Prof. R. Radha, for their minute suggestions and continuous assessment.

During my M.Sc. and Ph.D., I had the privilege of attending a few courses taught by Prof. V. Kannan, Prof. S. Kumaresan, Prof. T. Amaranath, Prof. R. Tandan in our department. Their instructions had a significant impact on me, and it tremendously motivated me in my studies.

I am grateful to all the faculty members School Deans, and staff who have provided administrative assistance and support throughout the years.

I would like to acknowledge the financial support provided by CSIR (award number: 09/414(1154)/2017-EMR-I).

I want to thank all my research scholars of our department, especially Dr. A. Mukherjee, Dr. P. N. Mandal, Laba, Akshay, Priyapada, Soumak and Sachin for their love, care, and company, which made my life more pleasurable.

My appreciation extends to the monks and professors of my alma mater, Ramakrishna Mission Residential College, Narendrapur (Kolkata), who encouraged me to pursue higher studies in Mathematics and provided financial support during my college days.

I am grateful to all my teachers during my school days, especially Mrs. Gouri

Halder, Mrs. Jayati Chatterjee, Mr. Sakha Halder, Mr. Arnab Sarkar, Mr. Mohan Mandal, Mr. Sumanta Sarkar, Mr. Uday Mukherjee, Mr. Joydip Mukherjee, and Mr. Soumen Pal, for their love, encouragement, and support.

I would also like to acknowledge the assistance provided by Late Mr. Samir Halder, Late Mr. Samar Sarkar, Mr. Dipak Kumar Mukherjee, Mr. Bijan Roy, Mrs. Snigdha Ghosh and Mr. Arjun Halder.

I want to thank all my friends for their cheerful company during school, college and university days. Specially, I like to thank Soumitra, Sourav, Sudipta, Ravishangkar, Suman, Kalyan, Sovan and Debraj. I fondly recall the countless moments I spent with Smrity, Snigdha, Soumitra, Sumanta, Swastik, Lili and Tripti. Without these people my life would not have been the same.

Finally, I would like to express my gratitude to my family for their constant love, support, and patience during my academic pursuit. Their encouragement and sacrifices have been a source of strength for me, and I am deeply indebted to them.

- Joydev Halder

ABSTRACT

This thesis consists of four chapters. Chapter 1 is dedicated to the introduction and the literature survey of the McKendrick–Von Foerster type equations.

In Chapter 2, an implicit finite difference scheme is presented to approximate the solution to the McKendrick–Von Foerster equation with diffusion (M-VD) with Robin condition at both the end points. The notion of upper solution is introduced and used effectively with aid of discrete maximum principle to study the wellposedness and stability of the numerical scheme. A relation between the numerical solutions to the M-V-D and the steady state problem is established.

In Chapter 3, a numerical scheme to find approximate solutions to the M-V-D with Robin condition at the left end point and Dirichlet boundary condition at right point is presented. The main difficulty in employing the standard analysis to study the properties of this scheme is due to presence of nonlinear and nonlocal term in the Robin boundary condition in the M-V-D. To overcome this, we use the abstract theory of discretizations based on the notion of stability threshold to analyze the scheme. Stability, and convergence of the proposed numerical scheme are established.

In Chapter 4, higher order numerical schemes to the McKendrick–Von Foerster equation are presented when the death rate has singularity at the maximum age. The third, fourth order schemes that are proposed are based on the characteristics (non intersecting lines in this case), and are multi-step methods with appropriate corrections at each step. In fact, the convergence analysis of the schemes are discussed in detail. Moreover, numerical experiments are provided to validate the orders of convergence of the proposed third order and fourth order schemes.

List of Publications and Preprints (part of the thesis work):

1. Joydev Halder, Suman Kumar Tumuluri, *A numerical scheme for a diffusion equation with nonlocal nonlinear boundary condition*, *Computational and Applied Mathematics*, Vol 42, No. 2, article number: 84, 2023.

2. Joydev Halder, Suman Kumar Tumuluri, *Numerical solution to a nonlinear McKendrick–Von Foerster equation with diffusion*, *Numerical Algorithms*, Vol 92, No. 2, pp 1007–1039, 2023.

3. Joydev Halder, Suman Kumar Tumuluri, *A survey of age–structured models in population dynamics*, *The Proceedings of Telangana Academy of Sciences*, Special Issue (Mathematical Sciences, Frontiers in Mathematics), Vol 1, No. 1, pp 156-168, 2020.

4. Joydev Halder, Suman Kumar Tumuluri, *A higher order numerical scheme to a nonlinear McKendrick–Von Foerster equation with singular mortality.* (communicated)

This thesis is dedicated to all of my teachers

For their unwavering support, encouragement, patience, and belief in me

Contents

Chapter 1

Introduction

1.1 Introduction

Population dynamics is one of the fundamental areas of ecology, forming both the basis for the study of more complex communities and of many applied questions. Understanding population dynamics is the key to understand the relative importance of competition for resources and predation in structuring ecological communities, which is a central question in ecology.

Population dynamics is the study of how populations change with respect to structures like age, size etc., and time. Important factors in population dynamics include rates of reproduction, death and migration etc.

Usage of differential equations in the modeling of population dynamics can be traced back to several centuries. One of the earliest models was due to Malthus (see [53]). In that model, Malthus has proposed that the rate of population growth/ decay is proportional to the size of the total population. The Malthus model does not refer to the effects of crowding or the limitation of resources. In 1938, Verhulst presented a model which incorporates the effect of limitation of resources. The Verhulst model is also known as the logistic equation. In the logistic model, the total population tends to the nontrivial steady state called the carrying capacity. The logistic model does not consider the correlation between the population size and the mean individual fitness (often measured as per capita population growth rate) of the population. A more realistic model of population growth would allow the Allee effect (see [80]).

1.2 Structured models

The structured population models distinguish individuals from one another according to characteristics such as age, size, location, status, and movement etc. to determine the birth, growth and death rates, interaction with each other and with the environment. The goal of the structured population models is to understand how these characteristics affect the dynamics of these models and thus the outcomes and consequences of the biological processes. Many authors considered age, size, spatial and maturity structured population models (see [31, 82, 83, 75]).

1.2.1 Age-structured models : Hyperbolic PDEs

In the modeling of population dynamics, the main step is to identify some significant variables called structured variables that allow the division of the population into homogeneous subgroups. Then, one can describe its dynamics through the interaction of these groups, ruled by mechanisms that depend on these variables. Age is one of the most natural and widely used structured variables. Let $u(x,t)$ denote the density of population that has age x at time t. Assume that μ and β are the age-specific mortality rate and the age-specific fertility rate, respectively. One of the earliest age-structured population models is due to A. G. McKendrick (see [55]) and is given by

$$\begin{cases} u_t(x,t) + u_x(x,t) + \mu(x)u(x,t) = 0, \ \ x > 0, t > 0, \\ u(0,t) = \displaystyle\int_0^{a_\dagger} \beta(x)u(x,t)dx, \ \ t > 0, \\ u(x,0) = u_0(x), \ \ x > 0, \end{cases} \tag{1.1}$$

where μ, β, u_0 are assumed to be non-negative functions. Model (1.1) is known as the renewal equation and has been rediscovered by von-Foerster. Henceforth, we refer (1.1) as the McKendrick–Von Foerster equation.

In McKendrick–Von Foerster equation (1.1), the fertility and the mortality rates merely depend on the age but not on the total populations. Practically it is not the case. As there is a competition among individuals for limited resources and individuals of different ages have different advantages (disadvantages) in this competition, it is natural to assume that the fertility and mortality rates depend on the weighted population. To this end, Gurtin and MaCamy introduced a nonlinear age-dependent population model where the fertility and mortality functions are density dependent (see[25]). The Gurtin-MacCamy model is given by

$$
\begin{cases}
u_t(x,t) + u_x(x,t) + \mu(x, s_1(t))u(x,t) = 0, \;\; x > 0, t > 0, \\
u(0,t) = \displaystyle\int_0^{a_\dagger} \beta(x, s_2(t))u(x,t)dx, \;\; t > 0, \\
u(x,0) = u_0(x), \;\; x > 0, \\
s_\nu(t) = \displaystyle\int_0^{a_\dagger} \psi_\nu(x)u(x,t)dx, \;\; t > 0, \;\; \nu = 1, 2,
\end{cases}
\tag{1.2}
$$

where ψ_1, ψ_2 are the competition weights. Henceforth, we call (1.2) as the nonlinear McKendrick–Von Foerster equation.

1.2.2 Age-structured models : Parabolic PDEs

In [12], the authors introduced the diffusion term in the McKendrick–Von Foerster equation to account the variability in the DNA content which can influence the 'biological age'. The McKendrick–Von Foerster equation with diffusion (M-V-D) is given by

$$
\begin{cases}
u_t(x,t) + u_x(x,t) + \mu(x, s(t))u(x,t) = u_{xx}(x,t), \;\; x \in (0, a_\dagger), \;\; t > 0, \\
u(0,t) - u_x(0,t) = \displaystyle\int_0^{a_\dagger} \beta_1(x, s_1(t))u(x,t)dx, \;\; t > 0, \\
u(a_\dagger, t) + u_x(a_\dagger, t) = \displaystyle\int_0^{a_\dagger} \beta_2(x, s_2(t))u(x,t)dx, \;\; t > 0, \\
u(x,0) = u_0(x), \;\; x > 0, \\
s(t) = \displaystyle\int_0^{a_\dagger} \psi(x)u(x,t)dx, \;\; s_\nu(t) = \displaystyle\int_0^{a_\dagger} \psi_\nu(x)u(x,t)dx, \;\; \nu = 1, 2, \;\; t > 0,
\end{cases}
\tag{1.3}
$$

where u and μ are as in (1.2) and the functions $s(t)$, $s_\nu(t)$ represent the weighted populations which influence the mortality and fertility rates μ , β_1 and β_2.

Since $a_\dagger$ is the maximum age, it is natural to impose the Dirichlet boundary condition at right boundary. Then (1.3) becomes

$$\begin{cases} u_t(x,t) + u_x(x,t) + \mu\big(x, s_1(t)\big)u(x,t) = u_{xx}(x,t), \ x \in (0, a_\dagger), \ t > 0 \\ u(0,t) - u_x(0,t) = \displaystyle\int_0^{a_\dagger} \beta\big(x, s_2(t)\big)u(x,t)dx, \quad t \geq 0, \\ u(a_\dagger, t) = 0, \ t \geq 0, \\ u(x,0) = u_0(x), \quad x \in (0, a_\dagger), \\ s_\nu(t) = \displaystyle\int_0^{a_\dagger} \psi_\nu(x)u(x,t)dx, \quad t \geq 0, \quad \nu = 1, 2. \end{cases} \tag{1.4}$$

In the recent years, the M-V-D has attracted interest of many engineers as well as mathematicians due to its applications in the modeling of thermoelasticity, neuronal networks etc. (see [18, 19, 36, 37, 56, 57, 58]). The main difficulty in the study of the M-V-D is due to the nonlocal nature of the PDE, and the boundary condition(s). Though numerical study of nonlocal equations got considerable focus, relatively less attention was paid to problems with the Robin boundary condition(s). In this thesis, we present numerical schemes to models (1.2), (1.3), and (1.4).

1.3 A stable scheme to M-V-D with Robin–Robin boundary condition

In Chapter 2, we provide a stable numerical scheme to (1.3) and investigate the long time behavior of the numerical solution to (1.3). In this section, we briefly present the concepts and main results that we have given in Chapter 2.
Before defining the numerical scheme, first we introduce the following notations. Let h and k be the spacial and temporal step sizes, respectively. Denote by (x_i, t_n) a typical grid point with $x_i = ih$, and $t_n = nk$. Moreover, we assume that $a_\dagger = Mh$ for some $M \in \mathbb{N}$ and define the set of grid points

$$\begin{cases} \Lambda = \{(x_i, t_n) : i = 1, 2, \dots, M-1, \ n = 1, 2, ...\}, \\ \bar{\Lambda} = \{(x_i, t_n) : i = 0, 1, \dots, M, \ n = 0, 1, ...\}. \end{cases}$$

At every grid point (x_i, t_n), let $U_{i,n}$ denote the approximate solution to (1.3), and

$$\Phi_i = u_0(x_i), \ \Psi_i = \psi(x_i), \ \boldsymbol{U}_n = (U_{0,n}, U_{1,n}, ..., U_{M,n}), \ \boldsymbol{\Psi} = (\Psi_0, \Psi_1, ..., \Psi_M),$$

$$\Psi_{\nu i} = \psi_\nu(x_i),\ \boldsymbol{\Psi}_\nu = (\Psi_{\nu 0}, \Psi_{\nu 1}, ..., \Psi_{\nu M}),\ \nu = 1,2,\ \mu_i(X) = \mu(x_i, X),$$

$$\beta_{\nu i}(X) = \beta_\nu(x_i, X),\ \boldsymbol{\beta}_\nu(X) = (\beta_{\nu 1}(X), \beta_{\nu 2}(X), \ldots, \beta_{\nu M}(X)),\ X \geq 0.$$

To approximate the integral terms in equation (1.3), we choose composite Simpson's–$\frac{1}{3}$ quadrature formula with weights $\{q_0, q_1, ..., q_M\}$. In other words, we approximate

$$\int_0^{a_\dagger} \psi(x)u(x,t)dx \sim \sum_{i=0}^{M} q_i \Psi_i U_{i,n} =: I(\boldsymbol{\Psi}\boldsymbol{U}_n),$$

$$\int_0^{a_\dagger} \psi_\nu(x)u(x,t)dx \sim \sum_{i=0}^{M} q_i \Psi_{\nu i} U_{i,n} =: I(\boldsymbol{\Psi}_\nu \boldsymbol{U}_n),\ \nu = 1,2.$$

Moreover, we approximate the integral terms in the boundary conditions with

$$\int_0^{a_\dagger} \beta_\nu(x, s_\nu(t))u(x,t)dx \sim \sum_{i=0}^{M} q_i \beta_{\nu i}(I(\boldsymbol{\Psi}_\nu \boldsymbol{U}_n))U_{i,n} = I(\boldsymbol{\beta}_\nu(I(\boldsymbol{\Psi}_\nu \boldsymbol{U}_n))\boldsymbol{U}_n),$$

where $\nu = 1,2$.

With the notation introduced so far, we propose the following implicit scheme:

$$\begin{cases} (1+2r)U_{i,n} - bU_{i+1,n} - cU_{i-1,n} = U_{i,n-1} - k\mu_i(I(\boldsymbol{\Psi}\boldsymbol{U}_n))U_{i,n},\ (i,n) \in \Lambda, \\ \left(1 + \dfrac{1}{h}\right) U_{0,n} - \dfrac{1}{h} U_{1,n} = I(\boldsymbol{\beta}_1(I(\boldsymbol{\Psi}_1 \boldsymbol{U}_n))\boldsymbol{U}_n),\ n \in \mathbb{N}, \\ \left(1 + \dfrac{1}{h}\right) U_{M,n} - \dfrac{1}{h} U_{M-1,n} = I(\boldsymbol{\beta}_2(I(\boldsymbol{\Psi}_2 \boldsymbol{U}_n))\boldsymbol{U}_n),\ n \in \mathbb{N}, \\ U_{i,0} = \Phi_i,\ 0 \leq i \leq M, \end{cases} \tag{1.5}$$

where $b = r - \frac{\lambda}{2}$, $c = r + \frac{\lambda}{2}$, $\lambda = \frac{k}{h}$ and $r = \frac{k}{h^2}$. Notice that (1.5) is a nonlinear scheme.

We now define the following finite difference operators

$$\mathcal{L}[U_{i,n}] = (1+2r)U_{i,n} - bU_{i+1,n} - cU_{i-1,n},\ (i,n) \in \Lambda,$$

$$\mathcal{BC}_1[U_{0,n}] = \left(1 + \frac{1}{h}\right) U_{0,n} - \left(\frac{1}{h}\right) U_{1,n},\ n \in \mathbb{N},$$

$$\mathcal{BC}_2[U_{M,n}] = \left(1 + \frac{1}{h}\right) U_{M,n} - \left(\frac{1}{h}\right) U_{M-1,n},\ n \in \mathbb{N}.$$

Then numerical scheme (1.5) using the finite difference operators is written as

$$\begin{cases} \mathcal{L}[U_{i,n}] = U_{i,n-1} - k\mu_i(I(\boldsymbol{\Psi}\boldsymbol{U}_n))U_{i,n}, \ (i,n) \in \Lambda, \\ \mathcal{BC}_1[U_{0,n}] = I(\boldsymbol{\beta}_1(I(\boldsymbol{\Psi}_1\boldsymbol{U}_n))\boldsymbol{U}_n), \ n \in \mathbb{N}, \\ \mathcal{BC}_2[U_{M,n}] = I(\boldsymbol{\beta}_2(I(\boldsymbol{\Psi}_2\boldsymbol{U}_n))\boldsymbol{U}_n), \ n \in \mathbb{N}, \\ U_{i,0} = \Phi_i, \ 0 \le i \le M. \end{cases} \tag{1.6}$$

Since (1.6) is a system of nonlinear equations, *a priori* it is not clear whether there exists a solution to it. In order to establish the existence and uniqueness of a solution to (1.6), we use the monotonicity arguments with the aid of notions of upper, and lower solutions (see [19, 37]). To this end, we begin with the following definition.

Definition 1.3.1 (Upper solution) A matrix $(\tilde{U}_{i,n})$ is called an upper solution to (1.6) if it satisfies

$$\begin{aligned} &\mathcal{L}[\tilde{U}_{i,n}] \ge \tilde{U}_{i,n-1} - k\mu_i(I(\boldsymbol{\Psi}\tilde{\boldsymbol{U}}_n))\tilde{U}_{i,n}, \ (i,n) \in \Lambda, \\ &\mathcal{BC}_1[\tilde{U}_{0,n}] \ge I(\boldsymbol{\beta}_1(I(\boldsymbol{\Psi}_1\tilde{\boldsymbol{U}}_n))\tilde{\boldsymbol{U}}_n), \ n \in \mathbb{N}, \\ &\mathcal{BC}_2[\tilde{U}_{M,n}] \ge I(\boldsymbol{\beta}_2(I(\boldsymbol{\Psi}_2\tilde{\boldsymbol{U}}_n))\tilde{\boldsymbol{U}}_n), \ n \in \mathbb{N}, \\ &\tilde{U}_{i,0} \ge \Phi_i, \ 0 \le i \le M. \end{aligned} \tag{1.7}$$

Similarly, $(\hat{U}_{i,n})$ is called a lower solution to (1.6) if it satisfies all inequalities of (1.7) in the reversed order. A pair of upper and lower solutions $(\tilde{U}_{i,n}, \hat{U}_{i,n})$ is said to be *ordered* if $\tilde{U}_{i,n} \ge \hat{U}_{i,n}$ on $\bar{\Lambda}$.
For a given pair of ordered upper and lower solutions $(\tilde{U}_{i,n}, \hat{U}_{i,n})$, we set

$$\langle \hat{U}_{i,n}, \tilde{U}_{i,n} \rangle := \{U_{i,n} : \hat{U}_{i,n} \le U_{i,n} \le \tilde{U}_{i,n}\}.$$

1.3.1 Existence and uniqueness

In this thesis, existence of a solution to (1.6) is proved in four cases: (i) $s \mapsto \mu(.,s)$ is decreasing and $s \mapsto \beta_\nu(.,s)$ is increasing, (ii) $s \mapsto \mu(.,s)$ is increasing and $s \mapsto \beta_\nu(.,s)$ are decreasing, (iii) $s \mapsto \mu(.,s)$ is decreasing and $s \mapsto \beta_\nu(.,s)$ is decreasing, (iv) $s \mapsto \mu(.,s)$ is increasing and $s \mapsto \beta_\nu(.,s)$ is increasing. The main results of case (i) are stated in this subsection. Results in the other cases, i.e., $(ii) - (iv)$ can be found in Chapter 2

Assume $\frac{\partial \mu}{\partial s}(.,s) \leq 0,\ \frac{\partial \beta_\nu}{\partial s}(.,s) \geq 0.$
Let $\hat{U}_{i,n}$ and $\tilde{U}_{i,n}$ be a pair of ordered lower and upper solutions to (1.6). Now, define

$$\omega = \sup\left\{\mu(x_i,s) \mid s = I(\boldsymbol{\Psi}\boldsymbol{U}_n),\ \hat{U}_{i,n} \leq U_{i,n} \leq \tilde{U}_{i,n},\ (i,n) \in \bar{\Lambda}\right\},$$

$$\xi = \sup\left\{\frac{\partial}{\partial s}\mu(x_i,s) \mid s = I(\boldsymbol{\Psi}\boldsymbol{U}_n),\ \hat{U}_{i,n} \leq U_{i,n} \leq \tilde{U}_{i,n},\ (i,n) \in \bar{\Lambda}\right\}.$$

We now introduce a linear operator

$$L[U_{i,n}] = \mathcal{L}[U_{i,n}] + k\left(\xi\hat{U}_{i,n}I(\boldsymbol{\Psi}\boldsymbol{U}_n) + \omega U_{i,n}\right). \tag{1.8}$$

Using this new operator, (1.6) can be written as

$$\begin{cases} L[U_{i,n}] = U_{i,n-1} + k\left(-\mu_i(I(\boldsymbol{\Psi}\boldsymbol{U}_n))U_{i,n} + \xi\hat{U}_{i,n}I(\boldsymbol{\Psi}\boldsymbol{U}_n) + \omega U_{i,n}\right), (i,n) \in \Lambda, \\ \mathcal{BC}_1[U_{0,n}] = I(\boldsymbol{\beta}_1(I(\boldsymbol{\Psi}_1\boldsymbol{U}_n))\boldsymbol{U}_n),\ n \in \mathbb{N}, \\ \mathcal{BC}_2[U_{M,n}] = I(\boldsymbol{\beta}_2(I(\boldsymbol{\Psi}_2\boldsymbol{U}_n))\boldsymbol{U}_n),\ n \in \mathbb{N}, \\ U_{i,0} = \Phi_i,\ 0 \leq i \leq M. \end{cases} \tag{1.9}$$

For $(i,n) \in \bar{\Lambda}$, we construct a sequence $\{U^m_{i,n}\}$ of approximations to a solution $\{U_{i,n}\}$ to (1.9) in the following manner. Let $\{U^m_{i,n}\}$ be the solution to

$$\begin{cases} L[U^m_{i,n}] = U^{m-1}_{i,n-1} + k\Big(-\mu_i(I(\boldsymbol{\Psi}\boldsymbol{U}^{m-1}_n))U^{m-1}_{i,n} + \xi\hat{U}_{i,n}I(\boldsymbol{\Psi}\boldsymbol{U}^{m-1}_n) \\ \qquad\qquad + \omega U^{m-1}_{i,n}\Big),\ (i,n) \in \Lambda,\ m \in \mathbb{N}, \\ \mathcal{BC}_1[U^m_{0,n}] = I(\boldsymbol{\beta}_1(I(\boldsymbol{\Psi}_1\boldsymbol{U}^{m-1}_n))\boldsymbol{U}^{m-1}_n),\ n \in \mathbb{N},\ m \in \mathbb{N}, \\ \mathcal{BC}_2[U^m_{M,n}] = I(\boldsymbol{\beta}_2(I(\boldsymbol{\Psi}_2\boldsymbol{U}^{m-1}_n))\boldsymbol{U}^{m-1}_n),\ n \in \mathbb{N},\ m \in \mathbb{N}, \\ U^m_{i,0} = \Phi_i,\ 0 \leq i \leq M,\ m \in \mathbb{N}. \end{cases} \tag{1.10}$$

To close the system, we need to fix the initial approximation $U^0_{i,n}$. If the initial approximation is taken to be an upper solution (a lower solution, resp.) to (1.6), then the solution to (1.10) is denoted by $\bar{U}^m_{i,n}$ ($\underline{U}^m_{i,n}$, resp.).
To state the existence and uniqueness result, we first introduce the following notation:

$$\sigma_1 = \min\{\xi\hat{U}_{i,n}I(\boldsymbol{\Psi}) + \omega \mid (i,n) \in \bar{\Lambda}, \hat{U}_{i,n} \leq U_{i,n} \leq \tilde{U}_{i,n}\}.$$

$$\gamma = \min\big\{\frac{\partial}{\partial s}\mu(x_i,s) : s = I(\boldsymbol{\Psi}\boldsymbol{U}_n),\ \hat{U}_{i,n} \le U_{i,n} \le \tilde{U}_{i,n}, (i,n) \in \bar{\Lambda}\big\},$$

$$\alpha = \min\big\{\mu(x_i,s) : s = I(\boldsymbol{\Psi}\boldsymbol{U}_n),\ \hat{U}_{i,n} \le U_{i,n} \le \tilde{U}_{i,n}, (i,n) \in \bar{\Lambda}\big\},$$

$$\sigma_3 = \min\{\gamma\tilde{U}_{i,n}I(\boldsymbol{\Psi}) + \alpha : (i,n) \in \bar{\Lambda}\},$$

$$\delta_1 = \sup\big\{\eta I(\boldsymbol{\Psi}_\nu)I(\tilde{\boldsymbol{U}}_n) + I(\boldsymbol{\beta}_\nu(I(\boldsymbol{\Psi}_\nu\tilde{\boldsymbol{U}}_n))) : n = 0,1,2,\ldots,\ \nu = 1,2\big\},$$

We are now ready to state the existence and uniqueness result for (1.6).

Theorem 1.3.2 (Existence and uniqueness) *Let $\hat{U}_{i,n}$, and $\tilde{U}_{i,n}$ be a pair of ordered lower and upper solutions to equation (1.6), respectively. Assume that $s \mapsto \mu(.,s)$ is decreasing, $s \mapsto \beta_\nu(.,s)$ is increasing, for $\nu = 1,2$ and $-k\sigma_1 < 1$. Then the following hold:*
(i) For every fixed $(i,n) \in \bar{\Lambda}$, both $\{\bar{U}^m_{i,n}\}$, $\{\underline{U}^m_{i,n}\}$ are monotone sequences. Moreover, we have

$$\hat{U}_{i,n} \le \underline{U}^m_{i,n} \le \underline{U}^{m+1}_{i,n} \le \underline{U}_{i,n} \le \bar{U}_{i,n} \le \bar{U}^{m+1}_{i,n} \le \bar{U}^m_{i,n} \le \tilde{U}_{i,n},\ \ (i,n) \in \bar{\Lambda},$$

for every $m \in \mathbb{N} \cup \{0\}$, where $\lim_{m\to\infty} \bar{U}^m_{i,n} = \bar{U}_{i,n}$, $\lim_{m\to\infty} \underline{U}^m_{i,n} = \underline{U}_{i,n}$.
(ii) Both $\bar{U}_{i,n}$ and $\underline{U}_{i,n}$ are solutions to (1.6).
(iii) If $U^*_{i,n}$ is another solution to (1.6) in $\langle\hat{U}_{i,n}, \tilde{U}_{i,n}\rangle$, then $\underline{U}_{i,n} \le U^*_{i,n} \le \bar{U}_{i,n}$ on $\bar{\Lambda}$.
(iv) If $\max\{-k\sigma_3, \delta_1\} < 1$, then (1.6) has a unique solution in $\langle\hat{U}_{i,n}, \tilde{U}_{i,n}\rangle$. □

For more details and a proof of this result, see Theorems 2.3.2, 2.3.3 and 2.4.1, in Chapter 2.

1.3.2 Steady state and the long time behavior

In Chapter 2, we study the long time behavior of the numerical solution to (1.3) also. Analysis of the long time behavior of the solution to (1.3) requires the study of the corresponding steady state problem. The steady state equation corresponding to (1.3) is the following boundary value problem

$$\begin{cases} v_x(x) + \mu(x,p)v(x) = v_{xx}(x), \;\; x \in (0, a_\dagger), \\ v(0) - v_x(0) = \displaystyle\int_0^{a_\dagger} \beta_1(y,p_1)v(y)dy, \\ v(a_\dagger) + v_x(a_\dagger) = \displaystyle\int_0^{a_\dagger} \beta_2(y,p_2)v(y)dy, \\ p = \displaystyle\int_0^{a_\dagger} \psi(x)v(x)dx, \;\; p_\nu = \displaystyle\int_0^{a_\dagger} \psi_\nu(x)v(x)dx, \;\; \nu = 1,2. \end{cases} \tag{1.11}$$

Set $\boldsymbol{V} = (V_0, V_1, ..., V_M)$. The numerical method that we propose to find an approximate solution to (1.11) is

$$\begin{cases} a'V_i - b'V_{i+1} - c'V_{i-1} = -\mu_i(I(\boldsymbol{\Psi V}))V_i, \;\; 1 \le i \le M-1, \\ \left(1 + \dfrac{1}{h}\right)V_0 - \left(\dfrac{1}{h}\right)V_1 = I(\boldsymbol{\beta}_1(I(\boldsymbol{\Psi}_1\boldsymbol{V}))\boldsymbol{V}), \\ \left(1 + \dfrac{1}{h}\right)V_M - \left(\dfrac{1}{h}\right)V_{M-1} = I(\boldsymbol{\beta}_2(I(\boldsymbol{\Psi}_2\boldsymbol{V}))\boldsymbol{V}), \end{cases} \tag{1.12}$$

where $a' = \frac{2}{h^2}$, $b' = \frac{1}{h^2} - \frac{1}{2h}$ and $c' = \frac{1}{h^2} + \frac{1}{2h}$. By introducing the following finite difference operators

$$\begin{aligned} \mathcal{L}^s[V_i] =& a'V_i - b'V_{i+1} - c'V_{i-1}, \\ \mathcal{BC}_1^s[V_0] =& \left(1 + \frac{1}{h}\right)V_0 - \left(\frac{1}{h}\right)V_1, \\ \mathcal{BC}_2^s[V_M] =& \left(1 + \frac{1}{h}\right)V_M - \left(\frac{1}{h}\right)V_{M-1}, \end{aligned}$$

we write finite difference scheme (1.12) as

$$\begin{cases} \mathcal{L}^s[V_i] = -\mu_i(I(\boldsymbol{\Psi V}))V_i, \;\; 1 \le i \le M-1, \\ \mathcal{BC}_1^s[V_0] = I(\boldsymbol{\beta}_1(I(\boldsymbol{\Psi}_1\boldsymbol{V}))\boldsymbol{V}), \\ \mathcal{BC}_2^s[V_M] = I(\boldsymbol{\beta}_2(I(\boldsymbol{\Psi}_2\boldsymbol{V}))\boldsymbol{V}). \end{cases} \tag{1.13}$$

Definition 1.3.3 A vector $(\tilde{V}_i)$ is called an upper solution to (1.13) if it satisfies the relation

$$\begin{aligned}
&\mathcal{L}^s[\tilde{V}_i] \geq -\mu_i(I(\boldsymbol{\Psi}\tilde{\boldsymbol{V}}))\tilde{V}_i,\ 1 \leq i \leq M-1,\\
&\mathcal{BC}_1^s[\tilde{V}_0] \geq I(\boldsymbol{\beta}_1(I(\boldsymbol{\Psi}_1\tilde{\boldsymbol{V}}))\tilde{\boldsymbol{V}}),\\
&\mathcal{BC}_2^s[\tilde{V}_M] \geq I(\boldsymbol{\beta}_2(I(\boldsymbol{\Psi}_2\tilde{\boldsymbol{V}}))\tilde{\boldsymbol{V}}).
\end{aligned} \tag{1.14}$$

Similarly, $(\hat{V}_i)$ is called a lower solution to equation (1.13) if it satisfies all the inequalities in (1.14) in the reverse order. A pair of upper solution $(\tilde{V}_i)$ and lower solution $(\hat{V}_i)$ is said to be ordered if $\tilde{V}_i \geq \hat{V}_i,\ 0 \leq i \leq M$.
For a given pair of ordered upper and lower solutions $\tilde{V}_i,\ \hat{V}_i$, we set $\langle \hat{V}_i, \tilde{V}_i\rangle \equiv \{V_i : \hat{V}_i \leq V_i \leq \tilde{V}_i\}$.
Observe that any ordered lower and upper solution to (1.14) is also an ordered upper and lower solution to (1.7). Let $\tilde{V}_i$ and $\hat{V}_i$ be a pair of upper and lower solutions to (1.13), respectively. Now, define

$$\omega_s = \max\big\{\mu(x_i,p) : p = I(\boldsymbol{\Psi}\boldsymbol{V}),\ \hat{V}_i \leq V_i \leq \tilde{V}_i,\ 0 \leq i \leq M\big\},$$

$$\xi_s = \max\big\{\frac{\partial}{\partial p}\mu(x_i,p) : p = I(\boldsymbol{\Psi}\boldsymbol{V}),\ \hat{V}_i \leq V_i \leq \tilde{V}_i,\ 0 \leq i \leq M\big\},$$

$$L^s[V_i] = \mathcal{L}^s[V_i] + \Big(\xi_s\hat{V}_i I(\boldsymbol{\Psi}\boldsymbol{V}) + \omega_s V_i\Big),\ 1 \leq i \leq M-1.$$

Thus (1.13) becomes

$$\begin{cases}
L^s[V_i] = \Big(-\mu_i(I(\boldsymbol{\Psi}\boldsymbol{V}))V_i + \xi_s\hat{V}_i I(\boldsymbol{\Psi}\boldsymbol{V}) + \omega_s V_i\Big),\ 1 \leq i \leq M-1,\\
\mathcal{BC}_1^s[V_0] = I(\boldsymbol{\beta}_1(I(\boldsymbol{\Psi}_1\boldsymbol{V}))\boldsymbol{V}),\\
\mathcal{BC}_2^s[V_M] = I(\boldsymbol{\beta}_2(I(\boldsymbol{\Psi}_2\boldsymbol{V}))\boldsymbol{V}).
\end{cases} \tag{1.15}$$

We now construct a sequence of approximations $\{V_i^m\}$ to (1.15) using the linear iteration process

$$\begin{cases}
L^s[V_i^m] = \Big(-\mu_i(I(\boldsymbol{\Psi}\boldsymbol{V}^{m-1}))V_i^{m-1} + \xi_s\hat{V}_i I(\boldsymbol{\Psi}\boldsymbol{V}^{m-1}) + \omega_s V_i^{m-1}\Big),\\
\qquad\qquad\qquad\qquad\qquad\qquad 1 \leq i \leq M-1,\ m \in \mathbb{N},\\
\mathcal{BC}_1^s[V_0^m] = I(\boldsymbol{\beta}_1(I(\boldsymbol{\Psi}_1\boldsymbol{V}^{m-1}))\boldsymbol{V}^{m-1}),\ m \in \mathbb{N},\\
\mathcal{BC}_2^s[V_M^m] = I(\boldsymbol{\beta}_2(I(\boldsymbol{\Psi}_2\boldsymbol{V}^{m-1}))\boldsymbol{V}^{m-1}),\ m \in \mathbb{N}.
\end{cases} \tag{1.16}$$

If V_i^0 is equal to an upper solution (lower solution, resp.) to (1.13) then denote the solution to (1.16) by $\bar{V}_i^m$ ($\underline{V}_i^m$, resp.).

The existence and uniqueness of solution to (1.13) is proved along the same lines of the existence and uniqueness of solution to (1.6). In particular, we show that $(\bar{V}_i^m)$, and $(\underline{V}_i^m)$ are monotone for each fixed i. The limits of these monotone sequences turnout to be solutions to (1.13) (See Theorems 2.5.2 and 2.5.3). For uniqueness of slution to (1.13) see Theorem 2.5.4 in Chapter 2.
We conclude this section with the statement of the result regarding the long time behavior of the solution.

Theorem 1.3.4 (Asymptotic behavior) *Let $\tilde{V}_i$ and $\hat{V}_i$ be a pair of ordered upper and lower solutions to (1.13), respectively. Assume that $\hat{U}_{i,n} \leq \hat{V}_i \leq \tilde{V}_i \leq \tilde{U}_{i,n}$. Let $\bar{Y}_{i,n}$ and $\underline{Y}_{i,n}$ be solutions to (1.6) with $\bar{Y}_{i,0} = \tilde{V}_i$ and $\underline{Y}_{i,0} = \hat{V}_i$, respectively. Then the following conclusions hold:*
(i) For each fixed $0 \leq i \leq M$, the sequence $(\bar{Y}_{i,n})$ is decreasing and $(\underline{Y}_{i,n})$ is increasing in n.
(ii) For each $0 \leq i \leq M$, set $\lim\limits_{n\to\infty} \bar{Y}_{i,n} = \bar{V}_i$, $\lim\limits_{n\to\infty} \underline{Y}_{i,n} = \underline{V}_i$. Then $\bar{V}_i$ and $\underline{V}_i$ are the maximal and minimal solutions to (1.13) in $\langle \hat{V}_i, \tilde{V}_i \rangle$, respectively.
(iii) Let $\Phi_i \in \langle \hat{V}_i, \tilde{V}_i \rangle$. Then $\lim\limits_{n\to\infty} U_{i,n} = \bar{V}_i = \underline{V}_i$. □

For more details see Theorem 2.6.2.

1.4 A convergent scheme to M-V-D with Robin–Dirichlet boundary data

In this section, our objective is to propose a convergent numerical scheme to find approximate solutions to (1.4) and provide the main results that are discussed in Chapter 3.
First fix $T > 0$, assume that $a_\dagger = 2(M' + 3)h$, for some $M' \in \mathbb{N}$ and $T = Nk$ for some $N \in \mathbb{N}$. To simplify the notations, we write $M = 2(M' + 3)$. For every grid point (x_i, t^n), we denote the numerical solution by U_i^n, and set

$$\begin{gathered}
\Psi_{\nu,i} = \psi_\nu(x_i), \;\; \boldsymbol{\Psi}_\nu = (\Psi_{\nu,1}, \Psi_{\nu,2}, \ldots, \Psi_{\nu,M-1}), \;\; \nu = 1, 2, \\
\boldsymbol{\beta}(\cdot) = \big(\beta(x_1, \cdot), \beta(x_2, \cdot), \ldots, \beta(x_{M-1}, \cdot)\big), \\
\boldsymbol{\mu}(\cdot) = \big(\mu(x_1, \cdot), \mu(x_2, \cdot), \ldots, \mu(x_{M-1}, \cdot)\big), \\
\boldsymbol{U}^n = (U_1^n, U_2^n, \ldots, U_{M-1}^n).
\end{gathered}$$

To approximate the integrals in (1.4), we use the following quadrature rule which is a combination of the composite Simpson–$\frac{1}{3}$ and Minle's rule. For $\boldsymbol{V} = (V_1, \dots, V_{M-1}) \in \mathbb{R}^{M-1}$, we define the quadrature formula

$$\begin{aligned}\mathcal{Q}_h(\boldsymbol{V}) = & \frac{4h}{3}(2V_1 - V_2 + 2V_3) + \frac{h}{3}\sum_{i=2}^{M'}(V_{2i} + 4V_{2i+1} + V_{2i+2}) \\ & + \frac{4h}{3}(2V_{2M'+3} - V_{2M'+4} + 2V_{2M'+5}).\end{aligned}$$

For $\boldsymbol{V} = (V_1, \dots, V_{M-1})$, $\boldsymbol{W} = (W_1, \dots, W_{M-1})$ in $\mathbb{R}^{M-1}$, define

$$\boldsymbol{V} \bullet \boldsymbol{W} = (V_1W_1, \dots, V_{M-1}W_{M-1}).$$

With the notation introduced so far, we propose the following scheme for (1.4) using the forward difference approximation for u_t, the backward difference for u_x, and the central difference for u_{xx}:

$$\begin{cases} \dfrac{U_i^n - U_i^{n-1}}{k} + \dfrac{U_i^{n-1} - U_{i-1}^{n-1}}{h} + \mu\big(x_i, \mathcal{Q}_h(\boldsymbol{\Psi}_1 \cdot \boldsymbol{U}^{n-1})\big)U_i^{n-1} \\ \qquad\qquad = \dfrac{U_{i+1}^{n-1} + U_{i-1}^{n-1} - 2U_i^{n-1}}{h^2}, \quad 1 \le i \le M-1,\ 1 \le n \le N, \\ \left(1 + \dfrac{1}{h}\right) U_0^n - \dfrac{1}{h}U_1^n = \mathcal{Q}_h\Big(\boldsymbol{\beta}\big(\mathcal{Q}_h(\boldsymbol{\Psi}_2 \cdot \boldsymbol{U}^n)\big) \cdot \boldsymbol{U}^n\Big), \quad 0 \le n \le N, \\ U_M^n = 0, \quad 0 \le n \le N, \\ U_i^0 = u_0(x_i), \quad 1 \le i \le M-1. \end{cases} \tag{1.17}$$

In order to carry out the analysis within an abstract theory of discretizations, we introduce the general discretization framework. For, we define the spaces

$$X_h = Y_h = \mathbb{R}^{N+1} \times (\mathbb{R}^{M-1})^{N+1} \times \mathbb{R}^{N+1}.$$

We also introduce the operator $\Phi_h \colon X_h \to Y_h$, defined through the formulae

$$\Phi_h(\boldsymbol{V_0}, \boldsymbol{V^0}, \boldsymbol{V^1}, ..., \boldsymbol{V^N}, \boldsymbol{V_M}) = (\boldsymbol{P_0}, \boldsymbol{P^0}, \boldsymbol{P^1}, ..., \boldsymbol{P^N}, \boldsymbol{P_M}),$$

where

$$
\begin{aligned}
&\boldsymbol{P}_0 = (P_0^0, P_0^1, \cdots, P_0^N),\\
&P_0^n = \left(1+\frac{1}{h}\right)V_0^n - \frac{1}{h}V_1^n - \mathcal{Q}_h\Big(\boldsymbol{\beta}\big(\mathcal{Q}_h(\boldsymbol{\Psi}_2\cdot\boldsymbol{V}^n)\big)\cdot\boldsymbol{V}^n\Big),\ 0\le n\le N,\\
&\boldsymbol{P}_M = (P_M^0, P_M^1, \cdots, P_M^N),\\
&P_M^n = \frac{V_M^n}{h}, \quad 0\le n\le N,\\
&\boldsymbol{P}^n = (P_1^n, P_2^n, \ldots, P_{M-1}^n), \quad 0\le n\le N,\\
&P_i^0 = V_i^0 - U_i^0, \quad 1\le i\le M-1,\\
&P_i^n = \frac{V_i^n - V_i^{n-1}}{k} + \frac{V_i^{n-1} - V_{i-1}^{n-1}}{h} + \mu\big(x_i, \mathcal{Q}_h(\boldsymbol{\Psi}_1\cdot\boldsymbol{V}^{n-1})\big)V_i^{n-1}\\
&\qquad - \frac{V_{i+1}^{n-1} + V_{i-1}^{n-1} - 2V_i^{n-1}}{h^2},\ 1\le n\le N, 1\le i\le M-1.
\end{aligned}
\tag{1.18}
$$

Now $\boldsymbol{U}_h = (\boldsymbol{U}_0, \boldsymbol{U}^0, \boldsymbol{U}^1, \cdots, \boldsymbol{U}^N) \in X_h$ is a solution to (1.17) if and only if it is a solution of the discrete problem

$$\Phi_h(\boldsymbol{U}_h) = \mathbf{0} \in Y_h. \tag{1.19}$$

To investigate how close $\boldsymbol{U_h}$ is to u, we first need to choose an element $\boldsymbol{u_h} \in X_h$, which is a suitable discrete representation of u. In particular, our choice is the set of nodal values of the theoretical solution u, namely

$$\boldsymbol{u}_h = (\boldsymbol{u}_0, \boldsymbol{u}^0, \ldots, \boldsymbol{u}^N, \boldsymbol{u}_M) \in X_h, \tag{1.20}$$

where

$$
\begin{cases}
\boldsymbol{u}_0 = (u_0^0, u_0^1, \ldots, u_0^N) \in \mathbb{R}^{N+1},\ u_0^n = u(0, t^n),\ 0\le n\le N,\\
\boldsymbol{u}^n = (u_1^n, u_2^n, \ldots, u_{M-1}^n) \in \mathbb{R}^{M-1},\ u_i^n = u(x_i, t^n), 1\le i\le M-1, 0\le n\le N,\\
\boldsymbol{u}_M = (u_M^0, u_M^1, \ldots, u_M^N) \in \mathbb{R}^{N+1},\ u_M^n = u(a_\dagger, t^n),\ 0\le n\le N.
\end{cases}
\tag{1.21}
$$

Then the global discretization error is defined to be the vector

$$\boldsymbol{e_h} = \boldsymbol{u_h} - \boldsymbol{U_h} \in X_h,$$

and the local discretization error is given by

$$\boldsymbol{I_h} = \Phi_h(\boldsymbol{u}_h) \in Y_h.$$

In order to measure the magnitude of errors, we define the following norms in the spaces X_h and Y_h:

$$\|(\boldsymbol{V}_0,\boldsymbol{V}^0,\boldsymbol{V}^1,\ldots,\boldsymbol{V}^N,\boldsymbol{V}_M)\|_{X_h}= h(\|\boldsymbol{V}_0\|_*+\|\boldsymbol{V}_M\|_*)+\max\{\|\boldsymbol{V}^0\|,\|\boldsymbol{V}^1\|,\ldots,\|\boldsymbol{V}^N\|\},$$

$$\|(\boldsymbol{P}_0,\boldsymbol{P}^0,\boldsymbol{P}^1,...,\boldsymbol{P}^N,\boldsymbol{P}_M)\|_{Y_h}=\left(\|\boldsymbol{P}_0\|_*^2+\|\boldsymbol{P}^0\|^2+h\|\boldsymbol{P}_M\|_*^2+\sum_{n=1}^{N}k\|\boldsymbol{P}^n\|^2\right)^{1/2},$$

where $\|\boldsymbol{V}^n\|^2 = \sum\limits_{i=1}^{M-1} h|V_i^n|^2$ and $\|\boldsymbol{V}_0\|_*^2 = \sum\limits_{n=0}^{N} k|V_0^n|^2$.
For $\boldsymbol{V} \in \mathbb{R}^{M-1}, \boldsymbol{Z} \in \mathbb{R}^{N+1}$, we define

$$\langle \boldsymbol{V}, \boldsymbol{W}\rangle = \sum_{i=1}^{M-1} hV_iW_i,$$

$$\|\boldsymbol{V}\|_\infty = \max_{1\le j\le M-1}|V_i|, \quad \|\boldsymbol{Z}\|^\infty = \max_{0\le n\le N}|Z^n|.$$

In order to state the main results, we give the following standard definitions.

Definition 1.4.1 (Consistency) Discretized equation (1.19) is said to be consistent with (1.4) if

$$\lim_{h\to 0}||\Phi_h(\boldsymbol{u}_h)||_{Y_h} = \lim_{h\to 0}||\boldsymbol{I}_h||_{Y_h} = 0.$$

Definition 1.4.2 (Stability) Discretized equation (1.19) is said to be stable restricted to the thresholds M_h if there exist two positive constants h_0 and S such that for each $0 < h \le h_0$ and for all $\boldsymbol{V}_h$, $\boldsymbol{W}_h$ in the open ball $B(\boldsymbol{u}_h, M_h) \subset X_h$

$$||\boldsymbol{V}_h - \boldsymbol{W}_h||_{X_h} \le S||\Phi_h(\boldsymbol{V}_h) - \Phi_h(\boldsymbol{W}_h)||_{Y_h}.$$

Definition 1.4.3 (Convergence) Discretized equation (1.19) is said to be convergent if there exists $h_0 > 0$ such that, for each $0 < h \le h_0$, the discretized equation has a solution $\boldsymbol{U}_h$ for which

$$\lim_{h\to 0}||\boldsymbol{u}_h - \boldsymbol{U}_h||_{X_h} = \lim_{h\to 0}||\boldsymbol{e}_h||_{X_h} = 0.$$

1.4.1 Consistency, stability and convergence

Using the notations introduced so far, we state the main theorems in Chapter 3 in the following.

Theorem 1.4.4 (Consistency) *Assume that μ, β, ψ_1 and ψ_2 are sufficiently smooth such that the solution u to (1.2) is four times continuously differentiable with bounded derivatives. Moreover, we assume that there exists $L > 0$ such that for every $0 \leq x \leq a_\dagger$, $s_1, s_2 > 0$,*

$$|\mu(x, s_1) - \mu(x, s_2)| \leq L|s_1 - s_2|,$$

and

$$|\beta(x, s_1) - \beta(x, s_2)| \leq L|s_1 - s_2|.$$

Then the local discretization error satisfies

$$\|\Phi_h(u_h)\|_{Y_h} = \{\|\boldsymbol{U}^0 - \boldsymbol{u}^0\|^2 + \mathcal{O}(h^2) + \mathcal{O}(k^2)\}^{1/2}, \quad \text{as } h \to 0.$$

□

Theorem 1.4.5 (Stability) *Assume the hypotheses of Theorem 1.4.4. Let r and λ be such that $k = rh^2 = \lambda h$, and $\lambda + 2r \leq 1$. Then discretization (1.19) is stable with thresholds $R_h = Rh$, where R is a fixed positive constant independent of h.* □

Theorem 1.4.6 (Convergence) *Assume the hypotheses of Theorem 1.4.5. If*

$$\|\boldsymbol{U}^0 - \boldsymbol{u}^0\|_{X_h} = \mathcal{O}(h), \ \text{as } h \to 0,$$

then discretization (1.19) is convergent. □

1.5 The McKendrick–Von Foerster equation with singularity

In this section, we outline the main results which are given in Chapter 4. In that chapter, we propose and analyze a numerical scheme to find approximate

solutions to (1.2) with the mortality function having singularity at $a = a_\dagger$.
When μ is linear, the survival probability

$$\pi(x) = \exp\Big(-\int_0^x \mu(y)dy\Big),$$

must be zero at the maximum age at $x = a_\dagger$, which indeed suggests us that

$$\int_0^{a_\dagger} \mu(y, s(\cdot))dy = +\infty. \tag{1.22}$$

This readily implies that μ has a singularity at $x = a_\dagger$.
Let u be the solution to (1.2). We define

$$d(x,t) = \begin{cases} \int\limits_{t-x}^{t} \mu\big(y + x - t, s_1(y)\big)dy, & t > x, \\ \int\limits_{0}^{x-t} \mu\big(y, s_1(0)\big)dy + \int\limits_{0}^{t} \mu\big(y + x - t, s_1(y)\big)dy, & t \le x, \end{cases} \tag{1.23}$$

$$\lambda(x,t) = \exp(-d(x,t)). \tag{1.24}$$

and

$$u(x,t) = \lambda(x,t)v(x,t),\ 0 \le x < a_\dagger,\ t \ge 0. \tag{1.25}$$

In view of (1.2), it is straightforward to obtain that v satisfies

$$\begin{cases} v_t(x,t) + v_x(x,t) = 0,\ 0 < x < a_\dagger,\ t > 0, \\ v(0,t) = \int_0^{a_\dagger} \beta(x, p(t))\lambda(x,t)v(x,t)dx,\ t > 0, \\ v(x,0) = \dfrac{u^0(x)}{\pi(x,0)},\ 0 \le x < a_\dagger, \\ p(t) = \int_0^{a_\dagger} \psi_2(x)\lambda(x,t)v(x,t)dx. \end{cases} \tag{1.26}$$

Moreover, one can observe that if v is a weak solution to (1.26) then u is also a weak solution to (1.2).
In order to define the scheme, we define step size $h = \frac{a_\dagger}{2M+2}$ for a given a positive integer M. Let $\lfloor \frac{a^*}{h} \rfloor = J^*$ for some $J^* \in \mathbb{N}$ and $\lfloor \frac{T}{h} \rfloor = N$. At every grid point (x_i, t^n), each U_i^n is the numerical approximation to $u(x_i, t^n)$ and V_i^n represents the numerical approximation to $v(x_i, t^n)$, $i = 0, 1, \dots, 2M+1$. Moreover, the

approximation of the survival probability $\lambda(x_i, t^n)$ is denoted by Λ_i^n.
At each time level t^n, $n = 0, 1, \ldots, N$, we denote

$$\boldsymbol{U^n} = [U_0^n, U_1^n, \ldots, U_{2M+1}^n],\ \boldsymbol{V^n} = [V_0^n, V_1^n, \ldots, V_{2M+1}^n] \in \mathbb{R}^{2M+2}.$$

and let the vector $\boldsymbol{\Lambda}^n = [\Lambda_0^n, \Lambda_1^n, \ldots, \Lambda_{2M+1}^n]$ approximate the survival probability
$$\boldsymbol{\lambda}^n = [\lambda(x_0, t^n), \lambda(x_1, t^n), \ldots, \lambda(x_{2M+1}, t^n)].$$
Also, we use this vector notation to represent the evaluations of the fertility rate
$$\boldsymbol{\beta}(\cdot) = [\beta(x_0, \cdot), \beta(x_1, \cdot), \ldots, \beta(x_{2M+1}, \cdot)].$$
To approximate the integral term that appears in the boundary condition, we use the following quadrature rule which is a combination of the composite Simpson $\frac{1}{3}$ and Milne's rules. For the vector $\boldsymbol{Y} = [Y_0, Y_1, \ldots, Y_{2M+1}]$, we define

$$\mathcal{Q}_h(\boldsymbol{Y}) = \frac{4h}{3}(2Y_1 - Y_2 + 2Y_3) + \sum_{i=2}^{M-2} \frac{h}{3}(Y_{2i} + 4Y_{2i+1} + Y_{2i+2}) + \frac{4h}{3}(2Y_{2M-1} - Y_{2M} + 2Y_{2M+1}). \tag{1.27}$$

With this notation, we propose following numerical scheme to (1.26) based on the method of characteristics:

$$\begin{cases} V_i^n = V_{i-1}^{n-1},\ i = 1, 2, \ldots, 2M+1,\ n = 1, 2, \ldots, N, \\ V_0^n = \mathcal{Q}_h(\boldsymbol{\beta}(P_\Lambda^n) \cdot \boldsymbol{\Lambda}^n \cdot \boldsymbol{V}^n),\ n = 1, 2, \ldots, N, \\ V_i^0 = \dfrac{U_i^0}{\Pi_i^0},\ i = 0, 1, \ldots, 2M+1, \\ P_\Lambda^n = \mathcal{Q}_h(\boldsymbol{\psi}_2 \cdot \boldsymbol{\Lambda}^n \cdot \boldsymbol{V}^n),\ n = 1, 2, \ldots, N. \end{cases} \tag{1.28}$$

Finally, to compute an approximate solution U_i^n to (1.2), we use the following relation

$$U_i^n = \Lambda_i^n V_i^n,\ i = 0, 1, \ldots, 2M+1,\ n = 1, \ldots, N. \tag{1.29}$$

The nontrivial part in (1.28) is to find an approximation of the survival probability Λ_i^n and we postpone the discussion on how to approximate Λ_i^n to Subsections 1.5.1 and 1.5.2.
In order to compare the numerical and analytical solutions at each grid point, we represent the restriction of the solution u to (1.2) to the grid by the vector $\boldsymbol{u}^n = [u(x_0, t^n), u(x_1, t^n), \ldots, u(x_{2M+1}^n, t^n)]$, $n = 0, 1, \ldots, N$. Similarly, the restriction of the solution v to (1.26) to the grid is denoted by the vector $\boldsymbol{v}^n = [v(x_0, t^n), v(x_1, t^n), \ldots, v(x_{2M+1}^n, t^n)]$, $n = 0, 1, \ldots, N$.

For a $\boldsymbol{Y} = [Y_0, Y_1, \ldots, Y_{2M+1}] \in \mathbb{R}^{2M+5}$, we define the following norms

$$\begin{aligned} ||\boldsymbol{Y}||_1 &= \sum_{i=0}^{2M+1} h|Y_i|, \\ ||\boldsymbol{Y}||_\infty &= \max_{0\le i\le 2M+1} |Y_i|. \end{aligned} \tag{1.30}$$

To state the approximation theorems of the survival probability (1.24), we make the following assumptions.

$(H1)$ Suppose u^0, β are continuous, bounded, and, μ, ψ_1, ψ_2 are nonnegative and sufficiently regular so that the solution to (1.2) is in $C^4([0, a_\dagger) \times [0, T])$.

Since ψ_1, ψ_2 are continuous on $[0, a_\dagger]$, for every bounded function u, the map $t \mapsto s_\nu(t)$ is a bounded function, i.e., there exists $K > 0$ such that $s_\nu(t) \le K$ for all $t \in [0, T]$, where $\nu = 1, 2$.

$(H2)$ For a given $s_1(t) \in C^4([0, T])$, let

$$\begin{cases} \int_0^{a_\dagger} \mu\big(y, s_1(y + t - a_\dagger)\big) dy = \infty, & t > a_\dagger, \\ \int_{a_\dagger - t}^{a_\dagger} \mu\big(y, s_1(y + t - a_\dagger)\big) dy = \infty, & t < a_\dagger. \end{cases} \tag{1.31}$$

$(H3)$ The function $\mu \in C^4([0, a_\dagger) \times (0, \infty))$ and $\frac{\partial^p \mu}{\partial s^p}$ are bounded in $[0, a_\dagger) \times [0, K]$, where $1 \le p \le 4$.

$(H4)$ There exists $C > 0$ such that $\frac{\partial^{(p+q)}\mu}{\partial x^p \partial s^q} \le C \frac{\partial^{(p+q)}\mu}{\partial x^{(p+q)}}$ holds in $[0, a_\dagger) \times [0, K]$, where $1 \le p \le 3$, $1 \le q \le 3$ and $p + q \le 4$.

$(H5)$ The functions

$$\varphi(y) = \frac{\partial^2 \mu}{\partial x^2}\big(y, s_1(0)\big) \exp\Big(- \int_{a^*}^{y} \mu(z, s_1(0)) dz \Big),$$

and

$$\rho(y) = \frac{\partial^4 \mu}{\partial x^4}\big(y, s_1(0)\big) \exp\Big(- \int_{a^*}^{y} \mu\big(z, s_1(0)\big) dz \Big),$$

are bounded on $[a^*, a_\dagger]$.

With this set of notation, we state one of our main theorems in Chapter 4 in the following (see [27]).

Theorem 1.5.1 (Convergence) *Assume that $\beta \in C^q([0, a_\dagger] \times (0, \infty))$, and $\mu \in C^q([0, a_\dagger) \times (0, \infty))$ satisfies (1.22). Let $u \in C^q([0, a_\dagger] \times [0, T])$ be the solution to*

(1.2) and v be a bounded solution to (1.26) on $[0, a_\dagger) \times [0, T]$. Assume that Λ_i^n denote an approximation to survival probability $\lambda(x_i, t^n)$ at each grid point such that

$$\max_{0 \le n \le N} \|\boldsymbol{\Lambda}^n - \boldsymbol{\lambda}^n\|_\infty \le Ch^l. \tag{1.32}$$

Furthermore, assume that the quadrature rule $\mathcal{Q}_h$ is of k-th order accuracy and $q = \max(l, k)$. Then the numerical approximations $\boldsymbol{U}^n$ and $\boldsymbol{V}^n$, $n = 0, 1, \ldots, N$, associated to u and v, respectively, that are obtained using numerical method (1.28)–(1.29), satisfy

$$\max_{0 \le n \le N} || \boldsymbol{V}^n - \boldsymbol{v}^n ||_\infty \le Ch^r,$$

and

$$\max_{0 \le n \le N} || \boldsymbol{U}^n - \boldsymbol{u}^n ||_\infty \le Ch^r,$$

where $q, l, k, r \in \mathbb{N}$, $r = \min(l, k)$. □

1.5.1 A third order aprroximation of λ

In this subsection, we approximate λ in the following three iterative steps. This is a predictor-corrector method in which we correct the approximate value of λ twice.

Step–1 First we define

$$\widehat{U}^0 = u_0(x_i), \ 0 \le i \le 2M + 1,$$
$$\widehat{\boldsymbol{S}}_\nu^0 = \mathcal{Q}_h(\boldsymbol{\psi}_\nu \cdot \widehat{\boldsymbol{U}}^0), \quad \nu = 1, 2,$$
$$D_i^0 = \frac{h}{6} \sum_{j=1}^{i} \Big[\mu\big((j-1)h, \widehat{\boldsymbol{S}}_1^0\big) + 4\mu\big((j - \frac{1}{2})h, \widehat{\boldsymbol{S}}_1^0\big) + \mu\big(jh, \widehat{\boldsymbol{S}}_1^0\big)\Big], \ 1 \le i \le 2M + 1,$$
$$\bar{D}_i^0 = \tilde{D}_i^0 = \hat{D}_i^0 = D_i^0, \ 1 \le i \le 2M + 1,$$
$$\bar{D}_0^n = \tilde{D}_0^n = \hat{D}_0^n = 0, \ 0 \le n \le N,$$

and

$$\bar{D}_i^n = \widehat{D}_{i-1}^{n-1} + \frac{h}{2}\Big[\mu\big((i-1)h, \widehat{\boldsymbol{S}}_1^{n-1}\big) + \mu\big(ih, \widehat{\boldsymbol{S}}_1^{n-1}\big)\Big], \quad n, i \ge 1, \tag{1.33}$$

where $\widehat{D}_{i-1}^{n-1}$ and $\widehat{S}_1^{n-1}$ are defined in Step-3. We approximate the survival probability function $\lambda(x,t)$ at each grid point by

$$\bar{\Lambda}_i^n = \exp(-\bar{D}_i^n), \quad 0 \le i \le 2M+1. \tag{1.34}$$

From (1.28)–(1.29) (on substituting $\Lambda_i^n = \bar{\Lambda}_i^n$), we get $\bar{U}_i^n$. Define

$$\bar{\boldsymbol{S}}_\nu^n = \mathcal{Q}_h(\boldsymbol{\psi}_\nu \cdot \bar{\boldsymbol{U}}^n), \quad \nu = 1, 2. \tag{1.35}$$

Step–2 In this step, we first update $\bar{D}_i^n$ to obtain

$$\widetilde{D}_i^n = \widehat{D}_{i-1}^{n-1} + \frac{h}{2}\Big[\mu\big((i-1)h, \widehat{\boldsymbol{S}}_1^{n-1}\big) + \mu\big(ih, \bar{\boldsymbol{S}}_1^n\big)\Big], \quad n, i \ge 1. \tag{1.36}$$

We now correct the approximated survival probability function Λ_i^n at each grid point by replacing $\bar{D}_i^n$ with $\widetilde{D}_i^n$, i.e.,

$$\widetilde{\Lambda}_i^n = \exp(-\widetilde{D}_i^n), \quad 0 \le i \le 2M+1. \tag{1.37}$$

As in the previous step, we substitute $\Lambda_i^n = \widetilde{\Lambda}_i^n$ in (1.28)–(1.29) to get $\widetilde{U}_i^n$. In this step, we correct the approximate weighted population to arrive at

$$\widetilde{\boldsymbol{S}}_\nu^n = \mathcal{Q}_h(\boldsymbol{\psi}_\nu \cdot \widetilde{\boldsymbol{U}}^n), \ \nu = 1, 2. \tag{1.38}$$

Step–3 We make the final correction to $\widetilde{D}$ to get

$$\widehat{D}_i^n = \begin{cases} \widehat{D}_{i-1}^{n-1} + \dfrac{h}{2}\Big[\mu\big((i-1)h, \widehat{\boldsymbol{S}}_1^{n-1}\big) + \mu\big(ih, \widetilde{\boldsymbol{S}}_1^n\big)\Big], & n = 1, \text{ or } i = 1, \\ \widehat{D}_{i-2}^{n-2} + \dfrac{h}{3}\Big[\mu\big((i-2)h, \widehat{\boldsymbol{S}}_1^{n-2}\big) + 4\mu\big((i-1)h, \widehat{\boldsymbol{S}}_1^{n-1}\big) + \mu\big(ih, \widetilde{\boldsymbol{S}}_1^n\big)\Big], & n, i \ge 2. \end{cases} \tag{1.39}$$

We correct $\widetilde{\Lambda}$ once more to find

$$\widehat{\Lambda}_i^n = \exp(-\widehat{D}_i^n), \quad 0 \le i \le 2M+1. \tag{1.40}$$

As before, we use (1.28)–(1.29), with $\Lambda_i^n = \widehat{\Lambda}_i^n$ to get the updated solution of (1.2) namely $\widehat{U}_i^n$. We define

$$\widehat{\boldsymbol{S}}_\nu^n = \mathcal{Q}_h(\boldsymbol{\psi}_\nu \cdot \widehat{\boldsymbol{U}}^n), \quad \nu = 1, 2. \tag{1.41}$$

Note that the survival probability vanishes only at the maximum age, but $a_\dagger$ is not a grid point. Now we present the result corresponding to third order approximation of λ.

Theorem 1.5.2 *Assume hypotheses $(H1)-(H5)$. Moreover assume that $\mu \in C^4([0,a_\dagger)\times(0,\infty))$, $\frac{d^2\mu}{dy^2}(y,s_1(y+\alpha)) \geq 0$ and $\frac{d^4\mu}{dy^4}(y,s_1(y+\alpha)) \geq 0$ for all $y\in[a^*,a_\dagger)$ and $\alpha \geq -a^*$. Let $u \in C^4([0,a_\dagger]\times[0,T])$ be the solution to (1.2). Then*

$$\|\boldsymbol{\Lambda}^n - \boldsymbol{\lambda}^n\|_\infty \leq Ch^4, \tag{1.42}$$

where C is a constant independent of n, h. □

For more details and a proof of this result, see Theorems 4.4.3 and 4.4.4 in Chapter 4.

1.5.2 A fourth order aprroximation of λ

In this subsection, we propose a fourth order numerical scheme to (1.2) by introducing two more corrections to the predictor corrector method presented in Subsecection 1.5.1. In other words, the method that we introduce here is a five step scheme and the first three steps are exactly the same as those defined in the previous section. Before defining the new steps, we need to introduce the notation $\widehat{U}^{n-\frac{1}{2}}_{i-\frac{1}{2}}$, $1\leq n\leq N$, $1\leq i\leq 2M+1$. We define $\widehat{U}^{n-\frac{1}{2}}_{i-\frac{1}{2}}$ with step size h as the approximation $\widehat{U}^{2n-1}_{2i-1}$ with the step size $\frac{h}{2}$ computed in Step–3 of the third order scheme in (1.33), (1.36) and (1.39) in the previous subsection.

Step–4 We define

$$\begin{aligned}
\widehat{\boldsymbol{S}}^{n-\frac{1}{2}}_\nu &= \mathcal{Q}_h(\boldsymbol{\psi}_\nu\cdot\widehat{\boldsymbol{U}}^{n-\frac{1}{2}}), \quad \nu=1,2,\\
\widehat{\widehat{D}}^n_i &= D^0_i, \quad 1\leq i\leq 2M+1,\\
\widehat{\widehat{D}}^n_0 &= D^n_0 = 0, \quad 0\leq n\leq N,
\end{aligned}$$

and

$$\widehat{\widehat{D}}^n_i = D^{n-1}_{i-1} + \frac{h}{6}\Big[\mu\big((i-1)h,\boldsymbol{S}^{n-1}_1\big) + 4\mu\big((i-\frac{1}{2})h,\widehat{\boldsymbol{S}}^{n-\frac{1}{2}}_1\big) + \mu\big(ih,\widehat{\boldsymbol{S}}^n_1\big)\Big], \quad n,i\geq 1, \tag{1.43}$$

where D_{i-1}^{n-1} and $\boldsymbol{S}_1^{n-1}$ are defined in Step–5. We approximate the survival probability function $\lambda(x,t)$ at each grid point by

$$\widehat{\widehat{\Lambda}}_i^n = \exp(-\widehat{\widehat{D}}_i^n), \quad 0 \le i \le 2M+1. \tag{1.44}$$

From (1.28)–(1.29) (on substituting $\Lambda_i^n = \widehat{\widehat{\Lambda}}_i^n$), we get $\widehat{\widehat{U}}_i^n$. We now define

$$\widehat{\widehat{\boldsymbol{S}}}_\nu^n = \mathcal{Q}_h(\boldsymbol{\psi}_\nu \cdot \widehat{\widehat{\boldsymbol{U}}}^n), \quad \nu = 1,2. \tag{1.45}$$

Step–5 Finally, we define

$$D_i^n = \begin{cases} D_{i-1}^{n-1} + \dfrac{h}{6}\Big[\mu\big((i-1)h, \boldsymbol{S}_1^{n-1}\big) + 4\mu\big((i-\dfrac{1}{2})h, \widehat{\boldsymbol{S}}_1^{n-\frac{1}{2}}\big) & \\ +\mu\big(ih, \widehat{\widehat{\boldsymbol{S}}}_1^n\big)\Big], & n=1, \text{ or } i=1, \\ D_{i-2}^{n-2} + \dfrac{h}{3}\Big[\mu\big((i-2)h, \boldsymbol{S}_1^{n-2}\big) + 4\mu\big((i-1)h, \widehat{\widehat{\boldsymbol{S}}}_1^{n-1}\big) & \\ +\mu\big(ih, \widehat{\widehat{\boldsymbol{S}}}_1^n\big)\Big], & n > i \ge 2. \end{cases} \tag{1.46}$$

We now correct $\widehat{\widehat{\Lambda}}_i^n$ once more to find

$$\Lambda_i^n = \exp(-D_i^n), \quad 0 \le i \le 2M+1. \tag{1.47}$$

As before, we use (1.28)–(1.29) to get the updated value of solution of (1.2) namely U_i^n. We now define

$$\boldsymbol{S}_\nu^n = \mathcal{Q}_h(\boldsymbol{\psi}_\nu \cdot \boldsymbol{U}^n), \quad \nu = 1,2. \tag{1.48}$$

With this set of notation, we state our main theorem corresponding to fourth order approximation of λ as follows.

Theorem 1.5.3 *Assume hypotheses $(H1)-(H5)$.Moreover assume that $\mu \in C^4([0,a_\dagger) \times (0,\infty))$, $\frac{d^2\mu}{dy^2}(y, s_1(y+\alpha)) \ge 0$ and $\frac{d^4\mu}{dy^4}(y, s_1(y+\alpha)) \ge 0$ for all $y \in [a^*, a_\dagger)$ and $\alpha \ge -a^*$. Let $u \in C^4([0,a_\dagger] \times [0,T])$ be the solution to (1.2). Then*

$$\|\boldsymbol{\Lambda}^n - \boldsymbol{\lambda}^n\|_\infty \le Ch^4, \tag{1.49}$$

where C is a constant independent of n, h. □

Finally, in order to validate the effectiveness of the proposed numerical scheme, we presented numerical simulations in which the order of convergence is computed (see Section 4.6).

Chapter 2

Numerical solution to a nonlinear McKendrick–Von Foerster equation with diffusion

2.1 Introduction

Reaction diffusion equations with nonlocal boundary condition are studied widely due to many applications in physical and biological phenomena (see [19, 23, 66, 68]). In the literature, various methods are introduced to deal with these types of equations (see [18, 19, 20, 23, 39, 49]). One of the methods to analize these equations, both analytically and numerically, is the method of upper and lower solutions (see [15, 24, 46, 64, 65, 76, 78]). Many authors use this technique to solve nonlinear diffusion equations with linear boundary conditions. However, in physical problems such as gas-liquid interaction problems, generally the nonlinearity occurs at the boundary conditions also (see [22, 54, 62, 74]). At the same time, the qualitative properties of solutions to those partial differential equations (PDEs) in the above mentioned references are studied widely compared to the numerical aspects of them (see [49]).

On the other hand, the McKendrick–Von Foerster equation is ubiquitous in the study of population dynamics (see [21, 60, 61, 72, 73, 81]). In particular, the McKendrick–Von Foerster equation with diffusion (M-V-D) arises naturally in the modeling of neuronal networks, thermoelasticity etc, (see [18, 19, 58]). The main difficulty in the study of the M-V-D is due to the nonlocal nature of the PDE, and the boundary condition(s). Though numerical study of non-local equations got considerable focus, relatively less attention was paid to problems with the Robin boundary conditions. The authors of [57] studied well-posedness and long time behavior of the solution to M-V-D with a nonlinear boundary condition. In [38], the authors presented a numerical scheme of the M-V-D with the Robin boundary condition in the positive quarter plane.

This paper is dedicated to the numerical study of the following nonlinear nonlocal M-V-D with nonlinear nonlocal Robin boundary conditions:

$$\begin{cases} u_t(x,t) + u_x(x,t) + d(x, s(t))u(x,t) = u_{xx}(x,t), \ x \in D, \ t > 0, \\ u(0,t) - u_x(0,t) = \displaystyle\int_0^{a_\dagger} B_1(y, s_1(t))u(y,t)dy, \ t > 0, \\ u(a_\dagger, t) + u_x(a_\dagger, t) = \displaystyle\int_0^{a_\dagger} B_2(y, s_2(t))u(y,t)dy, \ t > 0, \\ u(x,0) = u_0(x), \ x \in \bar{D}, \\ s(t) = \displaystyle\int_0^{a_\dagger} \psi(x)u(x,t)dx, \ s_\nu(t) = \displaystyle\int_0^{a_\dagger} \psi_\nu(x)u(x,t)dx, \ \nu = 1,2, \ t > 0, \end{cases} \tag{2.1}$$

where $a_\dagger > 0$, $D = (0, a_\dagger) \subset \mathbb{R}$. The functions d, B_1, B_2, ψ, ψ_1, ψ_2, u_0 are assumed to be non-negative and continuous, in their respective domains. In [37], the authors have proved the existence of a global solution to (2.1) when $d = d(x)$ and $B_\nu = B_\nu(x)$, $\nu = 1, 2$. Moreover, the authors have proved that the solution to (2.1) converges pointwise to the solution to its steady state equation as time tends to infinity. The author of [63, 64, 67, 69] presented a numerical scheme and introduced a monotone iterative method to find an approximate solution to the nonlinear nonlocal reaction diffusion equation. In [69], the author considered a class of nonlinear reaction-diffusion equations with linear nonlocal boundary conditions to investigates its the asymptotic behavior of the discrete solution.

Analysis of the long time behavior of the solutions to (2.1) requires the study of its steady state problem. The steady state equation corresponding to (2.1) is the following boundary value problem

$$
\begin{cases}
v_x(x) + d(x,p)v(x) = v_{xx}(x), \;\; x \in D, \\
v(0) - v_x(0) = \displaystyle\int_0^{a_\dagger} B_1(y,p_1)v(y)dy, \\
v(a_\dagger) + v_x(a_\dagger) = \displaystyle\int_0^{a_\dagger} B_2(y,p_2)v(y)dy, \\
p = \displaystyle\int_0^{a_\dagger} \psi(x)v(x)dx, \;\; p_\nu = \displaystyle\int_0^{a_\dagger} \psi_\nu(x)v(x)dx, \;\; \nu = 1,2.
\end{cases}
\tag{2.2}
$$

Using an implicit finite difference scheme, we discretize (2.1) to get a system of nonlinear equations. A similar nonlinear finite difference scheme is given for steady state problem (2.2). To slove this system of equations, we introduce a linear monotone iterative scheme. Moreover, we prove that the numerical solution to (2.1) converges to that of its steady state as time tends to infinity. The important difference between the present work and the earlier ones is due to the nonlinear and nonlocal nature of the term d and B_ν in (2.1), $\nu = 1,2$.

The chapter is organized as follows. In Section 2.2, we present a finite-difference scheme to find an approximate solution to equation (2.1). Moreover, we establish existence and uniqueness of solution to the nonlinear systems given by the numerical scheme in Section 2.3 and the uniqueness of the same is proved in Section 2.4. In Section 2.5, we present a numerical scheme for (2.2). We study the long time behavior of numerical solution to equation (2.1) in Section 2.6. In Section 2.7, a particular type of nonlinearity is considered where one can analyze the numerical scheme under weaker hypotheses. Finally, numerical examples are presented in Section 2.8 to re-validate the theoretical results.

2.2 Numerical scheme

In this section, we first discretize equation (2.1) using an implicit finite-difference scheme. Thus the numerical scheme that we propose turns out to be a nonlinear system of equations. Let h and k be the spacial and temporal step sizes, respectively. Denote by (x_i, t_n) a typical grid point with $x_i = ih$, and $t_n = nk$, respectively. Moreover, we assume that $a_\dagger = Mh$ for some $M \in \mathbb{N}$ and define the set of grid points

$$\begin{cases} \Lambda = \{(x_i, t_n) : i = 1, 2, ..., M-1,\ n = 1, 2, ...\}, \\ \bar{\Lambda} = \{(x_i, t_n) : i = 0, 1, ..., M,\ n = 0, 1, ...\}. \end{cases}$$

At every grid point (x_i, t_n), let $U_{i,n}$ denote the approximate solution to (2.1), and

$$\Phi_i = u_0(x_i),\ \Psi_i = \psi(x_i),\ \boldsymbol{U}_n = (U_{0,n}, U_{1,n}, ..., U_{M,n}),\ \boldsymbol{\Psi} = (\Psi_0, \Psi_1, ..., \Psi_M),$$

$$\Psi_{\nu i} = \psi_\nu(x_i),\ \boldsymbol{\Psi}_\nu = (\Psi_{\nu 0}, \Psi_{\nu 1}, ..., \Psi_{\nu M}),\ \nu = 1, 2,\ d_i(X) = d(x_i, X),$$

$$B_{\nu i}(X) = B_\nu(x_i, X),\ \boldsymbol{B}_\nu(X) = (B_{\nu 1}(X), B_{\nu 2}(X), \ldots, B_{\nu M}(X)),\ X \geq 0.$$

To approximate the integral terms in equation (2.1), we choose composite Simpson's $\frac{1}{3}$ quadrature formula with weights $\{q_0, q_1, ..., q_M\}$. In other words, we approximate

$$\int_0^{a_\dagger} \psi(x)u(x,t)dx \sim \sum_{i=0}^{M} q_i \Psi_i U_{i,n} = I(\boldsymbol{\Psi}\boldsymbol{U}_n),$$

$$\int_0^{a_\dagger} \psi_\nu(x)u(x,t)dx \sim \sum_{i=0}^{M} q_i \Psi_{\nu i} U_{i,n} = I(\boldsymbol{\Psi}_\nu \boldsymbol{U}_n),\ \nu = 1, 2.$$

Moreover, we approximate the integral terms in the boundary conditions with

$$\int_0^{a_\dagger} B_\nu(x, s_\nu(t))u(x,t)dx \sim \sum_{i=0}^{M} q_i B_{\nu,i}(I(\boldsymbol{\Psi}_\nu \boldsymbol{U}_n))U_{i,n} = I(\boldsymbol{B}_\nu(I(\boldsymbol{\Psi}_\nu \boldsymbol{U}_n))\boldsymbol{U}_n),$$

where $\nu = 1, 2$. In view of the results in [67], we avoid explicit, semi-implicit schemes, and present an implicit numerical scheme for (2.1). With the notation introduced so far, we propose the following implicit scheme for (2.1) using the backward difference approximation for u_t and the centered in space discretization for u_x, u_{xx}:

$$\begin{cases} (1+2r)U_{i,n} - bU_{i+1,n} - cU_{i-1,n} = U_{i,n-1} - kd_i(I(\boldsymbol{\Psi}\boldsymbol{U}_n))U_{i,n},\ (i,n) \in \Lambda, \\ \left(1 + \dfrac{1}{h}\right) U_{0,n} - \dfrac{1}{h} U_{1,n} = I(\boldsymbol{B}_1(I(\boldsymbol{\Psi}_1 \boldsymbol{U}_n))\boldsymbol{U}_n),\ n \in \mathbb{N}, \\ \left(1 + \dfrac{1}{h}\right) U_{M,n} - \dfrac{1}{h} U_{M-1,n} = I(\boldsymbol{B}_2(I(\boldsymbol{\Psi}_2 \boldsymbol{U}_n))\boldsymbol{U}_n),\ n \in \mathbb{N}, \\ U_{i,0} = \Phi_i,\ 0 \leq i \leq M, \end{cases} \tag{2.3}$$

where $b = r - \frac{\lambda}{2}$, $c = r + \frac{\lambda}{2}$, $\lambda = \frac{k}{h}$ and $r = \frac{k}{h^2}$.
We now define the following finite difference operators

$$\begin{cases} \mathcal{L}[U_{i,n}] = (1+2r)U_{i,n} - bU_{i+1,n} - cU_{i-1,n}, \ (i,n) \in \Lambda, \\ \mathcal{BC}_1[U_{0,n}] = \left(1 + \dfrac{1}{h}\right) U_{0,n} - \left(\dfrac{1}{h}\right) U_{1,n}, \ n \in \mathbb{N}, \\ \mathcal{BC}_2[U_{M,n}] = \left(1 + \dfrac{1}{h}\right) U_{M,n} - \left(\dfrac{1}{h}\right) U_{M-1,n}, \ n \in \mathbb{N}. \end{cases} \tag{2.4}$$

Then numerical scheme (2.3) using the finite difference operators is written as

$$\begin{cases} \mathcal{L}[U_{i,n}] = U_{i,n-1} - kd_i(I(\boldsymbol{\Psi U}_n))U_{i,n}, \ (i,n) \in \Lambda, \\ \mathcal{BC}_1[U_{0,n}] = I(\boldsymbol{B}_1(I(\boldsymbol{\Psi}_1\boldsymbol{U}_n))\boldsymbol{U}_n), \ n \in \mathbb{N}, \\ \mathcal{BC}_2[U_{M,n}] = I(\boldsymbol{B}_2(I(\boldsymbol{\Psi}_2\boldsymbol{U}_n))\boldsymbol{U}_n), \ n \in \mathbb{N}, \\ U_{i,0} = \Phi_i, \ 0 \le i \le M. \end{cases} \tag{2.5}$$

Since (2.5) is a system of nonlinear equations, *a priori* it is not clear whether there exists a solution to it. In the next section, we establish the existence of a solution to (2.5), and its uniqueness is discussed in Section 2.4. For, we use the monotonicity arguments with the aid of notions of upper, and lower solutions (see [19, 37]). To this end, we begin with following definition.

Definition 2.2.1 A matrix $(\tilde{U}_{i,n})$ is called an upper solution to (2.5) if it satisfies

$$\begin{cases} \mathcal{L}[\tilde{U}_{i,n}] \ge \tilde{U}_{i,n-1} - kd_i(I(\boldsymbol{\Psi}\tilde{\boldsymbol{U}}_n))\tilde{U}_{i,n}, \ (i,n) \in \Lambda, \\ \mathcal{BC}_1[\tilde{U}_{0,n}] \ge I(\boldsymbol{B}_1(I(\boldsymbol{\Psi}_1\tilde{\boldsymbol{U}}_n))\tilde{\boldsymbol{U}}_n), \ n \in \mathbb{N}, \\ \mathcal{BC}_2[\tilde{U}_{M,n}] \ge I(\boldsymbol{B}_2(I(\boldsymbol{\Psi}_2\tilde{\boldsymbol{U}}_n))\tilde{\boldsymbol{U}}_n), \ n \in \mathbb{N}, \\ \tilde{U}_{i,0} \ge \Phi_i, \ 0 \le i \le M. \end{cases} \tag{2.6}$$

Similarly, $(\hat{U}_{i,n})$ is called a lower solution to (2.5) if it satisfies all inequalities of (2.6) in the reversed order.

A pair of upper and lower solutions $(\tilde{U}_{i,n}, \hat{U}_{i,n})$ are said to be *ordered* if $\tilde{U}_{i,n} \ge \hat{U}_{i,n}$ on $\bar{\Lambda}$. For a given pair of ordered upper and lower solutions $(\tilde{U}_{i,n}, \hat{U}_{i,n})$, we set

$$\langle \hat{U}_{i,n}, \tilde{U}_{i,n} \rangle := \{U_{i,n} : \hat{U}_{i,n} \le U_{i,n} \le \tilde{U}_{i,n}\},$$

$$\eta = \sup\left\{\frac{\partial}{\partial s}B_\nu(x_i,s) \mid s = I(\boldsymbol{\Psi}_\nu \boldsymbol{U}_n), \hat{U}_{i,n} \leq U_{i,n} \leq \tilde{U}_{i,n}, (i,n) \in \bar{\Lambda}, \nu = 1,2\right\}.$$

We conclude this section with the following assumptions which are used throughout the paper:

$$\text{The spacial and temporal step sizes are such that } b > 0, \tag{2.7}$$

$$d \text{ is a nonnegetive } C^1 \text{ function, } s \mapsto d(.,s) \text{ is monotone,} \tag{2.8}$$

$$B_\nu \text{ is a nonnegetive } C^1 \text{ function, } s \mapsto B_\nu(.,s) \text{ is monotone, } \nu = 1,2, \tag{2.9}$$

$$\max\{\eta I(\boldsymbol{\Psi}_\nu)||\Phi||_\infty a_\dagger + I(\boldsymbol{B}_\nu(0)) \mid \nu = 1,2\} \leq 1. \tag{2.10}$$

Observe that under assumption (2.10) $\tilde{U}_{i,n} \equiv ||\Phi||_\infty$ and $\hat{U}_{i,n} \equiv 0$ are upper solution and lower solution to (2.5), respectively.

2.3 Existence of solution

In this section, we employ the monotonicity method along with a discrete maximum principle to establish the existence result to nonlinear system (2.5). We prove the existence of a solution to (2.5) in four cases: (i) $s \mapsto d(.,s)$ is decreasing and $s \mapsto B_\nu(.,s)$ is increasing, (ii) $s \mapsto d(.,s)$ is increasing and $s \mapsto B_\nu(.,s)$ are decreasing, (iii) $s \mapsto d(.,s)$ is decreasing and $s \mapsto B_\nu(.,s)$ is decreasing, (iv) $s \mapsto d(.,s)$ is increasing and $s \mapsto B_\nu(.,s)$ is increasing. The cases (i) and (ii) are given separately in the next subsections. Existence of solutions to (2.5) in the cases (iii) and (iv) can be proved using the similar arguments, thus the details are omitted.

2.3.1 The case $\frac{\partial d}{\partial s}(.,s) \leq 0$, $\frac{\partial B_\nu}{\partial s}(.,s) \geq 0$

Let $\hat{U}_{i,n}$ and $\tilde{U}_{i,n}$ be a pair of ordered lower and upper solutions to (2.5). Now, define

$$\beta = \sup\left\{d(x_i,s) \mid s = I(\boldsymbol{\Psi}\boldsymbol{U}_n),\ \hat{U}_{i,n} \leq U_{i,n} \leq \tilde{U}_{i,n},\ (i,n) \in \bar{\Lambda}\right\},$$

$$\xi = \sup\left\{\frac{\partial}{\partial s}d(x_i,s) \mid s = I(\boldsymbol{\Psi}\boldsymbol{U}_n),\ \hat{U}_{i,n} \leq U_{i,n} \leq \tilde{U}_{i,n},\ (i,n) \in \bar{\Lambda}\right\}.$$

We now introduce a linear operator

$$L[U_{i,n}] = \mathcal{L}[U_{i,n}] + k\left(\xi \hat{U}_{i,n} I(\boldsymbol{\Psi}\boldsymbol{U}_n) + \beta U_{i,n}\right). \tag{2.11}$$

Using this new operator, (2.5) can be written as

$$\begin{cases} L[U_{i,n}] = U_{i,n-1} + k\left(-d_i(I(\boldsymbol{\Psi}\boldsymbol{U}_n))U_{i,n} + \xi\hat{U}_{i,n}I(\boldsymbol{\Psi}\boldsymbol{U}_n) + \beta U_{i,n}\right), (i,n) \in \Lambda, \\ \mathcal{BC}_1[U_{0,n}] = I(\boldsymbol{B}_1(I(\boldsymbol{\Psi}_1\boldsymbol{U}_n))\boldsymbol{U}_n),\ n \in \mathbb{N}, \\ \mathcal{BC}_2[U_{M,n}] = I(\boldsymbol{B}_2(I(\boldsymbol{\Psi}_2\boldsymbol{U}_n))\boldsymbol{U}_n),\ n \in \mathbb{N}, \\ U_{i,0} = \Phi_i,\ 0 \le i \le M. \end{cases} \tag{2.12}$$

For $(i,n) \in \bar{\Lambda}$, we construct a sequence $\{U_{i,n}^m\}$ of approximations to a solution $\{U_{i,n}\}$ to (2.12) in the following manner. Let $\{U_{i,n}^m\}$ be the solution to

$$\begin{cases} L[U_{i,n}^m] = U_{i,n-1}^{m-1} + k\left(-d_i(I(\boldsymbol{\Psi}\boldsymbol{U}_n^{m-1}))U_{i,n}^{m-1} + \xi\hat{U}_{i,n}I(\boldsymbol{\Psi}\boldsymbol{U}_n^{m-1})\right. \\ \qquad\qquad \left.+\beta U_{i,n}^{m-1}\right),\ (i,n) \in \Lambda,\ m \in \mathbb{N}, \\ \mathcal{BC}_1[U_{0,n}^m] = I(\boldsymbol{B}_1(I(\boldsymbol{\Psi}_1\boldsymbol{U}_n^{m-1}))\boldsymbol{U}_n^{m-1}),\ n \in \mathbb{N},\ m \in \mathbb{N}, \\ \mathcal{BC}_2[U_{M,n}^m] = I(\boldsymbol{B}_2(I(\boldsymbol{\Psi}_2\boldsymbol{U}_n^{m-1}))\boldsymbol{U}_n^{m-1}),\ n \in \mathbb{N},\ m \in \mathbb{N}, \\ U_{i,0}^m = \Phi_i,\ 0 \le i \le M,\ m \in \mathbb{N}. \end{cases} \tag{2.13}$$

To close the system, we need to fix the initial approximation $U_{i,n}^0$. If the initial approximation is taken to be an upper solution (a lower solution, resp.) to (2.5), then the solution to (2.13) is denoted by $\bar{U}_{i,n}^m$ ($\underline{U}_{i,n}^m$, resp.).
We next show that the sequences of approximations $(\bar{U}_{i,n}^m)$ and $(\underline{U}_{i,n}^m)$ are indeed monotone at each grid point $(i,n) \in \bar{\Lambda}$.

Lemma 2.3.1 (Discrete maximum principle) *Assume that $s \mapsto d(.,s)$ is decreasing, $s \mapsto B_\nu(.,s)$ is increasing, $\nu = 1,2$. Assume (2.7) holds, and $-k\sigma_1 < 1$, where*

$$\sigma_1 = \min\{\xi\hat{U}_{i,n}I(\boldsymbol{\Psi}) + \beta \mid (i,n) \in \bar{\Lambda}, \hat{U}_{i,n} \le U_{i,n} \le \tilde{U}_{i,n}\}.$$

If $W_{i,n}$ satisfies

$$\begin{cases} L[W_{i,n}] \ge 0,\ (i,n) \in \Lambda, \\ \mathcal{BC}_1[W_{0,n}] \ge 0,\ n \in \mathbb{N}, \\ \mathcal{BC}_2[W_{M,n}] \ge 0,\ n \in \mathbb{N}, \\ W_{i,0} \ge 0,\ 0 \le i \le M, \end{cases} \tag{2.14}$$

then $W_{i,n} \ge 0,\ (i,n) \in \bar{\Lambda}$.

Proof. On the contrary, assume that for some $N \in \mathbb{N}$, there exists $(i', n') \in \bar{\Lambda}$ such that

$$W_{i',n'} = \min_{\substack{0 \le n \le N \\ 0 \le i \le M}} W_{i,n} < 0. \tag{2.15}$$

We first notice that $W_{i,0} \ge 0$ for $0 \le i \le M$, which gives $n' \neq 0$.
On the other hand, since $\mathcal{BC}_1[W_{0,n}] \ge 0$, we have

$$hW_{1,n'} \le (1+h)W_{0,n'},$$

which readily gives that $i' \neq 0$. Using the other boundary condition and the same argument, one can easily show that $i' \neq M$. Therefore we obtain $(i', n') \in \bar{\Lambda}$. Using the definition of b, c, and the fact that $b > 0$ with $2r = b + c$, we get

$$2rW_{i',n'} - bW_{i'+1,n'} - cW_{i'-1,n'} \le 0. \tag{2.16}$$

From (2.14)-(2.16) and the definition of L, we obtain

$$\begin{aligned} 0 &\le W_{i',n'} + k\left(\xi \hat{U}_{i',n'} I(\boldsymbol{\Psi}\boldsymbol{W}_{n'}) + \beta W_{i',n'}\right) \\ &\le W_{i',n'} + k\left(\xi \hat{U}_{i',n'} I(\boldsymbol{\Psi}) + \beta\right) W_{i',n'}. \end{aligned} \tag{2.17}$$

In view of (2.15) and (2.17), we deduce

$$0 \ge 1 + k\left(\xi \hat{U}_{i',n'} I(\boldsymbol{\Psi}) + \beta\right) \ge 1 + k\sigma_1,$$

which is a contradiction to the assumption $-k\sigma_1 < 1$. Hence, we find that

$$W_{i,n} \ge 0, \ (i,n) \in \bar{\Lambda}.$$

This completes the proof.

Theorem 2.3.2 *Let $\hat{U}_{i,n}$, and $\tilde{U}_{i,n}$ be a pair of ordered lower and upper solutions to equation (2.5), respectively. Assume that $s \mapsto d(.,s)$ is decreasing, $s \mapsto B_\nu(.,s)$ is increasing, for $\nu = 1, 2$ and $-k\sigma_1 < 1$. Then the following hold:*
(i) For every fixed $(i,n) \in \bar{\Lambda}$, both $\{\bar{U}^m_{i,n}\}$, $\{\underline{U}^m_{i,n}\}$ are monotone sequences. Moreover, we have

$$\hat{U}_{i,n} \le \underline{U}^m_{i,n} \le \underline{U}^{m+1}_{i,n} \le \underline{U}_{i,n} \le \bar{U}_{i,n} \le \bar{U}^{m+1}_{i,n} \le \bar{U}^m_{i,n} \le \tilde{U}_{i,n}, \ (i,n) \in \bar{\Lambda},$$

for every $m \in \mathbb{N} \cup \{0\}$*, where* $\lim_{m\to\infty} \bar{U}^m_{i,n} = \bar{U}_{i,n}$*,* $\lim_{m\to\infty} \underline{U}^m_{i,n} = \underline{U}_{i,n}$*.*
(ii) Both $\bar{U}_{i,n}$ *and* $\underline{U}_{i,n}$ *are solutions to* (2.5)*.*
(iii) If $U^*_{i,n}$ *is another solution to* (2.5) *in* $\langle \hat{U}_{i,n}, \tilde{U}_{i,n}\rangle$*, then* $\underline{U}_{i,n} \le U^*_{i,n} \le \bar{U}_{i,n}$ *on* $\bar{\Lambda}$*.*

Proof.(i) Set $\bar{W}^0_{i,n} = \bar{U}^0_{i,n} - \bar{U}^1_{i,n}$, $(i,n) \in \bar{\Lambda}$.

Claim 1: We first prove that $\bar{W}^0_{i,n} \ge 0$, $(i,n) \in \bar{\Lambda}$.
From (2.6) and (2.13), it follows that for $n \in \mathbb{N}$, we find

$$\begin{aligned}
\mathcal{BC}_1[\bar{W}^0_{0,n}] &= \mathcal{BC}_1[\tilde{U}_{0,n}] - \mathcal{BC}_1[\bar{U}^1_{0,n}] \\
&\ge I(\boldsymbol{B}_1(I(\boldsymbol{\Psi}_1\tilde{\boldsymbol{U}}_n))\tilde{\boldsymbol{U}}_n) - I(\boldsymbol{B}_1(I(\boldsymbol{\Psi}_1\tilde{\boldsymbol{U}}_n))\tilde{\boldsymbol{U}}_n) \\
&= 0.
\end{aligned} \tag{2.18}$$

Similarly, we have

$$\mathcal{BC}_2[\bar{W}^0_{M,n}] \ge 0, \;\; n \in \mathbb{N}. \tag{2.19}$$

Again, from (2.13) and (2.6), for $1 \le i \le M-1$, $\; n \in \mathbb{N}$, we get

$$\begin{aligned}
L[\bar{W}^0_{i,n}] &= L[\bar{U}^0_{i,n}] - L[\bar{U}^1_{i,n}] \\
&= \mathcal{L}[\bar{U}^0_{i,n}] + k\left(\xi\hat{U}_{i,n}I(\boldsymbol{\Psi}\bar{\boldsymbol{U}}^0_n) + \beta\bar{U}^0_{i,n}\right) - \bar{U}^0_{i,n-1} \\
&\quad - k\left(-d_i(I(\boldsymbol{\Psi}\bar{\boldsymbol{U}}^0_n))\bar{U}^0_{i,n} + \xi\hat{U}_{i,n}I(\boldsymbol{\Psi}\bar{\boldsymbol{U}}^0_n) + \beta\bar{U}^0_{i,n}\right) \\
&= \mathcal{L}[\bar{U}^0_{i,n}] - \bar{U}^0_{i,n-1} + kd_i(I(\boldsymbol{\Psi}\bar{\boldsymbol{U}}^0_n))\bar{U}^0_{i,n} \\
&\ge 0,
\end{aligned} \tag{2.20}$$

where the last inequality is due to the assumption that $\bar{U}^0_{i,n}$ is an upper solution to (2.5).
In view of Lemma 2.3.1, we conclude that

$$\bar{U}^0_{i,n} \ge \bar{U}^1_{i,n}, \;\; (i,n) \in \bar{\Lambda}. \tag{2.21}$$

Using the same argument employed to prove (2.21), one can easily prove that

$$\underline{U}^0_{i,n} \le \underline{U}^1_{i,n}, \;\; (i,n) \in \bar{\Lambda}.$$

Claim 2: We next prove that $\bar{U}^1_{i,n} \ge \underline{U}^1_{i,n}$.

For, we set $W^1_{i,n} = \bar{U}^1_{i,n} - \underline{U}^1_{i,n}$, and consider

$$\begin{aligned}
L[W^1_{i,n}] &= L[\bar{U}^1_{i,n}] - L[\underline{U}^1_{i,n}] \\
&= \bar{U}^0_{i,n-1} + k\left(-d_i(I(\boldsymbol{\Psi}\bar{\boldsymbol{U}}^0_n))\bar{U}^0_{i,n} + \xi\hat{U}_{i,n}I(\boldsymbol{\Psi}\bar{\boldsymbol{U}}^0_n) + \beta\bar{U}^0_{i,n}\right) - \underline{U}^0_{i,n-1} \\
&\quad - k\left(-d_i(I(\boldsymbol{\Psi}\underline{\boldsymbol{U}}^0_n))\underline{U}^0_{i,n} + \xi\hat{U}_{i,n}I(\boldsymbol{\Psi}\underline{\boldsymbol{U}}^0_n) + \beta\underline{U}^0_{i,n}\right) \\
&= \bar{W}^0_{i,n-1} + k\left(-d_i(I(\boldsymbol{\Psi}\underline{\boldsymbol{U}}^0_n))\bar{W}^0_{i,n} + [d_i(I(\boldsymbol{\Psi}\underline{\boldsymbol{U}}^0_n)) - d_i(I(\boldsymbol{\Psi}\bar{\boldsymbol{U}}^0_n))]\bar{U}^0_{i,n}\right. \\
&\quad \left. + \xi\hat{U}_{i,n}I(\boldsymbol{\Psi}\bar{\boldsymbol{W}}^0_n) + \beta\bar{W}^0_{i,n}\right) \\
&\geq \bar{W}^0_{i,n-1} + k\xi I(\boldsymbol{\Psi}\bar{\boldsymbol{W}}^0_n)(\hat{U}_{i,n} - \bar{U}^0_{i,n}) \\
&\geq 0,
\end{aligned} \tag{2.22}$$

where the last inequality follows from the fact that $\xi \leq 0$ and Claim 1. Using the boundary condition and the fact that $s \mapsto B_1(.,s)$ is increasing, one can easily prove that $\mathcal{BC}_1[W^1_{0,n}] \geq 0$, $\mathcal{BC}_2[W^1_{M,n}] \geq 0$, and $W^1_{i,0} = 0$.
From Lemma 2.3.1, it follows that $W^1_{i,n} \geq 0$.
Hence

$$\underline{U}^0_{i,n} \leq \underline{U}^1_{i,n} \leq \bar{U}^1_{i,n} \leq \bar{U}^0_{i,n}, \ (i,n) \in \bar{\Lambda}.$$

Claim 3: We now prove that $\bar{U}^{m+1}_{i,n} \leq \bar{U}^m_{i,n}$, $(i,n) \in \bar{\Lambda}$, $m \in \mathbb{N} \cup \{0\}$.
Let the following hold

$$\bar{U}^p_{i,n} \geq \bar{U}^{p+1}_{i,n}, \ (i,n) \in \bar{\Lambda}, \ p = 0, 1, ..., m. \tag{2.23}$$

Set $\bar{W}^{m+1}_{i,n} = \bar{U}^{m+1}_{i,n} - \bar{U}^{m+2}_{i,n}$, then from (2.6) and (2.13) it follows that, for $(i,n) \in \bar{\Lambda}$,

$$\begin{aligned}
L[\bar{W}^{m+1}_{i,n}] &= L[\bar{U}^{m+1}_{i,n}] - L[\bar{U}^{m+2}_{i,n}] \\
&= \bar{U}^m_{i,n-1} + k\left(-d_i(I(\boldsymbol{\Psi}\bar{\boldsymbol{U}}^m_n))\bar{U}^m_{i,n} + \xi\hat{U}_{i,n}I(\boldsymbol{\Psi}\bar{\boldsymbol{U}}^m_n) + \beta\bar{U}^m_{i,n}\right) - \bar{U}^{m+1}_{i,n-1} \\
&\quad - k\left(-d_i(I(\boldsymbol{\Psi}\bar{\boldsymbol{U}}^{m+1}_n))\bar{U}^{m+1}_{i,n} + \xi\hat{U}_{i,n}I(\boldsymbol{\Psi}\bar{\boldsymbol{U}}^{m+1}_n) + \beta\bar{U}^{m+1}_{i,n}\right) \\
&\geq \bar{U}^m_{i,n-1} - \bar{U}^{m+1}_{i,n-1} \\
&\geq 0,
\end{aligned}$$

where the last inequality is due to (2.23) and the technique employed in the proof of (2.22).

Again, from the linearity of the operator $\mathcal{BC}_1$, nonnegativity of Ψ, Ψ_1, Ψ_2 and the induction hypothesis, we find that $\mathcal{BC}_1[\bar{W}^{m+1}_{0,n}] \geq 0,\ \mathcal{BC}_2[\bar{W}^{m+1}_{M,n}] \geq 0,\ n \in \mathbb{N}$. Again in view of Lemma 2.3.1, we conclude that

$$\bar{U}^{m+1}_{i,n} \geq \bar{U}^{m+2}_{i,n},\ (i,n) \in \bar{\Lambda}.$$

Similarly, by the induction argument, it straightforward to show that

$$\hat{U}_{i,n} \leq \underline{U}^{m}_{i,n} \leq \underline{U}^{m+1}_{i,n} \leq \bar{U}^{m+1}_{i,n} \leq \bar{U}^{m}_{i,n} \leq \tilde{U}_{i,n},\ (i,n) \in \bar{\Lambda},\ m \in \mathbb{N} \cup \{0\}.$$

Now (i) is an immediate consequence of the previous inequality.

(ii) Since $d,\ B_\nu,\ \nu = 1,2$ are continuous functions, we let $m \to \infty$ in (2.13) to obtain that both $\bar{U}_{i,n}$ and $\underline{U}_{i,n}$ are solutions to (2.5).

(iii) Let $U^*_{i,n}$ be a solution to (2.5) in $\langle \hat{U}_{i,n}, \tilde{U}_{i,n} \rangle$. Hence it is clear that $\tilde{U}_{i,n} = \bar{U}^0_{i,n} \geq U^*_{i,n},\ (i,n) \in \bar{\Lambda}$. Set $W^1_{i,n} = \bar{U}^1_{i,n} - U^*_{i,n},\ (i,n) \in \bar{\Lambda}$.
As before, it is easy to verify that $L[W^1_{i,n}] \geq 0,\ (i,n) \in \Lambda,\ \mathcal{BC}_1[W^1_{0,n}] \geq 0,\ \mathcal{BC}_2[W^1_{M,n}] \geq 0,\ n \in \mathbb{N}$, and hence we conclude that $W^1_{i,n} \geq 0,\ (i,n) \in \bar{\Lambda}$.
Thus we have

$$U^*_{i,n} \leq \bar{U}^1_{i,n} \leq \bar{U}^0_{i,n},\ (i,n) \in \bar{\Lambda}.$$

By following the method used in the proof of (i), we can easily show that

$$\hat{U}_{i,n} \leq \underline{U}^{m}_{i,n} \leq U^*_{i,n} \leq \bar{U}^{m}_{i,n} \leq \tilde{U}_{i,n},\ (i,n) \in \bar{\Lambda},\ m \in \mathbb{N} \cup \{0\}. \tag{2.24}$$

Letting $m \to \infty$ in (2.37), we find that

$$\underline{U}_{i,n} \leq U^*_{i,n} \leq \bar{U}_{i,n},\ (i,n) \in \bar{\Lambda},$$

which completes the proof of (iii).

2.3.2 The case $\frac{\partial d}{\partial s}(.,s) \geq 0,\ \frac{\partial B_\nu}{\partial s}(.,s) \leq 0$

Now, define

$$\zeta = \inf\left\{\frac{\partial}{\partial s_\nu} B_\nu(x_i, s_\nu) \mid s_\nu = I(\mathbf{\Psi}_\nu \boldsymbol{U}_n), \hat{U}_{i,n} \leq U_{i,n} \leq \tilde{U}_{i,n}, (i,n) \in \bar{\Lambda}, \nu = 1,2\right\},$$

$$\theta = \inf\left\{B_\nu(x_i, s_\nu) \mid s_\nu = I(\mathbf{\Psi}_\nu \boldsymbol{U}_n),\ \hat{U}_{i,n} \leq U_{i,n} \leq \tilde{U}_{i,n}, (i,n) \in \bar{\Lambda},\ \nu = 1,2\right\}.$$

Consider the following linear operators

$$\begin{cases} L_*[U_{i,n}] = \mathcal{L}[U_{i,n}] + k\left(\xi\tilde{U}_{i,n}I(\boldsymbol{\Psi}\boldsymbol{U}_n) + \beta U_{i,n}\right), \ (i,n)\in\Lambda, \\ BC_1[U_{0,n}] = \mathcal{BC}_1[U_{0,n}] - \theta I(\boldsymbol{\Psi}_1\boldsymbol{U}_n) - \zeta I(\tilde{\boldsymbol{U}}_n)I(\boldsymbol{\Psi}_1\boldsymbol{U}_n), \ n\in\mathbb{N}, \\ BC_2[U_{M,n}] = \mathcal{BC}_2[U_{M,n}] - \theta I(\boldsymbol{\Psi}_2\boldsymbol{U}_n) - \zeta I(\tilde{\boldsymbol{U}}_n)I(\boldsymbol{\Psi}_2\boldsymbol{U}_n), \ n\in\mathbb{N}. \end{cases} \tag{2.25}$$

Using these new operators, scheme (2.5) can be written as

$$\begin{cases} L_*[U_{i,n}] = U_{i,n-1} + k\left(-d_i(I(\boldsymbol{\Psi}\boldsymbol{U}_n))U_{i,n} + \xi\tilde{U}_{i,n}I(\boldsymbol{\Psi}\boldsymbol{U}_n) + \beta U_{i,n}\right), (i,n)\in\Lambda, \\ BC_1[U_{0,n}] = I(\boldsymbol{B}_1(I(\boldsymbol{\Psi}_1\boldsymbol{U}_n))\boldsymbol{U}_n) - \theta I(\boldsymbol{U}_n) - \zeta I(\tilde{\boldsymbol{U}}_n)I(\boldsymbol{\Psi}_1\boldsymbol{U}_n), \ n\in\mathbb{N}, \\ BC_2[U_{M,n}] = I(\boldsymbol{B}_2(I(\boldsymbol{\Psi}_2\boldsymbol{U}_n))\boldsymbol{U}_n) - \theta I(\boldsymbol{U}_n) - \zeta I(\tilde{\boldsymbol{U}}_n)I(\boldsymbol{\Psi}_2\boldsymbol{U}_n), \ n\in\mathbb{N}, \\ U_{i,0} = \Phi_i, \ 0\le i\le M. \end{cases} \tag{2.26}$$

For $(i,n)\in\bar{\Lambda}$, we construct a sequence $\{U_{i,n}^m\}$ of approximations to a solution $\{U_{i,n}\}$ to (2.26) as follows. Let $\{U_{i,n}^m\}$ be the solution to

$$\begin{cases} L_*[U_{i,n}^m] = U_{i,n-1}^{m-1} + k\left(-d_i(I(\boldsymbol{\Psi}\boldsymbol{U}_n^{m-1}))U_{i,n}^{m-1} + \xi\tilde{U}_{i,n}I(\boldsymbol{\Psi}\boldsymbol{U}_n^{m-1}) + \beta U_{i,n}^{m-1}\right), \\ \qquad\qquad (i,n)\in\Lambda, \ m\in\mathbb{N}, \\ BC_1[U_{0,n}^m] = I(\boldsymbol{B}_1(I(\boldsymbol{\Psi}_1\boldsymbol{U}_n^{m-1}))\boldsymbol{U}_n^{m-1}) - \theta I(\boldsymbol{U}_n^{m-1}) - \zeta I(\tilde{\boldsymbol{U}}_n)I(\boldsymbol{\Psi}_1\boldsymbol{U}_n^{m-1}), \\ \qquad\qquad n\in\mathbb{N}, m\in\mathbb{N}, \\ BC_2[U_{M,n}^m] = I(\boldsymbol{B}_2(I(\boldsymbol{\Psi}_2\boldsymbol{U}_n^{m-1}))\boldsymbol{U}_n^{m-1}) - \theta I(\boldsymbol{U}_n^{m-1}) - \zeta I(\tilde{\boldsymbol{U}}_n)I(\boldsymbol{\Psi}_2\boldsymbol{U}_n^{m-1}), \\ \qquad\qquad n\in\mathbb{N}, \ m\in\mathbb{N}, \\ U_{i,0}^m = \Phi_i, \ 0\le i\le M, \ m\in\mathbb{N}. \end{cases} \tag{2.27}$$

If the initial approximation $U_{i,n}^0$ is taken to be an upper solution (a lower solution, resp.) to (2.5), then the solution to (2.27) is denoted by $\bar{U}_{i,n}^m$ ($\underline{U}_{i,n}^m$, resp.). The sequences of approximations $(\bar{U}_{i,n}^m)$ and $(\underline{U}_{i,n}^m)$ are indeed monotone at each grid point $(i,n)\in\bar{\Lambda}$ as in Theorem 2.3.2.

Theorem 2.3.3 *Let $\hat{U}_{i,n}$, and $\tilde{U}_{i,n}$ be a pair of ordered lower and upper solutions to equation (2.5), respectively. Assume that $s\mapsto d(.,s)$ is increasing, $s\mapsto B_\nu(.,s)$ is decreasing, $\nu=1,2$, $-k\sigma_2<1$ and $\delta<1$, where*

$$\delta = \inf\{\theta a_\dagger + \zeta I(\boldsymbol{\Psi}_\nu)I(\tilde{\boldsymbol{U}}_n) \mid \nu=1,2\},$$

$$\sigma_2 = \min\{\xi\tilde{U}_{i,n}I(\boldsymbol{\Psi}) + \beta \mid (i,n)\in\bar{\Lambda}, \hat{U}_{i,n}\le U_{i,n}\le\tilde{U}_{i,n}\}.$$

Then the following hold:
(i) For every fixed $(i,n) \in \bar{\Lambda}$, *both* $\{\bar{U}^m_{i,n}\}$, $\{\underline{U}^m_{i,n}\}$ *are monotone sequences. Moreover, we have*

$$\hat{U}_{i,n} \leq \underline{U}^m_{i,n} \leq \underline{U}^{m+1}_{i,n} \leq \underline{U}_{i,n} \leq \bar{U}_{i,n} \leq \bar{U}^{m+1}_{i,n} \leq \bar{U}^m_{i,n} \leq \tilde{U}_{i,n},\ (i,n) \in \bar{\Lambda},$$

for every $m \in \mathbb{N} \cup \{0\}$, *where* $\lim\limits_{m\to\infty} \bar{U}^m_{i,n} = \bar{U}_{i,n}$, $\lim\limits_{m\to\infty} \underline{U}^m_{i,n} = \underline{U}_{i,n}$.
(ii) The functions $\bar{U}_{i,n}$ *and* $\underline{U}_{i,n}$ *are solutions to* (2.5).
(iii) If $U^*_{i,n}$ *is another solution to* (2.5) *in* $\langle \hat{U}_{i,n}, \tilde{U}_{i,n} \rangle$, *then* $\underline{U}_{i,n} \leq U^*_{i,n} \leq \bar{U}_{i,n}$ *on* $\bar{\Lambda}$.

Proof. The proof is similar to that of Theorem 2.3.2 and we omit the details.

2.4 Uniqueness

In this section, we show that there exists indeed a unique solution to (2.5). To this end, we first introduce the following notation:

$$\gamma = \min\left\{\tfrac{\partial}{\partial s} d(x_i, s) : s = I(\mathbf{\Psi}\boldsymbol{U}_n),\ \hat{U}_{i,n} \leq U_{i,n} \leq \tilde{U}_{i,n}, (i,n) \in \bar{\Lambda}\right\},$$

$$\alpha = \min\left\{d(x_i, s) : s = I(\mathbf{\Psi}\boldsymbol{U}_n),\ \hat{U}_{i,n} \leq U_{i,n} \leq \tilde{U}_{i,n}, (i,n) \in \bar{\Lambda}\right\},$$

$$\sigma_3 = \min\{\gamma \tilde{U}_{i,n} I(\mathbf{\Psi}) + \alpha : (i,n) \in \bar{\Lambda}\},$$

$$\sigma_4 = \min\{\gamma \hat{U}_{i,n} I(\mathbf{\Psi}) + \alpha : (i,n) \in \bar{\Lambda}\},$$

$$\delta_1 = \sup\left\{\eta I(\mathbf{\Psi}_\nu) I(\tilde{\boldsymbol{U}}_{\boldsymbol{n}}) + I(\boldsymbol{B}_\nu(I(\mathbf{\Psi}_\nu \tilde{\boldsymbol{U}}_n))) : n = 0, 1, 2, \ldots,\ \nu = 1, 2\right\},$$

$$\delta_2 = \sup\left\{\eta I(\mathbf{\Psi}_\nu) I(\hat{\boldsymbol{U}}_{\boldsymbol{n}}) + I(\boldsymbol{B}_\nu(I(\mathbf{\Psi}_\nu \hat{\boldsymbol{U}}_n))) : n = 0, 1, 2, \ldots,\ \nu = 1, 2\right\}.$$

We are ready to prove the uniqueness result.

Theorem 2.4.1 (Uniqueness) *Assume one of the following conditions:*
(i) $s \mapsto d(., s)$ *is decreasing,* $s \mapsto B_\nu(., s)$ *is increasing and* $\max\{-k\sigma_3, \delta_1\} < 1$,
(ii) $s \mapsto d(., s)$ *is increasing,* $s \mapsto B_\nu(., s)$ *is increasing and* $\max\{-k\sigma_4, \delta_1\} < 1$,
(iii) $s \mapsto d(., s)$ *is decreasing,* $s \mapsto B_\nu(., s)$ *is decreasing and* $\max\{-k\sigma_3, \delta_2\} < 1$,
(iv) $s \mapsto d(., s)$ *is increasing,* $s \mapsto B_\nu(., s)$ *is decreasing and* $\max\{-k\sigma_4, \delta_2\} < 1$.
Then equation (2.5) *has a unique solution in* $\langle \hat{U}_{i,n}, \tilde{U}_{i,n} \rangle$.

Proof. We prove the theorem under the assumptions given in (i). The proof in the other cases follow from the same argument.
In view of Theorem 2.3.2(iii), to prove uniqueness of solution to equation (2.5), it suffices to show that $\bar{U}_{i,n} = \underline{U}_{i,n}$. To this end, let $X_{i,n} = \bar{U}_{i,n} - \underline{U}_{i,n}$. Note that

$X_{i,n} \geq 0$ in $\bar{\Lambda}$.
Define $W_{i,n} = (1-\rho)^n X_{i,n}$, for some constant $\rho > 0$ such that $-k\sigma_3 < \rho < 1$.
Claim $W_{i,n} \equiv 0,\ (i,n) \in \bar{\Lambda}$.
On the contrary, assume that there exists $N \in \mathbb{N}$, $(i', n') \in \bar{\Lambda}$ such that

$$W_{i',n'} = \max_{\substack{0 \leq n \leq N \\ 0 \leq i \leq M}} W_{i,n} > 0.$$

From the initial conditions, we get $n' \neq 0$. Let, if possible, $i' = 0$.
We observe from the left boundary term that

$$\begin{aligned}
&\left(1 + \frac{1}{h}\right) W_{0,n'} - \left(\frac{1}{h}\right) W_{1,n'} \\
&= (1-\rho)^{n'} \left(\left(1 + \frac{1}{h}\right) X_{0,n'} - \left(\frac{1}{h}\right) X_{1,n'} \right) \\
&= (1-\rho)^{n'} \left(I(\boldsymbol{B}_1(I(\boldsymbol{\Psi}_1 \bar{\boldsymbol{U}}_{n'}))\bar{\boldsymbol{U}}_{n'}) - I(\boldsymbol{B}_1(I(\boldsymbol{\Psi}_1 \underline{\boldsymbol{U}}_{n'}))\underline{\boldsymbol{U}}_{n'}) \right) \\
&= (1-\rho)^{n'} [I(\boldsymbol{B}_1(I(\boldsymbol{\Psi}_1 \bar{\boldsymbol{U}}_{n'}))\bar{\boldsymbol{U}}_{n'}) - I(\boldsymbol{B}_1(I(\boldsymbol{\Psi}_1 \bar{\boldsymbol{U}}_{n'}))\underline{\boldsymbol{U}}_{n'}) \\
&\qquad + I(\boldsymbol{B}_1(I(\boldsymbol{\Psi}_1 \bar{\boldsymbol{U}}_{n'}))\underline{\boldsymbol{U}}_{n'}) - I(\boldsymbol{B}_1(I(\boldsymbol{\Psi}_1 \underline{\boldsymbol{U}}_{n'}))\underline{\boldsymbol{U}}_{n'})] \\
&\leq (1-\rho)^{n'} (\bar{U}_{0,n'} - \underline{U}_{0,n'}) \left(I(\boldsymbol{B}_1(I(\boldsymbol{\Psi}_1 \tilde{\boldsymbol{U}}_{n'}))) + \eta I(\boldsymbol{\Psi}_1) I(\tilde{\boldsymbol{U}}_{\boldsymbol{n'}}) \right) \\
&\leq \delta_1 W_{0,n'} \\
&< W_{0,n'},
\end{aligned}$$

or

$$W_{0,n'} < W_{1,n'}. \tag{2.28}$$

In view of (2.28), we see that $i' \neq 0$. Using the same argument at the other boundary point, we get $i' \neq M$. This shows that $(i', n') \in \Lambda$.
Finally, we use the argument that was used to prove Claim 1 in Theorem 2.3.2(i) to get a contradiction. Since b, $c > 0$ and $b + c = 2r$, we readily obtain that

$$2rW_{i',n'} - bW_{i'+1,n'} - cW_{i'-1,n'} \geq 0.$$

Then from the definition of $\mathcal{L}$, we immediately get

$$W_{i',n'} \leq \mathcal{L}[W_{i',n'}]. \tag{2.29}$$

Thus from (2.5) and (2.29), it follows that

$$\begin{aligned}
W_{i',n'} &\leq (1-\rho)W_{i,n'-1} - k(1-\rho)^{n'}d_i(I(\boldsymbol{\Psi}\bar{\boldsymbol{U}}_{n'}))\bar{U}_{i,n'} + k(1-\rho)^{n'}d_i(I(\boldsymbol{\Psi}\underline{\boldsymbol{U}}_{n'}))\underline{U}_{i,n'} \\
&= (1-\rho)W_{i',n'-1} - k(1-\rho)^{n'}\left[\bar{U}_{i',n'}(d_{i'}(I(\boldsymbol{\Psi}\bar{\boldsymbol{U}}_{n'})) - d_{i'}(I(\boldsymbol{\Psi}\underline{\boldsymbol{U}}_{n'})))\right] \\
&\qquad - k(1-\rho)^{n'}\left[d_{i'}(I(\boldsymbol{\Psi}\underline{\boldsymbol{U}}_{n'}))(\bar{U}_{i',n'} - \underline{U}_{i',n'})\right] \\
&\leq (1-\rho)W_{i',n'-1} - kW_{i',n'}\left[\tilde{U}_{i',n'}\gamma I(\boldsymbol{\Psi}) + \alpha\right].
\end{aligned}$$

Therefore we find that

$$\begin{aligned}
(1-\rho)W_{i',n'-1} &\geq \left(1 + k\left[\tilde{U}_{i',n'}\gamma I(\boldsymbol{\Psi}) + \alpha\right]\right)W_{i',n'} \\
&\geq (1+k\sigma_3)W_{i',n'}.
\end{aligned}$$

Hence from the above relation, we obtain

$$(1+k\sigma_3)W_{i',n'} \leq (1-\rho)W_{i',n'-1} \leq (1-\rho)W_{i',n'},$$

which is impossible because $-k\sigma_3 < \rho$. Thus it follows that $W_{i,n} \equiv 0$ or $\bar{U}_{i,n} = \underline{U}_{i,n},\ (i,n) \in \bar{\Lambda}$, proving the uniqueness result.

2.5 Steady state

The objective of this section is to provide a numerical solution to (2.2). As in the unsteady case, we present an implicit numerical scheme to find an approximate solution to the steady state problem, and study its well posedness. Moreover, we introduce the notions of upper, lower solutions to address the existence of a solution to the nonlinear scheme.

2.5.1 Numerical scheme

In order to discretize the ordinary differential equation (ODE) given in (2.2), we use the notation from the earlier sections. Let $h, M, d, B_\nu,\ \{q_0, q_1, ..., q_M\}$ be as in Section 2.2, and V_i denote the approximate solution to (2.2) at the grid point $x_i = ih,\ 0 \leq i \leq M$. As before, we approximate the integrals in the ODE and the boundary conditions in (2.2) by

$$\int_0^{a_\dagger} \psi(x)v(x)dx \sim \sum_{i=0}^{M} q_i \Psi_i V_i = I(\boldsymbol{\Psi V}),$$

$$\int_0^{a_\dagger} \psi_\nu(x)v(x)dx \sim \sum_{i=0}^{M} q_i \Psi_{\nu i} V_i = I(\boldsymbol{\Psi}_\nu \boldsymbol{V}),\ \nu = 1, 2,$$

$$\int_0^{a_\dagger} B_\nu(x,p)v(x)dx \sim \sum_{i=0}^{M} q_i B_{\nu,i}(I(\boldsymbol{\Psi}_\nu \boldsymbol{V}))V_i = I(\boldsymbol{B}_\nu(I(\boldsymbol{\Psi}_\nu \boldsymbol{V}))\boldsymbol{V}),\ \nu = 1, 2,$$

where $\boldsymbol{V} = (V_0, V_1, ..., V_M)$.

The numerical method that we propose to find an approximate solution to (2.2) is based on the central difference approximation for v_{xx} and v_x. Therefore the numerical solution (V_i) of (2.2) is given by

$$\begin{cases} a'V_i - b'V_{i+1} - c'V_{i-1} = -d_i(I(\boldsymbol{\Psi V}))V_i,\ 1 \le i \le M-1, \\ \left(1 + \dfrac{1}{h}\right) V_0 - \left(\dfrac{1}{h}\right) V_1 = I(\boldsymbol{B}_1(I(\boldsymbol{\Psi}_1 \boldsymbol{V}))\boldsymbol{V}), \\ \left(1 + \dfrac{1}{h}\right) V_M - \left(\dfrac{1}{h}\right) V_{M-1} = I(\boldsymbol{B}_2(I(\boldsymbol{\Psi}_2 \boldsymbol{V}))\boldsymbol{V}), \end{cases} \tag{2.30}$$

where $a' = \frac{2}{h^2}$, $b' = \frac{1}{h^2} - \frac{1}{2h}$ and $c' = \frac{1}{h^2} + \frac{1}{2h}$.

By introducing following finite difference operators

$$\begin{cases} \mathcal{L}^s[V_i] = a'V_i - b'V_{i+1} - c'V_{i-1}, \\ \mathcal{BC}_1^s[V_0] = \left(1 + \dfrac{1}{h}\right) V_0 - \left(\dfrac{1}{h}\right) V_1, \\ \mathcal{BC}_2^s[V_M] = \left(1 + \dfrac{1}{h}\right) V_M - \left(\dfrac{1}{h}\right) V_{M-1}, \end{cases} \tag{2.31}$$

we write finite difference scheme (2.30) as

$$\begin{cases} \mathcal{L}^s[V_i] = -d_i(I(\boldsymbol{\Psi V}))V_i,\ 1 \le i \le M-1, \\ \mathcal{BC}_1^s[V_0] = I(\boldsymbol{B}_1(I(\boldsymbol{\Psi}_1 \boldsymbol{V}))\boldsymbol{V}), \\ \mathcal{BC}_2^s[V_M] = I(\boldsymbol{B}_2(I(\boldsymbol{\Psi}_2 \boldsymbol{V}))\boldsymbol{V}). \end{cases} \tag{2.32}$$

Notice that numerical scheme (2.32) is a system of nonlinear equations. We need to prove existence and uniqueness result for (2.32). For, we apply the monotonicity arguments that were used in Sections 2.3 and 2.4. To this end, we introduce the notion of upper (lower) solution to (2.32).

Definition 2.5.1 A vector $(\tilde{V}_i)$ is called an upper solution to (2.32) if it satisfies the relation

$$\begin{cases} \mathcal{L}^s[\tilde{V}_i] \geq -d_i(I(\boldsymbol{\Psi}\tilde{\boldsymbol{V}}))\tilde{V}_i, \ 1 \leq i \leq M-1, \\ \mathcal{BC}^s_1[\tilde{V}_0] \geq I(\boldsymbol{B}_1(I(\boldsymbol{\Psi}_1\tilde{\boldsymbol{V}}))\tilde{\boldsymbol{V}}), \\ \mathcal{BC}^s_2[\tilde{V}_M] \geq I(\boldsymbol{B}_2(I(\boldsymbol{\Psi}_2\tilde{\boldsymbol{V}}))\tilde{\boldsymbol{V}}). \end{cases} \tag{2.33}$$

Similarly, $(\hat{V}_i)$ is called a lower solution to equation (2.32) if it satisfies all the inequalities in (2.33) in the reverse order.

A pair of upper solution $(\tilde{V}_i)$ and lower solution $(\hat{V}_i)$ are said to be ordered if $\tilde{V}_i \geq \hat{V}_i$, $0 \leq i \leq M$. For a given pair of ordered upper and lower solutions $\tilde{V}_i$, $\hat{V}_i$, we set $\langle \hat{V}_i, \tilde{V}_i \rangle \equiv \{V_i : \hat{V}_i \leq V_i \leq \tilde{V}_i\}$.
Observe that any ordered lower and upper solution to (2.32) is also an ordered upper and lower solution to (2.5). Moreover, notice that if hypothesis (2.10) holds, then $\tilde{V}_i \equiv ||\Phi||_\infty$ and $\hat{V}_i \equiv 0$ are upper solution and lower solution to (2.32), respectively.

2.5.2 Existence

As in the unsteady case, we prove existence of solution to (2.32) in the following four cases: (i) $\frac{\partial d}{\partial p}(.,p) \leq 0$, $\frac{\partial B_\nu}{\partial p}(.,p) \geq 0$, (ii) $\frac{\partial d}{\partial p}(.,p) \geq 0$, $\frac{\partial B_\nu}{\partial p}(.,p) \leq 0$, (iii) $\frac{\partial d}{\partial p}(.,p) \geq 0$, $\frac{\partial B_\nu}{\partial p}(.,p) \geq 0$, (iv) $\frac{\partial d}{\partial p}(.,p) \leq 0$, $\frac{\partial B_\nu}{\partial p}(.,p) \leq 0$. Cases (i) and (ii) are discussed briefly in the next two subsubsections. On the other hand, existence of solution to (2.32) in cases (iii) and (iv) can be proved using the similar arguments.

The case $\frac{\partial d}{\partial p}(.,p) \leq 0$, $\frac{\partial B_\nu}{\partial p}(.,p) \geq 0$

Let $\tilde{V}_i$ and $\hat{V}_i$ be a pair of upper and lower solutions to (2.32), respectively. Now, define

$$\beta_s = \max\left\{d(x_i,p) : p = I(\boldsymbol{\Psi V}),\ \hat{V}_i \leq V_i \leq \tilde{V}_i,\ 0 \leq i \leq M\right\},$$

$$\xi_s = \max\left\{\tfrac{\partial}{\partial p} d(x_i,p) : p = I(\boldsymbol{\Psi V}),\ \hat{V}_i \leq V_i \leq \tilde{V}_i,\ 0 \leq i \leq M\right\},$$

$$L^s[V_i] = \mathcal{L}^s[V_i] + \left(\xi_s \hat{V}_i I(\boldsymbol{\Psi V}) + \beta_s V_i\right),\ 1 \leq i \leq M-1.$$

Thus (2.32) becomes

$$\begin{cases} L^s[V_i] = \left(-d_i(I(\mathbf{\Psi V}))V_i + \xi_s \hat{V}_i I(\mathbf{\Psi V}) + \beta_s V_i\right), \ 1 \le i \le M-1, \\ \mathcal{BC}_1^s[V_0] = I(\boldsymbol{B}_1(I(\mathbf{\Psi}_1 \boldsymbol{V}))\boldsymbol{V}), \\ \mathcal{BC}_2^s[V_M] = I(\boldsymbol{B}_2(I(\mathbf{\Psi}_2 \boldsymbol{V}))\boldsymbol{V}). \end{cases} \tag{2.34}$$

We now construct a sequence of approximations $\{V_i^m\}$ to (2.34) using the linear iteration process

$$\begin{cases} L^s[V_i^m] = \left(-d_i(I(\mathbf{\Psi V}^{m-1}))V_i^{m-1} + \xi_s \hat{V}_i I(\mathbf{\Psi V}^{m-1}) + \beta_s V_i^{m-1}\right), \\ \qquad\qquad\qquad\qquad 1 \le i \le M-1, \ m \in \mathbb{N}, \\ \mathcal{BC}_1^s[V_0^m] = I(\boldsymbol{B}_1(I(\mathbf{\Psi}_1 \boldsymbol{V}^{m-1}))\boldsymbol{V}^{m-1}), \ m \in \mathbb{N}, \\ \mathcal{BC}_2^s[V_M^m] = I(\boldsymbol{B}_2(I(\mathbf{\Psi}_2 \boldsymbol{V}^{m-1}))\boldsymbol{V}^{m-1}), \ m \in \mathbb{N}. \end{cases} \tag{2.35}$$

If V_i^0 is equal to an upper solution (lower solution, resp.) to (2.32) then denote the solution to (2.35) by $\bar{V}_i^m$ ($\underline{V}_i^m$, resp.). As in the earlier sections, we show that both $(\bar{V}_i^m)$ and $(\underline{V}_i^m)$ are monotone sequences for each $1 \le i \le M-1$. This is given in the next result.

Theorem 2.5.2 (Existence) *Let $\hat{V}_i$, and $\tilde{V}_i$ be a pair of ordered lower and upper solutions to equation (2.32), respectively. Assume that $p \mapsto d(.,p)$ is decreasing, $p \mapsto B_\nu(.,p)$ is increasing and $\mu_1 = \min\{\xi_s \hat{V}_i I(\mathbf{\Psi}) + \beta_s : 0 \le i \le M\} > 0$. Then the following hold:*
(i) For each $0 \le i \le M$, both $\{\bar{V}_i^m\}$, $\{\underline{V}_i^m\}$ are monotone. Moreover, we have

$$\hat{V}_i \le \underline{V}_i^m \le \underline{V}_i^{m+1} \le \underline{V}_i \le \bar{V}_i \le \bar{V}_i^{m+1} \le \bar{V}_i^m \le \tilde{V}_i,$$

for every $m \in \mathbb{N} \cup \{0\}$, where $\lim_{m\to\infty} \{\bar{V}_i^m\} = \bar{V}_i$, $\lim_{m\to\infty} \{\underline{V}_i^m\} = \underline{V}_i$.
(ii) Both $\bar{V}_i$ and $\underline{V}_i$ are solutions to (2.32).

(iii) If V_i^* is another solution to (2.32) in $\langle \hat{V}_i, \tilde{V}_i \rangle$ then $\underline{V}_i \le V_i^* \le \bar{V}_i$, for $0 \le i \le M$.

Proof. The proof follows from the same arguments used in the proof of Theorem 2.3.2.

The case $\frac{\partial d}{\partial p}(.,p) \geq 0$, $\frac{\partial B_\nu}{\partial p}(.,p) \leq 0$

Let

$$\theta_s = \min\left\{B_\nu(x_i,p_\nu) : p_\nu = I(\mathbf{\Psi}_\nu \boldsymbol{V}),\ \hat{V}_i \leq V_i \leq \tilde{V}_i,\ 0 \leq i \leq M, \nu = 1,2\right\},$$

$$\zeta_s = \min\left\{\tfrac{\partial}{\partial p_\nu} B_\nu(x_i,p_\nu) : p_\nu = I(\mathbf{\Psi}_\nu \boldsymbol{V}),\ \hat{V}_i \leq V_i \leq \tilde{V}_i,\ 0 \leq i \leq M, \nu = 1,2\right\}.$$

We now introduce the following linear operators

$$\begin{cases} L_*^s[V_i] = \mathcal{L}^s[V_i] + \Big(\xi_s \tilde{V}_i I(\mathbf{\Psi}\boldsymbol{V}) + \beta_s V_i\Big),\ 1 \leq i \leq M-1, \\ \mathcal{BC}_1^s[V_0] = I(\boldsymbol{B}_1(I(\mathbf{\Psi}_1\boldsymbol{V}))\boldsymbol{V}) - \theta_s I(\mathbf{\Psi}_1\boldsymbol{V}) - \zeta_s I(\tilde{\boldsymbol{V}}) I(\mathbf{\Psi}_1\boldsymbol{V}), \\ \mathcal{BC}_2^s[V_M] = I(\boldsymbol{B}_2(I(\mathbf{\Psi}_2\boldsymbol{V}))\boldsymbol{V}) - \theta_s I(\mathbf{\Psi}_2\boldsymbol{V}) - \zeta_s I(\tilde{\boldsymbol{V}}) I(\mathbf{\Psi}_2\boldsymbol{V}). \end{cases} \tag{2.36}$$

Thus (2.32) becomes

$$\begin{cases} L_*^s[V_i] = \Big(-d_i(I(\mathbf{\Psi}\boldsymbol{V}))V_i + \xi_s \tilde{V}_i I(\mathbf{\Psi}\boldsymbol{V}) + \beta_s V_i\Big),\ 1 \leq i \leq M-1, \\ \mathcal{BC}_1^s[V_0] = I(\boldsymbol{B}_1(I(\mathbf{\Psi}_1\boldsymbol{V}))\boldsymbol{V}) - \theta_s I(\mathbf{\Psi}_1\boldsymbol{V}) - \zeta_s I(\tilde{\boldsymbol{V}}) I(\mathbf{\Psi}_1\boldsymbol{V}), \\ \mathcal{BC}_2^s[V_M] = I(\boldsymbol{B}_2(I(\mathbf{\Psi}_2\boldsymbol{V}))\boldsymbol{V}) - \theta_s I(\mathbf{\Psi}_2\boldsymbol{V}) - \zeta_s I(\tilde{\boldsymbol{V}}) I(\mathbf{\Psi}_2\boldsymbol{V}). \end{cases} \tag{2.37}$$

We construct a sequence of approximations $\{V_i^m\}$ to (2.37) using the linear iteration process

$$\begin{cases} L_*^s[V_i^m] = \Big(-d_i(I(\mathbf{\Psi}\boldsymbol{V}^{m-1}))V_i^{m-1} + \xi_s \tilde{V}_i I(\mathbf{\Psi}\boldsymbol{V}^{m-1}) + \beta_s V_i^{m-1}\Big), \\ \qquad\qquad 1 \leq i \leq M-1,\ m \in \mathbb{N}, \\ \mathcal{BC}_1^s[V_0^m] = I(\boldsymbol{B}_1(I(\mathbf{\Psi}_1\boldsymbol{V}^{m-1}))\boldsymbol{V}^{m-1}) - \theta_s I(\mathbf{\Psi}_1\boldsymbol{V}^{m-1}) - \zeta_s I(\tilde{\boldsymbol{V}}) I(\mathbf{\Psi}_1\boldsymbol{V}^{m-1}), \\ \qquad\qquad m \in \mathbb{N}, \\ \mathcal{BC}_2^s[V_M^m] = I(\boldsymbol{B}_2(I(\mathbf{\Psi}_2\boldsymbol{V}^{m-1}))\boldsymbol{V}^{m-1}) - \theta_s I(\mathbf{\Psi}_2\boldsymbol{V}^{m-1}) - \zeta_s I(\tilde{\boldsymbol{V}}) I(\mathbf{\Psi}_2\boldsymbol{V}^{m-1}), \\ \qquad\qquad m \in \mathbb{N}. \end{cases} \tag{2.38}$$

If V_i^0 is equal to an upper solution (lower solution, resp.) to (2.32) then the solution to (2.38) is denoted by $\bar{V}_i^m$ ($\underline{V}_i^m$, resp.). As in Section 2.3, we show that both $(\bar{V}_i^m)$ and $(\underline{V}_i^m)$ are monotone sequences for each $1 \leq i \leq M-1$. This is given in the next result.

Theorem 2.5.3 (Existence) *Let $\hat{V}_i$, and $\tilde{V}_i$ be a pair of ordered lower and upper solutions to equation (2.32), respectively. Assume that $p \mapsto d(.,p)$ is increasing,*

$p \mapsto B_\nu(.,p)$ is decreasing, $\mu_2 = \min\{\xi_s \tilde{V}_i I(\mathbf{\Psi}) + \beta_s : 0 \leq i \leq M\} > 0$ and $\lambda = \max\{\theta a_\dagger + \zeta I(\mathbf{\Psi}_\nu) I(\tilde{\boldsymbol{V}}) \mid \nu = 1,2\} < 1$. Then the following hold:
(i) For each $0 \leq i \leq M$, both $\{\bar{V}_i^m\}$, $\{\underline{V}_i^m\}$ are monotone. Moreover, we have

$$\hat{V}_i \leq \underline{V}_i^m \leq \underline{V}_i^{m+1} \leq \underline{V}_i \leq \bar{V}_i \leq \bar{V}_i^{m+1} \leq \bar{V}_i^m \leq \tilde{V}_i,$$

for every $m \in \mathbb{N} \cup \{0\}$, where $\lim_{m\to\infty} \{\bar{V}_i^m\} = \bar{V}_i$, $\lim_{m\to\infty} \{\underline{V}_i^m\} = \underline{V}_i$.
(ii) Both $\bar{V}_i$ and $\underline{V}_i$ are solutions to (2.32).
(iii) If V_i^* is another solution to (2.32) in $\langle \hat{V}_i, \tilde{V}_i \rangle$ then $\underline{V}_i \leq V_i^* \leq \bar{V}_i$, for $0 \leq i \leq M$.

Proof. The proof follows from the same arguments used in the proof of Theorem 2.3.2.

2.5.3 Uniqueness

The objective of this subsection is to provide a statement of the uniqueness result to (2.32). In order to state the uniqueness result, we introduce the following notations:

$$\gamma_s = \min\left\{\tfrac{\partial}{\partial p} d(x,p) : p = I(\mathbf{\Psi}\boldsymbol{V}),\ \hat{V}_i \leq V_i \leq \tilde{V}_i,\ 0 \leq i \leq M\right\},$$
$$\alpha_s = \min\left\{d(x,p) : p = I(\mathbf{\Psi}\boldsymbol{V}),\ \hat{V}_i \leq V_i \leq \tilde{V}_i, 0 \leq i \leq M\right\},$$
$$\mu_3 = \min\{\gamma_s \tilde{V}_i I(\mathbf{\Psi}) + \alpha_s : 0 \leq i \leq M\},$$
$$\mu_4 = \min\{\gamma_s \hat{V}_i I(\mathbf{\Psi}) + \alpha_s : 0 \leq i \leq M\},$$
$$\eta_s = \max\left\{\tfrac{\partial}{\partial p_\nu} B_\nu(x_i,p_\nu) : p_\nu = I(\mathbf{\Psi}_\nu \boldsymbol{V}),\ \hat{V}_i \leq V_i \leq \tilde{V}_i,\ 0 \leq i \leq M, \nu = 1,2\right\},$$
$$\lambda_1 = \max\left\{I\left(\eta_s I(\mathbf{\Psi}_\nu)\tilde{V}_i + \boldsymbol{B}_\nu(I(\mathbf{\Psi}_\nu \tilde{\boldsymbol{V}}))\right) : \nu = 1,2\right\},$$
$$\lambda_2 = \max\left\{I\left(\eta_s I(\mathbf{\Psi}_\nu)\hat{V}_i + \boldsymbol{B}_\nu(I(\mathbf{\Psi}_\nu \tilde{\boldsymbol{V}}))\right) : \nu = 1,2\right\}.$$

We conclude the section with the following uniqueness theorem for system (2.32).

Theorem 2.5.4 (Uniqueness) *Assume one of the following conditions:*
(i) $p \mapsto d(.,p)$ is decreasing, $\mu_3 > 0$, $p \mapsto B_\nu(.,p)$ is increasing and $\lambda_1 < 1$,
(ii) $p \mapsto d(.,p)$ is increasing, $\mu_4 > 0$, $p \mapsto B_\nu(.,p)$ is increasing and $\lambda_1 < 1$,
(iii) $p \mapsto d(.,p)$ is decreasing, $\mu_3 > 0$, $p \mapsto B_\nu(.,p)$ is decreasing and $\lambda_2 < 1$,
(iv) $p \mapsto d(.,p)$ is increasing, $\mu_4 > 0$, $p \mapsto B_\nu(.,p)$ is decreasing and $\lambda_2 < 1$.
Then equation (2.32) has a unique solution in $\langle \hat{V}_i, \tilde{V}_i \rangle$.

2.6 Long time behavior

In this section, our aim is to establish the stability of numerical scheme (2.5) and a relation between $U_{i,n}$ and V_i. In particular, we show that if the initial data satisfies $\hat{V}_i \leq \Phi_i \leq \tilde{V}_i$, $0 \leq i \leq M$, then the corresponding numerical solution $U_{i,n}$ to (2.1) converges to the numerical solution V_i to (2.2). We first begin with the stability result.

Theorem 2.6.1 (Stability) *Assume the hypotheses of Theorem 2.4.1. Then scheme* (2.5) *is stable.*

Proof. We prove this result under hypotheses (i) in Theroem 2.4.1. The other cases follow using the same argument. First, fix $T > 0$. Let $N \in \mathbb{N}$, $k > 0$ be such that $Nk \leq T$. To prove stability of the numerical scheme, we show that $|| U_n ||_\infty \leq || \Phi ||_\infty$, $n \in \mathbb{N}$. We set $\tilde{U}_{i,n} = || \Phi ||_\infty$ and $\hat{U}_{i,n} = 0$. Observe that $\tilde{U}_{i,n}$ is an upper solution to (2.5), due to $\delta_1 < 1$. It is easy to verify that the constant zero matrix $(\hat{U}_{i,n})$ is a lower solution to (2.5). From Theorems 2.3.2 and 2.4.1, there exists a unique solution to (2.5), say $U_{i,n}$ satisfying, $0 \leq U_{i,n} \leq || \Phi ||_\infty$, $0 \leq i \leq M$, $0 \leq n \leq N$. We now prove the main theorem of this section.

Theorem 2.6.2 (Asymptotic behavior) *Let $\tilde{V}_i$ and $\hat{V}_i$ be a pair of ordered upper and lower solutions to* (2.32)*, respectively. Let the hypotheses of Theorem 2.4.1 hold. Assume that $\hat{U}_{i,n} \leq \hat{V}_i \leq \tilde{V}_i \leq \tilde{U}_{i,n}$. Let $\bar{Y}_{i,n}$ and $\underline{Y}_{i,n}$ be solutions to* (2.5) *with $\bar{Y}_{i,0} = \tilde{V}_i$ and $\underline{Y}_{i,0} = \hat{V}_i$, respectively. Then the following conclusions hold:*
(i) For each fixed $0 \leq i \leq M$, the sequence $(\bar{Y}_{i,n})$ is decreasing and $(\underline{Y}_{i,n})$ is increasing in n. Moreover, we have $\bar{Y}_{i,n} \geq \underline{Y}_{i,n}$ on $\bar{\Lambda}$.
(ii) If $U_{i,n}$ is a solution to (2.5) *with initial data $\Phi_i \in \langle \hat{V}_i, \tilde{V}_i \rangle$, then $\underline{Y}_{i,n} \leq U_{i,n} \leq \bar{Y}_{i,n}$.*
(iii) For each $0 \leq i \leq M$, set $\lim\limits_{n\to\infty} \bar{Y}_{i,n} = \bar{V}_i$, $\lim\limits_{n\to\infty} \underline{Y}_{i,n} = \underline{V}_i$. Then $\bar{V}_i$ and $\underline{V}_i$ are the maximal and minimal solutions to (2.32) *in $\langle \hat{V}_i, \tilde{V}_i \rangle$, respectively.*
(iv) Let $\Phi_i \in \langle \hat{V}_i, \tilde{V}_i \rangle$. Assume that $\mu_3 > 0$, and $\mu_4 > 0$ whenever $\frac{\partial d}{\partial s} \geq 0$, and $\frac{\partial d}{\partial s} < 0$, respectively. Then $\lim\limits_{n\to\infty} U_{i,n} = \bar{V}_i = \underline{V}_i$.

Proof. We prove the theorem under the assumptions given in (i) in the statement of Theroem 2.4.1. The other cases follow from the same argument.
(i) In order to prove (i), we use the same strategy employed in the proof of

Theorem 2.4.1.

Let $X_{i,n} = \bar{Y}_{i,n} - \bar{Y}_{i,n+1},\ (i,n) \in \bar{\Lambda}$.

Now define $\bar{W}_{i,n} = (1-\rho)^n(\bar{Y}_{i,n} - \bar{Y}_{i,n+1})$, for some constant $\rho > 0$ such that $-k\sigma_3 < \rho < 1$.

Claim $\bar{W}_{i,n} \geq 0$ on $\bar{\Lambda}$.

On the contrary, assume that for some $N \in \mathbb{N}$, there exists $(i',n') \in \bar{\Lambda}$ such that

$$\bar{W}_{i',n'} = \min_{\substack{0 \leq n \leq N \\ 0 \leq i \leq M}} \bar{W}_{i,n} < 0.$$

Observe that $\tilde{V}_i$ is also an upper solution to (2.5). In view of Theorems 2.3.2 and 2.4.1, we obtain, $\bar{W}_{i,0} = \bar{Y}_{i,0} - \bar{Y}_{i,1} = \tilde{V}_i - \bar{Y}_{i,1} \geq 0$. Thus we find that $n' \neq 0$. Let if possible $i' = 0$.

Then from the left boundary condition and hypothesis, we get

$$\begin{aligned}
&\left(1+\frac{1}{h}\right)W_{0,n'} - \left(\frac{1}{h}\right)W_{1,n'} \\
&= (1-\rho)^{n'}\left(\left(1+\frac{1}{h}\right)X_{0,n'} - \left(\frac{1}{h}\right)X_{1,n'}\right) \\
&= (1-\rho)^{n'}\left(I(\boldsymbol{B}_1(I(\boldsymbol{\Psi}_1\bar{\boldsymbol{Y}}_{n'}))\bar{\boldsymbol{Y}}_{n'}) - I(\boldsymbol{B}_1(I(\boldsymbol{\Psi}_1\bar{\boldsymbol{Y}}_{n'+1}))\bar{\boldsymbol{Y}}_{n'+1})\right) \\
&= (1-\rho)^{n'}[I(\boldsymbol{B}_1(I(\boldsymbol{\Psi}_1\bar{\boldsymbol{Y}}_{n'}))\bar{\boldsymbol{Y}}_{n'}) - I(\boldsymbol{B}_1(I(\boldsymbol{\Psi}_1\bar{\boldsymbol{Y}}_{n'}))\bar{\boldsymbol{Y}}_{n'+1}) \\
&\qquad + I(\boldsymbol{B}_1(I(\boldsymbol{\Psi}_1\bar{\boldsymbol{Y}}_{n'}))\bar{\boldsymbol{Y}}_{n'+1}) - I(\boldsymbol{B}_1(I(\boldsymbol{\Psi}_1\bar{\boldsymbol{Y}}_{n'+1}))\bar{\boldsymbol{Y}}_{n'+1})] \\
&\geq (1-\rho)^{n'}(\bar{Y}_{0,n'} - \bar{Y}_{0,n'+1})I\left(\boldsymbol{B}_1(I(\boldsymbol{\Psi}_1\tilde{\boldsymbol{U}}_{n'})) + \eta I(\boldsymbol{\Psi}_1)\tilde{U}_{i,n'+1}\right) \\
&\geq \delta_1 W_{0,n'} \\
&> W_{0,n'}.
\end{aligned} \tag{2.39}$$

In view of (2.39), we obtain $i' \neq 0$. Using the same argument at the other boundary, we get $i' \neq M$. Therefore we have $(i',n') \in \Lambda$.

Since

$$2r\bar{W}_{i',n'} - b\bar{W}_{i'+1,n'} - c\bar{W}^0_{i'-1,n'} \leq 0,$$

from the definition of $\mathcal{L}$, we deduce

$$\begin{aligned}
\bar{W}_{i',n'} &\geq \mathcal{L}[\bar{W}_{i',n'}] \\
&= (1-\rho)\bar{W}_{i',n'-1} - (1-\rho)^{n'} k[d_{i'}(I(\mathbf{\Psi}\bar{\boldsymbol{Y}}_{n'}))\bar{Y}_{i',n'} \\
&\quad - d_{i'}(I(\mathbf{\Psi}\bar{\boldsymbol{Y}}_{n'+1}))\bar{Y}_{i',n'+1}] \\
&= (1-\rho)\bar{W}_{i',n'-1} - (1-\rho)^{n'} k\left[\bar{Y}_{i',n'}(d_{i'}(I(\mathbf{\Psi}\bar{\boldsymbol{Y}}_{n'})) - d_{i'}(I(\mathbf{\Psi}\bar{\boldsymbol{Y}}_{n'+1})))\right] \\
&\quad - (1-\rho)^{n'} k\left[d_{i'}(I(\mathbf{\Psi}\bar{\boldsymbol{Y}}_{n'+1}))(\bar{Y}_{i',n'} - \bar{Y}_{i',n'+1})\right] \\
&\geq (1-\rho)\bar{W}_{i',n'-1} - k\left[\tilde{U}_{i',n'} I(\mathbf{\Psi})\gamma + \alpha\right]\bar{W}_{i',n'} \\
&\geq (1-\rho)\bar{W}_{i',n'-1} - k\sigma_3\bar{W}_{i',n'}.
\end{aligned}$$

In view of the above relation, we find that

$$(1+k\sigma_3)\,\bar{W}_{i',n'} \geq (1-\rho)\bar{W}_{i',n'-1} \geq (1-\rho)\bar{W}_{i',n'},$$

which is impossible because $-k\sigma_3 < \rho$. This contradiction shows that $\bar{W}_{i,n} \geq 0$. Hence

$$\bar{Y}_{i,n+1} \geq \bar{Y}_{i,n}, \ \ (i,n) \in \bar{\Lambda}. \tag{2.40}$$

A similar argument employed to prove (2.40) gives the relations $\underline{Y}_{i,n+1} \geq \underline{Y}_{i,n}$ and $\bar{Y}_{i,n} \geq \underline{Y}_{i,n}, \ \ (i,n) \in \bar{\Lambda}$.

(ii) Let $U_{i,n}$ be the solution to (2.5) with initial data $\Phi_i \in \langle \hat{V}_i, \tilde{V}_i \rangle$.
On setting $W_{i,n} = (1-\rho)^n(\bar{Y}_{i,n} - U_{i,n})$, and using the argument employed to prove (2.40), one can readily obtain $W_{i,n} \geq 0$, which yields $U_{i,n} \leq \bar{Y}_{i,n}$. Similarly, one can show that $\underline{Y}_{i,n} \leq U_{i,n}$.

(iii) We first notice that $\hat{V}_i \leq \underline{V}_i \leq \bar{V}_i \leq \tilde{V}_i$.
Using (i) and letting $n \to \infty$ in (2.5), we find that both $\bar{V}_i$ and $\underline{V}_i$ are solutions to equation (2.32).
Let V_i^* be a maximal solution to (2.32) in $\langle \hat{V}_i, \tilde{V}_i \rangle$. On setting $W_{i,n} = (1-\rho)^n(\bar{Y}_{i,n} - V_i^*)$, and using the argument employed to prove (i), one readily obtains $W_{i,n} \geq 0$. Again, let $n \to \infty$, to get $\bar{V}_i \geq V_i^*$. Maximality of V_i^* ensures that $\bar{V}_i = V_i^*$. Similarly, one can prove that $\underline{V}_i$ is a minimal solution to (2.32) in $\langle \hat{V}_i, \tilde{V}_i \rangle$.

(iv) Since $1 > \delta_1 \geq \lambda_1$, Theorem 2.5.4 ensures that (2.32) has a unique solution. *i.e.*, $\bar{V}_i = \underline{V}_i$, $0 \leq i \leq M$. In view of Theorem 2.6.2(ii) and (iii), we conclude that $\lim\limits_{n\to\infty} U_{i,n} = \bar{V}_i = \underline{V}_i$.

2.7 A special type of nonlinearity

In this section, we study the following nonlinear nonlocal M-V-D with nonlinear nonlocal Robin boundary conditions

$$\begin{cases} u_t(x,t) + u_x(x,t) + d(x, s(t))u(x,t) = u_{xx}(x,t), \ x \in D, \ t > 0, \\ u(0,t) - u_x(0,t) = g\left(\int_0^{a_\dagger} \bar{B}_1(y)u(y,t)dy\right), \ t > 0, \\ u(a_\dagger, t) + u_x(a_\dagger, t) = g\left(\int_0^{a_\dagger} \bar{B}_2(y)u(y,t)dy\right), \ t > 0, \\ u(x,0) = u_0(x), \ x \in \bar{D}, \\ s(t) = \int_0^{a_\dagger} \psi(x)u(x,t)dx, \ t > 0. \end{cases} \tag{2.41}$$

The functions d, $\bar{B}_1$, $\bar{B}_2$, ψ, g, u_0 are assumed to be non-negative and continuous. Notice that with the choice

$$\begin{cases} B_1(x,s) = \dfrac{g(s)}{s}\bar{B}_1(x), \ \psi_1 = \bar{B}_1, \\ B_2(x,s) = \dfrac{g(s)}{s}\bar{B}_2(x), \ \psi_2 = \bar{B}_2, \end{cases}$$

system (2.1) reduces to (2.41). In fact, this choice of B_ν has singularity at $s = 0$, for $\nu = 1, 2$. Notwithstanding the presence of the singularities, we study the existence, uniqueness and the long time behavior of approximate solutions to (2.41) analogous to the earlier sections.

As before, the steady state equation corresponding to (2.41) is given by

$$\begin{cases} v_x(x) + d(x,p)v(x) = v_{xx}(x), \ x \in D, \\ v(0) - v_x(0) = g\left(\int_0^{a_\dagger} \bar{B}_1(y)v(y)dy\right), \\ v(a_\dagger) + v_x(a_\dagger) = g\left(\int_0^{a_\dagger} \bar{B}_2(y)v(y)dy\right), \\ p = \int_0^{a_\dagger} \psi(x)v(x)dx. \end{cases} \tag{2.42}$$

2.7.1 Numerical scheme

Let $\bar{\boldsymbol{B}}_\nu = (\bar{B}_\nu(x_0), \bar{B}_\nu(x_1), \ldots, \bar{B}_\nu(x_M))$, $\nu = 1, 2$. Using the finite difference operators given in (2.4), we propose the following implicit scheme to find approximate solutions to (2.41):

$$\begin{cases} \mathcal{L}[U_{i,n}] = U_{i,n-1} - kd_i(I(\boldsymbol{\Psi}\boldsymbol{U}_n))U_{i,n}, \ (i,n) \in \Lambda, \\ \mathcal{BC}_1[U_{0,n}] = g\left(I(\bar{\boldsymbol{B}}_1\boldsymbol{U}_n)\right), \ n \in \mathbb{N}, \\ \mathcal{BC}_2[U_{M,n}] = g\left(I(\bar{\boldsymbol{B}}_2\boldsymbol{U}_n)\right), \ n \in \mathbb{N}, \\ U_{i,0} = \Phi_i, \ 0 \le i \le M. \end{cases} \tag{2.43}$$

We now introduce the notion of upper and lower solutions to (2.43).

Definition 2.7.1 A vector $(\tilde{U}_{i,n})$ is called an upper solution to (2.43) if

$$\begin{cases} \mathcal{L}[\tilde{U}_{i,n}] \ge \tilde{U}_{i,n-1} - kd_i(I(\boldsymbol{\Psi}\tilde{\boldsymbol{U}}_n))\tilde{U}_{i,n}, \ (i,n) \in \Lambda, \\ \mathcal{BC}_1[\tilde{U}_{0,n}] \ge g\left(I(\bar{\boldsymbol{B}}_1\tilde{\boldsymbol{U}}_n)\right), \ n \in \mathbb{N}, \\ \mathcal{BC}_2[\tilde{U}_{M,n}] \ge g\left(I(\bar{\boldsymbol{B}}_2\tilde{\boldsymbol{U}}_n)\right), \ n \in \mathbb{N}, \\ \tilde{U}_{i,0} \ge \Phi_i, \ 0 \le i \le M. \end{cases} \tag{2.44}$$

Similarly, $(\hat{U}_{i,n})$ is called a lower solution to (2.43) if it satisfies inequalities of (2.44) in the reversed order.

Throughout this section, we make the following hypotheses:

$$g \text{ is a } C^1 \text{ such that } g' > 0 \text{ and } g(Ax) \le x, \tag{2.45}$$

where $A = \max\{\sum_{i=0}^{M} q_i\bar{B}_{1,i}, \sum_{i=0}^{M} q_i\bar{B}_{2,i}\}$. We prove the existence result in the following two cases: (i) $s \mapsto d(.,s)$ is decreasing, (ii) $s \mapsto d(.,s)$ is increasing. We provide an outline of the existence result in case (i) and the other case can be delt with a similar technique.

To that end, using the notation introduced in (2.11), scheme (2.43) can be written as

$$\begin{cases} L[U_{i,n}] = U_{i,n-1} + k\left(-d_i(I(\boldsymbol{\Psi}\boldsymbol{U}_n))U_{i,n} + \xi\hat{U}_{i,n}I(\boldsymbol{\Psi}\boldsymbol{U}_n) + \beta U_{i,n}\right), (i,n) \in \Lambda, \\ \mathcal{BC}_1[U_{0,n}] = g\left(I(\bar{\boldsymbol{B}}_1\boldsymbol{U}_n)\right), \ n \in \mathbb{N}, \\ \mathcal{BC}_2[U_{M,n}] = g\left(I(\bar{\boldsymbol{B}}_2\boldsymbol{U}_n)\right), \ n \in \mathbb{N}, \\ U_{i,0} = \Phi_i, \ 0 \le i \le M. \end{cases} \tag{2.46}$$

For $(i,n)\in\bar{\Lambda}$, we construct a sequence $\{U^m_{i,n}\}$ of approximations to a solution $\{U_{i,n}\}$ to (2.46) as follows. Let $\{U^m_{i,n}\}$ be the solution to

$$\begin{cases} L[U^m_{i,n}] = U^{m-1}_{i,n-1} + k\left(-d_i(I(\boldsymbol{\Psi}\boldsymbol{U}^{m-1}_n))U^{m-1}_{i,n} + \xi\hat{U}_{i,n}I(\boldsymbol{\Psi}\boldsymbol{U}^{m-1}_n) + \beta U^{m-1}_{i,n}\right), \\ \qquad\qquad\qquad (i,n)\in\Lambda,\ m\in\mathbb{N}, \\ \mathcal{BC}_1[U^m_{0,n}] = g\left(I(\bar{\boldsymbol{B}}_1\boldsymbol{U}^{m-1}_n)\right),\ n\in\mathbb{N},\ m\in\mathbb{N}, \\ \mathcal{BC}_2[U^m_{M,n}] = g\left(I(\bar{\boldsymbol{B}}_2\boldsymbol{U}^{m-1}_n)\right),\ n\in\mathbb{N},\ m\in\mathbb{N}, \\ U^m_{i,0} = \Phi_i,\ 0\le i\le M,\ m\in\mathbb{N}. \end{cases} \tag{2.47}$$

If $U^0_{i,n}$ is equal to an upper solution (lower solution, resp.) to (2.43), then the solution to (2.47) is denoted by $\bar{U}^m_{i,n}$ ($\underline{U}^m_{i,n}$, resp.).
Observe that, in view of hypothesis (2.45), we get that $\tilde{U}_{i,n}\equiv\|\Phi\|_\infty$, $\hat{U}_{i,n}\equiv 0$ is a pair of ordered upper and lower solution to (2.43). We are ready to state an existence result whose proof is analogous to that of Theorem 2.3.2.

Theorem 2.7.2 (Existence) *Let $\hat{U}_{i,n}$, and $\tilde{U}_{i,n}$ be a pair of ordered lower and upper solutions to equation (2.43), respectively. Assume (2.45), $s\mapsto d(.,s)$ is a decreasing function and $-k\sigma_1<1$. Then the following hold:*
(i) For every fixed $(i,n)\in\bar{\Lambda}$, both $\{\bar{U}^m_{i,n}\}$, $\{\underline{U}^m_{i,n}\}$ are monotone sequences. Moreover, we have

$$\hat{U}_{i,n}\le\underline{U}^m_{i,n}\le\underline{U}^{m+1}_{i,n}\le\underline{U}_{i,n}\le\bar{U}_{i,n}\le\bar{U}^{m+1}_{i,n}\le\bar{U}^m_{i,n}\le\tilde{U}_{i,n},\ (i,n)\in\bar{\Lambda},$$

for every $m\in\mathbb{N}\cup\{0\}$, where $\lim_{m\to\infty}\bar{U}^m_{i,n}=\bar{U}_{i,n}$, $\lim_{m\to\infty}\underline{U}^m_{i,n}=\underline{U}_{i,n}$.
(ii) Both $\bar{U}_{i,n}$ and $\underline{U}_{i,n}$ are solutions to (2.43).
(iii) If $U^*_{i,n}$ is another solution to (2.43) in $\langle\hat{U}_{i,n},\tilde{U}_{i,n}\rangle$, then $\underline{U}_{i,n}\le U^*_{i,n}\le\bar{U}_{i,n}$ on $\bar{\Lambda}$.

When $s\mapsto d(.,s)$ is an increasing function, using the notation in (2.25), one can write (2.43) as

$$\begin{cases} L_*[U_{i,n}] = U_{i,n-1} + k\left(-d_i(I(\boldsymbol{\Psi}\boldsymbol{U}_n))U_{i,n} + \xi\tilde{U}_{i,n}I(\boldsymbol{\Psi}\boldsymbol{U}_n) + \beta U_{i,n}\right), (i,n)\in\Lambda, \\ \mathcal{BC}_1[U_{0,n}] = g\left(I(\bar{\boldsymbol{B}}_1\boldsymbol{U}_n)\right),\ n\in\mathbb{N}, \\ \mathcal{BC}_2[U_{M,n}] = g\left(I(\bar{\boldsymbol{B}}_2\boldsymbol{U}_n)\right),\ n\in\mathbb{N}, \\ U_{i,0} = \Phi_i,\ 0\le i\le M. \end{cases} \tag{2.48}$$

As before, for $(i,n)\in\bar{\Lambda}$, we construct a sequence $\{U^m_{i,n}\}$ of approximations to a solution $\{U_{i,n}\}$ to (2.48). The sequence $(i,n) \in \bar{\Lambda}$ is monotonic and its limit turns out to be the solution to (2.43).

Before stating the uniqueness result, we introduce the following notation:

$$\delta_* = \max\left\{g'(\zeta^\nu) : \zeta^\nu \in \left(I(\bar{\boldsymbol{B}}_\nu \hat{\boldsymbol{U}}_{\boldsymbol{n}}), I(\bar{\boldsymbol{B}}_\nu \tilde{\boldsymbol{U}}_{\boldsymbol{n}})\right), \nu = 1, 2\right\}.$$

Now we are ready to state the uniqueness theorem.

Theorem 2.7.3 (Uniqueness) *Assume one of the following conditions:*
(i) $s \mapsto d(.,s)$ *is decreasing,* $\max\{-k\sigma_3, A\delta_*\} < 1$,
(ii) $s \mapsto d(.,s)$ *is increasing,* $\max\{-k\sigma_4, A\delta_*\} < 1$.
Then equation (2.43) has a unique solution in $\langle \hat{U}_{i,n}, \tilde{U}_{i,n} \rangle$.

We now recall the finite difference operator given in (2.31) and propose the following implicit scheme for (2.42) which is immediate from (2.30)

$$\begin{cases} \mathcal{L}^s[V_i] = -d_i(I(\boldsymbol{\Psi V}))V_i, \ 1 \le i \le M-1, \\ \mathcal{BC}_1^s[V_0] = g\left(I(\bar{\boldsymbol{B}}_1 \boldsymbol{V})\right), \\ \mathcal{BC}_2^s[V_M] = g\left(I(\bar{\boldsymbol{B}}_2 \boldsymbol{V})\right). \end{cases} \tag{2.49}$$

Using the notion of upper and lower solution to (2.49), we can get the similar results as in Section 2.5. We conclude this section with the following result concerning asymptotic behavior.

Theorem 2.7.4 (Asymptotic behavior) *Let* $\tilde{V}_i$ *and* $\hat{V}_i$ *be a pair of ordered upper and lower solutions to (2.49), respectively. Let the hypothesis of Theorem 2.7.3 hold. Assume that* $\hat{U}_{i,n} \le \hat{V}_i \le \tilde{V}_i \le \tilde{U}_{i,n}$. *Let* $\bar{U}_{i,n}$ *and* $\underline{U}_{i,n}$ *be solutions to (2.43) corresponding to* $\Phi_i = \tilde{V}_i$ *and* $\Phi_i = \hat{V}_i$, *respectively. Then the following conclusions hold:*
(i) $\bar{U}_{i,n}$ *is decreasing and* $\underline{U}_{i,n}$ *is increasing in* n. *Moreover, we have* $\bar{U}_{i,n} \ge \underline{U}_{i,n}$ *on* $\bar{\Lambda}$.
(ii) If $U_{i,n}$ *is a solution to (2.43) with initial data* $\Phi_i \in \langle \hat{V}_i, \tilde{V}_i \rangle$, *then* $\underline{U}_{i,n} \le U_{i,n} \le \bar{U}_{i,n}$.
(iii) For each $0 \le i \le M$, *set* $\lim\limits_{n\to\infty} \bar{U}_{i,n} = \bar{V}_i$, $\lim\limits_{n\to\infty} \underline{U}_{i,n} = \underline{V}_i$. *Then* $\bar{V}_i$ *and* $\underline{V}_i$ *are the maximal and minimal solutions to (2.49) in* $\langle \hat{V}_i, \tilde{V}_i \rangle$, *respectively.*
(iv) Let $\Phi_i \in \langle \hat{V}_i, \tilde{V}_i \rangle$. *Assume that* $\mu_3 > 0$, *and* $\mu_4 > 0$ *whenever* $\frac{\partial d}{\partial s} \ge 0$, *and* $\frac{\partial d}{\partial s} < 0$, *respectively. Then we have* $\lim\limits_{n\to\infty} U_{i,n} = \bar{V}_i = \underline{V}_i$.

2.8 Numerical simulations

In this section, we present four examples in which the numerical solutions to time dependent problem (2.5) and corresponding steady state problem (2.32) are computed to validate the results in the earlier sections. In Examples 2.8.1–2.8.2, we demonstrate the facts that for each i, n $(\bar{U}^m_{i,n})$ is decreasing, $(\underline{U}^m_{i,n})$ is increasing and the approximate $U_{i,n}$ tends to V_i for each i, as n tends to ∞. If E_h denotes the magnitude of the error with step size h, then the experimental order of convergence can be computed using the standard formula

$$\text{order} = \frac{\log(E_h) - \log(E_{\frac{h}{2}})}{\log 2}.$$

Moreover, to demonstrate the advantage of the proposed numerical scheme over a standard implicit difference scheme, we present two examples in which analytical solutions are known explicitly. In these examples, we use the same notation that is introduced in Section 2.2. In particular, we compare our scheme with the following scheme (backward difference approximation for u_t and centered the in space discretization for u_x, and u_{xx}):

$$\begin{cases} (1+2r)X_{i,n} - bX_{i+1,n} - cX_{i-1,n} = \Big(1 - kd_i(I(\boldsymbol{\Psi}\boldsymbol{X}_{n-1}))\Big)X_{i,n-1}, \ (i,n) \in \Lambda, \\ \left(1+\frac{1}{h}\right)X_{0,n} - \frac{1}{h}X_{1,n} = I(\boldsymbol{B}_1(I(\boldsymbol{\Psi}_1\boldsymbol{X}_{n-1}))\boldsymbol{X}_{n-1}), \ n \in \mathbb{N}, \\ \left(1+\frac{1}{h}\right)X_{M,n} - \frac{1}{h}X_{M-1,n} = I(\boldsymbol{B}_2(I(\boldsymbol{\Psi}_2\boldsymbol{X}_{n-1}))\boldsymbol{X}_{n-1}), \ n \in \mathbb{N}, \\ X_{i,0} = \Phi_i, \ 0 \le i \le M, \end{cases} \tag{2.50}$$

where $X_{i,n}$ is a numerical approximation to u at the grid point (x_i, t^n).
All computations have been performed using Matlab 8.5. In all the examples, we have taken $a_\dagger = 1$ and $\psi(x) = \psi_1(x) = \psi_2(x) \equiv 1$. Moreover, in the first two examples we have taken $h = 0.01$, $k = 0.5 \times 10^{-4}$, and $u_0(x) = \frac{e^{-x}}{2}$, $x \in [0,1]$.

Example 2.8.1

In order to test our numerical scheme, we assume that d, B_1 and B_2 are given by

$$d(x,s) = (x+1) - \tfrac{s}{10},\ B_1(x,s) = \tfrac{x+s}{10},\ \ B_2(x,s) = 0,\ \ x \in (0,1),\ \ s \ge 0.$$

Taking into account of the definitions of upper and lower solutions to (2.5), we choose $\tilde{U}_{i,n} \equiv 1$ and $\hat{U} \equiv 0$. It is easy to verify that $\tilde{V}_i \equiv 1$ and $\hat{V}_i \equiv 0$ are upper and lower solutions to (2.32), respectively. On the other hand, one can easily check that d and B_ν satisfy hypotheses of Theorems 2.4.1 and 2.6.2. Hence (2.5) has a unique numerical solution. Note that, for the given set of functions, $v(x) \equiv 0$ is a unique solution to (2.32).

In Figure 2.1 (Left), we show the upper and lower solutions $\bar{U}^m_{i,n}$ and $\underline{U}^m_{i,n}$,

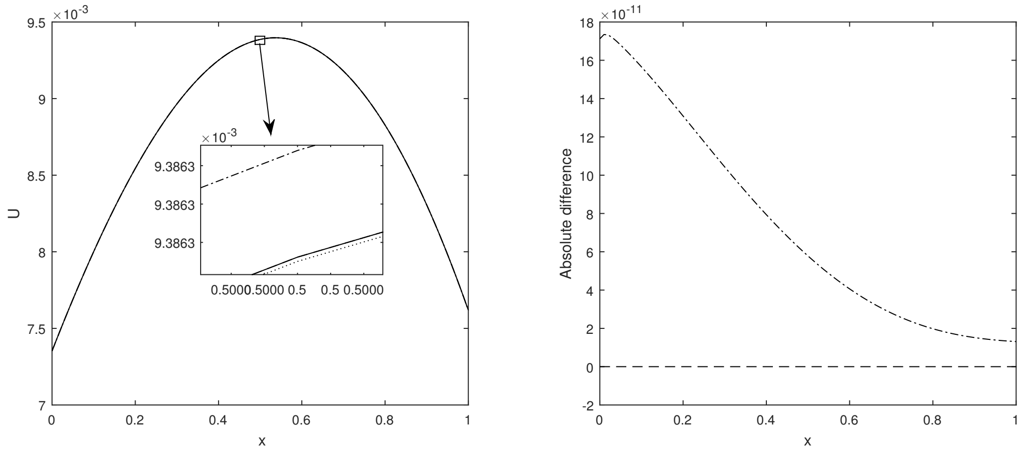

Figure 2.1: Approximate solutions to (2.1) with $d(x,s)$, $B_1(x,s)$, $B_2(x,s)$ given in Example 2.8.1; Left: $\bar{U}^3(x,1)$ (dash-dot line), $\bar{U}^4(x,1)$ (dashed line), $\underline{U}^3(x,1)$ (dotted line), $\underline{U}^4(x,1)$ (solid line) for $0 \leq x \leq 1$; Right: $|\bar{U}^3(x,1) - \underline{U}^3(x,1)|$ (dash-dot line) and $|\bar{U}^4(x,1) - \underline{U}^4(x,1)|$ (dashed line).

respectively, to (2.5) for $m = 3,\ 4$, and $t = 1$. From this figure, it is evident that for every fixed (i,n), $\bar{U}^m_{i,n}$ is decreasing with m and $\underline{U}^m_{i,n}$ is increasing with m. This phenomenon re-validates the results that are proved in Theorem 2.3.2. In Figure 2.1 (Right), we plot the absolute difference between $\bar{U}^m_{i,n}$ and $\underline{U}^m_{i,n}$ at $t = 1$, for $m = 3$ and 4. From this figure, one can observe that $\bar{U}^m_{i,n}$, $\underline{U}^m_{i,n}$ are very close to each other, and the sequence $(\bar{U}^m_{i,n})$ indeed converges to a unique solution $U_{i,n}$ as mentioned in Theorem 2.4.1. In the next figure, we turn towards the long time behavior of the numerical solution.

As the solution $U_{i,n}$ to (2.5) lies in the interval $(\bar{U}^m_{i,n}, \underline{U}^m_{i,n})$, if the length of the interval is too small, then without loss of generality, we take $U_{i,n}$ to be $\bar{U}^m_{i,n}$. In Figure 2.2, we present the numerical solutions to (2.5) at $t = 2, 3$ and the solution to the steady state problem. In particular, we have taken $U_{i,n} = \bar{U}^4_{i,n}$ at $t = 2$ and 3. Since the numerical solution V_i is identically 0, Figure 2.2 can be used for the error analysis also. From Figure 2.2, it is evident that $(U_{i,n})$ is very close to

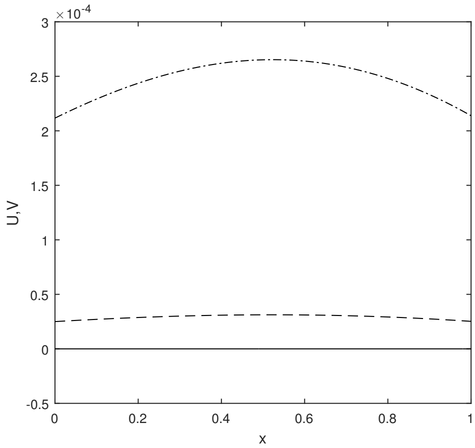

Figure 2.2: Approximate solutions to (2.5) and (2.32) with $d(x,s)$, $B_1(x,s)$, $B_2(x,s)$ given in Example 2.8.1; $U(x,2)$ (dash-dot line), $U(x,3)$ (dashed line), $V(x)$ (solid line) for $0 \le x \le 1$.

the trivial steady state (V_i) for sufficiently large n (it indeed converges to V_i), as demonstrated theoretically in Theorem 2.6.2.

Example 2.8.2

In this example, we validate the results presented in Section 2.7 when the special type of nonlinearity described in that section is considered. For the numerical simulations, we take d, g, $\bar{B}_1$ and $\bar{B}_2$ as

$$d(x,s) = (x+1) + \tfrac{s^2}{100},\; g(s) = \tfrac{\sqrt{s+1}}{2},\; \bar{B}_1(x) = \tfrac{1}{2},$$
$$\bar{B}_2(x) = e^{-x},\;\; x \in (0,1),\;\; x \in (0,1),\;\; s \ge 0.$$

In this example, we choose $\tilde{U}_{i,n} \equiv 1$ and $\hat{U} \equiv 0$ as the upper and lower solutions to (2.43) respectively. Furthermore, $\tilde{V}_i \equiv 1$ and $\hat{V}_i \equiv 0$ are chosen to be the upper and lower solutions to (2.49). One can easily check that d and g satisfy the hypotheses of Theorem 2.7.3. Hence (2.43) has a unique numerical solution.

In Figure 2.3 (Left), we present approximate solutions to (2.43) at $t = 1, 2$ and the solution to the steady state problem. Moreover, in Figure 2.3 (Right) the absolute errors $|\bar{U}_{i,n} - \bar{V}_i|$ are displayed at $t = 1$ and 2. From the these graphs, it is clear that $(U_{i,n})$ is very close to the nontrivial steady state (V_i) whenever n is large, as mentioned in Theorem 2.7.4.

Example 2.8.3

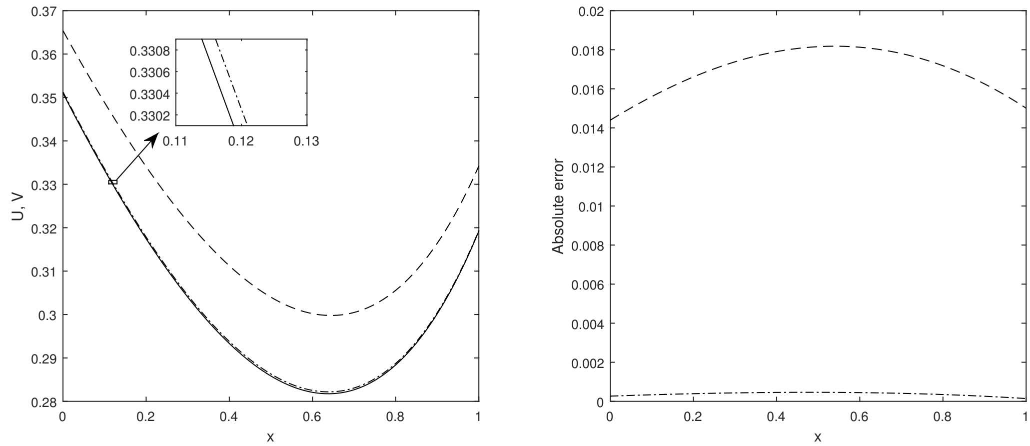

Figure 2.3: Approximate solutions to (2.43) and (2.49) with $d(x,s)$, $g(s)$, $\bar{B}_1(x)$, $\bar{B}_2(x)$ given in Example 2.8.2; Left: $U(x,1)$ (dashed line), $U(x,2)$ (dash-dot line), $V(x)$ (solid line) for $0 \le x \le 1$; Right: $|U(x,1) - V(x)|$ (dashed line) and $|U(x,2) - V(x)|$ (dash-dot line).

In this example, we choose the vital rates d, B_1, B_2 and the initial data u_0 such that the solution to (2.1) is known in the closed form. In particular, let

$$d(x,s) = 1 + \frac{2x-1}{4} + \frac{(2x-1)^2}{16} - \frac{s}{2\int_0^1 e^{-\frac{(2x-1)^2}{16}}dx}, \; u_0(x) = e^{-\frac{(2x-1)^2}{16}},$$

$$B_1(x,s) = B_2(x,s) = \frac{3e^{-1/16}}{4\int_0^1 e^{-\frac{(2x-1)^2}{16}}dx}, \;\; x \in (0,1), \;\; s \ge 0.$$

Now it is easy to verify that $u(x,t) = \frac{2}{1+4e^t}e^{-\frac{(2x-1)^2}{16}}$ is the solution to (2.1). On the other hand, to compute approximate solutions using (2.3), we first choose $\tilde{U}_{i,n} = e^{-\frac{(2ih-1)^2}{16}}$ and $\hat{U} \equiv 0$ as an upper solution and a lower solution to (2.5), respectively. Moreover, one can easily check that d and B_ν satisfy hypotheses of Theorem 2.4.1. Hence (2.5) has a unique numerical solution.

We now compare the numerical solutions and the exact solution at $t = 1$. The plots of $\bar{U}^2_{i,n}$ and $\underline{U}^2_{i,n}$ for $0 \le x \le 1$, $t = 1$, are presented in Figure 2.4(a). In Figure 2.4(b), the absolute difference $|\bar{U}^2_{i,n} - \underline{U}^2_{i,n}|$ is shown. When $m = 3$, the graphs of $\bar{U}^3_{i,n}$ and $\underline{U}^3_{i,n}$, for $0 \le x \le 1$ at $t = 1$ are depicted in Figure 2.4(c) and the absolute difference $|\bar{U}^3_{i,n} - \underline{U}^3_{i,n}|$ at $t = 1$ is presented in Figure 2.4 (d). From these numerical experiments, in particular from Figures 2.4(b), and 2.4(d), it is evident that the approximate solutions $\bar{U}^m_{i,n}$ and $\underline{U}^m_{i,n}$ are very close to each other as m grows. In this case $m = 3$ gives a good approximation. This verifies the conclusions of Theorem 2.3.2.

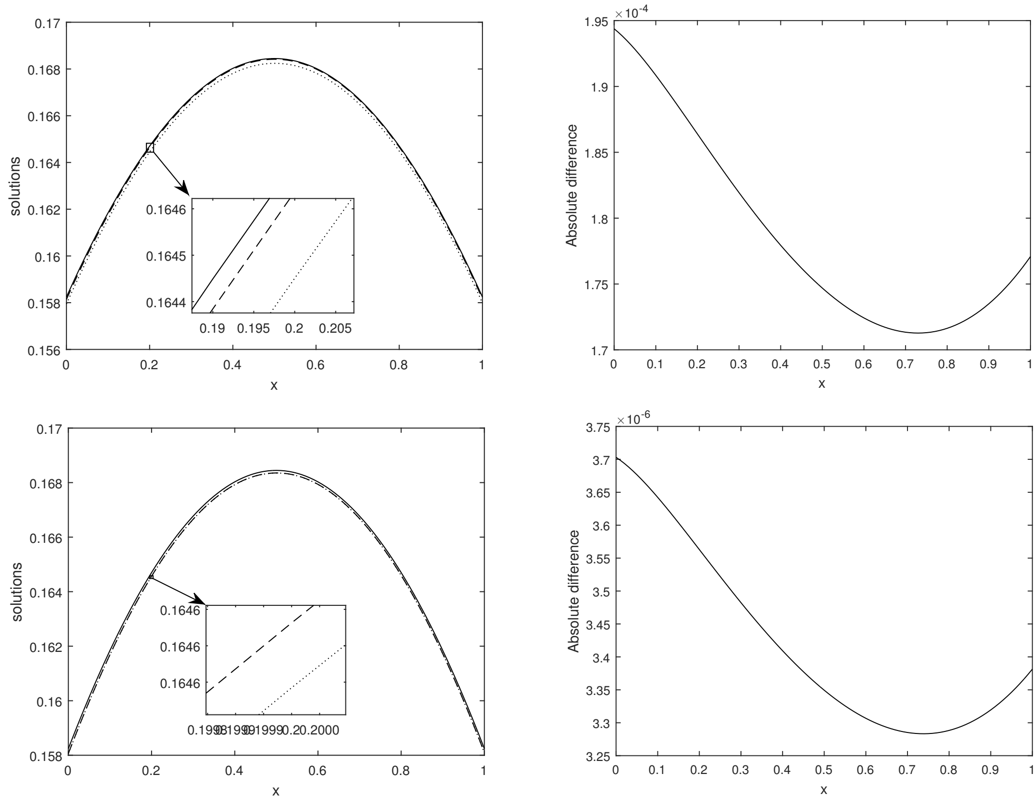

Figure 2.4: The exact solution to (2.1) and approximate solutions to (2.5) with $d(x,s)$, $B_1(x,s)$, $B_2(x,s)$ given in Example 2.8.3 with $h = 0.01$, $k = 0.01$; (a): $u(x,1)$ (solid line), $\bar{U}^2_{i,n}$ (dashed line) and $\underline{U}^2_{i,n}$ (dotted line); (b): $|\bar{U}^2_{i,n} - \underline{U}^2_{i,n}|$ at $t = 1$; (c): $u(x,1)$ (solid line), $\bar{U}^3_{i,n}$ (dashed line) and $\underline{U}^5_{i,n}$ (dotted line); (d): $|\bar{U}^3_{i,n} - \underline{U}^3_{i,n}|$ at $t = 1$.

Since $U_{i,n}$ lies in the interval $(\underline{U}^3_{i,n}, \bar{U}^3_{i,n})$ and the length of the interval is sufficiently small, we take the numerical solution at $t = 1$ to be $\bar{U}^3_{i,n}$. In Figure 2.5, we discuss convergence of numerical scheme (2.5). In particular, we present the exact solution u and the numerical solutions $U_{i,n}$ to (2.5) at $t = 1$ with $h = 0.01$, $k = 0.01$ in Figure 2.5(a). We show the absolute difference $|u(\cdot,1) - U_{i,n}|$ at $t = 1$ in Figure 2.5(b) for the same values of h and k. At $t = 1$, we have computed $U_{i,n}$ with smaller step sizes. In particular, we show $U_{i,n}$ with $h = 0.1 \times 10^{-2}$, $k = 0.1 \times 10^{-3}$, and u in Figure 2.5(c), and the corresponding the absolute difference $|u(\cdot,1) - U_{i,n}|$ in Figure 2.5(d). These numerical simulations show that the numerical solution U indeed converges to the exact solution u at $t = 1$ as $h, k \to 0$.

In Table 2.1, we display the magnitude of the discretization error and the experi-

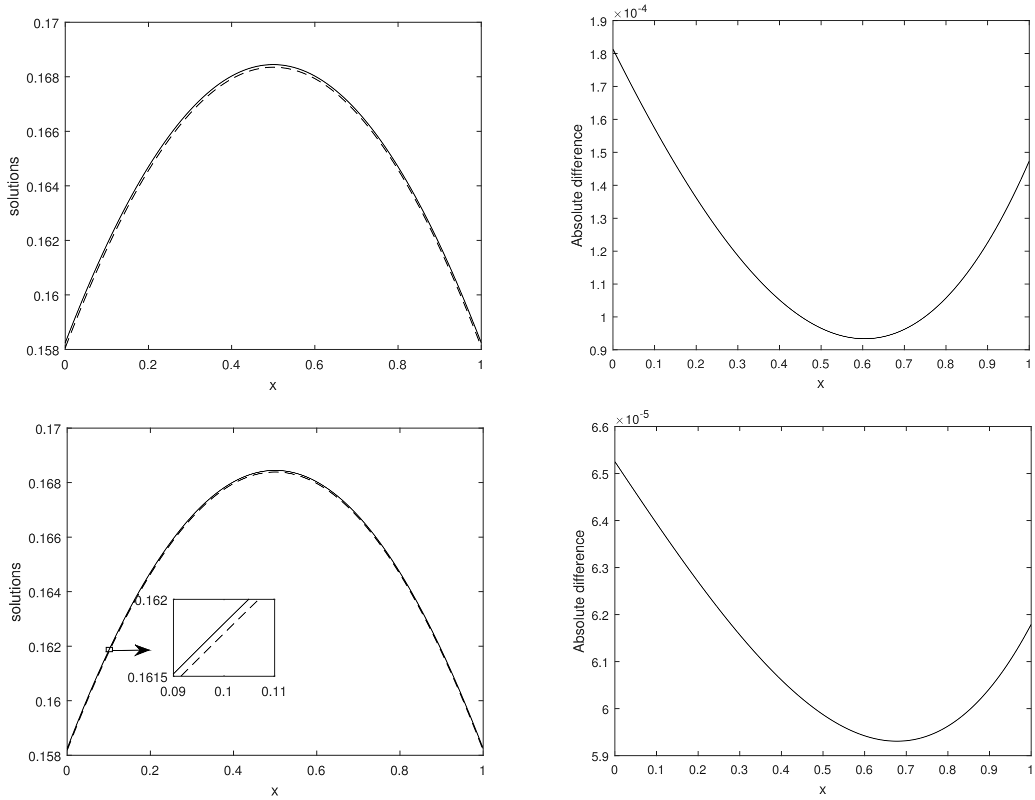

Figure 2.5: The exact solution to (2.1) and approximate solutions to (2.5) with d, B_1, B_2 given in Example 2.8.3; (a): $u(x,1)$ (solid line) and $U_{i,n}$ (dashed line) at $t=1$ with $h=0.01,\ k=0.01$; (b): $|u(x,1)-U_{i,n}|$ (solid line) at $t=1$ with $h=0.01,\ k=0.01$; (c): $u(x,1)$ (solid line) and $U_{i,n}$ (dashed line), at $t=1$ with $h=0.1\times10^{-2},\ k=0.1\times10^{-3}$; (d): $|u(x,1)-U_{i,n}|$ (solid line) at $t=1$ with $h=0.1\times10^{-2},\ k=0.1\times10^{-3}$.

mental order of convergence for different choices of h and k. In the third column, we present the maximum absolute error at $t=1$, and in the fourth column the experimental order of convergence is shown. From Table 2.1, we can observe that the order of convergence of the proposed numerical scheme (2.5) is one.

Our next objective is to demonstrate the advantage of scheme (2.3) over (2.50). To this end, in Table 2.2, we show the absolute error and the time required to compute approximate solutions using (the computational time) (2.3) and (2.50). In particular, we present the equation number of the scheme and the corresponding absolute error in the first and fourth column of Table 2.2 for different choices of $h,\ k$, respectively, at $t=1$. Moreover, we display the corresponding computational time in the fifth column. From the first two rows of Table 2.2, it is clear that at $t=1$ when $h=0.05,\ k=0.1$ scheme (2.3) gives better approximation

h	k	$\max\limits_{0\le i\le M}\{\lvert U_{i,N}-u(x_i,t^N)\rvert\}$	order
0.1	0.01	0.006939	0.9888
0.05	0.0025	0.003496	0.9941
0.02	0.0004	0.001405	0.9977
0.01	0.0001	0.000703	0.9988

Table 2.1: Magnitude of the discretization error and the experimental order of convergence for different choices of h and k at $t = 1$ with d, B_1, B_2 given in Example 2.8.3

Scheme	h	k	$\max\limits_{0\le i\le M}\{\lvert U_{i,N}-u(x_i,t^N)\rvert\}$	Computational time (sec)
(2.3)	0.05	0.1	1.35×10^{-3}	0.113
(2.50)	0.05	0.1	1.88×10^{-2}	0.109
(2.50)	0.02	0.1	1.49×10^{-3}	0.150
(2.3)	0.02	0.02	3.81×10^{-4}	0.177
(2.50)	0.02	0.02	3.23×10^{-3}	0.145
(2.50)	0.01	0.005	4.57×10^{-4}	0.295
(2.3)	0.01	0.008	2.87×10^{-4}	0.468
(2.50)	0.01	0.008	1.15×10^{-3}	0.196
(2.50)	0.005	0.004	5.78×10^{-4}	0.522

Table 2.2: The absolute difference between the exact solution and the computed solutions, and the computational time for different choices of h and k at $t = 1$ with d, B_1, B_2 given in Example 2.8.3

than (2.50). In order to get the absolute error close to 1.35×10^{-3} using (2.50), we need to take smaller step sizes. From the third row of Table 2.2, we observe that with $h = 0.02,\ k = 0.1$, semi-implicit (2.50) gives an approximate solution with the absolute error 1.49×10^{-3}. Moreover, the computational time to get an approximate solution with this accuracy using scheme (2.50) is more than that of scheme (2.3). Similarly, with different step sizes, we observe the same phenomena (see Rows 4-9 of Table 2.2). Thus from Table 2.2, we deduce that proposed implicit scheme (2.3) takes less computational time than (2.50) to get the same accuracy. Therefore from these calculations, it is evident that proposed scheme (2.3) is more efficient than standard semi-implicit scheme (2.50).

Example 2.8.4

Let the vital rates d, B_1, B_2 and the initial data u_0 be given by

$$d(x,s) = 1 + \tfrac{2x-1}{4} + \tfrac{(2x-1)^2}{16} - \left(\frac{s}{2\int_0^1 e^{-\frac{(2x-1)^2}{16}}dx}\right)^2,\ u_0(x) = e^{-\frac{(2x-1)^2}{16}},$$

$$B_1(x,s) = B_2(x,s) = \frac{3e^{-1/16}}{4\int_0^1 e^{-\frac{(2x-1)^2}{16}}dx},\ \ x \in (0,1),\ \ s \geq 0.$$

One can easily check that $u(x,t) = \frac{2}{\sqrt{1+24e^{2t}}}e^{-\frac{(2x-1)^2}{16}}$ is the solution to (2.1). In order to compute approximate solutions, we set $\tilde{U}_{i,n} = e^{-\frac{(2ih-1)^2}{16}}$ and $\hat{U} \equiv 0$. Moreover, one can easily verify that d and B_ν satisfy hypotheses of Theorem 2.4.1. Hence (2.5) admits a unique numerical solution.

In Figure 2.6, we compare the numerical solutions to (2.13) at $t = 1$. In particular, the graphs of $\bar{U}^2_{i,n}$ and $\underline{U}^2_{i,n}$ for $0 \leq x \leq 1$ at $t = 1$ are shown in Figure 2.6(a). Moreover, the absolute difference $|\bar{U}^2_{i,n} - \underline{U}^2_{i,n}|$ is shown in Figure 2.6(b). The plots of $\bar{U}^3_{i,n}$ and $\underline{U}^3_{i,n}$, for $0 \leq x \leq 1$ at $t = 1$ are depicted in Figure 2.6(c), and the absolute difference $|\bar{U}^3_{i,n} - \underline{U}^3_{i,n}|$ at $t = 1$ in Figure 2.6 (d). It is clear from Figures 2.6(b), and 2.6(d) that the approximate solutions $\bar{U}^m_{i,n}$ and $\underline{U}^m_{i,n}$ are close to each other as m grows. Therefore in this case, we got a good approximation with $m = 3$. This revalidates the conclusions of Theorem 2.3.2.

Since the length of the interval $(\underline{U}^3_{i,n}, \bar{U}^3_{i,n})$ is too small (see Figure 2.6 (d)), as in the previous example, we take $U_{i,n}$ to be $\bar{U}^3_{i,n}$. In Figure 2.7, we present the exact solution and numerical solutons to (2.1) at time $t = 1$ with different choices of $h,\ k$, which help us to discuss numerical convergence of scheme (2.5). To be more specific, we show the exact solution u and numerical solutions $U_{i,n}$ to (2.5) at $t = 1$ with $h = 0.01,\ \ k = 0.01$ in Figure 2.7(a), and the absolute

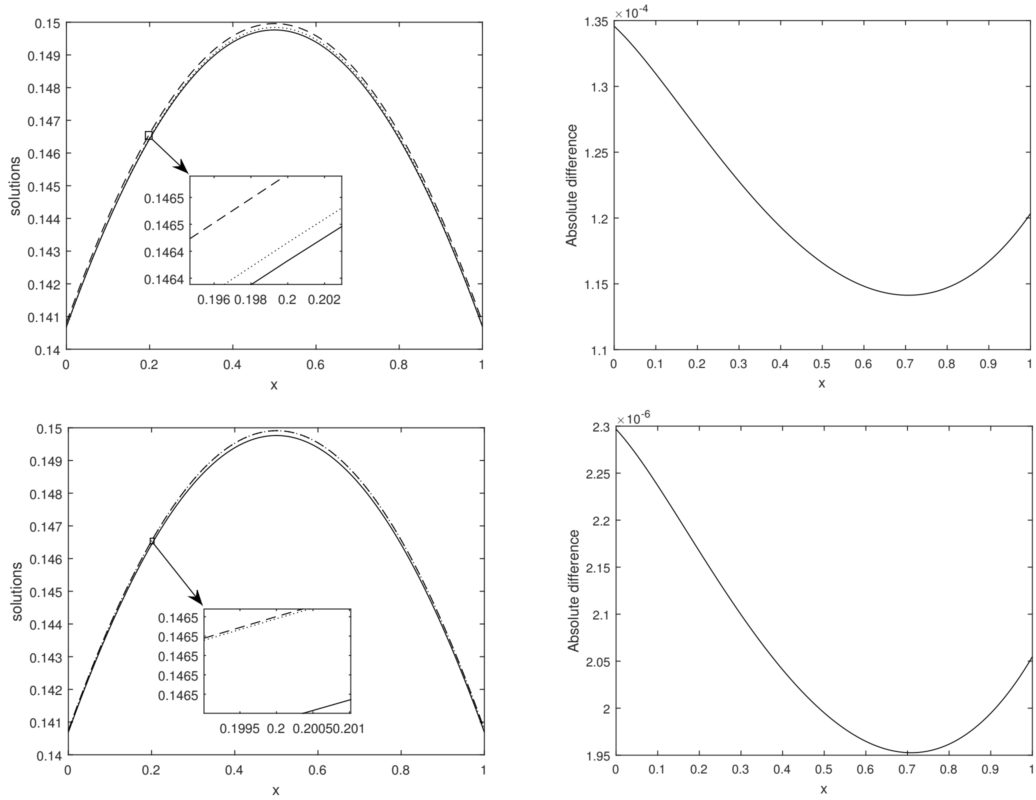

Figure 2.6: The exact solution to (2.1) and approximate solutions to (2.5) with $d(x,s)$, $B_1(x,s)$, $B_2(x,s)$ given in Example 2.8.4 with $h = 0.01$, $k = 0.01$; (a): $u(x,1)$ (solid line), $\bar{U}^2_{i,n}$ (dashed line) and $\underline{U}^3_{i,n}$ (dotted line); (b): $|\bar{U}^2_{i,n} - \underline{U}^2_{i,n}|$ at $t = 1$; (c): $u(x,1)$ (solid line), $\bar{U}^3_{i,n}$ (dashed line) and $\underline{U}^3_{i,n}$ (dotted line); (d): $|\bar{U}^3_{i,n} - \underline{U}^3_{i,n}|$ at $t = 1$.

differences $|u(\cdot,1) - U_{i,n}|$ at $t = 1$ in Figure 2.7(b). We present $U_{i,n}$ which is computed using smaller step sizes, namely, $h = 0.1 \times 10^{-2}$, $k = 0.1 \times 10^{-3}$ in Figure 2.7(c) and the corresponding absolute difference $|u(\cdot,1) - U_{i,n}|$ in Figure 2.7(d). From these numerical simulations, one can observe that the numerical solution U indeed converges to the exact solution u as the step sizes tend to 0. In Table 2.3, we show the computational error and the experimental order of convergence for different choices of h and k. In particular, in the third column, we display the maximum absolute error at $t = 1$ and in the fourth column the experimental order of convergence is shown. From Table 2.3, one can conclude that the experimental order of convergence of the proposed numerical scheme (2.5) is one.

In Table 2.4, we present the absolute difference between the exact solution to

h	k	$\max_{0\le i\le M}\{\lvert U_{i,N}-u(x_i,t^N)\rvert\}$	order
0.1	0.01	0.005847	0.9921
0.05	0.0025	0.002939	0.9857
0.02	0.0004	0.001190	0.9929
0.01	0.0001	0.000598	0.9963

Table 2.3: The magnitude of the error and the order of convergence for different choices of h and k at $t = 1$ with d, B_1, B_2 given in Example 2.8.4

Scheme	h	k	$\max_{0\le i\le M}\{\lvert U_{i,N}-u(x_i,t^N)\rvert\}$	Computational time (sec)
(2.3)	0.05	0.1	3.55×10^{-3}	0.101
(2.50)	0.05	0.1	1.74×10^{-2}	0.094
(2.50)	0.02	0.04	7.09×10^{-3}	0.107
(2.3)	0.02	0.02	2.84×10^{-4}	0.127
(2.50)	0.02	0.02	2.98×10^{-3}	0.118
(2.50)	0.01	0.005	4.46×10^{-4}	0.189
(2.3)	0.01	0.008	7.51×10^{-5}	0.505
(2.50)	0.01	0.008	1.07×10^{-3}	0.174
(2.50)	0.005	0.004	5.38×10^{-4}	0.578

Table 2.4: The absolute difference between the exact solution and the computed solutions, and the computational time for different choices of h and k at $t = 1$ with d, B_1, B_2 given in Example 2.8.4

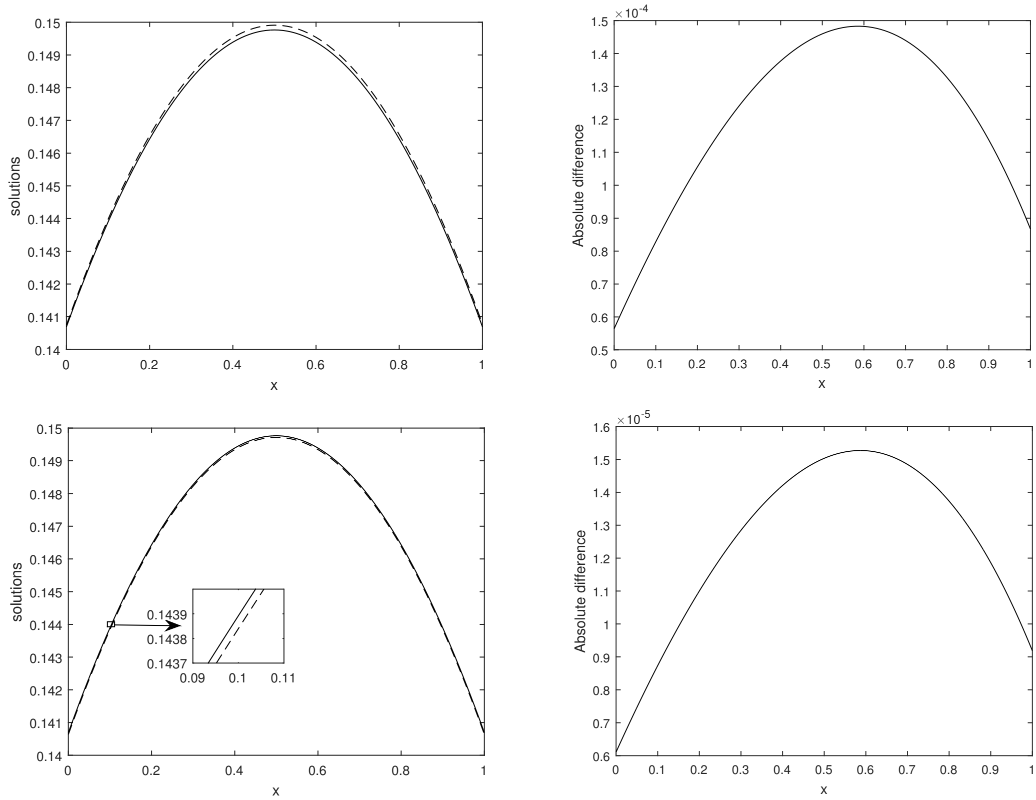

Figure 2.7: The exact solution to (2.1) and the approximate solutions to (2.5) with d, B_1, B_2 given in Example 2.8.4; (a): $u(x, 1)$ (solid line) and $U_{i,n}$ (dashed line) at $t = 1$ with $h = 0.01,\ k = 0.01$; (b): $|u(x, 1) - U_{i,n}|$ (solid line) at $t = 1$ with $h = 0.01,\ k = 0.01$; (c): $u(x, 1)$ (solid line) and $U_{i,n}$ (dashed line), at $t = 1$ with $h = 0.1 \times 10^{-2},\ k = 0.1 \times 10^{-3}$; (d): $|u(x, 1) - U_{i,n}|$ (solid line) at $t = 1$ with $h = 0.1 \times 10^{-2},\ k = 0.1 \times 10^{-3}$.

(2.1) and the approximated solutions that are obtained using (2.3) and (2.50), and the computational time for different values of h, k. As in the previous example, we display the equation number of the scheme, the absolute error and computation time in the first, fourth and fifth columns of Table 2.4, respectively. From the first three rows of Table 2.4, it is easy to observe that scheme (2.50) takes more computational time compared to (2.3) to achieve the same accuracy due to the requirement of smaller step sizes. It is evident from Table 2.4 that proposed scheme (2.3) is more efficient than standard semi-implicit scheme (2.50).

Chapter 3

A numerical scheme for a diffusion equation with nonlocal nonlinear boundary condition

3.1 Introduction

The McKendrick–Von Foerster equation arises naturally in many areas of mathematical biology such as cell proliferation, and demography modeling (see [2, 21, 60, 61, 72, 73, 81]). In particular, the McKendrick–Von Foerster equation is one amongst the important models whenever age structure is a vital feature in the modeling (see [3, 28, 33, 35, 47]). In the recent years, the McKendrick–Von Foerster equation with diffusion (M-V-D) has attracted interest of many engineers as well as mathematicians due to its applications in the modeling of thermoelasticity, neuronal networks etc., (see [18, 19, 36, 37, 57, 58]). The main difficulty in the study of the M-V-D is due to the nonlocal nature of the partial differential equation (PDE) and the boundary condition. The qualitative properties of the M-V-D have been developed by many authors. Though, numerical study of nonlocal equations got considerable focus, relatively less attention was paid to problems with the Robin boundary condition.

In this paper, our objective is to propose and analyze a numerical scheme to find approximate solutions to the following nonlinear diffusion equation

$$\begin{cases} u_t(x,t) + u_x(x,t) + d\big(x, s_1(t)\big)u(x,t) = u_{xx}(x,t), \ x \in (0, a_\dagger), \ t > 0 \\ u(0,t) - u_x(0,t) = \displaystyle\int_0^{a_\dagger} B\big(x, s_2(t)\big)u(x,t)dx, \quad t \geq 0, \\ u(a_\dagger, t) = 0, \ t \geq 0, \\ u(x,0) = u_0(x), \quad x \in (0, a_\dagger), \\ s_\nu(t) = \displaystyle\int_0^{a_\dagger} \psi_\nu(x)u(x,t)dx, \quad t \geq 0, \quad \nu = 1, 2, \end{cases} \tag{3.1}$$

where $a_\dagger > 0$. In the given model, the unknown function $u(x,t)$ represents the age-specific density of individuals of age x at time t. The function d represents the death rate and it depends on x and the environmental factor s_1. Similarly, the fertility rate B depends on the age x and the environmental factor s_2. Both the functions ψ_1 and ψ_2 are called the competition weights. Moreover, the functions d and B are assumed to be non-negative. Without loss of generality, we take the diffusion rate is equal to one.

In [36], the authors considered the M-V-D with nonlinear nonlocal Robin boundary condition and studied the existence and uniqueness of the solution. The authors of [38] proposed a convergent numerical scheme to the M-V-D. On the other hand, the existence of a global solution to the M-V-D in a bounded domain with nonlinear nonlocal Robin boundary condition was proved when $d = d(x)$ in [37]. Moreover, the authors of [13, 14] designed numerical schemes to compute the basic reproduction number R_0 for general continuously structured population models, in particular for models with boundary conditions of Robin type. Regarding the basic reproduction number for diffusion equation (1), taking the approach developed in [11], one can get $R_0 = \frac{2}{1+\sqrt{1+4d_0}} \int_0^\infty B(x,0)\, e^{(1-\sqrt{1+4d_0})\frac{x}{2}}\, dx$ under the assumptions that the mortality rate is a constant d_0 and $a_\dagger = \infty$. Recently in [30], an implicit finite difference scheme was introduced to approximate the solution to the M-V-D in a bounded domain with nonlinear nonlocal Robin boundary condition at both the boundary points. Moreover, the wellposedness and the stability of the numerical scheme were proved using the method of upper and lower solution with the aid of the discrete maximum principle.

The author of [50] presented an upwind scheme for a nonlinear hyperbolic integro-differential equation with nonlocal boundary condition. The analysis was carried out employing the general analytic framework developed in [52, 51, 77]. The notion of 'stability with threshold' and a result due to Stetter (see [79], Lemma 1.2.1) were the most important tools for the analysis.

The above mentioned results inspired us to propose and analyze an explicit finite difference numerical scheme to (3.1). The main difficulty in the analysis of the proposed numerical scheme is due to the nonlinearity and the Robin boundary condition that are presented in (3.1). The objective of this paper is to establish the stability and the convergence of our numerical method. Since the scheme is of the form $U_i^{n+1} = F(U_0^n, \dots, U_M^n)$, where F is a nonlinear function, the standard techniques of proving stability (for instance, the Lax theory etc.) can not be used. Instead, the notion of nonlinear stability (with threshold) is used to arrive at the convergence result.

This chapter is organized as follows. In Section 3.2, we present a finite difference scheme and define the required norms to use the general discretization framework. Moreover, we introduce the notion of stability with h-dependent thresholds. We prove consistency, stability and convergence results in Section 3.3. In Section 3.4, numerical schemes to (3.1) with other types of boundary conditions are discussed. Finally, numerical examples are provided in Section 3.5 to justify the convergence results that are proved.

3.2 The numerical scheme

Let h, k be the spatial and temporal step sizes. Denote by (x_i, t^n) a typical grid point, where $x_i = ih$, and $t^n = nk$. Moreover, we fix $T > 0$, assume that $a_\dagger = 2(M' + 3)h$ for some $M' \in \mathbb{N}$ and $T = Nk$ for some $N \in \mathbb{N}$. To simplify the notations, we write $M = 2(M' + 3)$. For every grid point (x_i, t^n), we denote the numerical solution by U_i^n, and set

$\Psi_{\nu,i} = \psi_\nu(x_i)$, $\boldsymbol{\Psi}_\nu = (\Psi_{\nu,1}, \Psi_{\nu,2}, \dots, \Psi_{\nu,M-1})$, $\nu = 1, 2$,

$\boldsymbol{B}(\cdot) = \big(B(x_1, \cdot), B(x_2, \cdot), \dots, B(x_{M-1}, \cdot)\big)$,

$\boldsymbol{d}(\cdot) = \big(d(x_1, \cdot), d(x_2, \cdot), \dots, d(x_{M-1}, \cdot)\big)$,

$\boldsymbol{U}^n = (U_1^n, U_2^n, \dots, U_{M-1}^n)$.

To approximate the integrals in (3.1), we use the following quadrature rule which is a combination of the composite Simpson–$\frac{1}{3}$ and Minle's rules. For

$\boldsymbol{V} = (V_1, \dots, V_{M-1}) \in \mathbb{R}^{M-1}$, we define the quadrature formula

$$\mathcal{Q}_h(\boldsymbol{V}) = \frac{4h}{3}(2V_1 - V_2 + 2V_3) + \frac{h}{3}\sum_{i=2}^{M'}(V_{2i} + 4V_{2i+1} + V_{2i+2}) + \frac{4h}{3}(2V_{2M'+3} - V_{2M'+4} + 2V_{2M'+5}).$$

If $\boldsymbol{V} = (V_1, \dots, V_{M-1})$, $\boldsymbol{W} = (W_1, \dots, W_{M-1})$ are in $\mathbb{R}^{M-1}$, then $\boldsymbol{V} \boldsymbol{\cdot} \boldsymbol{W}$ denotes the vector in $\mathbb{R}^{M-1}$ which is obtained by the element wise multiplication of $\boldsymbol{V}$ and $\boldsymbol{W}$, i.e.,

$$\boldsymbol{V} \boldsymbol{\cdot} \boldsymbol{W} = (V_1 W_1, \dots, V_{M-1} W_{M-1}).$$

With the notation introduced so far, we propose the following scheme for (3.1) using the forward difference approximation for u_t, the backward difference for u_x, and the central difference for u_{xx}:

$$\begin{cases} \dfrac{U_i^n - U_i^{n-1}}{k} + \dfrac{U_i^{n-1} - U_{i-1}^{n-1}}{h} + d\big(x_i, \mathcal{Q}_h(\boldsymbol{\Psi}_1 \cdot \boldsymbol{U}^{n-1})\big)U_i^{n-1} \\ \qquad = \dfrac{U_{i+1}^{n-1} + U_{i-1}^{n-1} - 2U_i^{n-1}}{h^2}, \quad 1 \le i \le M-1, \ 1 \le n \le N, \\ \left(1 + \dfrac{1}{h}\right) U_0^n - \dfrac{1}{h} U_1^n = \mathcal{Q}_h\Big(\boldsymbol{B}\big(\mathcal{Q}_h(\boldsymbol{\Psi}_2 \cdot \boldsymbol{U}^n)\big) \cdot \boldsymbol{U}^n\Big), \quad 0 \le n \le N, \\ U_M^n = 0, \quad 0 \le n \le N, \\ U_i^0 = u_0(x_i), \quad 1 \le i \le M-1. \end{cases} \tag{3.2}$$

In order to carry out the analysis within an abstract theory of discretizations, we introduce the general discretization framework. For, we define the spaces

$$X_h = Y_h = \mathbb{R}^{N+1} \times (\mathbb{R}^{M-1})^{N+1} \times \mathbb{R}^{N+1}.$$

We also introduce the operator $\Phi_h \colon X_h \to Y_h$, defined through the formulae

$$\Phi_h(\boldsymbol{V_0}, \boldsymbol{V^0}, \boldsymbol{V^1}, ..., \boldsymbol{V^N}, \boldsymbol{V_M}) = (\boldsymbol{P_0}, \boldsymbol{P^0}, \boldsymbol{P^1}, ..., \boldsymbol{P^N}, \boldsymbol{P_M}),$$

where

$$\begin{aligned}
&\boldsymbol{P}_0 = (P_0^0, P_0^1, \cdots, P_0^N),\\
&P_0^n = \left(1+\frac{1}{h}\right)V_0^n - \frac{1}{h}V_1^n - \mathcal{Q}_h\Big(\boldsymbol{B}\big(\mathcal{Q}_h(\boldsymbol{\Psi}_2\cdot\boldsymbol{V}^n)\big)\cdot\boldsymbol{V}^n\Big),\ 0\le n\le N,\\
&\boldsymbol{P}_M = (P_M^0, P_M^1, \cdots, P_M^N),\\
&P_M^n = \frac{V_M^n}{h},\quad 0\le n\le N,\\
&\boldsymbol{P}^n = (P_1^n, P_2^n, \ldots, P_{M-1}^n),\quad 0\le n\le N,\\
&P_i^0 = V_i^0 - U_i^0,\quad 1\le i\le M-1,\\
&P_i^n = \frac{V_i^n - V_i^{n-1}}{k} + \frac{V_i^{n-1}-V_{i-1}^{n-1}}{h} + d\big(x_i, \mathcal{Q}_h(\boldsymbol{\Psi}_1\cdot\boldsymbol{V}^{n-1})\big)V_i^{n-1}\\
&\qquad - \frac{V_{i+1}^{n-1}+V_{i-1}^{n-1}-2V_i^{n-1}}{h^2},\ 1\le n\le N, 1\le i\le M-1.
\end{aligned} \tag{3.3}$$

Now $\boldsymbol{U}_h = (\boldsymbol{U}_0, \boldsymbol{U}^0, \boldsymbol{U}^1, \cdots, \boldsymbol{U}^N) \in X_h$ is a solution to (3.2) if and only if it is a solution of the discrete problem

$$\Phi_h(\boldsymbol{U}_h) = \boldsymbol{0} \in Y_h. \tag{3.4}$$

To investigate how close $\boldsymbol{U_h}$ is to u, we first need to choose an element $\boldsymbol{u_h} \in X_h$, which is a suitable discrete representation of u. In particular, our choice is the set of nodal values of the theoretical solution u, namely

$$\boldsymbol{u}_h = (\boldsymbol{u}_0, \boldsymbol{u}^0, \ldots, \boldsymbol{u}^N, \boldsymbol{u}_M) \in X_h, \tag{3.5}$$

where

$$\begin{cases}
\boldsymbol{u}_0 = (u_0^0, u_0^1, \ldots, u_0^N) \in \mathbb{R}^{N+1},\ u_0^n = u(0,t^n),\ 0\le n\le N,\\
\boldsymbol{u}^n = (u_1^n, u_2^n, \ldots, u_{M-1}^n) \in \mathbb{R}^{M-1},\ u_i^n = u(x_i,t^n), 1\le i\le M-1, 0\le n\le N,\\
\boldsymbol{u}_M = (u_M^0, u_M^1, \ldots, u_M^N) \in \mathbb{R}^{N+1},\ u_M^n = u(a_\dagger,t^n),\ 0\le n\le N.
\end{cases} \tag{3.6}$$

Then the global discretization error is defined to be the vector

$$\boldsymbol{e_h} = \boldsymbol{u_h} - \boldsymbol{U_h} \in X_h,$$

and the local discretization error is given by

$$\boldsymbol{I_h} = \Phi_h(\boldsymbol{u}_h) \in Y_h.$$

In order to measure the magnitude of errors, we define the following norms in the spaces X_h and Y_h:

$$\|(\boldsymbol{V}_0,\boldsymbol{V}^0,\boldsymbol{V}^1,\ldots,\boldsymbol{V}^N,\boldsymbol{V}_M)\|_{X_h} = h(\|\boldsymbol{V}_0\|_* + \|\boldsymbol{V}_M\|_*) + \max\{\|\boldsymbol{V}^0\|,\|\boldsymbol{V}^1\|,\ldots,\|\boldsymbol{V}^N\|\},$$

$$\|(\boldsymbol{P}_0,\boldsymbol{P}^0,\boldsymbol{P}^1,...,\boldsymbol{P}^N,\boldsymbol{P}_M)\|_{Y_h} = \left(\|\boldsymbol{P}_0\|_*^2 + \|\boldsymbol{P}^0\|^2 + h\|\boldsymbol{P}_M\|_*^2 + \sum_{n=1}^{N} k\|\boldsymbol{P}^n\|^2\right)^{1/2},$$

where $\|\boldsymbol{V}^n\|^2 = \sum\limits_{i=1}^{M-1} h|V_i^n|^2$ and $\|\boldsymbol{V}_0\|_*^2 = \sum\limits_{n=0}^{N} k|V_0^n|^2$.
For $\boldsymbol{V},\boldsymbol{W} \in \mathbb{R}^{M-1}$ and $\boldsymbol{Z} \in \mathbb{R}^{N+1}$, we define

$$\langle \boldsymbol{V},\boldsymbol{W}\rangle = \sum_{i=1}^{M-1} hV_iW_i,$$

$$\|\boldsymbol{V}\|_\infty = \max_{1\le j\le M-1}|V_i|, \quad \|\boldsymbol{Z}\|^\infty = \max_{0\le n\le N}|Z^n|.$$

Throughout the chapter, we use C to denote the generic positive constant which does not depend on the step sizes, grid points and it need not be the same constant as in the preceding calculations.
For the sake of completeness, we give the following standard definitions (see [50]).

Definition 3.2.1 (Consistency) Discretization (3.4) is said to be consistent with (3.1) if

$$\lim_{h\to 0}\|\Phi_h(\boldsymbol{u}_h)\|_{Y_h} = \lim_{h\to 0}\|\boldsymbol{I}_h\|_{Y_h} = 0.$$

Moreover, if $\|\boldsymbol{I}_h\|_{Y_h} = \mathcal{O}(h^p) + \mathcal{O}(k^q)$ then we say that (p,q) is the order of the consistency.

Definition 3.2.2 (Stability) Discretization (3.4) is said to be stable restricted to the thresholds R_h if there exist two positive constants h_0 and S such that

$$\|\boldsymbol{V}_h - \boldsymbol{W}_h\|_{X_h} \le S\|\Phi_h(\boldsymbol{V}_h) - \Phi_h(\boldsymbol{W}_h)\|_{Y_h},$$

whenever $h \in (0, h_0]$, $\boldsymbol{V}_h, \boldsymbol{W}_h \in B(\boldsymbol{u}_h, R_h)$, where $B(\boldsymbol{u}_h, R_h) = \{z \in X_h \mid \|z - \boldsymbol{u}_h\|_{X_h} < R_h\}$.

Definition 3.2.3 (Convergence) Discretization (3.4) is said to be convergent if there exists $h_0 > 0$ such that, for all $0 < h \leq h_0$, (3.4) has a solution $\boldsymbol{U}_h$ for which

$$\lim_{h \to 0} \|\boldsymbol{u}_h - \boldsymbol{U}_h\|_{X_h} = \lim_{h \to 0} \|\boldsymbol{e}_h\|_{X_h} = 0.$$

The following theorem which is established in [51] is based on a result due to Stetter (see [79]), and plays an important role in the proof of convergence of (3.2).

Theorem 3.2.4 *(Cf. [51]) Assume that* (3.4) *is consistent and stable with thresholds M_h. If Φ_h is continuous in $B(u_h, M_h)$ and $\|I_h\| = \mathcal{O}(M_h)$ as $h \to 0$, then the following hold.*
(i) For sufficiently small $h > 0$, discrete equation (3.4) *admits a unique solution in $B(u_h, M_h)$.*
(ii) The solutions to (3.4) *converge to the solution to* (3.2) *as $h \to 0$. Furthermore, the order of convergence is not smaller than the order of consistency.*

3.3 Consistency, stability and convergence

In this section, we prove that numerical scheme (3.2) is consistent and stable. In order to obtain the stability result, we first need to prove an elementary inequality. Next, with the help of Theorem 3.2.4, we establish the convergence result. We begin with the consistency result in the following theorem.

Theorem 3.3.1 (Consistency) *Assume that d, B, ψ_i, $i = 1, 2$, are sufficiently smooth such that the solution u to* (3.1) *is four times continuously differentiable with bounded derivatives. Moreover, we assume that there exists $L > 0$ such that for every $0 \leq x \leq a_\dagger$, $s_1, s_2 > 0$,*

$$|d(x, s_1) - d(x, s_2)| \leq L|s_1 - s_2|,$$

and

$$|B(x, s_1) - B(x, s_2)| \leq L|s_1 - s_2|.$$

Then the local discretization error satisfies

$$\|\Phi_h(u_h)\|_{Y_h} = \{\|\boldsymbol{U}^0 - \boldsymbol{u}^0\|^2 + \mathcal{O}(h^2) + \mathcal{O}(k^2)\}^{1/2}, \quad \textit{as } h \to 0.$$

Proof. Using the notation introduced in (3.6), it is standard to verify that

$$\sup_{i,n} \left| \frac{u_i^n - u_i^{n-1}}{k} - u_t(x_i, t^{n-1}) \right| = \mathcal{O}(k), \text{ as } k \to 0, \tag{3.7}$$

$$\sup_{i,n} \left| \frac{u_i^{n-1} - u_{i-1}^{n-1}}{h} - u_x(x_i, t^{n-1}) \right| = \mathcal{O}(h), \text{ as } h \to 0, \tag{3.8}$$

and

$$\sup_{i,n} \left| \frac{u_{i+1}^{n-1} + u_{i-1}^{n-1} - 2u_i^{n-1}}{h^2} - u_{xx}(x_i, t^{n-1}) \right| = \mathcal{O}(h^2), \text{ as } h \to 0. \tag{3.9}$$

On the other hand, it is well known that if $f \in \mathcal{C}^4[0, a_\dagger]$, then

$$|\int_0^{a_\dagger} f(x)dx - \mathcal{Q}_h(\boldsymbol{f})| \leq Ch^4, \tag{3.10}$$

where $C > 0$ is independent of h.
Lipschitz continuity of d on compact sets readily implies

$$\begin{aligned} |d\big(x_i, s_1(t^{n-1})\big)u_i^{n-1} - & d\big(x_i, \mathcal{Q}_h(\boldsymbol{\psi}_1 \cdot \boldsymbol{u}^{n-1})\big)u_i^{n-1}| \\ & \leq L|u_i^{n-1}||s_1(t^{n-1}) - \mathcal{Q}_h(\boldsymbol{\psi}_1 \boldsymbol{u}^{n-1})| \\ & \leq LCh^4|u_i^{n-1}|. \end{aligned}$$

Hence we get

$$\sup_{i,n} |d\big(x_i, s_1(t^{n-1})\big)u_i^{n-1} - d\big(x_i, \mathcal{Q}_h(\boldsymbol{\psi}_1 \cdot \boldsymbol{u}^{n-1})\big)u_i^{n-1}| = \mathcal{O}(h^4), \text{ as } h \to 0. \tag{3.11}$$

From the boundary condition, it follows that

$$\begin{aligned}
&\Big| \int_0^{a_\dagger} B\big(x, s_2(t^n)\big) u(x,t^n) dx - \mathcal{Q}_h\Big(\boldsymbol{B}\big(\mathcal{Q}_h(\boldsymbol{\psi}_2 \cdot \boldsymbol{u}^n)\big) \cdot \boldsymbol{u}^n\Big)\Big| \\
&\le \Big| \int_0^{a_\dagger} B\big(x, s_2(t^n)\big) u(x,t^n) dx - \mathcal{Q}_h\Big(\boldsymbol{B}\big(s_2(t^n)\big) \cdot \boldsymbol{u}^n\Big)\Big| \\
&\quad + \Big| \mathcal{Q}_h\Big(\boldsymbol{B}\big(s_2(t^n)\big) \cdot \boldsymbol{u}^n\Big) - \mathcal{Q}_h\Big(\boldsymbol{B}\big(\mathcal{Q}_h(\boldsymbol{\psi}_2 \cdot \boldsymbol{u}^n)\big) \cdot \boldsymbol{u}^n\Big)\Big| \\
&\le Ch^4 + |\mathcal{Q}_h\big(|s_2(t^n) - \mathcal{Q}_h(\boldsymbol{\Psi}_2 \cdot \boldsymbol{u}^n)| L\boldsymbol{u}^n\big)| \\
&\le Ch^4 + LCh^4 a_\dagger \|\boldsymbol{u}^n\|_\infty.
\end{aligned} \tag{3.12}$$

Therefore we can write

$$\sup_n \Big| \int_0^{a_\dagger} B\big(x, s_2(t^n)\big) u(x,t^n) dx - \mathcal{Q}_h\Big(\boldsymbol{B}\big(\mathcal{Q}_h(\boldsymbol{\psi}_2 \cdot \boldsymbol{u}^n)\big) \cdot \boldsymbol{u}^n\Big)\Big| = \mathcal{O}(h^4), \text{ as } h \to 0. \tag{3.13}$$

Using (3.7), (3.8), (3.9), (3.11) and (3.13), one can easily conclude the proof of the required result. To prove numerical scheme (3.2) is stable, we need the following lemma.

Lemma 3.3.2 *If x, y, a, b and h are positive real numbers such that $\left(1 + \frac{1}{h}\right) x - \frac{1}{h} y \le a + b$, then $\left(1 + \frac{1}{h}\right) x^2 - \frac{1}{h} y^2 \le 2(a^2 + b^2)$.*

Proof. Consider

$$\begin{aligned}
\left(1 + \frac{1}{h}\right) x^2 - \frac{1}{h} y^2 &\le \left(1 + \frac{1}{h}\right) \left(\frac{ah + bh + y}{h+1}\right)^2 - \frac{1}{h} y^2 \\
&= \frac{a^2h^2 + b^2h^2 + 2abh^2 + y^2 + 2yh(a+b)}{h(h+1)} - \frac{1}{h} y^2 \\
&\le \frac{2h(h+1)(a^2+b^2) + (h+1)y^2}{h(h+1)} - \frac{1}{h} y^2 \\
&= 2(a^2 + b^2).
\end{aligned}$$

This completes the proof of the lemma. Now, we are ready to establish the following stability theorem.

Theorem 3.3.3 (Stability) *Assume the hypotheses of Theorem 3.3.1. Let r and λ be such that $k = rh^2 = \lambda h$, and $\lambda + 2r \le 1$. Then discretization (3.4) is stable with thresholds $R_h = Rh$, where R is a fixed positive constant independent of h.*

Proof. Assume that $\boldsymbol{u}_h \in X_h$ is the discrete representation of u given in (3.5)–(3.6). Suppose $\boldsymbol{V}_h$, $\boldsymbol{W}_h$ belong to the ball $B(\boldsymbol{u}_h, R_h)$. We set

$$\boldsymbol{V}_h = (\boldsymbol{V_0}, \boldsymbol{V^0}, \boldsymbol{V^1}, ..., \boldsymbol{V^N}, \boldsymbol{V_M}), \quad \Phi(\boldsymbol{V}_h) = (\boldsymbol{P_0}, \boldsymbol{P^0}, \boldsymbol{P^1}, ..., \boldsymbol{P^N}, \boldsymbol{P_M}),$$

$$\boldsymbol{W}_h = (\boldsymbol{W_0}, \boldsymbol{W^0}, \boldsymbol{W^1}, ..., \boldsymbol{W^N}, \boldsymbol{W_M}), \quad \Phi(\boldsymbol{W}_h) = (\boldsymbol{R_0}, \boldsymbol{R^0}, \boldsymbol{R^1}, ..., \boldsymbol{R^N}, \boldsymbol{R_M}).$$

Then from the definition of the norm in X_h, we find that

$$\begin{aligned} Rh &\geq \|\boldsymbol{V}_h - \boldsymbol{u}_h\|_{X_h} \\ &= h(\|\boldsymbol{V}_0 - \boldsymbol{u}_0\|_* + \|\boldsymbol{V}_M - \boldsymbol{u}_M\|_*) + \max_{0\leq n\leq N}\{\|\boldsymbol{V}^n - \boldsymbol{u}^n\|\} \\ &\geq \left(\sum_{i=1}^{M-1} h|V_i^n - u_i^n|^2\right)^{\frac{1}{2}}, \end{aligned}$$

or

$$R\sqrt{h} \geq |V_i^n - u_i^n|, \; 0 \leq n \leq N, \; 1 \leq i \leq M-1.$$

This readily implies

$$R\sqrt{h} \geq \|\boldsymbol{V}^n - \boldsymbol{u}^n\|_\infty, \; 0 \leq n \leq N.$$

Therefore there exists $C > 0$, independent of n, such that

$$\|\boldsymbol{V}^n\|_\infty \leq R\sqrt{h} + \|\boldsymbol{u}^n\|_\infty \leq C, \; 0 \leq n \leq N. \tag{3.14}$$

On the other hand, from the definition of Φ_h, we obtain

$$\begin{aligned} V_i^n - W_i^n =& (1-\lambda-2r)(V_i^{n-1} - W_i^{n-1}) + (r+\lambda)(V_{i-1}^{n-1} - W_{i-1}^{n-1}) \\ &+ r(V_{i+1}^{n-1} - W_{i+1}^{n-1}) + k(P_i^n - R_i^n) - k\big[d\big(x_i, Q_h(\boldsymbol{\Psi}_1 \cdot \boldsymbol{V}^{n-1})\big)V_i^{n-1} \\ &- d\big(x_i, Q_h(\boldsymbol{\Psi}_1 \cdot \boldsymbol{W}^{n-1})\big)W_i^{n-1}\big], \end{aligned} \tag{3.15}$$

for $1 \leq n \leq N$, $1 \leq i \leq M-1$. Multiply (3.15) with $h(V_i^n - W_i^n)$, take summation over $1 \leq i \leq M-1$, use $2r + \lambda \leq 1$, and the Cauchy-Schwarz inequality to arrive at

$$\begin{aligned}\|\boldsymbol{V}^n - \boldsymbol{W}^n\|^2 \leq & \frac{1}{2}\|\boldsymbol{V}^{n-1} - \boldsymbol{W}^{n-1}\|^2 + (\frac{1}{2} + k)\|\boldsymbol{V}^n - \boldsymbol{W}^n\|^2 \\ & + \frac{k}{2}\|\boldsymbol{d}\big(Q_h(\boldsymbol{\Psi}_1 \cdot \boldsymbol{V}^{n-1})\big)\boldsymbol{V}^{n-1} - \boldsymbol{d}\big(Q_h(\boldsymbol{\Psi}_1 \cdot \boldsymbol{W}^{n-1})\big)\boldsymbol{W}^{n-1}\|^2 \\ & + \frac{k}{2}\|\boldsymbol{P}^n - \boldsymbol{R}^n\|^2 + \frac{k}{2}\left(\left(1+\frac{1}{h}\right)|V_0^{n-1} - W_0^{n-1}|^2 - \frac{1}{h}|V_1^{n-1} - W_1^{n-1}|^2\right. \\ & \left. - \left(1 + \frac{1}{h}\right)|V_{M-1}^{n-1} - W_{M-1}^{n-1}|^2 + \frac{1}{h}|V_M^{n-1} - W_M^{n-1}|^2\right). \end{aligned} \tag{3.16}$$

Now consider

$$\begin{aligned}&\|\boldsymbol{d}\big(Q_h(\boldsymbol{\Psi}_1 \cdot \boldsymbol{V}^{n-1})\big)\boldsymbol{V}^{n-1} - \boldsymbol{d}\big(Q_h(\boldsymbol{\Psi}_1 \cdot \boldsymbol{W}^{n-1})\big)\boldsymbol{W}^{n-1}\| \\ &\leq \|\boldsymbol{d}\big(Q_h(\boldsymbol{\Psi}_1 \cdot \boldsymbol{V}^{n-1})\big)\|_\infty \|\boldsymbol{V}^{n-1} - \boldsymbol{W}^{n-1}\| \\ &\quad + \|\boldsymbol{W}^{n-1}\|_\infty \|\boldsymbol{d}\big(Q_h(\boldsymbol{\Psi}_1 \cdot \boldsymbol{V}^{n-1})\big) - \boldsymbol{d}\big(Q_h(\boldsymbol{\Psi}_1 \cdot \boldsymbol{W}^{n-1})\big)\| \\ &\leq C\|\boldsymbol{V}^{n-1} - \boldsymbol{W}^{n-1}\|, \end{aligned} \tag{3.17}$$

for some $C > 0$ independent of h, k. Thus (3.16)–(3.17) together give

$$\begin{aligned}(1 - 2k)\|\boldsymbol{V}^n - \boldsymbol{W}^n\|^2 \leq & (1 + Ck)\|\boldsymbol{V}^{n-1} - \boldsymbol{W}^{n-1}\|^2 + k\|\boldsymbol{P}^n - \boldsymbol{R}^n\|^2 \\ & + k\left(\left(1 + \frac{1}{h}\right)|V_0^{n-1} - W_0^{n-1}|^2 - \frac{1}{h}|V_1^{n-1} - W_1^{n-1}|^2\right. \\ & \left. + \frac{1}{h}|V_M^{n-1} - W_M^{n-1}|^2\right). \end{aligned} \tag{3.18}$$

Using (3.14) and the left boundary condition, we can write

$$
\begin{aligned}
(1+\frac{1}{h})|V_0^n - W_0^n| - \frac{1}{h}|V_1^n - W_1^n| \\
&\le |P_0^n - R_0^n| + \Big|\mathcal{Q}_h\Big(\boldsymbol{B}\big(\mathcal{Q}_h(\boldsymbol{\Psi}_2\cdot\boldsymbol{V}^n)\big)\cdot\boldsymbol{V}^n\Big) \\
&\quad - \mathcal{Q}_h\Big(\boldsymbol{B}\big(\mathcal{Q}_h(\boldsymbol{\Psi}_2\cdot\boldsymbol{W}^n)\big)\cdot\boldsymbol{W}^n\Big)\Big| \\
&\le |P_0^n - R_0^n| + \Big|\mathcal{Q}_h\Big(\boldsymbol{B}\big(\mathcal{Q}_h(\boldsymbol{\Psi}_2\cdot\boldsymbol{V}^n)\big)\cdot(\boldsymbol{V}^n - \boldsymbol{W}^n)\Big)\Big| \\
&\quad + \Big|\mathcal{Q}_h\Big(\Big(\boldsymbol{B}\big(\mathcal{Q}_h(\boldsymbol{\Psi}_2\cdot\boldsymbol{V}^n)\big) - \boldsymbol{B}\big(\mathcal{Q}_h(\boldsymbol{\Psi}_2\cdot\boldsymbol{W}^n)\big)\Big)\cdot\boldsymbol{W}^n\Big)\Big| \\
&\le |P_0^n - R_0^n| + \|\boldsymbol{B}\|_\infty|\mathcal{Q}_h(\boldsymbol{V}^n - \boldsymbol{W}^n)| \\
&\quad + La_\dagger\|\boldsymbol{\Psi}_2\|_\infty|\mathcal{Q}_h(\boldsymbol{V}^n - \boldsymbol{W}^n)|\ \|\boldsymbol{W}^n\|_\infty \\
&\le |P_0^n - R_0^n| + C\|\boldsymbol{V}^n - \boldsymbol{W}^n\|, \qquad (3.19)
\end{aligned}
$$

for some $C > 0$ independent of mesh sizes h and k. From (3.19) and Lemma 3.3.2, we deduce that

$$
\begin{aligned}
(1+\frac{1}{h})|V_0^{n-1} - W_0^{n-1}|^2 - \frac{1}{h}|V_1^{n-1} - W_1^{n-1}|^2 \\
\le C\left(\|\boldsymbol{V}^{n-1} - \boldsymbol{W}^{n-1}\|^2 + |P_0^{n-1} - R_0^{n-1}|^2\right).
\end{aligned} \tag{3.20}
$$

On substituting this bound in (3.18), we obtain

$$
\begin{aligned}
\|\boldsymbol{V}^n - \boldsymbol{W}^n\|^2 \le \frac{1+Ck}{1-2k}\|\boldsymbol{V}^{n-1} - \boldsymbol{W}^{n-1}\|^2 + \frac{Ck}{1-2k}\left(\|\boldsymbol{P}^n - \boldsymbol{R}^n\|^2\right. \\
\left. + |P_0^{n-1} - R_0^{n-1}|^2 + h|P_M^{n-1} - R_M^{n-1}|^2\right).
\end{aligned} \tag{3.21}
$$

From the discrete Gronwall lemma, there exists C_T depending solely on T such that

$$
\begin{aligned}
\|\boldsymbol{V}^n - \boldsymbol{W}^n\|^2 \le C_T\Bigg\{\|\boldsymbol{V}^0 - \boldsymbol{W}^0\|^2 + \frac{Ck}{1-2k}\sum_{m=1}^{n}\Big(\|\boldsymbol{P}^m - \boldsymbol{R}^m\|^2 \\
+ |P_0^{m-1} - R_0^{m-1}|^2 + h|P_M^{m-1} - R_M^{m-1}|^2\Big)\Bigg\}.
\end{aligned} \tag{3.22}
$$

Thus for k sufficiently small, this immediately gives

$$\|\boldsymbol{V}^n - \boldsymbol{W}^n\| \leq C_T \Bigg\{ \|\boldsymbol{P}^0 - \boldsymbol{R}^0\|^2 + C\left(\sum_{m=1}^{N} k\|\boldsymbol{P}^m - \boldsymbol{R}^m\|^2\right) \\ + C\|\boldsymbol{P}_0 - \boldsymbol{R}_0\|_*^2 + h\|\boldsymbol{P}_M - \boldsymbol{R}_M\|_*^2 \Bigg\}^{\frac{1}{2}}. \tag{3.23}$$

Again, from (3.19), we have

$$(1+h)|V_0^n - W_0^n| - |V_1^n - W_1^n| \leq h\left(C\|\boldsymbol{V}^n - \boldsymbol{W}^n\| + |P_0^n - R_0^n|\right).$$

On multiplying both sides with $|V_0^n - W_0^n|$ and using the AM-GM inequality, we get

$$|V_0^n - W_0^n|^2 \leq |V_1^n - W_1^n|^2 + h\left(C\|\boldsymbol{V}^n - \boldsymbol{W}^n\|^2 + |P_0^n - R_0^n|^2\right). \tag{3.24}$$

On multiplying both sides by hk, taking summation on n, we find that

$$h\|\boldsymbol{V}_0 - \boldsymbol{W}_0\|_*^2 \leq \sum_{n=0}^{N} hk|V_1^n - W_1^n|^2 + \sum_{n=0}^{N} kh^2\left(C\|\boldsymbol{V}^n - \boldsymbol{W}^n\|^2 + |P_0^n - R_0^n|^2\right) \\ \leq (1 + Ch^2)\sum_{n=0}^{N} k\|\boldsymbol{V}^n - \boldsymbol{W}^n\|^2 + h^2\|\boldsymbol{P}_0 - \boldsymbol{R}_0\|_*^2. \tag{3.25}$$

The second boundary condition immediately gives

$$\|\boldsymbol{V}_M - \boldsymbol{W}_M\|_* = h\|\boldsymbol{P}_M - \boldsymbol{R}_M\|_*. \tag{3.26}$$

From (3.23), (3.25) and (3.26), we observe that

$$h\Big(\|\boldsymbol{V}_0 - \boldsymbol{W}_0\|_* + \|\boldsymbol{V}_M - \boldsymbol{W}_M\|_*\Big) \\ + \max\Big\{\|\boldsymbol{V}^0 - \boldsymbol{W}^0\|, \|\boldsymbol{V}^1 - \boldsymbol{W}^1\|, \dots, \|\boldsymbol{V}^N - \boldsymbol{W}^N\|\Big\} \\ \leq K\left(\|\boldsymbol{P}_0 - \boldsymbol{R}_0\|_*^2 + \|\boldsymbol{P}^0 - \boldsymbol{R}^0\|^2 + h\|\boldsymbol{P}_M - \boldsymbol{R}_M\|_*^2 + \sum_{m=1}^{N} k\|\boldsymbol{P}^m - \boldsymbol{R}^m\|^2\right)^{\frac{1}{2}},$$

where K is a constant. This completes the proof. In the following result, we establish that (3.2) is indeed a convergent scheme.

Theorem 3.3.4 (Convergence) *Assume the hypotheses of Theorem 3.3.3. If*

$$\|\boldsymbol{U}^0 - \boldsymbol{u}^0\|_{X_h} = \mathcal{O}(h), \;\; \text{as } h \to 0,$$

then discretization (3.4) is convergent.

Proof. The proof is an immediate consequence of Theorems 3.2.4–3.3.3.

3.4 Other types of boundary conditions

In this section, we discuss the M-V-D with two other boundary conditions. In particular, we study (3.1) when the right boundary codition is non-homogeneous instead of homogeneous. On the other hand, in Subsection 3.4.2, we consider Robin boundary condition at both the end points.

3.4.1 Non-homogeneous boundary condition at $x = a_\dagger$

In this subsection, we consider (3.1) with non-homogeneous Dirichlet boundary condition, i.e.,

$$\begin{cases} u_t(x,t) + u_x(x,t) + d\big(x, s_1(t)\big)u(x,t) = u_{xx}(x,t), \;\; x \in (0, a_\dagger), \;\; t > 0, \\ u(0,t) - u_x(0,t) = \displaystyle\int_0^{a_\dagger} B\big(x, s_2(t)\big)u(x,t)dx, \quad t \geq 0, \\ u(a_\dagger, t) = g(t), \;\; t \geq 0, \\ u(x,0) = u_0(x), \quad x \in (0, a_\dagger), \\ s_\nu(t) = \displaystyle\int_0^{a_\dagger} \psi_\nu(x)u(x,t)dx, \quad t \geq 0, \quad \nu = 1, 2, \end{cases} \tag{3.27}$$

where g is a given smooth function. In order to discretize (3.27), we use the notations from the previous section. Let $h,\ k,\ T,\ M$ be as in Section 3.2 and U_i^n denote the approximate solution to (3.27) at the grid point (x_i, t^n). Moreover, we define $g^n = g(t^n)$, $0 \leq n \leq N$.

By discretizing (3.27) as in Section 3.2, we arrive at the following finite difference scheme (see (3.2))

$$\begin{cases} \dfrac{U_i^n - U_i^{n-1}}{k} + \dfrac{U_i^{n-1} - U_{i-1}^{n-1}}{h} + d\big(x_i, \mathcal{Q}_h(\boldsymbol{\Psi}_1 \cdot \boldsymbol{U}^{n-1})\big)U_i^{n-1} \\ \qquad\qquad = \dfrac{U_{i+1}^{n-1} + U_{i-1}^{n-1} - 2U_i^{n-1}}{h^2}, \ 1 \le i \le M-1, \ 1 \le n \le N, \\ \left(1 + \dfrac{1}{h}\right) U_0^n - \dfrac{1}{h} U_1^n = \mathcal{Q}_h\Big(\boldsymbol{B}\big(\mathcal{Q}_h(\boldsymbol{\Psi}_2 \cdot \boldsymbol{U}^n)\big) \cdot \boldsymbol{U}^n\Big), \quad 0 \le n \le N, \\ U_M^n = g^n, \quad 0 \le n \le N, \\ U_i^0 = u_0(x_i), \quad 1 \le i \le M-1. \end{cases} \tag{3.28}$$

As before, to carry out the analysis, we use the spaces X_h and Y_h that are introduced in Section 3.2. Moreover, we consider the operator $\widetilde{\Phi}_h \colon X_h \to Y_h$, defined through the formulae

$$\widetilde{\Phi}_h(\boldsymbol{V_0}, \boldsymbol{V^0}, \boldsymbol{V^1}, ..., \boldsymbol{V^N}, \boldsymbol{V_M}) = (\boldsymbol{P_0}, \boldsymbol{P^0}, \boldsymbol{P^1}, ..., \boldsymbol{P^N}, \boldsymbol{P_M}),$$

where

$$\begin{aligned} &\boldsymbol{P}_0 = (P_0^0, P_0^1, \cdots, P_0^N), \\ &P_0^n = \left(1 + \frac{1}{h}\right) V_0^n - \frac{1}{h} V_1^n - \mathcal{Q}_h\Big(\boldsymbol{B}\big(\mathcal{Q}_h(\boldsymbol{\Psi}_2 \cdot \boldsymbol{V}^n)\big) \cdot \boldsymbol{V}^n\Big), 0 \le n \le N, \\ &\boldsymbol{P}_M = (P_M^0, P_M^1, \cdots, P_M^N), \\ &P_M^n = \frac{V_M^n - g^n}{h}, \quad 0 \le n \le N, \\ &\boldsymbol{P}^n = (P_1^n, P_2^n, \ldots, P_{M-1}^n), \quad 0 \le n \le N, \\ &P_i^0 = V_i^0 - U_i^0, \quad 1 \le i \le M-1, \\ &P_i^n = \frac{V_i^n - V_i^{n-1}}{k} + \frac{V_i^{n-1} - V_{i-1}^{n-1}}{h} + d\big(x_i, \mathcal{Q}_h(\boldsymbol{\Psi}_1 \cdot \boldsymbol{V}^{n-1})\big)V_i^{n-1} \\ &\qquad - \frac{V_{i+1}^{n-1} + V_{i-1}^{n-1} - 2V_i^{n-1}}{h^2}, \ 1 \le n \le N, 1 \le i \le M-1. \end{aligned} \tag{3.29}$$

Using the definition of $\widetilde{\Phi}_h$, and the arguments used in Theorems 3.3.1–3.3.4, one can easily show that (3.28) is indeed a convergent scheme whenever the hypotheses in Theorem 3.3.4 hold.

3.4.2 Robin condition at both $x = 0,\ a_\dagger$

Consider the following M-V-D with nonlinear nonlocal Robin boundary conditions:

$$\begin{cases} u_t(x,t) + u_x(x,t) + d\big(x, s_1(t)\big)u(x,t) = u_{xx}(x,t),\ x \in (0,a_\dagger),\ t > 0, \\ u(0,t) - u_x(0,t) = \displaystyle\int_0^{a_\dagger} B_1\big(x, s_2(t)\big)u(x,t)dx, \quad t \geq 0, \\ u(a_\dagger,t) + u_x(a_\dagger,t) = \displaystyle\int_0^{a_\dagger} B_2\big(x, s_3(t)\big)u(x,t)dx, \quad t \geq 0, \\ u(x,0) = u_0(x), \quad x \in (0,a_\dagger), \\ s_\nu(t) = \displaystyle\int_0^{a_\dagger} \psi_\nu(x)u(x,t)dx, \quad t \geq 0 \quad \nu = 1,2,3. \end{cases} \tag{3.30}$$

In view of [11], equation (3.30) can be interpreted as a model for population living in a one-dimensional habitat. In that case, x represents the spatial position instead of age. In the right boundary condition, $B_2 = 0$ is an important case which represents the nonflux condition at $x = a_\dagger$. The authors of [30] designed a numerical scheme to (3.30), and studied wellposedness and long time behavior of the solution of that numerical scheme. Their numerical scheme is nonlinear and it is proved that the scheme is indeed stable. In this subsection, we propose a numerical scheme to (3.30) and establish its convergence.

For, we use the notation from the earlier sections. Moreover, we denote
$\Psi_{\nu,i} = \psi_\nu(x_i)$, $\boldsymbol{\Psi}_\nu = (\Psi_{\nu,1}, \Psi_{\nu,2}, \ldots, \Psi_{\nu,M-1})$, $\nu = 1,2,3$,
$\boldsymbol{B_1(\cdot)} = (B_1(x_1,\cdot), B_1(x_2,\cdot), \ldots, B_1(x_{M-1},\cdot))$, and
$\boldsymbol{B_2(\cdot)} = (B_2(x_1,\cdot), B_2(x_2,\cdot), \ldots, B_2(x_{M-1},\cdot))$.
Now we discretize (3.30) to get the following finite difference scheme

$$\begin{cases} \dfrac{U_i^n - U_i^{n-1}}{k} + \dfrac{U_i^{n-1} - U_{i-1}^{n-1}}{h} + d\Big(x_i, \mathcal{Q}_h(\boldsymbol{\Psi}_1 \cdot \boldsymbol{U}^{n-1})\Big)U_i^{n-1} \\ \qquad\qquad = \dfrac{U_{i+1}^{n-1} + U_{i-1}^{n-1} - 2U_i^{n-1}}{h^2},\ 1 \leq i \leq M-1,\ 1 \leq n \leq N, \\ \left(1 + \dfrac{1}{h}\right) U_0^n - \dfrac{1}{h}U_1^n = \mathcal{Q}_h\Big(\boldsymbol{B}_1\big(\mathcal{Q}_h(\boldsymbol{\Psi}_2 \cdot \boldsymbol{U}^n)\big) \cdot \boldsymbol{U}^n\Big), \quad 0 \leq n \leq N, \\ \left(1 + \dfrac{1}{h}\right) U_M^n - \dfrac{1}{h}U_{M-1}^n = \mathcal{Q}_h\Big(\boldsymbol{B}_2\big(\mathcal{Q}_h(\boldsymbol{\Psi}_3 \cdot \boldsymbol{U}^n)\big) \cdot \boldsymbol{U}^n\Big), \quad 0 \leq n \leq N, \\ U_i^0 = u_0(x_i), \quad 1 \leq i \leq M-1. \end{cases} \tag{3.31}$$

In order to establish the convergence of the solution of (3.31) to the solution to (3.30), we introduce the operator $\widehat{\Phi}_h\colon X_h \to Y_h$ given by

$$\widehat{\Phi}_h(\boldsymbol{V_0}, \boldsymbol{V^0}, \boldsymbol{V^1}, ..., \boldsymbol{V^N}, \boldsymbol{V_M}) = (\boldsymbol{P_0}, \boldsymbol{P^0}, \boldsymbol{P^1}, ..., \boldsymbol{P^N}, \boldsymbol{P_M}),$$

where

$$\begin{aligned}
\boldsymbol{P}_0 &= (P_0^0, P_0^1, \cdots, P_0^N),\\
P_0^n &= \left(1+\frac{1}{h}\right) V_0^n - \frac{1}{h} V_1^n - \mathcal{Q}_h\Big(\boldsymbol{B}_1\big(\mathcal{Q}_h(\boldsymbol{\Psi}_2\cdot \boldsymbol{V}^n)\big)\cdot \boldsymbol{V}^n\Big), \quad 0\le n\le N,\\
\boldsymbol{P}_M &= (P_M^0, P_M^1, \cdots, P_M^N),\\
P_M^n &= \left(1+\frac{1}{h}\right) V_M^n - \frac{1}{h} V_{M-1}^n - \mathcal{Q}_h\Big(\boldsymbol{B}_2\big(\mathcal{Q}_h(\boldsymbol{\Psi}_3\cdot \boldsymbol{V}^n)\big)\cdot \boldsymbol{V}^n\Big), \quad 0\le n\le N,\\
\boldsymbol{P}^n &= (P_1^n, P_2^n, \dots, P_{M-1}^n), \quad 0\le n\le N,\\
P_i^0 &= V_i^0 - U_i^0, \quad 1\le i\le M-1,\\
P_i^n &= \frac{V_i^n - V_i^{n-1}}{k} + \frac{V_i^{n-1} - V_{i-1}^{n-1}}{h} + d\big(x_i, \mathcal{Q}_h(\boldsymbol{\Psi}_1\cdot \boldsymbol{V}^{n-1})\big) V_i^{n-1}\\
&\quad - \frac{V_{i+1}^{n-1} + V_{i-1}^{n-1} - 2V_i^{n-1}}{h^2}, \; 1\le n\le N, 1\le i\le M-1.
\end{aligned} \tag{3.32}$$

Now, observe that (3.16) can be written as

$$\begin{aligned}
\|\boldsymbol{V}^n - \boldsymbol{W}^n\|^2 \le& \frac{1}{2}\|\boldsymbol{V}^{n-1} - \boldsymbol{W}^{n-1}\|^2 + (\frac{1}{2}+k)\|\boldsymbol{V}^n - \boldsymbol{W}^n\|^2\\
&+ \frac{k}{2}\|\boldsymbol{d}\big(Q_h(\boldsymbol{\Psi}_1\cdot \boldsymbol{V}^{n-1})\big)\boldsymbol{V}^{n-1} - \boldsymbol{d}\big(Q_h(\boldsymbol{\Psi}_1\cdot \boldsymbol{W}^{n-1})\big)\boldsymbol{W}^{n-1}\|^2\\
&+ \frac{k}{2}\|\boldsymbol{P}^n - \boldsymbol{R}^n\|^2 + \frac{k}{2}\Bigg((1+\frac{1}{h})|V_0^{n-1} - W_0^{n-1}|^2\\
&- \frac{1}{h}|V_1^{n-1} - W_1^{n-1}|^2 - \frac{1}{h}|V_{M-1}^{n-1} - W_{M-1}^{n-1}|^2\\
&+(1+\frac{1}{h})|V_M^{n-1} - W_M^{n-1}|^2\Bigg).
\end{aligned} \tag{3.33}$$

Using the same argument to establish (3.20), we obtain

$$\begin{aligned}
(1+\frac{1}{h})|V_M^{n-1} - W_M^{n-1}|^2 - \frac{1}{h}|V_{M-1}^{n-1} - W_{M-1}^{n-1}|^2&\\
\le C\left(\|\boldsymbol{V}^{n-1} - \boldsymbol{W}^{n-1}\|^2 + |P_M^{n-1} - R_M^{n-1}|^2\right)&.
\end{aligned} \tag{3.34}$$

Using (3.33)–(3.34), the definition of $\widetilde{\Phi}_h$, and the arguments used in Theorems 3.3.1–3.3.4, it is straightforward to show that (3.28) is indeed a convergent scheme whenever the hypotheses in Theorem 3.3.4 hold.

3.5 Numerical simulations

In this section, we present some examples in which the numerical solutions to (3.1), (3.27) and (3.30) are computed using (3.2), (3.28) and (3.31), respectively, to validate the results in the earlier sections. If E_h denotes the magnitude of the error with step size h, then the experimental order of convergence can be computed using the standard formula

$$\text{order} = \frac{\log(E_h) - \log(E_{\frac{h}{2}})}{\log 2}.$$

All the computations that are presented in this section have been performed using Matlab 8.5 (R2015a). In all the examples, we have taken $a_\dagger = 1$, $\psi_1(x) \equiv \psi_2(x) \equiv \psi_3(x) \equiv 1$ and $r = \frac{k}{h^2} = 0.4$.

Example 3.5.1

In order to test the efficacy of the numerical scheme, we assume that u_0, d, and B are given by

$$u_0(x) = e - e^x,\ d(x,s) = 1,\ B(x,s) = e,\ \ x \in (0,1),\ \ s \geq 0.$$

Note that given vital rates (d and B) are constant. Therefore, the first equation in (3.1) becomes linear. We now seek a solution to (3.1) of the form $u(x,t) = (c_1 e^{(\Lambda_1 x)} + c_2 e^{(\Lambda_2 x)})e^{(\lambda t)}$. On substituting u in (3.1), an easy computation gives $\Lambda_{1,2} = \frac{(1 \pm \sqrt{1+4(d+\lambda)})}{2}$, where λ is a solution of the characteristic equation

$$\det \begin{pmatrix} e^{\Lambda_1} & e^{\Lambda_2} \\ 1 - \Lambda_1 + \frac{1-e^{\Lambda_1}}{\Lambda_1} & 1 - \Lambda_2 + \frac{1-e^{\Lambda_2}}{\Lambda_2} \end{pmatrix} = 0. \tag{3.35}$$

One can easily verify that $\lambda = -1$ is a solution of (3.35). This readily gives us that $\Lambda_1 = 0$, $\Lambda_2 = 1$. After substituting $u(x,t) = (c_1 e + c_2 e^x)e^{-t}$ in the initial condition and the right boundary condition given in (3.1), we find $c_1 = 1$ and $c_2 = -1$. Hence for the given set of vital rates, $u(x,t) = (e - e^x)e^{-t}$ is the solution to (3.1). It is straightforward to check that d and B satisfy the hypotheses of

h	$\|\boldsymbol{U}_0 - \boldsymbol{u}_0\|_*$	order	$\max\limits_{1\leq n\leq N}\{\|\boldsymbol{U}^n - \boldsymbol{u}^n\|\}$	order	$\|\boldsymbol{e}_h\|_{X_h}$	order
0.1	0.0212	1.1009	0.0391	0.9805	0.0412	1.0212
0.05	0.0099	1.0509	0.0198	0.9921	0.0203	1.0105
0.02	0.0037	1.0204	0.0079	0.9972	0.0080	1.0041
0.01	0.0018	1.0102	0.0039	0.9986	0.0040	1.0020
0.005	0.0009	1.0051	0.0020	0.9993	0.0020	1.0010

Table 3.1: The magnitude of the global discretization error and the order of convergence for different choices of h at $t = 0.2$ with d, B given in Example 3.5.1.

Theorem 3.3.4. Hence (3.2) is a convergent numerical scheme.

In Figure 3.1, we show the absolute difference between the exact solution and the

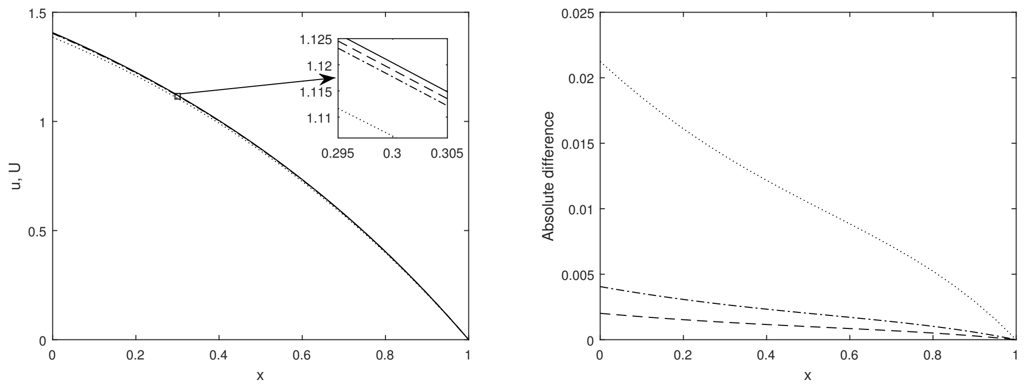

Figure 3.1: The exact solution to (3.1), and the approximate solutions using (3.2) at $t = 0.2$ with $d(x, s)$, $B(x, s)$ given in Example 3.5.1; Left: $u(x, 0.2)$ (solid line), $\boldsymbol{U}_{0.05}$ (dotted line), $\boldsymbol{U}_{0.01}$ (dash-dotted line), $\boldsymbol{U}_{0.005}$ (dashed line) for $0 \leq x \leq 1$, Right: $|u(x, 0.2) - \boldsymbol{U}_{0.05}|$ (dotted line), $|u(x, 0.2) - \boldsymbol{U}_{0.01}|$ (dash-dotted line) and $|u(x, 0.2) - \boldsymbol{U}_{0.005}|$ (dashed line).

computed solution. In Figure 3.1 (left), we present the exact solution u to (3.1) and the corresponding numerical solutions using (3.2) with $h = 0.05,\ 0.01,\ 0.005$ at $t = 0.2$. From this figure, it is evident that $\boldsymbol{U}_{0.05}$, $\boldsymbol{U}_{0.01}$ and $\boldsymbol{U}_{0.005}$ are very close to u at $t = 0.2$. This phenomenon re-validates the result that is proved in Theorem 3.3.4. In Figure 3.1 (right), the difference between $u(x, 0.2)$ and $\boldsymbol{U}_h$ at $t = 0.2$, with $h = 0.05,\ 0.01,\ 0.005$ are shown. From these figures, we can conclude that the sequence $\boldsymbol{U}_h$ indeed converges to the solution u as h tends to zero at $t = 0.2$, as mentioned in Theorem 3.3.4.

In Table 3.1, we display the magnitude of the global discretization error and the experimental order of convergence in $[0, 1] \times [0, 0.2]$ for different choices of h. In the second column of Table 3.1, we show the error at the boundary point $x = 0$, and in the fourth column the interior error i.e., $\max\limits_{1\leq n\leq N} \|\boldsymbol{U}^n - \boldsymbol{u}^n\|$ is shown. In the third, and fifth columns, the experimental order of convergence corresponding to the boundary $x = 0$, interior of the domain are given, respectively. Finally, the experimental order of convergence corresponding to the global discretization error is shown in the last column. From Table 3.1, one can easily observe that the order of convergence of the proposed numerical scheme is one.

Example 3.5.2

In this example, we consider the non-homogeneous case described in Subsection 3.4.1. In particular, we consider (3.27) with u_0, d, B, and g are given by

$$u_0 = \tfrac{e^{-x}}{2},\ d(x,s) = 1 + \tfrac{s}{1-e^{-1}},\ B(x,s) = 2e^{x},\ \ x \in (0,1),\ \ s \geq 0,$$
$$g(t) = \tfrac{e^{-1}}{1+e^{-t}},\ t > 0.$$

We observe that d and B satisfy hypotheses of Theorem 3.3.4. Therefore (3.28) is a convergent numerical scheme. On the other hand, it is easy to check that for the given set of functions, the function

$$u(x,t) = \tfrac{e^{-x}}{1+e^{-t}},\ x \in (0,1),\ t \geq 0,$$

is a solution to (3.27).

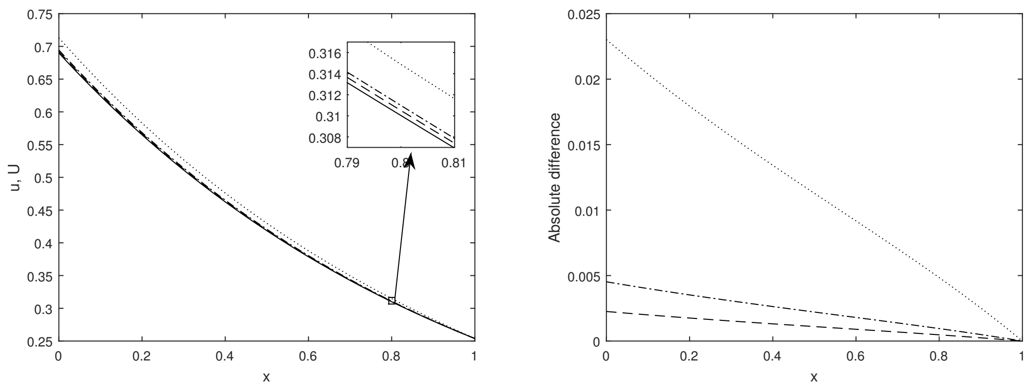

Figure 3.2: The exact solution to (3.27) and the approximate solutions using (3.28) at $t = 0.8$ with $d(x,s)$, $B(x,s)$, $g(t)$ given in Example 3.5.2; Left: $u(x,0.8)$ (solid line), $\boldsymbol{U}_{0.05}$ (dotted line), $\boldsymbol{U}_{0.01}$ (dash-dotted line), $\boldsymbol{U}_{0.005}$ (dashed line) for $0 \leq x \leq 1$, Right: $|u(x,0.8) - \boldsymbol{U}_{0.05}|$ (dotted line), $|u(x,0.8) - \boldsymbol{U}_{0.01}|$ (dash-dotted line) and $|u(x,0.8) - \boldsymbol{U}_{0.005}|$ (dashed line).

h	$\|\boldsymbol{U}_0 - \boldsymbol{u}_0\|_*$	order	$\max_{1\le n\le N}\{\|\boldsymbol{U}^n - \boldsymbol{u}^n\|\}$	order	$\|\boldsymbol{e}_h\|_{X_h}$	order
0.1	0.0451	1.0404	0.0416	0.9425	0.0461	1.0197
0.05	0.0219	1.0202	0.0216	0.9722	0.0227	1.0086
0.02	0.0086	1.0080	0.0088	0.9891	0.0090	1.0031
0.01	0.0042	1.0040	0.0044	0.9946	0.0045	1.0015
0.005	0.0021	1.0020	0.0022	0.9973	0.0023	1.0007

Table 3.2: The magnitude of the global discretization error and the order of convergence for different choices of h at $t = 0.8$ with $d(x,s)$, $B(x,s)$, $g(t)$ given in Example 3.5.2.

We display the exact solution u to (3.27) and the numerical solutions U using (3.28) in Figure 3.2. In Figure 3.2 (left), the exact solution u to (3.27) and numerical solutions using (3.28) with $h = 0.05,\ 0.01,\ 0.005$ at $t = 0.8$ are presented. From this figure, it is evident that $\boldsymbol{U}_{0.05}$, $\boldsymbol{U}_{0.01}$ and $\boldsymbol{U}_{0.005}$ are approaching to u at $t = 0.8$. In Figure 3.2 (right), we show the absolute difference between u and $\boldsymbol{U}_h$ at $t = 0.8$, with $h = 0.05,\ 0.01,\ 0.005$. We conclude from these figures that the sequence of numerical solutions $\boldsymbol{U}_h$ indeed converges to the solution u at $t = 0.8$ as h tends to 0.

In Table 3.2, we show computational errors and their experimental order of convergence for various choices of h at $t = 0.8$. In particular, we display the error at the boundary point $x = 0$, the maximum error in the interior of domain and the global discretization error in the second, fourth and sixth columns of the table, respectively. On the other hand, the experimental order of convergence corresponding to the error at the boundary point $x = 0$, the maximum error in the interior of domain and the global discretization error are presented in the third, fifth and seventh columns of the table, respectively. From Table 3.2, we observe that the experimental order of convergence of the proposed scheme is indeed one.

Example 3.5.3

In this example, we take the nonflux boundary condition at the right boundary described in Subsection 3.4.2, i.e., $B_2 = 0$. Let the vital rates d, B_1, B_2 and the initial data u_0 be given by

$$u_0(x) = e^{-x},\ d(x,s) = 2 + 4\Big(\tfrac{s}{1-e^{-1}}\Big)^{\frac{1}{4}},$$
$$B_1(x,s) = 2e^x,\ B_2(x,s) = 0,\ x \in (0,1),\ \ s \ge 0.$$

Once again, using the ansatz $u(x,t) = X(x)T(t)$ and substituting it in (3.30), we obtain that $u(x,t) = \frac{e^{-x}}{(1+t)^4}$ is the solution to (3.30). Moreover, it is easy to verify that d, B_1 and B_2 satisfy hypotheses of Theorem 3.3.4. Therefore (3.31) is a convergent numerical scheme.

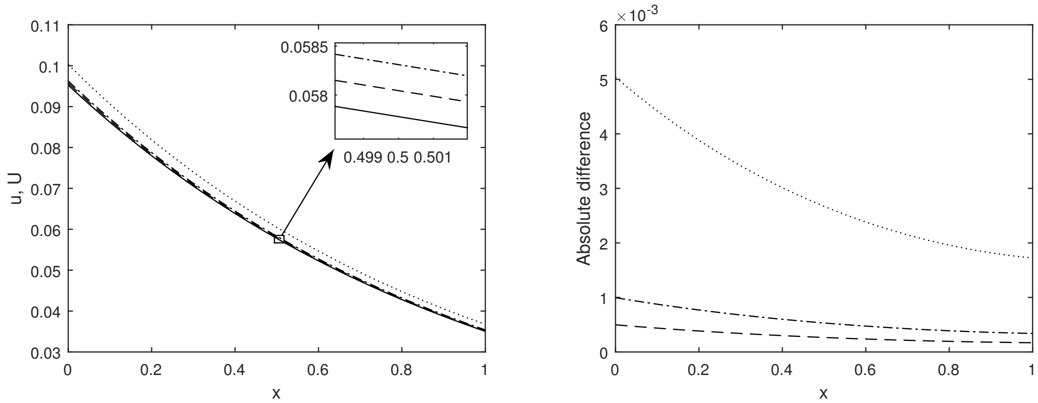

Figure 3.3: The exact solution to (3.30) and the approximate solutions using (3.31) at $t = 0.8$ with $d(x,s)$, $B_1(x,s)$, $B_2(x,s)$ given in Example 3.5.3; Left: $u(x,0.8)$ (solid line), $\boldsymbol{U}_{0.05}$ (dotted line), $\boldsymbol{U}_{0.01}$ (dash-dotted line), $\boldsymbol{U}_{0.005}$ (dashed line) for $0 \le x \le 1$, Right: $|u(x,0.8) - \boldsymbol{U}_{0.05}|$ (dotted line), $|u(x,0.8) - \boldsymbol{U}_{0.01}|$ (dash-dotted line) and $|u(x,0.8) - \boldsymbol{U}_{0.005}|$ (dashed line).

We compare the exact solution to (3.30) and the approximate solutions that are computed using (3.31) for different values of h at $t = 0.8$ in Figure 3.3. In particular, the exact solution to (3.30) and approximate solutions to (3.30) with $h = 0.05,\ 0.01,\ 0.005$ at $t = 0.8$ are shown in Figure 3.3 (left). Moreover, we plot the absolute difference between $u(x,0.8)$ and $\boldsymbol{U}_h$ with $h = 0.05,\ 0.01,\ 0.005$ at $t = 0.8$ in Figure 3.3 (right). From these graphs, it is clear that $\boldsymbol{U}_h$ approaches $u(x,0.8)$ as h goes to zero at $t = 0.8$. Furthermore, one can conclude that the numerical scheme (3.31) converges.

In Table 3.3, we present the absolute error $|u_i^n - U_i^n|$ and the experimental order of convergence for different choice of h at $t = 0.8$. In particular, we show the error at the boundary point $x = 1$ and the maximum error in the interior of domain in the second and fourth columns, respectively. In the third and fifth columns, we display the experimental order of convergence corresponding to the boundary point $x = 1$ and the interior of domain, respectively. Moreover, the global discretization error and corresponding experimental order of convergence are shown in the sixth and seventh columns of the table, respectively. From Table 3.3, one can conclude that the experimental order of convergence of the proposed

h	$\|\boldsymbol{U}_M - \boldsymbol{u}_M\|_*$	order	$\max\limits_{1\le n\le N}\{\|\boldsymbol{U}^n - \boldsymbol{u}^n\|\}$	order	$\|\boldsymbol{e}_h\|_{X_h}$	order
0.1	0.0076	1.2307	0.0141	0.8375	0.0169	0.9790
0.05	0.0032	1.0394	0.0079	0.9180	0.0085	0.9788
0.02	0.0012	0.9942	0.0033	0.9671	0.0035	0.9898
0.01	0.0006	0.9932	0.0017	0.9835	0.0017	0.9947
0.005	0.0003	0.9956	0.0008	0.9917	0.0008	0.9973

Table 3.3: The magnitude of the global discretization error and the order of convergence for different choices of h at $t = 0.8$ with $d(x, s)$, $B_1(x, s)$, $B_2(x, s)$ given in Example 3.5.3.

numerical scheme (3.30) is one.

Example 3.5.4

In this example, we choose the vital rates d, B_1, B_2 and the initial data u_0 such that the solution to (3.30) is known in the closed form. In particular, let u_0, d, B_1 and B_2 be given by

$$u_0(x) = e^{-\frac{(2x-1)^2}{16}},\ d(x,s) = 1 + \tfrac{2x-1}{4} + \tfrac{(2x-1)^2}{16} - \frac{s}{2\int_0^1 e^{-\frac{(2x-1)^2}{16}}dx},$$
$$B_1(x,s) = B_2(x,s) = \frac{3e^{-1/16}}{4\int_0^1 e^{-\frac{(2x-1)^2}{16}}dx},\quad x \in (0,1),\ \ s \geq 0.$$

Now it is straightforward to verify that $u(x,t) = \frac{2}{1+4e^t}e^{-\frac{(2x-1)^2}{16}}$ is the solution to (3.30). On the other hand, it is easy to check that d, B_1 and B_2 satisfy hypotheses of Theorem 3.3.4. Therefore (3.31) is a convergent numerical scheme.

In Figure 3.4, we plot the exact solution to (3.30) and computed solutions using (3.31) for different values of h at $t = 0.8$. In Figure 3.4 (left), the exact, and approximate solutions to (3.30) with $h = 0.05,\ 0.01,\ 0.005$ at $t = 0.8$ are presented. From these figures, it is straightforward to see that $u(x, 0.8)$ is closer to $\boldsymbol{U}_{0.005}$ than $\boldsymbol{U}_{0.01}$ and $\boldsymbol{U}_{0.05}$ at $t = 0.8$. In Figure 3.4 (right), we plot the absolute difference between $u(x, 0.8)$ and $\boldsymbol{U}_h$ with $h = 0.05,\ 0.01,\ 0.005$ at $t = 0.8$. From these graphs, one can observe that the numerical solutions $\boldsymbol{U}_h$ converge.

We display various discretization errors and their experimental orders of convergence for different choice of h at $t = 0.8$ in Table 3.4. We present the error at the boundary point $x = 0$ and the maximum error in the interior of domain in the second and fourth columns, respectively. In the third and fifth columns, we show the experimental order of convergence corresponding to the boundary point

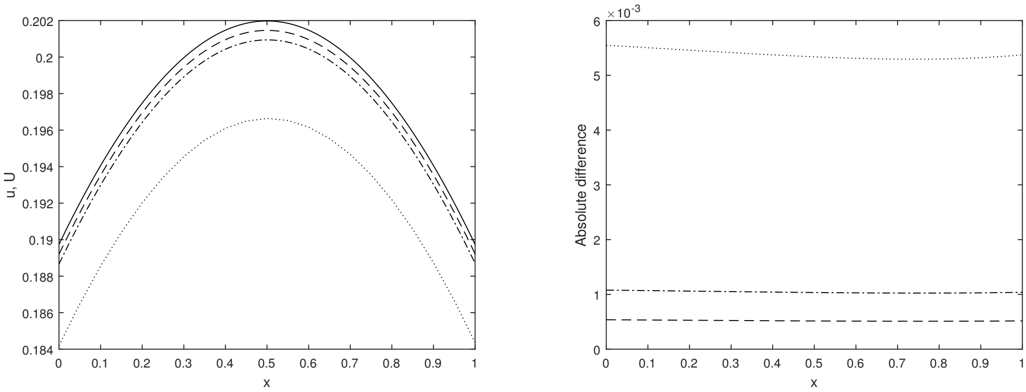

Figure 3.4: The exact solution to (3.30) and the approximate solutions using (3.31) at $t = 0.8$ with $d(x,s)$, $B_1(x,s)$, $B_2(x,s)$ given in Example 3.5.4; Left: $u(x,0.8)$ (solid line), $\boldsymbol{U}_{0.05}$ (dotted line), $\boldsymbol{U}_{0.01}$ (dash-dotted line), $\boldsymbol{U}_{0.005}$ (dashed line) for $0 \le x \le 1$, Right: $|u(x,0.8) - \boldsymbol{U}_{0.05}|$ (dotted line), $|u(x,0.8) - \boldsymbol{U}_{0.01}|$ (dash-dotted line) and $|u(x,0.8) - \boldsymbol{U}_{0.005}|$ (dashed line).

h	$\Vert\boldsymbol{U}_0 - \boldsymbol{u}_0\Vert_*$	order	$\max\limits_{1\le n\le N}\{\Vert\boldsymbol{U}^n - \boldsymbol{u}^n\Vert\}$	order	$\Vert\boldsymbol{e}_h\Vert_{X_h}$	order
0.1	0.0120	1.0586	0.0114	1.0457	0.0136	1.1717
0.05	0.0057	1.0290	0.0055	1.0225	0.0060	1.0888
0.02	0.0022	1.0115	0.0021	1.0089	0.0022	1.0367
0.01	0.0011	1.0057	0.0010	1.0044	0.0010	1.0186
0.005	0.0005	1.0028	0.0005	1.0022	0.0005	1.0093

Table 3.4: The magnitude of the global discretization error and the order of convergence for different choices of h at $t = 0.8$ with $d(x,s)$, $B_1(x,s)$, $B_2(x,s)$ given in Example 3.5.4.

$x = 0$ and the interior domain, respectively. Moreover, the global discretization error and the corresponding experimental order of convergence are given in the sixth and seventh columns of the table, respectively. From Table 3.4, it is easy to observe that the experimental order of convergence of the proposed scheme is one.

Example 3.5.5

In order to test our numerical scheme, we assume that d, B and u_0 are given by

$$u_0(x) = e - e^x,\ d(x,s) = 2 + x^2 + \tfrac{s^2}{2},\ B(x,s) = 2e^x + s,\ \ x \in (0,1),\ \ s \ge 0.$$

Note that, the given set of functions d, B and u_0 satisfy hypotheses of Theorem 3.3.4. Hence (3.2) is a convergent numerical scheme.

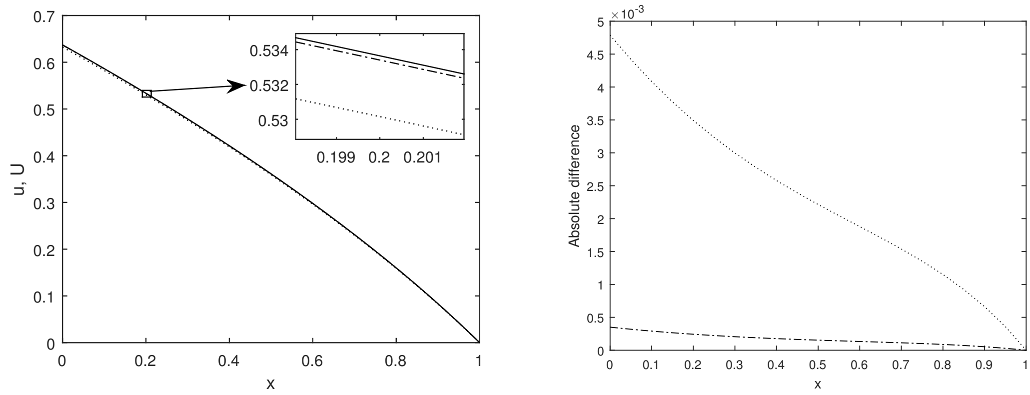

Figure 3.5: The approximate solutions to (3.1) at $t = 0.8$ with $d(x,s)$, $B_1(x,s)$, $B_2(x,s)$ given in Example 3.5.5; Left: $\boldsymbol{U}_{0.05}$ (dotted line), $\boldsymbol{U}_{0.01}$ (dash-dotted line), $\boldsymbol{U}_{0.005}$ (solid line) for $0 \le x \le 1$ at $t = 0.8$, Right: $|\boldsymbol{U}_{0.005} - \boldsymbol{U}_{0.05}|$ (dotted line) and $|\boldsymbol{U}_{0.005} - \boldsymbol{U}_{0.01}|$ (dash-dotted line).

In Figure 3.5 (left), we present approximate solutions to (3.1) at $t = 0.8$ for $h = 0.05,\ 0.01,\ 0.005$. On the other hand, we display the absolute difference $|\boldsymbol{U}_h - \boldsymbol{U}_{0.005}|$ at $t = 0.8$ for $h = 0.05,\ 0.01$ in Figure 3.5 (right). From this figure, it is evident that $\boldsymbol{U}_h$'s are very close to each other as h goes to zero, and the limit of the sequence $\boldsymbol{U}_h$ indeed converges to the solution of (3.1) as mentioned in Theorem 3.3.4.

Chapter 4

A higher order numerical scheme to a nonlinear McKendrick–Von Foerster equation with singular mortality

4.1 Introduction

Among the structured population models, one of the earliest one is due to McKendrick (later rediscovered by Von Foerster) which is popularly known as the McKendrick–Von Foerster equation (see [10, 28, 35, 82, 48, 33]). Assume that $u(x,t)$, μ, β, and $a_\dagger > 0$ denote the population density of individuals with age x at time t, the mortality rate, the fertility rate and the maximum age upto which any individual can survive, respectively. The age-structured linear McKendrick–Von Foerster equation is given by

$$\begin{cases} u_t(x,t) + u_x(x,t) + \mu(x)u(x,t) = 0, \ 0 < x < a_\dagger, \ t > 0, \\ u(0,t) = \displaystyle\int_0^{a_\dagger} \beta(x)u(x,t)dx, \ t > 0, \\ u(x,0) = u^0(x), \ 0 \le x < a_\dagger, \ 0 < x < a_\dagger, \end{cases} \tag{4.1}$$

This model is an improvement of the unstructured Verhulst model (see [28]). In the linear model (4.1), the population is assumed to be isolated and consisting of individuals living in an invariant environment with unlimited resources. Except their age, all individuals are identical. The fertility and mortality rates in this model solely depend on age. In reality, individuals compete with one another due to limited resources, and in this competition distinct advantages are there for individuals of different cohorts. To incorporate this, Gurtin and MacCamy developed a nonlinear age-dependent population model in which the mortality and fertility functions depend on the age and the total population size (see [26]). In both linear and nonlinear models, it is necessary to consider unbounded mortality rate in order to obtain that the probability of any individual to survive till or beyond the maximum age $a_\dagger$ is zero (see [42, 7, 41, 43, 44, 6, 16, 34]). However, this assumption on the mortality rate leads to additional complications while designing and analyzing numerical schemes.

In this paper, our objective is to propose and analyze a numerical scheme to find approximate solutions to the following nonlinear age-structured model

$$\begin{cases} u_t(x,t) + u_x(x,t) + \mu(x, s_1(t))u(x,t) = 0, \; 0 < x < a_\dagger, \; t > 0, \\ u(0,t) = \displaystyle\int_0^{a_\dagger} \beta(x, s_2(t))u(x,t)dx, \; t > 0, \\ u(x,0) = u^0(x), \; 0 \leq x < a_\dagger, \; 0 < x < a_\dagger, \\ s_\nu(t) = \displaystyle\int_0^{a_\dagger} \psi_\nu(x)u(x,t)dx, \; \nu = 1,2, \; t > 0, \end{cases} \tag{4.2}$$

when μ has singularity. As before, the unknown function $u(x,t)$ in (4.2) represents the age-specific density of individuals at time t. The death rate is represented by the function μ which depends on the variables x and the weighted population s_1. Similarly, the fertility rate β depends on x and s_2. Moreover, the fertility rate β, the mortality rate μ and the competition weights ψ_1 and ψ_2 are assumed to be non-negative.
In the theoretical study of (4.1), the survival probability

$$\pi(x) = \exp\left(- \int_0^x \mu(y)dy \right),$$

must be zero at the maximum age at $x = a_\dagger$, which indeed suggests us that

$$\int_0^{a_\dagger} \mu(y, s(\cdot))dy = +\infty. \tag{4.3}$$

This readily implies that μ has a singularity at $x = a_\dagger$.

Finding explicit analytical solutions of population models is infeasible except in very special cases. Therefore many authors proposed numerical schemes to age-structured model (see [1, 3, 5, 8, 17, 30, 28, 29, 40, 45, 59, 70, 71]). In particular, the numerical approximation to (4.1) and (4.2) can be obtained by different methods. Usually, in order to get convergence of the numerical schemes, uniform bounds on vital functions are required. In [34], authors considered (4.1) and pointed out that when the mortality function is unbounded, the standard finite-difference methods fail near the maximum age due to the difficulty in approximating the survival probability function. To overcome this difficulty, under some assumptions on μ, authors of [3] approximated the survival probability associated to (4.1) with a second order method. Using this result in [3], the authors of [4] obtained a second order finite diffrerence scheme to (4.1). On the other hand, the authors of [42] have designed numerical solution to (4.2) using a collocation method (Gauss–Legendre method; fourth order implicit Runge–Kutta method of two stages) which is a fourth order convergent scheme. In this work, they have considered a particular type of mortality function $\mu(x,s) = m(x)+M(x,s)$, where $m(x)$ is the natural mortality which is assumed to be in the form $m(x) = \frac{c}{(a_\dagger - x)^\alpha}$, for some $\alpha > 1,\ c > 0$ (see [32, 42]).

Above mentioned results inspired us to propose finite difference schemes to (4.2) when μ has singularity at $x = a_\dagger$. We present a third order scheme and a fourth order scheme. The main advantage of our schemes is the following. Our schemes are convergent though the mortality rate has 'essential singularity' at $x = a_\dagger$. For instance, if $\mu = e^{\frac{1}{(1-x)}}$ then the methods described in [42] are not applicable because the ubounded part of μ does not have the structure of 'pole'.

This chapter is organized as follows. In Section 4.2, we introduce a new variable λ and use it to reduce (4.2) to a nonlocal simple transport equation. Moreover, we present a finite difference scheme to approximate λ and with its help a finite difference scheme to (4.2) is proposed. We prove the main convergence theorem for the proposed schemes in Section 4.3. In Section 4.4, we establish the third order convergence of the approximation of λ. Moreover, with the help of results proved in Section 4.4, we present a fourth order approximation of λ in Section 4.5. In addition, we present a fourth order one step method to approximate λ associated to (4.1) in section 4.5. Finally, numerical examples are given in Section 4.6 to re-validate the convergence results that are proved in the earlier sections.

4.2 Scheme

Let u be the solution to (4.2). We define

$$d(x,t)=\begin{cases}\int\limits_{t-x}^{t}\mu\big(y+x-t,s_1(y)\big)dy, & t>x,\\ \int\limits_{0}^{x-t}\mu\big(y,s_1(0)\big)dy+\int\limits_{0}^{t}\mu\big(y+x-t,s_1(y)\big)dy, & t\leq x,\end{cases}\tag{4.4}$$

and

$$\lambda(x,t)=\exp(-d(x,t)).\tag{4.5}$$

From the definition, it immediately follows that λ satisfies $0\leq\lambda\leq 1$ whenever $\mu\geq 0$. We now define a new function $v(x,t)$ given by

$$u(x,t)=\lambda(x,t)v(x,t),\ 0\leq x<a_\dagger,\ t\geq 0.\tag{4.6}$$

In view of (4.2), it is straightforward to obtain

$$\begin{cases}v_t(x,t)+v_x(x,t)=0,\ 0<x<a_\dagger,\ t>0,\\ v(0,t)=\displaystyle\int_0^{a_\dagger}\beta(x,p(t))\lambda(x,t)v(x,t)dx,\ t>0,\\ v(x,0)=\dfrac{u^0(x)}{\pi(x,0)},\ 0\leq x<a_\dagger,\\ p(t)=\displaystyle\int_0^{a_\dagger}\psi_2(x)\lambda(x,t)v(x,t)dx.\end{cases}\tag{4.7}$$

For each $x\in(0,a_\dagger)$ and $\tau>0$, we know that the first equation of (4.7) satisfies

$$v(x,t)=v(x-\tau,t-\tau),\ \ x,t>\tau.\tag{4.8}$$

In fact, our method of finding the numerical approximation to (4.7) is based on (4.8).

Moreover, one can observe that if v is a weak solution to (4.7) then u is also a weak solution to (4.2).

As mentioned in the previous section, different methods were proposed to approximate the survival probability in the finite life-span case. In [3, 4, 6, 42], the authors considered a particular type of mortality profiles which were widely employed in biology problems. However, a specific behaviour of the mortality

rate was assumed near the maximum age, i.e., over an age interval $[a^*, a_\dagger)$, for the theoretical analysis of these methods. As in [3, 4, 6, 42, 43], we assume that after age a^* the mortality rate μ satisfies some growth conditions which will be described at the end of this section.
Now, given a positive integer M, we define step size $h = \frac{a_\dagger}{2M+2}$. Let $\lfloor \frac{a^*}{h} \rfloor = j_*$ for some $j_* \in \mathbb{N}$ and $\lfloor \frac{T}{h} \rfloor = N$. Denote by (x_i, t^n) a typical grid point with $x_i = ih$ and $t^n = nh$, where $0 \leq i \leq 2M+1$, $0 \leq n \leq N$.
At every grid point (x_i, t^n), let U_i^n and V_i^n denote the approximate solutions to (4.2) and (4.7), respectively. In other words, each U_i^n is the numerical approximation to $u(x_i, t^n)$ and V_i^n represents the numerical approximation to $v(x_i, t^n)$, $i = 0, 1, \dots, 2M+1$. Moreover, the approximation of the survival probability $\lambda(x_i, t^n)$ is denoted by Λ_i^n.
At each time level t^n, $n = 0, 1, \dots, N$, the numerical solution to (4.2) and (4.7) are described by the vectors

$$\boldsymbol{U^n} = [U_0^n, U_1^n, \dots, U_{2M+1}^n],\ \boldsymbol{V^n} = [V_0^n, V_1^n, \dots, V_{2M+1}^n] \in \mathbb{R}^{2M+2}.$$

Let the vector $\boldsymbol{\Lambda}^n = [\Lambda_0^n, \Lambda_1^n, \dots, \Lambda_{2M+1}^n]$ approximates the survival probability

$$\boldsymbol{\lambda}^n = [\lambda(x_0, t^n), \lambda(x_1, t^n), \dots, \lambda(x_{2M+1}, t^n)].$$

Also, we use this vector notation to represent the evaluations of the fertility rate

$$\boldsymbol{\beta}(\cdot) = [\beta(x_0, \cdot), \beta(x_1, \cdot), \dots, \beta(x_{2M+1}, \cdot)].$$

To approximate the integral term that appears in the boundary condition, we use the following quadrature rule which is a combination of the composite Simpson $\frac{1}{3}$ and Milne's rule. For the vector $\boldsymbol{Y} = [Y_0, Y_1, \dots, Y_{2M+1}]$, we define

$$\mathcal{Q}_h(\boldsymbol{Y}) = \frac{4h}{3}(2Y_1 - Y_2 + 2Y_3) + \sum_{i=2}^{M-2} \frac{h}{3}(Y_{2i} + 4Y_{2i+1} + Y_{2i+2}) + \frac{4h}{3}(2Y_{2M-1} - Y_{2M} + 2Y_{2M+1}). \tag{4.9}$$

On the other hand, for any two vectors $\boldsymbol{Y}$, $\boldsymbol{Z} \in \mathbb{R}^{2M+2}$, let $\boldsymbol{Y} \cdot \boldsymbol{Z}$ represent the usual dot product, i.e., $\boldsymbol{Y} \cdot \boldsymbol{Z} = [Y_0 Z_0, Y_1 Z_1, \dots, Y_{2M+1} Z_{2M+1}]$.
With this notation, we propose the following numerical scheme to (4.7) based on

the method of characteristics:

$$\begin{cases} V_i^n = V_{i-1}^{n-1}, \ i = 1, 2, \dots, 2M+1, \ n = 1, 2, \dots, N, \\ V_0^n = \mathcal{Q}_h(\boldsymbol{\beta}(P_\Lambda^n) \cdot \boldsymbol{\Lambda}^n \cdot \boldsymbol{V}^n), \ n = 1, 2, \dots, N, \\ V_i^0 = \dfrac{U_i^0}{\Pi_i^0}, \ i = 0, 1, \dots, 2M+1, \\ P_\Lambda^n = \mathcal{Q}_h(\boldsymbol{\psi}_2 \cdot \boldsymbol{\Lambda}^n \cdot \boldsymbol{V}^n), \ n = 1, 2, \dots, N. \end{cases} \tag{4.10}$$

Finally, to compute an approximate solution U_i^n to (4.2), we use the following relation

$$U_i^n = \Lambda_i^n V_i^n, \ i = 0, 1, \dots, 2M+1, \ n = 1, \dots, N. \tag{4.11}$$

The nontrivial part in (4.10) is to find the approximation Λ_i^n of the survival probability λ_i^n and we postpone the discussion on how to do it to Sections 4.4 and 4.5.

In order to compare the numerical and analytical solutions at each grid point, we represent the restriction of the solution u to (4.2) to the grid by the vector $\boldsymbol{u}^n = [u(x_0, t^n), u(x_1, t^n), \dots, u(x_{2M+1}^n, t^n)]$, $n = 0, 1, \dots, N$. Similarly, the restriction of the solution v to (4.7) to the grid is denoted by the vector

$$\boldsymbol{v}^n = [v(x_0, t^n), v(x_1, t^n), \dots, v(x_{2M+1}^n, t^n)], \ n = 0, 1, \dots, N.$$

For a $\boldsymbol{Y} = [Y_0, Y_1, \dots, Y_{2M+1}] \in \mathbb{R}^{2M+2}$, we define the following norms

$$\begin{aligned} ||\boldsymbol{Y}||_1 &= \sum_{i=0}^{2M+1} h|Y_i|, \\ ||\boldsymbol{Y}||_\infty &= \max_{0 \le i \le 2M+1} |Y_i|. \end{aligned} \tag{4.12}$$

It is straightforward to verify that

$$||\boldsymbol{Y}||_1 \le a_\dagger ||\boldsymbol{Y}||_\infty. \tag{4.13}$$

Then from the definition of $\mathcal{Q}_h$ given in (4.9), for every $\boldsymbol{Y},\ \boldsymbol{Z} \in \mathbb{R}^{2M+1}$, we have

$$
\begin{aligned}
|\mathcal{Q}_h(\boldsymbol{Y}\cdot\boldsymbol{Z})| \leq & \frac{4h}{3}(2|Y_1Z_1| + |Y_2Z_2| + 2|Y_3Z_3|) \\
& + \sum_{i=2}^{M-1} \frac{h}{3}(|Y_{2i}Z_{2i}| + 4|Y_{2i+1}Z_{2i+1}| + |Y_{2i+2}Z_{2i+2}|) \\
& + \frac{4h}{3}(2|Y_{2M-1}Z_{2M-1}| + |Y_{2M}Z_{2M}| + 2|Y_{2M+1}Z_{2M+1}|) \\
\leq & \frac{8}{3}||\boldsymbol{Y}||_\infty ||\boldsymbol{Z}||_1.
\end{aligned} \tag{4.14}
$$

Throughout the chapter, we make the following assumptions.
$(H1)$ Suppose $u^0,\ \beta$ are continuous, bounded, and, $\mu,\ \psi_1,\ \psi_2$ are nonnegative and sufficiently regular so that the solution to (4.2) is in $C^4([0,a_\dagger)\times[0,T])$.
Since $\psi_1,\ \psi_2$ are continuous on $[0,a_\dagger]$, for every bounded function u, the map $t\mapsto s_\nu(t)$ is a bounded function, i.e., there exists $K>0$ such that $s_\nu(t)\leq K$ for all $t\in[0,T]$, where $\nu=1,2$.
$(H2)$ For a given $s_1(t)\in C^4([0,T])$, let

$$
\begin{cases}
\int\limits_0^{a_\dagger} \mu\big(y, s_1(y+t-a_\dagger)\big)dy = \infty, & t > a_\dagger, \\
\int\limits_{a_\dagger - t}^{a_\dagger} \mu\big(y, s_1(y+t-a_\dagger)\big)dy = \infty, & t < a_\dagger.
\end{cases} \tag{4.15}
$$

$(H3)$ The function $\mu\in C^4([0,a_\dagger)\times(0,\infty))$ and $\frac{\partial^p\mu}{\partial s^p}$ are bounded in $[0,a_\dagger)\times[0,K]$, where $1\leq p\leq 4$.
$(H4)$ There exists $C>0$ such that $\frac{\partial^{(p+q)}\mu}{\partial x^p\partial s^q}\leq C\frac{\partial^{(p+q)}\mu}{\partial x^{(p+q)}}$ holds in $[0,a_\dagger)\times[0,K]$, where $1\leq p\leq 3$, $1\leq q\leq 3$ and $p+q\leq 4$.
$(H5)$ The functions

$$
\varphi(y) = \tfrac{\partial^2\mu}{\partial x^2}\big(y, s_1(0)\big)\exp\Big(-\int\limits_{a^*}^{y}\mu(z, s_1(0))dz\Big),
$$

and

$$
\rho(y) = \tfrac{\partial^4\mu}{\partial x^4}\big(y, s_1(0)\big)\exp\Big(-\int\limits_{a^*}^{y}\mu\big(z, s_1(0)\big)dz\Big),
$$

are bounded on $[a^*, a_\dagger]$.

Remark 4.2.1 From hypothesis $(H2)$, one can easily get that

$$\lim_{x\to a_\dagger} \lambda(x,\cdot) = 0. \tag{4.16}$$

Authors of [6, 32, 42] have considered the case in which the mortality rate is in the form

$$\mu(x,s) = m(x) + M(x,s), \tag{4.17}$$

where the function m is called the natural mortality that has singularity at $a_\dagger$, and the function M is called the external mortality caused due to resource competition. The mortality μ given in (4.17) satisfies hypothesis $(H2)$ due to (4.3). Moreover, it is easy to observe that μ given in (4.17) satisfies $(H3)-(H4)$. Therefore the mortality rate that we consider in this chapter is more generic one than that of (4.17).

Following theorem is ensures that at every $t > 0$ the population density vanishes at $a = a_\dagger$.

Theorem 4.2.2 *Assume* $(H1)$, *and* $v(x,0)$ *is a bounded function. Then,* v *is a bounded solution to* (4.7) *on* $[0,a_\dagger)\times[0,T]$. *Further, if* μ *satisfies* $(H2)$, *then*

$$\lim_{x\to a_\dagger} u(x,t) = 0, \quad 0 < t \le T. \tag{4.18}$$

Proof. For, $0 < t \le a_\dagger$, (4.7) gives

$$\begin{aligned}
|v(0,t)| &\le \int_0^{a_\dagger} |\beta(x,p(t))\lambda(x,t)v(x,t)|dx \\
&\le \|\beta\|_\infty\Big(\int_0^t |v(0,s)|ds + \int_0^{a_\dagger - t} |v(s,0)|ds\Big) \\
&\le \|\beta\|_\infty\Big(\int_0^t |v(0,s)|ds + a_\dagger\|v(\cdot,0)\|_\infty\Big).
\end{aligned}$$

Now, from Grönwall's lemma, we have

$$|v(0,t)| \le a_\dagger\|\beta\|_\infty\|v(\cdot,0)\|_\infty \exp(\|\beta\|_\infty a_\dagger), \ 0 < t \le a_\dagger. \tag{4.19}$$

From (4.19) and the fact $v(x,0)$ is bounded, one can get that v is a bounded on $[0,a_\dagger)\times[0,T]$.

Finally, since v is bounded, thanks to (4.16), we conclude that (4.18) holds. Throughout the chapter, we use C to denote the generic positive constant which need not be the same constant as in the preceding calculations.

4.3 A convergence result

In this section, we prove a convergence theorem provided we can approximate the survival probability λ. Notice that the quadrature rule $\mathcal{Q}_h$ given in (4.9) gives fourth order approximation. However, in the following convergence theorem, we consider a generic quadrature rule $\mathcal{Q}_h$ which is of k-th order accuracy.

Theorem 4.3.1 (Convergence) *Assume (H1)–(H5). Moreover assume that $\beta \in C^q([0,a_\dagger] \times (0,\infty))$, and $\mu \in C^q([0,a_\dagger) \times (0,\infty))$ satisfies (4.3). Let $u \in C^q([0,a_\dagger] \times [0,T])$ be the solution to (4.2). Assume that Λ_i^n denote an approximation to survival probability $\lambda(x_i,t^n)$ at each grid point such that*

$$\max_{0\le n\le N} \|\boldsymbol{\Lambda}^n - \boldsymbol{\lambda}^n\|_\infty \le Ch^l. \tag{4.20}$$

Furthermore, assume that the quadrature rule $\mathcal{Q}_h$ is of k-th order accuracy and $q = \max(l,k)$. Then the numerical approximations $\boldsymbol{U}^n$ and $\boldsymbol{V}^n$, $n = 0,1,\ldots,N$, associated to u and v, respectively, that are obtained using numerical method (4.10)–(4.11), satisfy

$$\max_{0\le n\le N} \| \boldsymbol{V}^n - \boldsymbol{v}^n \|_\infty \le Ch^r,$$

and

$$\max_{0\le n\le N} \| \boldsymbol{U}^n - \boldsymbol{u}^n \|_\infty \le Ch^r,$$

where $r = \min(l,k)$.

Proof.Step - 1: In this step, we prove that $(\|V^n\|_1)$, $(\|V^n\|_\infty)$ are bounded sequences.

From the boundary condition in (4.10), it follows that

$$
\begin{aligned}
|V_0^n| =& |\mathcal{Q}_h(\boldsymbol{\beta}(P_\Lambda^n)\cdot \mathbf{\Lambda}^n \cdot \mathbf{V}^n)| \\
\leq& \|\boldsymbol{\beta}\|_\infty \|\mathbf{\Lambda}^n\|_\infty |\mathcal{Q}_h(\mathbf{V}^n)| \\
\leq& \frac{8}{3}\|\boldsymbol{\beta}\|_\infty \|\mathbf{\Lambda}^n\|_\infty \sum_{i=1}^{2M+5} h|V_i^n| \\
\leq& C\|\boldsymbol{V}^{n-1}\|_1,
\end{aligned} \tag{4.21}
$$

for some $C > 0$. From (4.10) and (4.21), one can easily get that

$$\|\boldsymbol{V}^n\|_1 \leq (1 + Ch)\|\boldsymbol{V}^{n-1}\|_1.$$

From the discrete Gronwall lemma, there exists C_T depending solely on T such that

$$\|\boldsymbol{V}^n\|_1 \leq C_T\|\boldsymbol{V}^0\|_1, \;\; 1 \leq n \leq N. \tag{4.22}$$

From the recursive relation, for $i = 1, 2, \ldots, 2M + 1$, we can get

$$|V_i^n| = \begin{cases} |V_{i-n}^0|, & \text{if } i \geq n, \\ |V_0^{n-i}|, & \text{if } i < n. \end{cases} \tag{4.23}$$

From (4.13), (4.21), (4.22) and (4.23), we can conclude that

$$\|V^n\|_\infty \leq C\|V^0\|_\infty, \tag{4.24}$$

for some $C > 0$.

Step - 2: In this step, we estimate $||\boldsymbol{V}^n - \boldsymbol{v}^n||_1$.

Let the errors due to quadrature formula (4.9) be denoted by ε_1, ε_2, i.e.,

$$
\begin{aligned}
\varepsilon_1(t^n) =& | \; \mathcal{Q}_h(\boldsymbol{\psi}_1 \cdot \boldsymbol{\lambda}^n \cdot \boldsymbol{v}^n) - \int_0^{a_\dagger} \psi_1(x)\lambda(x,t)v(x,t)dx \; | \leq Ch^k, \\
\varepsilon_2(t^n) =& | \; \mathcal{Q}_h(\boldsymbol{\beta}(p(t^n)) \cdot \boldsymbol{\lambda}^n \cdot \boldsymbol{v}^n) - \int_0^{a_\dagger} \beta(x, p(t^n))\lambda(x,t)v(x,t^n)dx \; | \leq Ch^k,
\end{aligned} \tag{4.25}
$$

for some $C > 0$ independent of n and h, where $n = 0, 1, \dots, N$. Furthermore, we have

$$| V_i^n - v(x_i, t^n) | = | V_{i-1}^{n-1} - v(x_{i-1}, t^{n-1}) |, \ i = 1, 2, \dots, 2M+1. \tag{4.26}$$

We define $p_\Lambda^n = \mathcal{Q}_h(\boldsymbol{\psi}_2 \cdot \boldsymbol{\Lambda}^n \cdot \boldsymbol{v}^n)$ and $p_\lambda^n = \mathcal{Q}_h(\boldsymbol{\psi}_2 \cdot \boldsymbol{\lambda}^n \cdot \boldsymbol{v}^n)$.
On the other hand, from the boundary condition, we obtain

$$\begin{aligned}
| V_0^n - v(0, t^n) | = & \ | \mathcal{Q}_h(\boldsymbol{\beta}(P_\Lambda^n) \cdot \boldsymbol{\Lambda}^n \cdot \boldsymbol{V}^n) - \int_0^{a_\dagger} \beta(x, p(t^n))\lambda(x,t)v(x,t^n)dx | \\
\le & \ | \mathcal{Q}_h(\boldsymbol{\beta}(P_\Lambda^n) \cdot \boldsymbol{\Lambda}^n \cdot \boldsymbol{V}^n) - \mathcal{Q}_h(\boldsymbol{\beta}(p_\Lambda^n) \cdot \boldsymbol{\Lambda}^n \cdot \boldsymbol{V}^n) | \\
& + | \mathcal{Q}_h(\boldsymbol{\beta}(p_\Lambda^n) \cdot \boldsymbol{\Lambda}^n \cdot \boldsymbol{V}^n) - \mathcal{Q}_h(\boldsymbol{\beta}(p_\lambda^n) \cdot \boldsymbol{\Lambda}^n \cdot \boldsymbol{V}^n) | \\
& + | \mathcal{Q}_h(\boldsymbol{\beta}(p_\lambda^n) \cdot \boldsymbol{\Lambda}^n \cdot \boldsymbol{V}^n) - \mathcal{Q}_h(\boldsymbol{\beta}(p(t^n)) \cdot \boldsymbol{\Lambda}^n \cdot \boldsymbol{V}^n) | \\
& + | \mathcal{Q}_h(\boldsymbol{\beta}(p(t^n)) \cdot \boldsymbol{\Lambda}^n \cdot \boldsymbol{V}^n) - \mathcal{Q}_h(\boldsymbol{\beta}(p(t^n)) \cdot \boldsymbol{\Lambda}^n \cdot \boldsymbol{v}^n) | \\
& + | \mathcal{Q}_h(\boldsymbol{\beta}(p(t^n)) \cdot \boldsymbol{\Lambda}^n \cdot \boldsymbol{v}^n) - \mathcal{Q}_h(\boldsymbol{\beta}(p(t^n)) \cdot \boldsymbol{\lambda}^n \cdot \boldsymbol{v}^n) | \\
& + | \mathcal{Q}_h(\boldsymbol{\beta}(p(t^n)) \cdot \boldsymbol{\lambda}^n \cdot \boldsymbol{v}^n) - \int_0^{a_\dagger} \beta(x, p(t^n))\lambda(x,t)v(x,t^n)dx | \\
\le & C||\boldsymbol{V}^n - \boldsymbol{v}^n||_1 + C||\boldsymbol{\Lambda}^n - \boldsymbol{\lambda}^n||_\infty + \varepsilon_1(t^n) + \varepsilon_2(t^n).
\end{aligned} \tag{4.27}$$

Therefore from (4.26) and (4.27), it is follows that

$$\begin{aligned}
||\boldsymbol{V}^n - \boldsymbol{v}^n||_1 = & \sum_{i=0}^{2M+1} h|V_i^n - v(x_i, t^n)| \\
= & h|V_0^n - v(0, t^n)| + \sum_{i=0}^{2M} h|V_{i+1}^n - v(x_{i+1}, t^n)| \\
\le & h\Big(C||\boldsymbol{V}^n - \boldsymbol{v}^n||_1 + C||\boldsymbol{\Lambda}^n - \boldsymbol{\lambda}^n||_\infty + \varepsilon_1(t^n) + \varepsilon_2(t^n)\Big) \\
& + ||\boldsymbol{V}^{n-1} - \boldsymbol{v}^{n-1}||_1.
\end{aligned} \tag{4.28}$$

For sufficiently small h, the discrete Gronwall lemma gives

$$||\boldsymbol{V}^n - \boldsymbol{v}^n||_1 = C \left(||\boldsymbol{V}^0 - \boldsymbol{v}^0||_1 + h \sum_{j=0}^{n} \left[||\boldsymbol{\Lambda}^j - \boldsymbol{\lambda}^j||_\infty + \varepsilon_1(t^j) + \varepsilon_2(t^j) \right] \right), \tag{4.29}$$

where C is independent of h. In view of $||\boldsymbol{V}^0 - \boldsymbol{v}^0||_\infty = 0$, (**??**), (4.25) and (4.29), we have

$$||\boldsymbol{V}^n - \boldsymbol{v}^n||_1 \leq Ch^r, \ n = 0, 1, 2, \ldots, N, \tag{4.30}$$

for some $C > 0$ independent of n and h, where $r = \min(l, k)$.

Step - 3: We now estimate the error $||\boldsymbol{V}^n - \boldsymbol{v}^n||_\infty, \ n = 1, 2, \ldots, N$. For, due to (4.25), (4.27) and (4.30), it follows that

$$|V_0^n - v(0, t^n)| \leq Ch^r, \ n = 0, 1, 2, \ldots, N. \tag{4.31}$$

From the definition of V_i^n, for $i = 1, 2, \ldots, 2M + 1$, we can get

$$|V_i^n - v(x_i, t^n)| = \begin{cases} |V_{i-n}^0 - v(x_{i-n}, 0)|, & \text{if } i \geq n, \\ |V_0^{n-i} - v(0, t^{n-i})|, & \text{if } i < n. \end{cases} \tag{4.32}$$

Now from (4.31)–(4.32), and $V_i^0 = v(x_i, 0)$, $1 \leq i \leq 2M + 1$, we obtain

$$|V_i^n - v(x_i, t^n)| \leq Ch^r, \ 0 \leq n \leq N,$$

or

$$\max_{0 \leq n \leq N} || \ \boldsymbol{V}^n - \boldsymbol{v}^n \ ||_\infty \leq Ch^r. \tag{4.33}$$

Step - 4: We estimate $\|\boldsymbol{U}^n - \boldsymbol{u}^n\|_\infty$ in this step.

Consider

$$\begin{aligned} |U_i^n - u(x_i, t^n)| &= |\Lambda_i^n V_i^n - \lambda(x_i, t^n) v(x_i, t^n)| \\ &\leq |\Lambda_i^n||V_i^n - v(x_i, t^n)| + |v(x_i, t^n)||\Lambda_i^n - \lambda(x_i, t^n)|. \end{aligned} \tag{4.34}$$

Finally, from (**??**), (4.33) and (4.34), we conclude that

$$\max_{0 \leq n \leq N} \|\boldsymbol{U}^n - \boldsymbol{u}^n\|_\infty \leq Ch^r. \tag{4.35}$$

This completes the proof.

Remark 4.3.2 Step 1 of Theorem 4.3.1 readily implies that scheme (4.10) is stable in L^∞ norm.

4.4 A third order approximation of λ

In this section, we approximate λ in the following three iterative steps. This is a predictor-corrector method in which we correct the approximate value of λ twice.
Step–1 First we define

$$\begin{aligned}
&\widehat{U}^0 = u_0(x_i),\ 0 \le i \le 2M+1, && (4.36)\\
&\widehat{\boldsymbol{S}}^0_\nu = \mathcal{Q}_h(\boldsymbol{\psi}_\nu \cdot \widehat{\boldsymbol{U}}^0), \quad \nu = 1, 2, && (4.37)\\
&D^0_i = \frac{h}{6}\sum_{j=1}^{i}\Big[\mu\big((j-1)h, \widehat{\boldsymbol{S}}^0_1\big) + 4\mu\big((j-\frac{1}{2})h, \widehat{\boldsymbol{S}}^0_1\big) + \mu\big(jh, \widehat{\boldsymbol{S}}^0_1\big)\Big], && (4.38)\\
&\bar{D}^0_i = \tilde{D}^0_i = \hat{D}^0_i = D^0_i,\ 1 \le i \le 2M+1,\\
&\bar{D}^n_0 = \tilde{D}^n_0 = \hat{D}^n_0 = 0,\ 0 \le n \le N,
\end{aligned}$$

and

$$\bar{D}^n_i = \widehat{D}^{n-1}_{i-1} + \frac{h}{2}\Big[\mu\big((i-1)h, \widehat{\boldsymbol{S}}^{n-1}_1\big) + \mu\big(ih, \widehat{\boldsymbol{S}}^{n-1}_1\big)\Big], \quad n, i \ge 1, \tag{4.39}$$

where $\widehat{D}^{n-1}_{i-1}$ and $\widehat{S}^{n-1}_1$ are defined in Step-3. We approximate the survival probability function $\lambda(x,t)$ at each grid point by

$$\bar{\Lambda}^n_i = \exp(-\bar{D}^n_i). \tag{4.40}$$

Now, from (4.10)–(4.11) (on substituting $\Lambda^n_i = \bar{\Lambda}^n_i$), we get $\bar{U}^n_i$. Set

$$\bar{\boldsymbol{S}}^n_\nu = \mathcal{Q}_h(\boldsymbol{\psi}_\nu \cdot \bar{\boldsymbol{U}}^n), \quad \nu = 1, 2. \tag{4.41}$$

Step–2 In this step, we first update $\bar{D}^n_i$ to obtain

$$\widetilde{D}^n_i = \widehat{D}^{n-1}_{i-1} + \frac{h}{2}\Big[\mu\big((i-1)h, \widehat{\boldsymbol{S}}^{n-1}_1\big) + \mu\big(ih, \bar{\boldsymbol{S}}^n_1\big)\Big], \quad n, i \ge 1. \tag{4.42}$$

We now correct the approximated survival probability function Λ^n_i at each grid point by replacing $\bar{D}^n_i$ with $\widetilde{D}^n_i$, i.e.,

$$\widetilde{\Lambda}^n_i = \exp(-\widetilde{D}^n_i). \tag{4.43}$$

As in the previous step, we substitute $\Lambda_i^n = \widetilde{\Lambda}_i^n$ in (4.10)–(4.11) to get $\widetilde{U}_i^n$. In this step, we correct the approximate weighted population to arrive at

$$\widetilde{\boldsymbol{S}}_\nu^n = \mathcal{Q}_h(\boldsymbol{\psi}_\nu \cdot \widetilde{\boldsymbol{U}}^n). \tag{4.44}$$

Step–3 We now make the final correction to $\widetilde{D}$ to get

$$\widehat{D}_i^n = \begin{cases} \widehat{D}_{i-1}^{n-1} + \dfrac{h}{2}\Big[\mu\big((i-1)h, \widehat{\boldsymbol{S}}_1^{n-1}\big) + \mu\big(ih, \widetilde{\boldsymbol{S}}_1^n\big)\Big], \quad n = 1, \text{ or } i = 1, \\ \widehat{D}_{i-2}^{n-2} + \dfrac{h}{3}\Big[\mu\big((i-2)h, \widehat{\boldsymbol{S}}_1^{n-2}\big) + 4\mu\big((i-1)h, \widehat{\boldsymbol{S}}_1^{n-1}\big) \\ +\mu\big(ih, \widetilde{\boldsymbol{S}}_1^n\big)\Big], \quad n, i \geq 2. \end{cases} \tag{4.45}$$

We now correct $\widetilde{\Lambda}$ once more to find

$$\widehat{\Lambda}_i^n = \exp(-\widehat{D}_i^n). \tag{4.46}$$

As before, we use (4.10)–(4.11), with $\Lambda_i^n = \widehat{\Lambda}_i^n$ to get the updated value of solution of (4.2) namely $\widetilde{U}_i^n$. We now define

$$\widehat{\boldsymbol{S}}_\nu^n = \mathcal{Q}_h(\boldsymbol{\psi}_\nu \cdot \widehat{\boldsymbol{U}}^n), \quad \nu = 1, 2. \tag{4.47}$$

Note that the survival probability vanishes only at the maximum age, but $a_\dagger$ is not a grid point.

We prove the following technical lemma, which plays an important role in obtaining the convergence of $\widehat{\Lambda}_i^n$ to λ_i^n.

Lemma 4.4.1 *Let $u \in C^4([0, a_\dagger] \times [0, T])$ be the solution to (4.2) and U_i^n be an approximation of $u(x, t)$ at every grid points (x_i, t^n) with r-th order accuracy, where $2 \leq r \leq 4$. Assume that $\mu \in C^4([0, a_\dagger) \times (0, \infty))$ and $\|\frac{\partial \mu}{\partial s}\|_\infty$ bounded on $[0, a_\dagger) \times [0, K]$. Then there exit $0 < \eta_1,\ \eta_2,\ \eta_3 < h$ such that*

$$\begin{aligned} &\left| \int_{t^{n-1}}^{t^n} \mu\big(y + x_i - t^n, s_1(y)\big) dy - \frac{h}{2}\Big[\mu\big((i-1)h, \boldsymbol{S}_1^{n-1}\big) + \mu\big(ih, \boldsymbol{S}_1^n\big)\Big] \right| \\ \leq &\left| \frac{d^2}{dy^2}[\mu\big(\eta_1 + x_i - t^n, s_1(\eta_1)\big)] \right| \frac{h^3}{12} + Ch^3, \end{aligned} \tag{4.48}$$

$$\begin{aligned}
&\Big|\int\limits_{t^{n-1}}^{t^n} \mu\big(y+x_i-t^n, s_1(y)\big)dy - \frac{h}{2}\Big[\mu\big((i-1)h, \boldsymbol{S}_1^{n-1}\big)+\mu\big(ih, \boldsymbol{S}_1^{n-1}\big)\Big]\Big| \\
\le& \Big|\frac{d^2}{dy^2}[\mu\big(\eta_2+x_i-t^n, s(\eta_2)\big)]\Big|\frac{h^3}{12}+Ch^2,
\end{aligned} \tag{4.49}$$

and

$$\begin{aligned}
&\Big|\int\limits_{t^{n-2}}^{t^n} \mu\big(y+x_i-t^n, s_1(y)\big)dy - \frac{h}{3}\Big[\mu\big((i-2)h, \boldsymbol{S}_1^{n-2}\big)+4\mu\big((i-1)h, \boldsymbol{S}_1^{n-1}\big) \\
&+\mu\big(ih, \boldsymbol{S}_1^{n}\big)\Big]\Big| \le \Big|\frac{d^4}{dy^4}[\mu\big(\eta_3+x_i-t^n, s_1(\eta_3)\big)]\Big|\frac{h^5}{90}+Ch^{r+1},
\end{aligned} \tag{4.50}$$

for $1 \le i \le 2M+1$, $1 \le n \le N$.

Proof. Since ψ_1 is a bounded function, for $n = 1, 2, \dots, N$, we have the following

$$|\boldsymbol{s}_1^{n-1} - \boldsymbol{S}_1^{n-1}| = |\mathcal{Q}_h(\boldsymbol{\psi}_1 \cdot \boldsymbol{u}^{n-1}) - \mathcal{Q}_h(\boldsymbol{\psi}_1 \cdot \boldsymbol{U}^{n-1})| \le Ch^r. \tag{4.51}$$

Using (4.51), we obtain

$$\begin{aligned}
|\mu\big((i-1)h, \boldsymbol{s}_1^{n-1}\big) - \mu\big((i-1)h, \boldsymbol{S}_1^{n-1}\big)| \le& \|\frac{\partial\mu}{\partial s}\|_\infty |\boldsymbol{s}_1^{n-1} - \boldsymbol{S}_1^{n-1}| \\
\le& Ch^r,
\end{aligned} \tag{4.52}$$

for every $n = 1, 2, \dots, N, \;\; i = 1, \dots, j_*$. Since the quadrature formula $\mathcal{Q}_h$ that we use is of fourth order, it follows that

$$|\mu\big((i-1)h, s_1(t^{n-1})\big) - \mu\big((i-1)h, \boldsymbol{s}_1^{n-1}\big)| \le Ch^4. \tag{4.53}$$

From the trapezoidal rule (see [9]), we get that, for $n = 1, 2, \dots, N$, and $1 \le i \le 2M+1$,

$$\begin{aligned}
&\frac{h}{2}\Big[\mu\big((i-1)h, s_1(t^{n-1})\big)+\mu\big(ih, s_1(t^n)\big)\Big] - \int\limits_{t^{n-1}}^{t^n} \mu\big(y+x_i-t^n, s_1(y)\big)dy \\
=& \frac{d^2}{dy^2}[\mu\big(y+x_i-t^n, s_1(y)\big)]\Big|_{y=\eta_1}\frac{h^3}{12},
\end{aligned} \tag{4.54}$$

where $\eta_1 \in (0,h)$.
On the other hand, in view of (4.52)–(4.54) we find that

$$\begin{aligned}
&\Big|\int_{t^{n-1}}^{t^n} \mu\big(y+x_i-t^n, s_1(y)\big)dy - \frac{h}{2}\Big[\mu\big((i-1)h, \boldsymbol{S}_1^{n-1}\big)+\mu\big(ih, \boldsymbol{S}_1^{n}\big)\Big]\Big| \\
\leq &\Big|\int_{t^{n-1}}^{t^n} \mu\big(y+x_i-t^n, s_1(y)\big)dy - \frac{h}{2}\Big[\mu\big((i-1)h, s_1(t^{n-1})\big)+\mu\big(ih, s_1(t^{n})\big)\Big]\Big| \\
&+\frac{h}{2}\Big|\mu\big((i-1)h, s_1(t^{n-1})\big)+\mu\big(ih, s_1(t^{n})\big)-\mu\big((i-1)h, \boldsymbol{s}_1^{n-1}\big) \\
&-\mu\big(ih, \boldsymbol{s}_1^{n}\big)\Big| + \frac{h}{2}\Big|\mu\big((i-1)h, \boldsymbol{s}_1^{n-1}\big)+\mu\big(ih, \boldsymbol{s}_1^{n}\big) \\
&-\mu\big((i-1)h, \boldsymbol{S}_1^{n-1}\big)-\mu\big(ih, \boldsymbol{S}_1^{n}\big)\Big| \\
\leq &\Big|\frac{d^2}{dy^2}[\mu\big(\eta_1+x_i-t^n, s_1(\eta_1)\big)]\Big|\frac{h^3}{12}+Ch^{r+1}.
\end{aligned} \tag{4.55}$$

This proves (4.48). On repeating similar calculations in the derivation of (4.55), we can write

$$\begin{aligned}
&\Big|\int_{t^{n-1}}^{t^n} \mu\big(y+x_i-t^n, s_1(y)\big)dy - \frac{h}{2}\Big[\mu\big((i-1)h, \boldsymbol{S}_1^{n-1}\big)+\mu\big(ih, \boldsymbol{S}_1^{n-1}\big)\Big]\Big| \\
\leq &\Big|\frac{d^2}{dy^2}[\mu\big(\eta_2+x_i-t^n, s_1(\eta_2)\big)]\Big|\frac{h^3}{12}+Ch^3+\frac{h}{2}\Big|\mu\big(ih, s_1(t^n)\big)-\mu\big(ih, s_1(t^{n-1})\big)\Big| \\
\leq &\Big|\frac{d^2}{dy^2}[\mu\big(\eta_2+x_i-t^n, s(\eta_2)\big)]\Big|\frac{h^3}{12}+Ch^2.
\end{aligned} \tag{4.56}$$

This completes the proof of (4.49). We use the same strategy to prove (4.50). For, from the Simpson's $\frac{1}{3}$ quadrature rule (see [9]), we obtain that for $n = 1, 0, \ldots, N$, $i = 0, 1, \ldots, 2M+1$

$$\begin{aligned}
&\frac{h}{3}\Big[\mu\big((i-2)h, s_1(t^{n-2})\big)+4\mu\big((i-1)h, s_1(t^{n-1})\big)+\mu\big(ih, s_1(t^n)\big)\Big] \\
&-\int_{t^{n-2}}^{t^n} \mu\big(y+x_i-t^n, s_1(y)\big)dy = \frac{d^4}{dy^4}[\mu\big(\eta_1+x_i-t^n, s_1(\eta_1)\big)]\frac{h^5}{90},
\end{aligned} \tag{4.57}$$

for some $\eta_2 \in (0, 2h)$.
Moreover, in view of (4.52), (4.53) and (4.57) we get that

$$\begin{aligned}
&\Big|\int_{t^{n-2}}^{t^n} \mu\big(y + x_i - t^n, s_1(y)\big)dy - \frac{h}{3}\Big[\mu\big((i-2)h, \boldsymbol{S}_1^{n-2}\big) \\
&+ 4\mu\big((i-1)h, \boldsymbol{S}_1^{n-1}\big) + \mu\big(ih, \boldsymbol{S}_1^{n}\big)\Big]\Big| \\
\leq&\Big|\int_{t^{n-2}}^{t^n} \mu\big(y + x_i - t^n, s_1(y)\big)dy - \frac{h}{3}\Big[\mu\big((i-2)h, s_1(t^{n-2})\big) \\
&+ 4\mu\big((i-1)h, s_1(t^{n-1})\big) + \mu\big(ih, s_1(t^{n})\big)\Big]\Big| \\
&+ \frac{h}{3}\Big|\mu\big((i-2)h, s_1(t^{n-2})\big) + 4\mu\big((i-1)h, s_1(t^{n-1})\big) + \mu\big(ih, s_1(t^{n})\big) \\
&- \mu\big((i-2)h, \boldsymbol{s}_1^{n-2}\big) - 4\mu\big((i-1)h, \boldsymbol{s}_1^{n-1}\big) - \mu\big(ih, \boldsymbol{s}_1^{n}\big)\Big| \\
&+ \frac{h}{3}\Big|\mu\big((i-2)h, \boldsymbol{s}_1^{n-2}\big) + 4\mu\big((i-1)h, \boldsymbol{s}_1^{n-1}\big) + \mu\big(ih, \boldsymbol{s}_1^{n}\big) \\
&- \mu\big((i-2)h, \boldsymbol{S}_1^{n-2}\big) - 4\mu\big((i-1)h, \boldsymbol{S}_1^{n-1}\big) - \mu\big(ih, \boldsymbol{S}_1^{n}\big)\Big| \\
\leq&\Big|\frac{d^4}{dy^4}[\mu\big(\eta_3 + x_i - t^n, s_1(\eta_3)\big)]\Big|\frac{h^5}{90} + Ch^{r+1},
\end{aligned} \tag{4.58}$$

which readily gives (4.50). This proves the promised result. Besides this lemma the following standard inequality is also very useful in this section

$$|e^{-x} - e^{-y}| \leq |x - y|, \ \forall x, y \geq 0. \tag{4.59}$$

In the following, we show that $\widehat{\boldsymbol{\Lambda}}$ is indeed a third order approximation of $\boldsymbol{\lambda}$ in $[0, x_{j_*}]$.

Theorem 4.4.2 *Assume hypotheses (H1)–(H5). Moreover assume that* $\mu \in C^4([0, a_\dagger) \times (0, \infty))$, $\frac{d^2\mu}{dy^2}(y, s_1(y + \alpha)) \geq 0$ *and* $\frac{d^4\mu}{dy^4}(y, s_1(y + \alpha)) \geq 0$ *for all* $y \in [a^*, a_\dagger)$ *and* $\alpha \geq -a^*$. *Let* $u \in C^4([0, a_\dagger] \times [0, T])$ *be the solution to (4.2). Then*

$$\|\widehat{\boldsymbol{\Lambda}}^n - \boldsymbol{\lambda}^n\|_\infty \leq Ch^3, \quad 0 \leq n \leq N, \tag{4.60}$$

where C is a constant independent of n, h.

In view of the assumptions on the behavior of μ around the singularity, we prove Theorem 4.4.2 in two parts. In the first part, we estimate $|\widehat{\Lambda}_i^n - \lambda(x_i, t^n)|$ when $0 \le i \le j_*$. In the other part, we estimate the same near the singularity i.e., $j_* + 1 \le i \le 2M + 1$.

Theorem 4.4.3 *Assume the hypotheses of Theorem 4.4.2. Then*

$$\max_{0 \le i \le j_*} |\widehat{\Lambda}_i^n - \lambda(x_i, t^n)| \le Ch^3, \quad 0 \le n \le N, \tag{4.61}$$

where C is a constant independent of n, h.

Theorem 4.4.4 *Assume the hypotheses of Theorem 4.4.2. Then*

$$\max_{j_*+1 \le i \le 2M+1} |\widehat{\Lambda}_i^n - \lambda(x_i, t^n)| \le Ch^3, \quad 0 \le n \le N, \tag{4.62}$$

where C is a constant independent of n, h.

Due to the nature of numerical scheme (4.10), at each stage proofs of Theorem 4.4.3 and 4.4.4 depend on each other. In particular, the proof of Step–1 of Theorem 4.4.4 depends on Step–1 of Theorem 4.4.3. To prove Step–2 of Theorem 4.4.3, we need Step–1 of both the Theorems. We prove Step–2 of Theorem 4.4.4 using Step–2 of Theorem 4.4.3 and Step–1 of both the Theorems. We follow the same strategy to prove the others steps. We have adopted this way of presenting proofs because the proof of Theorem 4.4.3 is too long.

Proof of Theorem 4.4.3. Observe that $\mu(x, s)$ is fourth times continuously differentiable when $x \in [0, a^*]$ and it has bounded derivatives with respect to s. Therefore from (4.48)–(4.50), we obtain that

$$\left| \int_{t^{n-1}}^{t^n} \mu\big(y + x_i - t^n, s_1(y)\big)dy - \frac{h}{2}\Big[\mu\big((i-1)h, \boldsymbol{S}_1^{n-1}\big) + \mu\big(ih, \boldsymbol{S}_1^n\big)\Big]\right| \le Ch^3, \tag{4.63}$$

$$\left| \int_{t^{n-1}}^{t^n} \mu\big(y + x_i - t^n, s_1(y)\big)dy - \frac{h}{2}\Big[\mu\big((i-1)h, \boldsymbol{S}_1^{n-1}\big) + \mu\big(ih, \boldsymbol{S}_1^{n-1}\big)\Big]\right| \le Ch^2, \tag{4.64}$$

and

$$\Big|\int_{t^{n-2}}^{t^n} \mu\big(y+x_i-t^n, s_1(y)\big)dy - \frac{h}{3}\Big[\mu\big((i-2)h, \boldsymbol{S}_1^{n-2}\big) + 4\mu\big((i-1)h, \boldsymbol{S}_1^{n-1}\big)$$
$$+ \mu\big(ih, \boldsymbol{S}_1^{n}\big)\Big]\Big| \leq Ch^4, \tag{4.65}$$

where $2 \leq r \leq 4$. In view of (4.39), (4.42) and (4.45), we find that

$$\widehat{\Lambda}_0^n = \lambda(0, t^n),\ \ n = 0, 1, \ldots, N.$$

Step–1: Consider $n = 0$ and $i = 1, \ldots, j_*$. Since

$$\Big|\int_0^{x_i} \mu\big(y, s_1(0)\big)dy - \frac{h}{6}\sum_{j=1}^{i}\Big[\mu\big((j-1)h, \widehat{\boldsymbol{S}}_1^0\big) + 4\mu\big((j-\frac{1}{2})h, \widehat{\boldsymbol{S}}_1^0\big)$$
$$+ \mu\big(jh, \widehat{\boldsymbol{S}}_1^0\big)\Big]\Big| \leq Ch^4, \tag{4.66}$$

from (4.59), we conclude that

$$|\widehat{\Lambda}_i^0 - \lambda(x_i, t^0)| \leq Ch^4,\ \ i = 0, 1, \ldots, j_*.$$

Step–2: Let $n = 1$ and $i = 1, \ldots, j_*$.
From (4.63) and (4.66), it follows that

$$\begin{aligned}
&|d(x_i, t^1) - \bar{D}_i^1| \\
=&\Big|\int_0^{x_i-t^1} \mu\big(y, s_1(0)\big)dy + \int_0^{t^1} \mu\big(y+x_i-t^1, s_1(y)\big)dy - \widehat{D}_{i-1}^0 \\
&-\frac{h}{2}\Big[\mu\big((i-1)h, \widehat{\boldsymbol{S}}_1^0\big) + \mu\big(ih, \widehat{\boldsymbol{S}}_1^0\big)\Big]\Big| \\
\leq& Ch^4 + Ch^2 \leq Ch^2.
\end{aligned} \tag{4.67}$$

Using (4.59) and (4.67), we conclude that

$$|\bar{\Lambda}_i^1 - \lambda(x_i, t^1)| \leq Ch^2, \quad i = 0, 1, \ldots, j_*. \tag{4.68}$$

From Step–2 of Theorem 4.4.4, it follows that

$$|\bar{\Lambda}_i^1 - \lambda(x_i, t^1)| \le Ch^2, \quad i = j_* + 1, \dots, 2M + 1. \tag{4.69}$$

On taking $\Lambda_i^1 = \bar{\Lambda}_i^1$, $U_i^1 = \bar{U}_i^1$ in Theorem 4.3.1 and using (4.68)–(4.69), we get

$$\| \bar{\boldsymbol{U}}^1 - \boldsymbol{u}^1 \|_\infty \le Ch^3. \tag{4.70}$$

Again from (4.63) and (4.66), we get

$$\begin{aligned}
&|d(x_i, t^1) - \widetilde{D}_i^1| \\
\le &\left| \int_0^{t^1} \mu\big(y + x_i - t^1, s_1(y)\big) dy - \frac{h}{2}\Big[\mu\big((i-1)h, \widehat{\boldsymbol{S}}_1^0\big) + \mu\big(ih, \bar{\boldsymbol{S}}_1^1\big)\Big] \right| + Ch^4 \\
\le &Ch^4 + Ch^3 \le Ch^3.
\end{aligned} \tag{4.71}$$

As before using (4.59) and (4.71), we obtain

$$|\widetilde{\Lambda}_i^1 - \lambda(x_i, t^1)| \le Ch^3, \;\; i = 0, 1, \dots, j_*. \tag{4.72}$$

On taking $\Lambda_i^1 = \widetilde{\Lambda}_i^1$ and $U_i^1 = \widetilde{U}_i^1$ in Theorem 4.3.1 and using the similar argument employed to prove (4.89), we find that

$$\| \tilde{\boldsymbol{U}}^1 - \boldsymbol{u}^1 \|_\infty \le Ch^3. \tag{4.73}$$

Now using the same argument, we can easily prove that

$$|\widehat{\Lambda}_i^1 - \lambda(x_i, t^1)| \le Ch^3, \;\; i = 0, 1, \dots, j_*, \tag{4.74}$$

and

$$\| \tilde{\boldsymbol{U}}^1 - \boldsymbol{u}^1 \|_\infty \le Ch^3. \tag{4.75}$$

Step–3: Assume $n = 2$ and $i = 1, \dots, j_*$.
There are two possibilities in this case, viz., one is $i \ge 2$ and the other one is $i \in \{0, 1\}$. We consider the case $i \ge 2$ now, and the other situation can be dealt in a similar way.

Using the similar argument to obtain (4.72)–(4.73), we get

$$|\widetilde{\Lambda}_i^2 - \lambda(x_i, t^2)| \le Ch^3, \ i = 0, 1, \ldots, j_*. \tag{4.76}$$

and

$$\| \tilde{\boldsymbol{U}}^1 - \boldsymbol{u}^1 \|_\infty \le Ch^3. \tag{4.77}$$

From (4.65)–(4.66) and (4.76)–(4.77), we obtain

$$\begin{aligned}
&|d(x_i, t^2) - \widehat{D}_i^2| \\
\le& \Big| \int_0^{t^2} \mu\big(y + x_i - t^2, s_1(y)\big) dy - \frac{h}{3}\Big[\mu\big((i-2)h, \widehat{\boldsymbol{S}}_1^0\big) + 4\mu\big((i-1)h, \widehat{\boldsymbol{S}}_1^1\big) \\
&\quad + \mu\big(ih, \widetilde{\boldsymbol{S}}_1^2\big)\Big] + Ch^4 \\
\le& Ch^4.
\end{aligned} \tag{4.78}$$

From (4.78), thanks to (4.59), it immediately follows that

$$|\widehat{\Lambda}_i^2 - \lambda(x_i, t^2)| \le 2Ch^4, \ i = 2, 3, \ldots, j_*.$$

As before, on substituting $\Lambda_i^2 = \widehat{\Lambda}_i^2$ in Theorem 4.3.1, we obtain $U_i^2 = \widehat{U}_i^2$ which satisfies

$$\| \hat{\boldsymbol{U}}^2 - \boldsymbol{u}^2 \|_\infty \le Ch^3. \tag{4.79}$$

Step–4: In this we employ the induction argument to prove the required the result.
For, Assume

$$\begin{aligned}
|d(x_i, t^m) - \widehat{D}_i^m| \le& \Big\lfloor m - 2\lfloor\frac{m}{2}\rfloor\Big\rfloor C_1 h^3 + \left(1 + \lfloor\frac{m}{2}\rfloor\right) C_2 h^4 \\
\le& Ch^3, \ i = m, \ldots, j_*, \ m = 0, 1, \ldots, n-1,
\end{aligned} \tag{4.80}$$

and

$$\begin{aligned}
|d(x_i, t^m) - \widehat{D}_i^m| \le& \Big\lfloor i - 2\lfloor\frac{i}{2}\rfloor\Big\rfloor C_1 h^3 + \lfloor\frac{i}{2}\rfloor C_2 h^4 \\
\le& Ch^3, \ i = 0, 1, \ldots, m-1, \ m = 0, 1, \ldots, n-1,
\end{aligned} \tag{4.81}$$

where $\lfloor\cdot\rfloor$ denote the floor function. The motivation for assumptions (4.80)–(4.81) lies in the calculations presented in the earlier steps. First, consider the case $i \geq n$.

Now from (4.63) and (4.80), we obtain

$$
\begin{aligned}
&\left|d(x_i,t^n)-\bar{D}_i^n\right| \\
=&\Big|\int\limits_0^{x_i-t^n}\mu\big(y,s_1(0)\big)dy+\int\limits_0^{t^n}\mu\big(y+x_i-t^m,s_1(y)\big)dy-\widehat{D}_{i-1}^{n-1} \\
&-\frac{h}{2}\Big[\mu\big((i-1)h,\widehat{\boldsymbol{S}}_1^{n-1}\big)+\mu\big(ih,\widehat{\boldsymbol{S}}_1^{n-1}\big)\Big]\Big| \\
=&\Big|\int\limits_0^{x_{i-1}-t^{n-1}}\mu\big(y,s_1(0)\big)dy+\int\limits_0^{t^{n-1}}\mu\big(y+x_{i-1}-t^{n-1},s_1(y)\big)dy \\
&+\int\limits_{t^{n-1}}^{t^n}\mu\big(y+x_i-t^n,s_1(y)\big)dy-\widehat{D}_{i-1}^{n-1}-\frac{h}{2}\Big[\mu\big((i-1)h,\widehat{\boldsymbol{S}}_1^{n-1}\big)+\mu\big(ih,\widehat{\boldsymbol{S}}_1^{n-1}\big)\Big]\Big| \\
\leq&\Big|\int\limits_{t^{n-1}}^{t^n}\mu\big(y+x_i-t^n,s_1(y)\big)dy-\frac{h}{2}\Big[\mu\big((i-1)h,\widehat{\boldsymbol{S}}_1^{n-1}\big)+\mu\big(ih,\widehat{\boldsymbol{S}}_1^{n-1}\big)\Big]\Big| \\
&+\Big[(n-1)-2\lfloor\frac{n-1}{2}\rfloor\Big]C_1h^3+\left(1+\lfloor\frac{n-1}{2}\rfloor\right)C_2h^4 \\
\leq&Ch^2+\Big[(n-1)-2\lfloor\frac{n-1}{2}\rfloor\Big]C_1h^3+\left(1+\lfloor\frac{n-1}{2}\rfloor\right)C_2h^4\leq Ch^2.
\end{aligned}
\tag{4.82}
$$

Next, we proceed to the situation where $n > i$.
Then from (4.64) and (4.81), we readily get

$$
|d(x_i,t^n)-\bar{D}_i^n|\leq Ch^2+\Big[(i-1)-2\lfloor\frac{i-1}{2}\rfloor\Big]C_1h^3+\lfloor\frac{i-1}{2}\rfloor C_2h^4\leq Ch^2.
\tag{4.83}
$$

Thus (4.59), (4.82)–(4.83), together give us

$$
|\bar{\Lambda}_i^n-\lambda(x_i,t^n)|\leq Ch^2,\ i=1,\ldots,j_*,
$$

and as before Theorem 4.3.1 grants us (on substituting $\Lambda_i^n = \bar{\Lambda}_i^n$)

$$\| \bar{\boldsymbol{U}}^n - \boldsymbol{u}^n \|_\infty \leq Ch^2. \tag{4.84}$$

Using similar arguments, one can prove that

$$|d(x_i, t^n) - \widetilde{D}_i^n| \leq Ch^3 + \Big\lfloor (i-1) - 2\lfloor \frac{i-1}{2} \rfloor \Big\rfloor C_1 h^3 + \lfloor \frac{i-1}{2} \rfloor C_2 h^4 \leq Ch^3, \quad i \geq n, \tag{4.85}$$

and

$$|d(x_i, t^n) - \widetilde{D}_i^n| \leq Ch^3 + \Big\lfloor (i-1) - 2\lfloor \frac{i-1}{2} \rfloor \Big\rfloor C_1 h^3 + \lfloor \frac{i-1}{2} \rfloor C_2 h^4 \leq Ch^3, \quad i < n. \tag{4.86}$$

Using (4.59) and (4.85)–(4.86), we conclude that

$$|\widetilde{\Lambda}_i^n - \lambda(x_i, t^n)| \leq Ch^3, \; i = 1, \ldots, j_*. \tag{4.87}$$

From Step–4 of Theorem 4.4.4, it follows that

$$|\widetilde{\Lambda}_i^n - \lambda(x_i, t^n)| \leq Ch^3, \quad i = j_* + 1, \ldots, 2M + 1. \tag{4.88}$$

On taking $\Lambda_i^1 = \widetilde{\Lambda}_i^1$, $U_i^1 = \widetilde{U}_i^1$ in Theorem 4.3.1 and using (4.87)–(4.88), we get

$$\| \tilde{\boldsymbol{U}}^n - \boldsymbol{u}^n \|_\infty \leq Ch^3. \tag{4.89}$$

Due to (4.65) and (4.80) for $i \geq n$, we find that

$$\begin{aligned}
&|d(x_i,t^n)-\widehat{D}_i^n| \\
=&|\int_0^{x_i-t^n}\mu\big(y,s_1(0)\big)dy+\int_0^{t^n}\mu\big(y+x_i-t^n,s_1(y)\big)dy-\widehat{D}_{i-2}^{n-2} \\
&-\frac{h}{3}\Big[\mu\big((i-2)h,\widehat{\boldsymbol{S}}_1^{n-2}\big)+4\mu\big((i-1)h,\widehat{\boldsymbol{S}}_1^{n-1}\big)+\mu\big(ih,\widetilde{\boldsymbol{S}}_1^{n}\big)\Big]| \\
=&|d(x_{i-2},t^{n-2})+\int_{t^{n-2}}^{t^n}\mu\big(y+x_i-t^n,s_1(y)\big)dy-\widehat{D}_{i-2}^{n-2} \\
&-\frac{h}{3}\Big[\mu\big((i-2)h,\widehat{\boldsymbol{S}}_1^{n-2}\big)+4\mu\big((i-1)h,\widehat{\boldsymbol{S}}_1^{n-1}\big)+\mu\big(ih,\widetilde{\boldsymbol{S}}_1^{n}\big)\Big]| \\
\leq&Ch^4+\Big|(n-2)-2\lfloor\frac{n-2}{2}\rfloor\Big|C_1h^3+\left(1+\lfloor\frac{n-2}{2}\rfloor\right)C_2h^4\leq Ch^3.
\end{aligned} \tag{4.90}$$

On the other hand, using the same strategy from (4.65) and (4.81), we get

$$\begin{aligned}
&|d(x_i,t^n)-\widehat{D}_i^n| \\
=&|\int_{t^n-x_i}^{t^n}\mu\big(y+x_i-t^n,s_1(y)\big)dy-\widehat{D}_{i-2}^{n-2}-\frac{h}{3}\Big[\mu\big((i-2)h,\widehat{\boldsymbol{S}}_1^{n-2}\big) \\
&+4\mu\big((i-1)h,\widehat{\boldsymbol{S}}_1^{n-1}\big)+\mu\big(ih,\widetilde{\boldsymbol{S}}_1^{n}\big)\Big]| \\
=&|d(x_{i-2},t^{n-2})+\int_{t^{n-2}}^{t^n}\mu\big(y+x_i-t^n,s_1(y)\big)dy \\
&-\widehat{D}_{i-2}^{n-2}-\frac{h}{3}\Big[\mu\big((i-2)h,\widehat{\boldsymbol{S}}_1^{n-2}\big)+4\mu\big((i-1)h,\widehat{\boldsymbol{S}}_1^{n-1}\big)+\mu\big(ih,\widetilde{\boldsymbol{S}}_1^{n}\big)\Big]| \\
\leq&Ch^4+\Big|(i-2)-2\lfloor\frac{i-2}{2}\rfloor\Big|C_1h^3+\lfloor\frac{i-2}{2}\rfloor C_2h^4\leq Ch^3,\quad i<n.
\end{aligned} \tag{4.91}$$

Finally, from (4.59), (4.90)–(4.91), we conclude that

$$|\widehat{\Lambda}_i^n-\lambda(x_i,t^n)|\leq Ch^3,\ i=1,\dots,j_*. \tag{4.92}$$

This completes the proof. Now we present a result which is quite useful in estimating $|\Lambda_i^n-\lambda(x_i,t^n)|$ for $i>j_*$.

Lemma 4.4.5 *Let $u\in C^4([0,a_\dagger]\times[0,T])$ be the solution to (4.2). Assume that* *and* $\mu \in C^4([0,a_\dagger)\times(0,\infty))$ *and satisfies (H1)–(H5). Then the functions*

$$\zeta(x,t,y,x_{j_*})$$
$$=\frac{d^2}{dy^2}[\mu\big(y+x-t,s_1(y)\big)]\exp\Big(-\int\limits_{x_{j_*}}^{x-t}\mu\big(z,s_1(0)\big)dz-\int\limits_0^t\mu\big(z+x-t,s_1(z)\big)dz\Big)$$

and

$$\xi(x,t,y,x_{j_*})$$
$$=\frac{d^4}{dy^4}[\mu\big(y+x-t,s_1(y)\big)]\exp\Big(-\int\limits_{x_{j_*}}^{x-t}\mu\big(z,s_1(0)\big)dz-\int\limits_0^t\mu\big(z+x-t,s_1(z)\big)dz\Big)$$

are bounded on $[a^*,a_\dagger]\times[0,K]\times[a^*,a_\dagger]$.

Proof.We begin with the observation

$$\begin{aligned}
&\mu\big(y+x-t,s_1(y)\big)\\
=&\mu\big(y+x-t,s_1(0)\big)+\frac{\partial\mu}{\partial s}\big(y+x-t,s_1(\eta_5)\big)\big(s_1(y)-s_1(0)\big)\\
=&\mu\big(y+x-t,s_1(0)\big)+y\frac{\partial\mu}{\partial s}\big(y+x-t,s_1(\eta_5)\big)\int_0^{a_\dagger}\psi(x)\frac{\partial u}{\partial t}(x,\eta_6)dx,
\end{aligned}\tag{4.93}$$

for some $\eta_5,\ \eta_6\in(0,y)$, and

$$\exp\Big\{-\int\limits_0^t\Big(y\frac{\partial\mu}{\partial s}\big(y+x-t,s_1(\eta_5)\big)\int_0^{a_\dagger}\psi(x)\frac{\partial u}{\partial t}(x,\eta_6)dx\Big)dy\Big\}\le C,\tag{4.94}$$

for some positive constant C. From (4.94), we can conclude that

$$\exp\Big(-\int\limits_{x_{j_*}}^{x-t}\mu\big(z,s_1(0)\big)dz-\int\limits_0^t\mu\big(z+x-t,s_1(z)\big)dz\Big)\le C\exp\Big(-\int\limits_{x_{j_*}}^{x}\mu\big(z,s_1(0)\big)dz\Big).\tag{4.95}$$

On the other hand, a straight forward computation gives

$$\begin{aligned}
&\frac{d^2}{dy^2}[\mu\big(y+x-t,s_1(y)\big)]\\
=&\Big[\frac{\partial^2\mu}{\partial x^2}+2\frac{ds_1}{dy}\frac{\partial^2\mu}{\partial x\partial s_1}+\Big(\frac{ds_1}{dy}\Big)^2\frac{\partial^2\mu}{\partial s_1^2}+\frac{d^2s_1}{dy^2}\frac{\partial\mu}{\partial s_1}\Big]\big(y+x-t,s_1(y)\big).
\end{aligned} \tag{4.96}$$

From hypothesis $(H4)$ and (4.96), we get

$$\begin{aligned}
&\frac{d^2}{dy^2}[\mu\big(y+x-t,s_1(y)\big)]\\
\leq&\Big[C_2\frac{\partial^2\mu}{\partial x^2}\Big]\big(y+x-t,s_1(0)\big)+\Big[\Big(\frac{ds_1}{dy}\Big)^2\frac{\partial^2\mu}{\partial s_1^2}+\frac{d^2s_1}{dy^2}\frac{\partial\mu}{\partial s_1}\Big]\big(y+x-t,s_1(y)\big).
\end{aligned} \tag{4.97}$$

On multiplying with $\exp\Big(-\int\limits_{x_{j*}}^{x-t}\mu\big(z,s_1(0)\big)dz-\int\limits_0^t\mu\big(z+x-t,s_1(z)\big)dz\Big)$ on both sides of (4.97) and using (4.95), we obtain

$$\zeta(x,t,y,x_{j_*})\leq C_3\varphi(y)+C_4, \tag{4.98}$$

where C_3 and C_4 are constants. Similarly, consider

$$\begin{aligned}
&\frac{d^4}{dy^4}[\mu\big(y+x-t,s_1(y)\big)]\\
=&\Big[\frac{\partial^4\mu}{\partial x^4}+4\frac{\partial^4\mu}{\partial^3x\partial s_1}\frac{ds_1}{dy}+6\frac{\partial^4\mu}{\partial^2x\partial^2s_1}\Big(\frac{ds_1}{dy}\Big)^2+4\frac{\partial^4\mu}{\partial x\partial^3s_1}\Big(\frac{ds_1}{dy}\Big)^3+\frac{\partial^4\mu}{\partial^4s_1}\Big(\frac{ds_1}{dy}\Big)^4\\
&+6\frac{\partial^3\mu}{\partial^2x\partial s_1}\frac{d^2s_1}{dy^2}+12\frac{\partial^3\mu}{\partial x\partial^2s_1}\frac{ds_1}{dy}\frac{d^2s_1}{dy^2}+6\frac{\partial^3\mu}{\partial^3s_1}\Big(\frac{ds_1}{dy}\Big)^2\frac{d^2s_1}{dy^2}\\
&+4\frac{\partial^2\mu}{\partial x\partial s_1}\frac{d^3s_1}{dy^3}+\frac{\partial^2\mu}{\partial^2s_1}\Big(3\big(\frac{d^2s_1}{dy^2}\big)^2+4\frac{ds_1}{dy}\frac{d^3s_1}{dy^3}\Big)+\frac{\partial\mu}{\partial s_1}\frac{d^4s_1}{dy^4}\Big]\big(y+x-t,s_1(y)\big).
\end{aligned} \tag{4.99}$$

From (4.99) and $(H4)-(H5)$, it readily follows that

$$\xi(x,t,y,x_{j_*})\leq C_3\rho(y)+C_4.$$

for some $C_4>0$. This completes the proof. Now we are ready to give a proof of Theorem 4.4.4 which estimates $|\widehat{\Lambda}_i^n-\lambda(x_i,t^n)|$ when the grid points are close to the singularity.

Proof of Theorem 4.4.4. We prove the proposition in the case when $x_i > a^*$, $t^n \leq x_i$. The proof in the case when $t^n > x_i > a^*$ follows from the same argument.

Step–1: Assume $n = 0$.

Consider the following estimate

$$\begin{aligned}
&|\widehat{\Lambda}_i^0 - \lambda(x_i, t^0)| \\
=&\Bigg| \exp\Big\{ - \widehat{D}^0_{j_*} \Big\} \exp\Big\{ - \frac{h}{6} \sum_{j=j_*+1}^{i} \Big[\mu\big((j-1)h, \widehat{\boldsymbol{S}}_1^0\big) + 4\mu\big((j-\frac{1}{2})h, \widehat{\boldsymbol{S}}_1^0\big) \\
&+ \mu\big(jh, \widehat{\boldsymbol{S}}_1^0\big)\Big]\Big\} - \exp\Big\{ - \int_0^{x_{j_*}} \mu\big(y, s_1(0)\big) dy \Big\} \exp\Big\{ - \int_{x_{j_*}}^{x_i} \mu\big(y, s_1(0)\big) dy \Big\} \Bigg| \\
\leq&\Bigg| \exp\Big\{ - \widehat{D}^0_{j_*} \Big\} - \exp\Big\{ - \int_0^{x_{j_*}} \mu\big(y, s_1(0)\big) dy \Big\} \Bigg| \exp\Big\{ - \int_{x_{j_*}}^{x_i} \mu\big(y, s_1(0)\big) dy \Big\} \\
&+ \Bigg| \exp\Big\{ - \frac{h}{6} \sum_{j=j_*+1}^{i} \Big[\mu\big((j-1)h, \widehat{\boldsymbol{S}}_1^0\big) + 4\mu\big((j-\frac{1}{2})h, \widehat{\boldsymbol{S}}_1^0\big) + \mu\big(jh, \widehat{\boldsymbol{S}}_1^0\big)\Big] \Big\} \\
&- \exp\Big\{ - \int_{x_{j_*}}^{x_i} \mu\big(y, s_1(0)\big) dy \Big\} \Bigg| \exp\Big\{ - \widehat{D}^0_{j_*} \Big\} \\
:=&I_1 + I_2. \qquad (4.100)
\end{aligned}$$

We now estimate I_1 and I_2 separately. Since $\frac{\partial^4 \mu}{\partial x^4} \geq 0$ and from (4.50) and (4.99), one can obtain

$$\begin{aligned}
\int_{x_{j_*}}^{x_i} \mu\big(y, s_1(0)\big) dy \leq& \frac{h}{6} \sum_{j=j_*+1}^{i} \Big[\mu\big((j-1)h, \widehat{\boldsymbol{S}}_1^0\big) + 4\mu\big((j-\frac{1}{2})h, \widehat{\boldsymbol{S}}_1^0\big) \\
&+ \mu\big(jh, \widehat{\boldsymbol{S}}_1^0\big)\Big] + Ch^4. \qquad (4.101)
\end{aligned}$$

Using (4.101) and (4.50), we obtain

$$
\begin{aligned}
I_2 \leq & \Big| \exp\Big\{ -\frac{h}{6}\sum_{j=j_*+1}^{i}\Big[\mu\big((j-1)h,\widehat{\boldsymbol{S}}_1^0\big)+4\mu\big((j-\frac{1}{2})h,\widehat{\boldsymbol{S}}_1^0\big)+\mu\big(jh,\widehat{\boldsymbol{S}}_1^0\big)\Big]\Big\} \\
& - \exp\Big\{-\int_{x_{j_*}}^{x_i}\mu\big(y,s_1(0)\big)dy\Big\}\Big| \\
\leq & \exp\Big\{-\int_{x_{j_*}}^{x_i}\mu\big(y,s_1(0)\big)dy + Ch^4\Big\}\Big| -\frac{h}{6}\sum_{j=j_*+1}^{i}\Big[\mu\big((j-1)h,\widehat{\boldsymbol{S}}_1^0\big) \\
& + 4\mu\big((j-\frac{1}{2})h,\widehat{\boldsymbol{S}}_1^0\big)+\mu\big(jh,\widehat{\boldsymbol{S}}_1^0\big)\Big] + \int_{x_{j_*}}^{x_i}\mu\big(y,s_1(0)\big)dy\Big| \\
\leq & C\exp\Big\{-\int_{x_{j_*}}^{x_i}\mu\big(y,s_1(0)\big)dy\Big\}\Big|\frac{d^4}{dy^4}[\mu\big(\eta_3,s_1(0)\big)]\Big|(x_i-x_{j_*})\frac{h^4}{12} \\
\leq & C\big|\rho(\eta_3)\big|(x_i-x_{j_*})\frac{h^4}{12},
\end{aligned}
\tag{4.102}
$$

where $\eta_3 \in (x_{j_*}, x_i)$.
From the fact that ρ is a bounded function, and form (4.102), we conclude that $I_2 \leq Ch^4$. From Theorem 4.4.3, it follows that $I_1 \leq Ch^4$. Hence form (4.100) conclude

$$
|\widehat{\Lambda}_i^0 - \lambda(x_i,t^0)| \leq Ch^4, \quad i = j_*+1,\dots,2M+1.
$$

Step–2 Suppose $n = 1$. Consider the following estimate

$$
\begin{aligned}
&|\bar{\Lambda}_i^1 - \lambda(x_i, t^1)| \\
=&\Bigg| \exp\Big\{ - \widehat{D}_{j_*}^0 \Big\} \exp\Big\{ - \frac{h}{6} \sum_{j=j_*+1}^{i-1} \Big[\mu\big((j-1)h, \widehat{\boldsymbol{S}}_1^0\big) + 4\mu\big((j-\frac{1}{2})h, \widehat{\boldsymbol{S}}_1^0\big) \\
&+ \mu\big(jh, \widehat{\boldsymbol{S}}_1^0\big)\Big] \Big\} \exp\Big\{ - \frac{h}{2}\Big[\mu\big((i-1)h, \widehat{\boldsymbol{S}}_1^0\big) + \mu\big(ih, \widehat{\boldsymbol{S}}_1^0\big)\Big]\Big\} \\
&- \exp\Big\{ - \int_0^{x_{j*}} \mu\big(y, s_1(0)\big) dy \Big\} \exp\Big\{ - \int_{x_{j*}}^{x_i - t^1} \mu\big(y, s_1(0)\big) dy \\
&- \int_0^{t^1} \mu\big(y + x_i - t^1, s_1(y)\big) dy \Big\} \Bigg| \\
\le&\Bigg| \exp\Big\{ - \widehat{D}_{j_*}^0 \Big\} - \exp\Big\{ - \int_0^{x_{j*}} \mu\big(y, s_1(0)\big) dy \Big\} \Bigg| \exp\Big\{ - \int_{x_{j*}}^{x_i - t^1} \mu\big(y, s_1(0)\big) dy \\
&- \int_0^{t^1} \mu\big(y + x_i - t^1, s_1(y)\big) dy \Big\} + \Bigg| \exp\Big\{ - \frac{h}{6} \sum_{j=j_*+1}^{i-1} \Big[\mu\big((j-1)h, \widehat{\boldsymbol{S}}_1^0\big) \\
&+ 4\mu\big((j-\frac{1}{2})h, \widehat{\boldsymbol{S}}_1^0\big) + \mu\big(jh, \widehat{\boldsymbol{S}}_1^0\big)\Big] - \frac{h}{2}\Big[\mu\big((i-1)h, \widehat{\boldsymbol{S}}_1^0\big) + \mu\big(ih, \widehat{\boldsymbol{S}}_1^0\big)\Big]\Big\} \\
&- \exp\Big\{ - \int_{x_{j*}}^{x_i - t^1} \mu\big(y, s_1(0)\big) dy - \int_0^{t^1} \mu\big(y + x_i - t^1, s_1(y)\big) dy \Big\} \Bigg| \exp\Big\{ - \widehat{D}_{j_*}^0 \Big\} \\
:=& I_3 + I_4.
\end{aligned}
\tag{4.103}
$$

Since $\frac{\partial^2 \mu}{\partial x^2} \ge 0$ and from (4.49) and (4.96), one can obtain

$$
\begin{aligned}
&\int_{x_{j*}}^{x_i - t^1} \mu\big(y, s_1(0)\big) dy + \int_0^{t^1} \mu\big(y + x_i - t^1, s_1(y)\big) dy \\
\le& \frac{h}{6} \sum_{j=j_*+1}^{i-1} \Big[\mu\big((j-1)h, \widehat{\boldsymbol{S}}_1^0\big) + 4\mu\big((j-\frac{1}{2})h, \widehat{\boldsymbol{S}}_1^0\big) + \mu\big(jh, \widehat{\boldsymbol{S}}_1^0\big)\Big] \\
&+ \frac{h}{2}\Big[\mu\big((i-1)h, \widehat{\boldsymbol{S}}_1^0\big) + \mu\big(ih, \widehat{\boldsymbol{S}}_1^0\big)\Big] + Ch^2.
\end{aligned}
\tag{4.104}
$$

Using (4.104), (4.49), (4.50) and the Lagrange theorem, we obtain

$$
\begin{aligned}
I_4 \leq & \Bigg| \exp\Big\{ -\frac{h}{6} \sum_{j=j_*+1}^{i-1} \Big[\mu\big((j-1)h, \widehat{\boldsymbol{S}}_1^0\big) + 4\mu\big((j-\frac{1}{2})h, \widehat{\boldsymbol{S}}_1^0\big) + \mu\big(jh, \widehat{\boldsymbol{S}}_1^0\big)\Big] \\
& - \frac{h}{2}\Big[\mu\big((i-1)h, \widehat{\boldsymbol{S}}_1^0\big) + \mu\big(ih, \widehat{\boldsymbol{S}}_1^0\big)\Big]\Big\} \\
& - \exp\Big\{ - \int\limits_{x_{j*}}^{x_i - t^1} \mu\big(y, s_1(0)\big)dy - \int\limits_0^{t^1} \mu\big(y + x_i - t^1, s_1(y)\big)dy \Big\}\Bigg| \\
\leq & \exp\Big\{ - \int\limits_{x_{j*}}^{x_i - t^1} \mu\big(y, s_1(0)\big)dy - \int\limits_0^{t^1} \mu\big(y + x_i - t^1, s_1(y)\big)dy + Ch^2\Big\} \\
& \Bigg| -\frac{h}{6} \sum_{j=j_*+1}^{i-1} \Big[\mu\big((j-1)h, \widehat{\boldsymbol{S}}_1^0\big) + 4\mu\big((j-\frac{1}{2})h, \widehat{\boldsymbol{S}}_1^0\big) + \mu\big(jh, \widehat{\boldsymbol{S}}_1^0\big)\Big] \\
& - \frac{h}{2}\Big[\mu\big((i-1)h, \widehat{\boldsymbol{S}}_1^0\big) + \mu\big(ih, \widehat{\boldsymbol{S}}_1^0\big)\Big] + \int\limits_{x_{j*}}^{x_i - t^1} \mu\big(y, s_1(0)\big)dy \\
& + \int\limits_0^{t^1} \mu\big(y + x_i - t^1, s_1(y)\big)dy\Bigg| \\
\leq & C\Big(\Big|\frac{d^4}{dy^4}[\mu\big(\eta_3, s_1(0)\big)]\Big|(x_{i-1} - x_{j_*})\frac{h^4}{90} \\
& + \Big|\frac{d^2}{dy^2}[\mu\big(\eta_4 + x_i - t^1, s_1(\eta_4)\big)]\Big|(x_i - x_{i-1})\frac{h^2}{12}\Big) \\
\leq & C\Big|\rho(\eta_3) + \zeta(x_i, t^n, \eta_4, x_{j_*})\Big|(x_i - x_{j_*})\frac{h^2}{12},
\end{aligned}
\tag{4.105}
$$

where $\eta_3 \in (x_{j_*}, x_{i-1})$ and $0 \leq \eta_4 \leq h$.
From the fact that ρ and ξ are bounded functions, and from (4.105), we conclude that $I_4 \leq Ch^2$. From Theorem 4.4.3, it follows that $I_3 \leq Ch^4$. Using these fact, from (4.103) we conclude

$$
|\bar{\Lambda}_i^1 - \lambda(x_i, t^1)| \leq Ch^2, \quad i = j_* + 1, \ldots, 2M + 1. \tag{4.106}
$$

From Step–2 of Theorem 4.4.3, it follows that

$$
|\bar{\Lambda}_i^1 - \lambda(x_i, t^1)| \leq Ch^2, \quad i = 1, \ldots, j_*. \tag{4.107}
$$

On taking $\Lambda_i^1 = \bar{\Lambda}_i^1$, $U_i^1 = \bar{U}_i^1$ in Theorem 4.3.1 and using (4.106)–(4.107), we get

$$|| \bar{\boldsymbol{U}}^1 - \boldsymbol{u}^1 ||_\infty \leq Ch^2. \tag{4.108}$$

Using similar arguments, we can prove that

$$|\widetilde{\Lambda}_i^1 - \lambda(x_i, t^1)| \leq Ch^3, \quad i = j_* + 1, \ldots, 2M + 1, \tag{4.109}$$

$$|| \widetilde{\boldsymbol{U}}^1 - \boldsymbol{u}^1 ||_\infty \leq Ch^3, \tag{4.110}$$

and

$$|\widehat{\Lambda}_i^1 - \lambda(x_i, t^1)| \leq Ch^3, \quad i = j_* + 1, \ldots, 2M + 1, \tag{4.111}$$

$$|| \widehat{\boldsymbol{U}}^1 - \boldsymbol{u}^1 ||_\infty \leq Ch^3, \tag{4.112}$$

Step–3 Consider the case when $n = 2$.
Using the similar arguments to get (4.106), (4.125)–(4.110), we obtain

$$|\bar{\Lambda}_i^2 - \lambda(x_i, t^2)| \leq Ch^2, \quad i = j_* + 1, \ldots, 2M + 1, \tag{4.113}$$

$$|| \bar{\boldsymbol{U}}^2 - \boldsymbol{u}^2 ||_\infty \leq Ch^2, \tag{4.114}$$

and

$$|\widetilde{\Lambda}_i^2 - \lambda(x_i, t^2)| \leq Ch^3, \quad i = j_* + 1, \ldots, 2M + 1, \tag{4.115}$$

$$|| \widetilde{\boldsymbol{U}}^2 - \boldsymbol{u}^2 ||_\infty \leq Ch^3. \tag{4.116}$$

Case–1 Suppose $n = 2$ and $i = j_* + 1$.
Consider

$$
\begin{aligned}
&|\widehat{\Lambda}^2_{j_*+1} - \lambda(x_{j_*+1}, t^2)| \\
=&\Big| \exp\Big\{ -\widehat{D}^0_{j_*-1}\Big\} \exp\Big\{ -\frac{h}{3}\Big[\mu\big(x_{j_*+1} - t^2, \widehat{\boldsymbol{S}}^0_1\big) + 4\mu\big(h + x_{j_*+1} - t^2, \widehat{\boldsymbol{S}}^1_1\big) \\
&+ \mu\big(2h + x_{j_*+1} - t^2, \widetilde{\boldsymbol{S}}^2_1\big)\Big]\Big\} - \exp\Big\{ -\int_0^{x_{j_*-1}} \mu\big(y, s_1(0)\big)dy\Big\} \\
&\exp\Big\{ -\int_0^{t^2} \mu\big(y + x_{j_*+1} - t^2, s_1(y)\big)dy\Big\}\Big| \\
\leq&\Big| \exp\Big\{ -\widehat{D}^0_{j_*-1}\Big\} - \exp\Big\{ -\int_0^{x_{j_*-1}} \mu\big(y, s_1(0)\big)dy\Big\}\Big| \\
&\exp\Big\{ -\int_0^{t^2} \mu\big(y + x_{j_*+1} - t^2, s_1(y)\big)dy\Big\} \\
&+ \Big| \exp\Big\{ -\frac{h}{3}\Big[\mu\big(x_{j_*+1} - t^2, \widehat{\boldsymbol{S}}^0_1\big) + 4\mu\big(h + x_{j_*+1} - t^2, \widehat{\boldsymbol{S}}^1_1\big) \\
&+ \mu\big(2h + x_{j_*+1} - t^2, \widetilde{\boldsymbol{S}}^2_1\big)\Big]\Big\} \\
&- \exp\Big\{ -\int_0^{t^2} \mu\big(y + x_{j_*+1} - t^2, s_1(y)\big)dy\Big\}\Big| \exp\Big\{ -\widehat{D}^0_{j_*-1}\Big\} \\
:=& I_5 + I_6.
\end{aligned}
\tag{4.117}
$$

Since $\frac{\partial^2 \mu}{\partial x^2} \geq 0$ and from (4.50) and (4.96), one can obtain

$$
\begin{aligned}
\int_0^{t^2} \mu\big(y + x_{j_*+1} - t^2, s_1(y)\big)dy \leq& \frac{h}{3}\Big[\mu\big(x_{j_*+1} - t^2, \widehat{\boldsymbol{S}}^0_1\big) + 4\mu\big(h + x_{j_*+1} - t^2, \widehat{\boldsymbol{S}}^1_1\big) \\
&+ \mu\big(2h + x_{j_*+1} - t^2, \widetilde{\boldsymbol{S}}^2_1\big)\Big] + Ch^2.
\end{aligned}
\tag{4.118}
$$

This implies

$$
\begin{aligned}
I_6 \leq & \Bigg| \exp\Bigg\{ -\frac{h}{3}\Big[\mu\big(x_{j_*+1}-t^2, \widehat{\boldsymbol{S}}_1^0\big) + 4\mu\big(h+x_{j_*+1}-t^2, \widehat{\boldsymbol{S}}_1^1\big) \\
& + \mu\big(2h+x_{j_*+1}-t^2, \widetilde{\boldsymbol{S}}_1^2\big)\Big]\Bigg\} - \exp\Bigg\{ -\int_0^{t^2} \mu\big(y+x_{j_*+1}-t^2, s_1(y)\big)dy\Bigg\}\Bigg| \\
\leq & \exp\Bigg\{ -\int_0^{t^2} \mu\big(y+x_{j_*+1}-t^2, s_1(y)\big)dy + Ch^2\Bigg\} \\
& \Bigg| -\frac{h}{3}\Big[\mu\big(x_{j_*+1}-t^2, \widehat{\boldsymbol{S}}_1^0\big) + 4\mu\big(h+x_{j_*+1}-t^2, \widehat{\boldsymbol{S}}_1^1\big) + \mu\big(2h+x_{j_*+1}-t^2, \widetilde{\boldsymbol{S}}_1^2\big)\Big] \\
& + \int_0^{t^2} \mu\big(y+x_{j_*+1}-t^2, s_1(y)\big)dy\Bigg| \\
\leq & C\left|\frac{d^4}{dy^4}[\mu\big(\eta_3+x_{j_*+1}-t^2, s_1(\eta_3)\big)]\right|\big(x_{j_*+1}-x_{j_*-1}\big)\frac{h^4}{12} \\
\leq & C\left|\xi(x_{j_*+1}, t^2, \eta_5, x_{j_*-1})\right|\big(x_{j_*+1}-x_{j_*-1}\big)\frac{h^4}{12},
\end{aligned} \tag{4.119}
$$

where $\eta_5 \in (0, 2h)$. Using the fact that ξ are bounded functions, and from (4.119), one can conclude that $I_6 \leq Ch^4$. From Theorem 4.4.3, it follows that $I_5 \leq Ch^3$. Using these fact, from (4.117) we conclude

$$
|\widehat{\Lambda}_i^2 - \lambda(x_i, t^2)| \leq Ch^3, \quad i = j_* + 1. \tag{4.120}
$$

Case–2 We now assume $n = 2$ and $j_* + 2 \le i \le 2M + 1$.
We estimate

$$\begin{aligned}
&|\widehat{\Lambda}_i^2 - \lambda(x_i, t^2)| \\
\le& \Big| \exp\Big\{ - \widehat{D}_{j_*}^0 \Big\} - \exp\Big\{ - \int_0^{x_{j_*}} \mu\big(y, s_1(0)\big) dy \Big\} \Big| \\
&+ \Big| \exp\Big\{ - \frac{h}{6} \sum_{j=j_*+1}^{i-2} \Big[\mu\big((j-1)h, \widehat{\boldsymbol{S}}_1^0\big) + 4\mu\big((j - \frac{1}{2})h, \widehat{\boldsymbol{S}}_1^0\big) + \mu\big(jh, \widehat{\boldsymbol{S}}_1^0\big) \Big] \\
&- \frac{h}{3} \Big[\mu\big(x_i - t^2, \widehat{\boldsymbol{S}}_1^0\big) + 4\mu\big(h + x_i - t^2, \widehat{\boldsymbol{S}}_1^1\big) + \mu\big(2h + x_i - t^2, \widetilde{\boldsymbol{S}}_1^2\big) \Big] \\
&- \exp\Big\{ - \int_{x_{j*}}^{x_i - t^2} \mu\big(y, s_1(0)\big) dy - \int_0^{t^2} \mu\big(y + x_i - t^2, s_1(y)\big) dy \Big\} \Big| \\
:=& I_7 + I_8, \qquad (4.121)
\end{aligned}$$

and

$$\begin{aligned}
I_8 =& \Big| \exp\Big\{ - \frac{h}{6} \sum_{j=j_*+1}^{i-2} \Big[\mu\big((j-1)h, \widehat{\boldsymbol{S}}_1^0\big) + 4\mu\big((j - \frac{1}{2})h, \widehat{\boldsymbol{S}}_1^0\big) + \mu\big(jh, \widehat{\boldsymbol{S}}_1^0\big) \Big] \\
&- \frac{h}{3} \Big[\mu\big(x_i - t^2, \widehat{\boldsymbol{S}}_1^0\big) + 4\mu\big(h + x_i - t^2, \widehat{\boldsymbol{S}}_1^1\big) + \mu\big(2h + x_i - t^2, \widetilde{\boldsymbol{S}}_1^2\big) \Big] \\
&- \exp\Big\{ - \int_{x_{j*}}^{x_i - t^2} \mu\big(y, s_1(0)\big) dy - \int_0^{t^2} \mu\big(y + x_i - t^2, s_1(y)\big) dy \Big\} \Big| \\
\le& C \Big| \rho(\eta_6) + \xi(x_i, t^2, \eta_7, x_{j_*}) \Big| (x_i - x_{j_*}) \frac{h^4}{90}, \qquad (4.122)
\end{aligned}$$

where $\eta_6 \in (x_{j_*}, x_{i-2})$ and $0 \le \eta_7 \le 2h$.
From the fact that ρ and ξ are bounded function, and form (4.122) , we conclude that $I_8 \le Ch^4$. From Theorem 4.4.3, it follows that $I_7 \le Ch^3$. Using these fact, from (4.121) we conclude

$$|\widehat{\Lambda}_i^2 - \lambda(x_i, t^2)| \le Ch^3, \quad i = j_* + 2, \dots, 2M + 1. \qquad (4.123)$$

From Step–3 of Theorem 4.4.3, it follows that

$$|\widehat{\Lambda}_i^2 - \lambda(x_i, t^2)| \leq Ch^3, \quad i = 1, \ldots, j_*. \tag{4.124}$$

On taking $\Lambda_i^2 = \widehat{\Lambda}_i^2$, $U_i^2 = \widehat{U}_i^2$ in Theorem 4.3.1 and using (4.120), (4.123)–(4.124), we get

$$|| \ \widehat{\boldsymbol{U}}^2 - \boldsymbol{u}^2 \ ||_\infty \leq Ch^3. \tag{4.125}$$

Step–4: We complete the proof of the required result using the induction argument.

For, assume

$$\begin{aligned} |\lambda(x_i, t^m) - \widehat{\Lambda}_i^m| \leq & \lfloor m - 2\lfloor \frac{m}{2} \rfloor \rfloor Ch^3 + \left(1 + \lfloor \frac{m}{2} \rfloor\right) Ch^4 \\ \leq & Ch^3, \ \ i = j_* + 1, \ldots, 2M + 1, \ \ m = 0, 1, \ldots, n - 1. \end{aligned} \tag{4.126}$$

Consider the following estimate

$$
\begin{aligned}
&|\bar{\Lambda}_i^n - \lambda(x_i,t^n)| \\
=&\Bigg| \exp\Big\{ -\widehat{D}^0_{j_*}\Big\} \exp\Big\{ -\frac{h}{6}\sum_{j=j_*+1}^{i-n}\Big[\mu\big((j-1)h,\widehat{\boldsymbol{S}}_1^0\big) + 4\mu\big((j-\frac{1}{2})h,\widehat{\boldsymbol{S}}_1^0\big) \\
&+\mu\big(jh,\widehat{\boldsymbol{S}}_1^0\big)\Big]\Big\} \exp\Big\{ -\frac{h}{3}\sum_{j=1}^{\frac{n-1}{2}}\Big[\mu\big((i-n+2j-2)h,\widehat{\boldsymbol{S}}_1^{2j-2}\big) \\
&+4\mu\big((i-n+2j-1)h,\widehat{\boldsymbol{S}}_1^{2j-1}\big) + \mu\big((i-n+2j)h,\widehat{\boldsymbol{S}}_1^{2j}\big)\Big]\Big\} \\
&\exp\Big\{ -\frac{h}{2}\Big[\mu\big((i-1)h,\widehat{\boldsymbol{S}}_1^{n-1}\big) + \mu\big(ih,\widehat{\boldsymbol{S}}_1^{n-1}\big)\Big]\Big\} - \exp\Big\{ -\int_0^{x_{j_*}}\mu\big(y,s_1(0)\big)dy\Big\} \\
&\exp\Big\{ -\int_{x_{j*}}^{x_i-t^n}\mu\big(y,s_1(0)\big)dy - \int_0^{t^n}\mu\big(y+x_i-t^n,s_1(y)\big)dy\Big\}\Bigg| \\
\le&\Bigg|\exp\Big\{ -\widehat{D}^0_{j_*}\Big\} - \exp\Big\{ -\int_0^{x_{j_*}}\mu\big(y,s_1(0)\big)dy\Big\}\Bigg| \\
&\exp\Big\{ -\int_{x_{j*}}^{x_i-t^n}\mu\big(y,s_1(0)\big)dy - \int_0^{t^n}\mu\big(y+x_i-t^n,s_1(y)\big)dy\Big\} \\
&+\Bigg|\exp\Big\{ -\frac{h}{6}\sum_{j=j_*+1}^{i-n}\Big[\mu\big((j-1)h,\widehat{\boldsymbol{S}}_1^0\big) + 4\mu\big((j-\frac{1}{2})h,\widehat{\boldsymbol{S}}_1^0\big) + \mu\big(jh,\widehat{\boldsymbol{S}}_1^0\big)\Big] \\
&-\frac{h}{3}\sum_{j=1}^{\frac{n-1}{2}}\Big[\mu\big((i-n+2j-2)h,\widehat{\boldsymbol{S}}_1^{2j-2}\big) + 4\mu\big((i-n+2j-1)h,\widehat{\boldsymbol{S}}_1^{2j-1}\big) \\
&+\mu\big((i-n+2j)h,\widehat{\boldsymbol{S}}_1^{2j}\big)\Big] - \frac{h}{2}\Big[\mu\big((i-1)h,\widehat{\boldsymbol{S}}_1^{n-1}\big) + \mu\big(ih,\widehat{\boldsymbol{S}}_1^{n-1}\big)\Big]\Big\} \\
&-\exp\Big\{ -\int_{x_{j*}}^{x_i-t^n}\mu\big(y,s_1(0)\big)dy - \int_0^{t^n}\mu\big(y+x_i-t^n,s_1(y)\big)dy\Big\}\Bigg| \exp\Big\{ -\widehat{D}^0_{j_*}\Big\} \\
:=&I_9 + I_{10}.
\end{aligned}
\tag{4.127}
$$

Since $\frac{\partial^2 \mu}{\partial x^2} \geq 0$ and from (4.49) and (4.96), one can obtain

$$\begin{aligned}
&\int\limits_{x_{j*}}^{x_i - t^n} \mu\big(y, s_1(0)\big)dy + \int\limits_{0}^{t^n} \mu\big(y + x_i - t^n, s_1(y)\big)dy \\
&\leq \frac{h}{6} \sum_{j=j_*+1}^{i-n} \Big[\mu\big((j-1)h, \widehat{\boldsymbol{S}}_1^0\big) + 4\mu\big((j-\frac{1}{2})h, \widehat{\boldsymbol{S}}_1^0\big) + \mu\big(jh, \widehat{\boldsymbol{S}}_1^0\big)\Big] \\
&+ \frac{h}{3} \sum_{j=1}^{\frac{n-1}{2}} \Big[\mu\big((i-n+2j-2)h, \widehat{\boldsymbol{S}}_1^{2j-2}\big) + 4\mu\big((i-n+2j-1)h, \widehat{\boldsymbol{S}}_1^{2j-1}\big) \\
&+ \mu\big((i-n+2j)h, \widehat{\boldsymbol{S}}_1^{2j}\big)\Big] + \frac{h}{2}\Big[\mu\big((i-1)h, \widehat{\boldsymbol{S}}_1^{n-1}\big) + \mu\big(ih, \widehat{\boldsymbol{S}}_1^{n-1}\big)\Big] + Ch^2.
\end{aligned} \tag{4.128}$$

Using (4.128), (4.49), (4.50) and the Lagrange theorem, we obtain

$$\begin{aligned}
I_{10} \leq & \Big| \exp\Big\{ -\frac{h}{6}\sum_{j=j_*+1}^{i-n}\Big[\mu\big((j-1)h,\widehat{\boldsymbol{S}}_1^0\big)+4\mu\big((j-\frac{1}{2})h,\widehat{\boldsymbol{S}}_1^0\big)+\mu\big(jh,\widehat{\boldsymbol{S}}_1^0\big)\Big] \\
& -\frac{h}{3}\sum_{j=1}^{\frac{n-1}{2}}\Big[\mu\big((i-n+2j-2)h,\widehat{\boldsymbol{S}}_1^{2j-2}\big)+4\mu\big((i-n+2j-1)h,\widehat{\boldsymbol{S}}_1^{2j-1}\big) \\
& +\mu\big((i-n+2j)h,\widehat{\boldsymbol{S}}_1^{2j}\big)\Big]-\frac{h}{2}\Big[\mu\big((i-1)h,\widehat{\boldsymbol{S}}_1^{n-1}\big)+\mu\big(ih,\widehat{\boldsymbol{S}}_1^{n-1}\big)\Big]\Big\} \\
& -\exp\Big\{-\int_{x_{j*}}^{x_i-t^n}\mu\big(y,s_1(0)\big)dy-\int_0^{t^n}\mu\big(y+x_i-t^n,s_1(y)\big)dy\Big\}\Big| \\
\leq & \exp\Big\{-\int_{x_{j*}}^{x_i-t^n}\mu\big(y,s_1(0)\big)dy-\int_0^{t^n}\mu\big(y+x_i-t^n,s_1(y)\big)dy+Ch^2\Big\} \\
& \Big| -\frac{h}{6}\sum_{j=j_*+1}^{i-n}\Big[\mu\big((j-1)h,\widehat{\boldsymbol{S}}_1^0\big)+4\mu\big((j-\frac{1}{2})h,\widehat{\boldsymbol{S}}_1^0\big)+\mu\big(jh,\widehat{\boldsymbol{S}}_1^0\big)\Big] \\
& -\frac{h}{3}\sum_{j=1}^{\frac{n-1}{2}}\Big[\mu\big((i-n+2j-2)h,\widehat{\boldsymbol{S}}_1^{2j-2}\big)+4\mu\big((i-n+2j-1)h,\widehat{\boldsymbol{S}}_1^{2j-1}\big) \\
& +\mu\big((i-n+2j)h,\widehat{\boldsymbol{S}}_1^{2j}\big)\Big]-\frac{h}{2}\Big[\mu\big((i-1)h,\widehat{\boldsymbol{S}}_1^{n-1}\big)+\mu\big(ih,\widehat{\boldsymbol{S}}_1^{n-1}\big)\Big] \\
& +\int_{x_{j*}}^{x_i-t^n}\mu\big(y,s_1(0)\big)dy+\int_0^{t^n}\mu\big(y+x_i-t^n,s_1(y)\big)dy\Big| \\
\leq & \exp\Big\{-\int_{x_{j*}}^{x_i-t^n}\mu\big(y,s_1(0)\big)dy-\int_0^{t^n}\mu\big(y+x_i-t^n,s_1(y)\big)dy\Big\} \\
& \Big(\Big|\frac{d^4}{dy^4}[\mu\big(\eta_8,s_1(0)\big)]\Big|(x_{i-n}-x_{j_*})\frac{h^4}{90} \\
& +\Big|\frac{d^2}{dy^2}[\mu\big(\eta_9+x_i-t^n,s_1(\eta_9)\big)]\Big|(x_{i-1}-x_{i-n})\frac{h^4}{90} \\
& +\Big|\frac{d^2}{dy^2}[\mu\big(\eta_{10}+x_i-t^n,s_1(\eta_{10})\big)]\Big|(x_i-x_{i-1})\frac{h^2}{12}\Big) \\
\leq & C\big|\rho(\eta_8)+\xi(x_i,t^n,\eta_9,x_{j_*})+\zeta(x_i,t^n,\eta_{10},x_{j_*})\big|(x_i-x_{j_*})\frac{h^2}{12}, \qquad (4.129)
\end{aligned}$$

where $\eta_8 \in (x_{j_*}, x_{i-n})$, $\eta_9 \in (x_{i-n}, x_{i-1})$ and $\eta_{10} \in (x_{i-1}, x_i)$.
From the fact that ρ, ζ and ξ are bounded functions, and from (4.129), one can show that $I_{10} \leq Ch^2$. From Theorem 4.4.3, it follows that $I_9 \leq Ch^3$. Using these fact, from (4.127) we conclude

$$|\bar{\Lambda}_i^n - \lambda(x_i, t^n)| \leq Ch^2, \quad i = j_* + 1, \ldots, 2M + 1.$$

Now it is straightforward to conclude that

$$|\widetilde{\Lambda}_i^n - \lambda(x_i, t^n)| \leq Ch^3, \quad i = j_* + 1, \ldots, 2M + 1, \tag{4.130}$$

and

$$|\widehat{\Lambda}_i^n - \lambda(x_i, t^n)| \leq Ch^3, \quad i = j_* + 1, \ldots, 2M + 1. \tag{4.131}$$

4.5 A fourth order approximation of λ

In this section, we propose a fourth order numerical scheme to (4.2) by introducing two more corrections to the predictor corrector method presented in Section 4.4. In other words, the method that we introduce here is a five step scheme and first three steps are exactly the same as those defined in the previous section. Before defining the new steps, we need to introduce the notation $\widehat{U}_{i-\frac{1}{2}}^{n-\frac{1}{2}}$, $1 \leq n \leq N$, $1 \leq i \leq 2M+1$. We define $\widehat{U}_{i-\frac{1}{2}}^{n-\frac{1}{2}}$ with step size h as $\widehat{U}_{2i-1}^{2n-1}$ with the step size $\frac{h}{2}$ and it is computed using the methods described in the previous section.

Step–4 We define

$$\begin{aligned} \widehat{\boldsymbol{S}}_\nu^{n-\frac{1}{2}} &= \mathcal{Q}_h(\boldsymbol{\psi}_\nu \cdot \widehat{\boldsymbol{U}}^{n-\frac{1}{2}}), \quad \nu = 1, 2, \\ \widehat{\widehat{D}}_i^n &= D_i^0, \quad 1 \leq i \leq 2M+1, \\ \widehat{\widehat{D}}_0^n &= D_0^n = 0, \quad 0 \leq n \leq N, \end{aligned} \tag{4.132}$$

and

$$\widehat{\widehat{D}}_i^n = D_{i-1}^{n-1} + \frac{h}{6}\Big[\mu\big((i-1)h, \boldsymbol{S}_1^{n-1}\big) + 4\mu\big((i-\frac{1}{2})h, \widehat{\boldsymbol{S}}_1^{n-\frac{1}{2}}\big) + \mu\big(ih, \widehat{\boldsymbol{S}}_1^n\big)\Big], \;\; n, i \geq 1, \tag{4.133}$$

where D_{i-1}^{n-1} and $\boldsymbol{S}_1^{n-1}$ are defined in Step–5. We approximate the survival probability function $\lambda(x,t)$ at each grid point by

$$\widehat{\widehat{\Lambda}}_i^n = \exp(-\widehat{\widehat{D}}_i^n). \tag{4.134}$$

From (4.10)–(4.11) (on substituting $\Lambda_i^n = \widehat{\widehat{\Lambda}}_i^n$), we get $\widehat{\widehat{U}}_i^n$. We now define

$$\widehat{\widehat{\boldsymbol{S}}}_\nu^n = \mathcal{Q}_h(\boldsymbol{\psi}_\nu \cdot \widehat{\widehat{\boldsymbol{U}}}^n), \quad \nu = 1, 2. \tag{4.135}$$

Step–5 Finally, we set

$$D_i^n = \begin{cases} D_{i-1}^{n-1} + \dfrac{h}{6}\Big[\mu\big((i-1)h, \boldsymbol{S}_1^{n-1}\big) + 4\mu\big((i-\dfrac{1}{2})h, \widehat{\boldsymbol{S}}_1^{n-\frac{1}{2}}\big) & \\ +\mu\big(ih, \widehat{\widehat{\boldsymbol{S}}}_1^n\big)\Big], & n = 1, \text{ or } i = 1, \\ D_{i-2}^{n-2} + \dfrac{h}{3}\Big[\mu\big((i-2)h, \boldsymbol{S}_1^{n-2}\big) + 4\mu\big((i-1)h, \widehat{\widehat{\boldsymbol{S}}}_1^{n-1}\big) & \\ +\mu\big(ih, \widehat{\widehat{\boldsymbol{S}}}_1^n\big)\Big], & n > i \geq 2. \end{cases} \tag{4.136}$$

We now correct $\widehat{\widehat{\Lambda}}_i^n$ once more to find

$$\Lambda_i^n = \exp(-D_i^n). \tag{4.137}$$

As before, we use (4.10)–(4.11) to get the updated value of solution of (4.2) namely U_i^n. We now define

$$\boldsymbol{S}_\nu^n = \mathcal{Q}_h(\boldsymbol{\psi}_\nu \cdot \boldsymbol{U}^n), \quad \nu = 1, 2. \tag{4.138}$$

Theorem 4.5.1 *Assume hypotheses $(H1)$–$(H5)$. Moreover assume that $\mu \in C^4([0, a_\dagger) \times (0, \infty))$, $\frac{d^2\mu}{dy^2}(y, s_1(y+\alpha)) \geq 0$ and $\frac{d^4\mu}{dy^4}(y, s_1(y+\alpha)) \geq 0$ for all $y \in [a^*, a_\dagger)$ and $\alpha \geq -a^*$. Let $u \in C^4([0, a_\dagger] \times [0, T])$ be the solution to (4.2).*

Then

$$\|\boldsymbol{\Lambda}^n - \boldsymbol{\lambda}^n\|_\infty \leq Ch^4, \tag{4.139}$$

where C is a constant independent of n, h.

Proof.To prove the theorem, we need to consider all the cases which are considered in Theroems 4.4.3 and 4.4.4. In this proof, we show the steps which play crucial role to get the fourth order.
We prove the required result using the induction argument. For, assume

$$\begin{aligned}|d(x_i,t^m) - D_i^m| \leq & \Big\lfloor (m-1) - 2\lfloor\frac{m-1}{2}\rfloor\Big\rfloor C_1h^4 + \left((i-m) + \lfloor\frac{m-1}{2}\rfloor\right)C_2h^5 \qquad (4.140)\\ \leq & Ch^3,\ i = m, \ldots, j_*,\ m = 0, 1, \ldots, n-1,\end{aligned}$$

and

$$\begin{aligned}|d(x_i,t^m) - \widehat{D}_i^m| \leq & \Big\lfloor i - 2\lfloor\frac{i}{2}\rfloor\Big\rfloor C_1h^4 + \lfloor\frac{i}{2}\rfloor C_2h^5 \qquad (4.141)\\ \leq & Ch^3,\ i = 0, 1, \ldots, m-1,\ m = 0, 1, \ldots, n-1.\end{aligned}$$

Using (4.65) and Theorem 4.3.1, we obtain

$$\begin{aligned}&|d(x_i,t^n) - \widehat{\widehat{D}}_i^n|\\ \leq & \Bigg|\int_{t^{n-1}}^{t^n} \mu\big(y + x_i - t^n, s_1(y)\big)dy - \frac{h}{6}\Big[\mu\big((i-1)h, \boldsymbol{S}_1^{n-1}\big) + 4\mu\big((i-\frac{1}{2})h, \widehat{\boldsymbol{S}}_1^{n-\frac{1}{2}}\big)\\ &+ \mu\big(ih, \widehat{\boldsymbol{S}}_1^n\big)\Big]\Bigg| + \Big\lfloor (n-1) - 2\lfloor\frac{n-1}{2}\rfloor\Big\rfloor C_1h^4 + \left((i-n) + \lfloor\frac{n-1}{2}\rfloor\right)C_2h^5\\ \leq & Ch^4 + \Big\lfloor (n-1) - 2\lfloor\frac{n-1}{2}\rfloor\Big\rfloor C_1h^4 + \left((i-n) + \lfloor\frac{n-1}{2}\rfloor\right)C_2h^5. \qquad (4.142)\end{aligned}$$

Similarly, using (4.65) and Theorem 4.3.1, we get

$$
\begin{aligned}
&|d(x_i,t^n)-D_i^n|\\
\le&\Bigg|\int_{t^{n-2}}^{t^n}\mu\big(y+x_i-t^n,s_1(y)\big)dy-\frac{h}{3}\Big[\mu\big((i-2)h,\boldsymbol{S}_1^{n-2}\big)+4\mu\big((i-1)h,\widehat{\widehat{\boldsymbol{S}}}_1^{n-1}\big)\\
&+\mu\big(ih,\widehat{\widehat{\boldsymbol{S}}}_1^{n}\big)\Big]\Bigg|+\Big|(n-2)-2\lfloor\frac{n-2}{2}\rfloor\Big|C_1h^4+\left(1+\lfloor\frac{n-2}{2}\rfloor\right)C_2h^5\\
\le&Ch^5+\Big|(n-2)-2\lfloor\frac{n-2}{2}\rfloor\Big|C_1h^5+\left((i-n)+\lfloor\frac{n-2}{2}\rfloor\right)C_2h^5\le Ch^4.
\end{aligned}
\tag{4.143}
$$

Using the similar arguments to get (4.92) and (4.131), from (4.143) one can obtain

$$
|\Lambda_i^n-\lambda(x_i,t^n)|\le Ch^4,\ i=j_*+1,\dots,2M+1,\ n=0,1,\dots,N. \tag{4.144}
$$

This completes the proof.

4.5.1 A special case

In this subsection, we discuss approximations of λ when μ is depends solely on x, i.e., $\mu(x,s)=f(x)$, $x\in[0,1)$. Then (4.4) reduces to

$$
d_s(x)=\int_0^x f(y)dy,\ x\in[0,a_\dagger), \tag{4.145}
$$

and

$$
\lambda_s(x)=\exp(-d_s(x)),\ x\in[0,a_\dagger). \tag{4.146}
$$

To approximate λ, we use the composite Simpson's $\frac{1}{3}$ quadrature rule. For, we define

$$
G_i=\frac{h}{6}\sum_{j=1}^{i}\Big[f\big((j-1)h\big)+4f\big((j-\frac{1}{2})h\big)+f\big(jh\big)\Big]. \tag{4.147}
$$

As before, we define

$$
\Lambda_{si}=\exp(-G_i). \tag{4.148}
$$

We are ready to state following proposition whose proof can be given using the arguments given in Theorems 4.4.3–4.4.4.

Theorem 4.5.2 *Let $f \in \mathcal{C}^4[0, a_\dagger)$ and $f^{(iv)}$ denote the fourth derivative of f. Assume that f satisfies the following assumptions.*
(H4) The function $f^{(iv)}(x) \geq 0$, for $x \in [0, a_\dagger)$,
(H5) The function $\varphi(x) = f^{(iv)}(x)\exp(-\int\limits_{a^*}^{x} f(y)dy)$, is bounded on $[a^*, a_\dagger]$.
Then for given $T > 0$, we have

$$\|\mathbf{\Lambda}_s - \boldsymbol{\lambda}_s\|_\infty \leq Ch^4. \tag{4.149}$$

4.6 Numerical simulations

In order to validate the effectiveness of the proposed numerical scheme, we present some examples in this section. To compute the experimental order of convergence, we use the following formula

$$\text{order} = \frac{\log(E_h) - \log(E_{\frac{h}{2}})}{\log 2},$$

where E_h denotes the magnitude of the error with step size h.
All the computations that are presented in this section have been performed using Matlab 8.5. In all the examples, we have taken $a_\dagger = 1$, and $\psi_1(x) \equiv \psi_2(x) \equiv 1$.

Example 4.6.1

In order to test our numerical scheme, we assume that u_0, μ, and β are given by

$u_0(x) = \exp\left(-\int_0^x e^{\frac{1}{1-y}}dy\right)$, $\mu(x) = e^{\frac{1}{1-x}} + as$, $\beta(x,s) = b(1-x)^2$, $x \in [0,1)$, $s \geq 0$,

where $\frac{1}{a} = \int\limits_0^1 \exp\left(-\int_0^x e^{\frac{1}{1-y}}dy\right)dx \approx 0.2553$, and $\frac{1}{b} = \int\limits_0^1 (1-x)^2 \exp\left(-\int_0^x e^{\frac{1}{1-y}}dy\right)dx \approx$ 0.1720.
Note that, for these set of functions $u(x,t) = \frac{\exp\left(-\int_0^x e^{\frac{1}{1-y}}dy\right)}{(1+t)}$ is a solution to (4.2).
From (4.4)–(4.5), we get

$$\lambda(x,t) = \begin{cases} u(x,t)e^{-x+t}, & x \geq t, \\ u(x,t)(1-x+t), & x < t. \end{cases}$$

h	$\|\boldsymbol{U}^N - \boldsymbol{u}^N\|_\infty$	order(u)	$\|\boldsymbol{\Lambda}^N - \boldsymbol{\lambda}^N\|_\infty$	order(λ)
0.1/2	4.7221×10^{-4}	3.6091	6.0334×10^{-5}	2.6719
0.1/3	1.0381×10^{-4}	3.3609	2.1055×10^{-5}	2.8290
0.1/4	3.8698×10^{-5}	3.2711	9.4679×10^{-6}	2.8858
0.1/5	1.8376×10^{-5}	3.2052	5.0143×10^{-6}	2.9146
0.1/6	1.0104×10^{-5}	3.1450	2.9631×10^{-6}	2.9321
0.1/8	4.0087×10^{-6}	3.0197	1.2810×10^{-6}	2.9525

Table 4.1: The order of convergence for different choices of h with u_0, μ and β given in Example 4.6.1 using (4.36)–(4.47) and (4.10)–(4.11)

h	$\|\boldsymbol{U}^N - \boldsymbol{u}^N\|_\infty$	order(u)	$\|\boldsymbol{\Lambda}^N - \boldsymbol{\lambda}^N\|_\infty$	order(λ)
0.1/2	1.6668×10^{-4}	4.9733	1.7616×10^{-5}	3.7483
0.1/3	2.2412×10^{-5}	4.9871	3.9422×10^{-6}	3.8728
0.1/4	5.3061×10^{-6}	4.7665	1.3109×10^{-6}	3.9248
0.1/5	1.7338×10^{-6}	4.2071	5.5028×10^{-7}	3.9527

Table 4.2: The order of convergence for different choices of u_0, h with μ and β given in Example 4.6.1 using (4.132)–(4.138) and (4.10)–(4.11)

Now it is easy to verify that u, v, μ and β satisfy the hypotheses of Theorem 4.3.1. Hence (4.10) is a convergent numerical scheme.

In Table 4.1, we display the discretization error and the experimental order of convergence using (4.36)–(4.47) and (4.10) for different choices of h. On the other hand, we show the discretization error and the experimental order of convergence using (4.132)–(4.138) and (4.10) for different choices of h in Table 4.2. In the second column of the both tables, we show the maximum error of $\|\boldsymbol{U}^N - \boldsymbol{u}^N\|_\infty$ and in the fourth column of the both tables the maximum error of $\|\boldsymbol{\Lambda}^N - \boldsymbol{\lambda}^N\|_\infty$ is presented at $t = 1$. From Tables 4.1 and 4.2, one can conclude that the orders of convergence of proposed schemes (4.36)–(4.47) and (4.132)–(4.138) are three and four, respectively. Moreover, from the second and fourth columns of Tables 4.1 and 4.2, one can conclude that the approximate solution U, and Λ indeed converge to solution u, and λ, respectively as $h \to 0$.

In Figure 4.1, we display the exact and computed solution to (4.2) and (4.5). Moreover, we present the absolute difference between the exact solutions and the corresponding numerical solutions in Figure 4.1. In particular, we show the exact and approximate solutions to (4.2), and (4.5) in Figure 4.1(a) and 4.1(c), respectively, using (4.36)–(4.47) and (4.11) with $h = 0.025$ at $t = 2, 3$. The

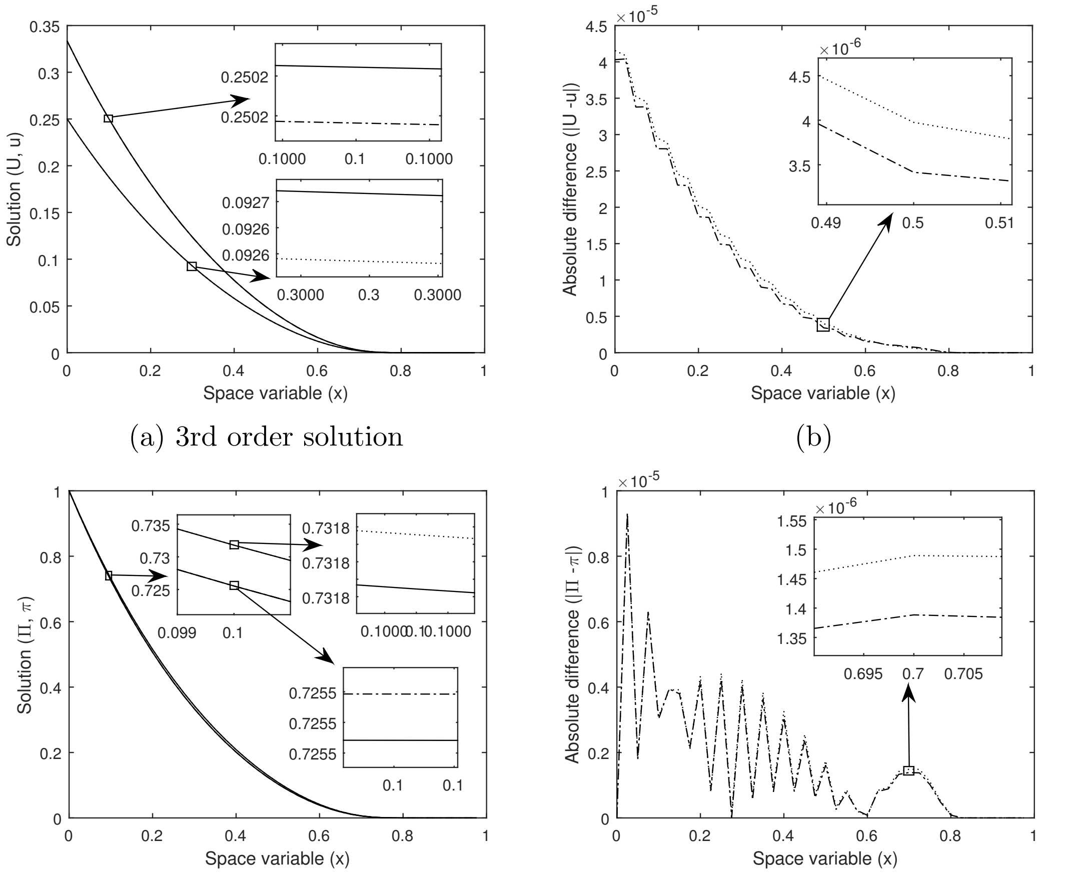

(a) 3rd order solution (b)

(c) 4th order solution (d)

Figure 4.1: The exact solutions and the approximate solutions to (4.2) using (4.11) and the third order approximation of λ at $t = 2,\ 3$ for $0 \leq x < 1$ with $\mu(x, s)$, $\beta(x, s)$ given in Example 4.6.1; (a): $u(x, 2), u(x, 3)$ (solid line), $U(x, 2)$ (dash-dotted line), $U(x, 3)$ (dotted line), (b): $\mid u(x, 2) - U(x, 2) \mid$ (dash-dotted line), $\mid u(x, 3) - U(x, 3) \mid$ (dotted line), (c): $\lambda(x, 2), \lambda(x, 3)$ (solid line), $\Lambda(x, 2)$ (dash-dotted line), $\Lambda(x, 3)$ (dotted line), (d): $\mid \lambda(x, 2) - \Lambda(x, 2) \mid$ (dash-dotted line), $\mid \lambda(x, 3) - \Lambda(x, 3) \mid$ (dotted line).

absolute differences $|u(x, t) - U(x, t)|$ and $|\lambda(x, t) - \Lambda(x, t)|$ at $t = 2, 3$ with $h = 0.025$ are presented in Figure 4.1(b) and Figure 4.1(d), respectively.

Similarly, we display the exact and computed solutions to (4.2) and (4.5), and their absolute differences at different times in Figure 4.2. In Figure 4.2(a), we present the exact solution to (4.2) and the approximate solutions to (4.2) using the fourth order method (4.132)–(4.138) and (4.10) at $t = 2, 3$ with $h = 0.025$. We also show the exact and the computed solutions to (4.5) in Figure 4.2(c). On the other hand, we show the absolute differences $|u(x, t) - U(x, t)|$ and $|\lambda(x, t) -$

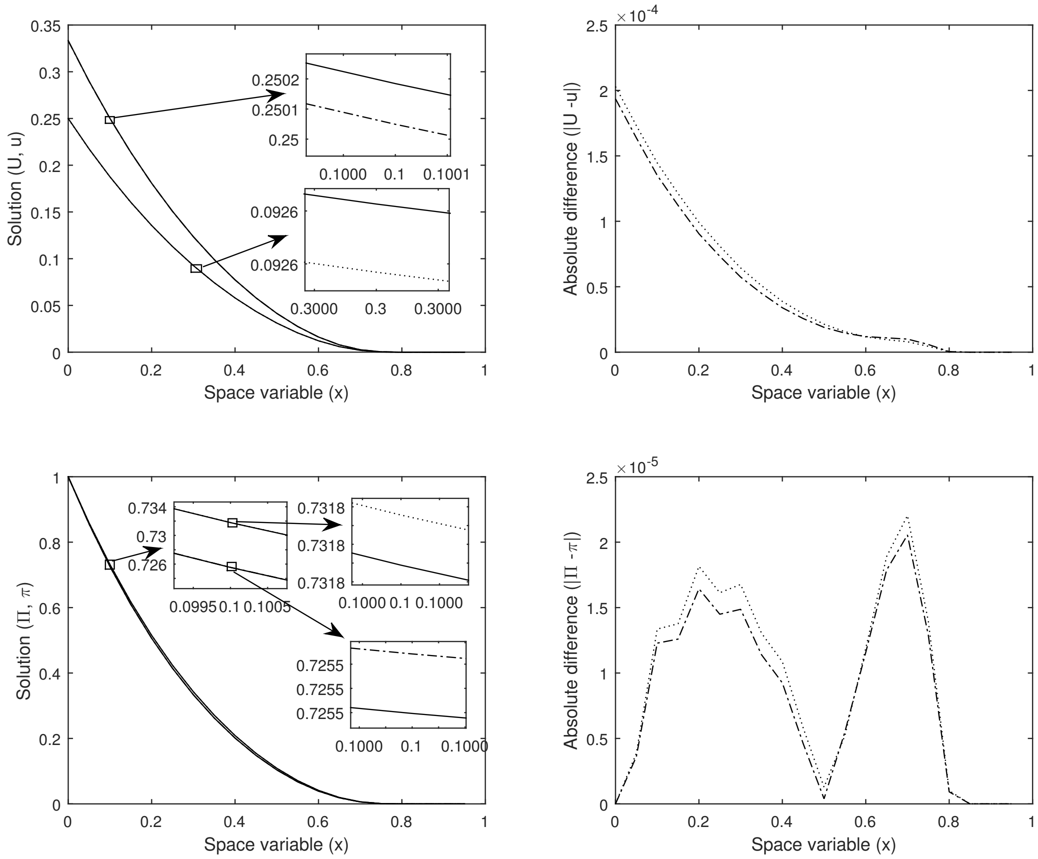

Figure 4.2: The exact solutions and the approximate solutions to (4.2) using (4.11) and the fourth order approximation of λ at $t = 2,\ 3$ for $0 \leq x < 1$ with $\mu(x, s)$, $\beta(x, s)$ given in Example 4.6.1; (a): $u(x, 2), u(x, 3)$ (solid line), $U(x, 2)$ (dash-dotted line), $U(x, 3)$ (dotted line), (b): $\mid u(x, 2) - U(x, 2) \mid$ (dash-dotted line), $\mid u(x, 3) - U(x, 3) \mid$ (dotted line), (c): $\lambda(x, 2), \lambda(x, 3)$ (solid line), $\Lambda(x, 2)$ (dash-dotted line), $\Lambda(x, 3)$ (dotted line), (d): $\mid \lambda(x, 2) - \Lambda(x, 2) \mid$ (dash-dotted line), $\mid \lambda(x, 3) - \Lambda(x, 3) \mid$ (dotted line).

$\Lambda(x, t)|$ at $t = 2, 3$ with $h = 0.1/4$ in Figures 4.2(b) and 4.2(d), respectively.

Example 4.6.2

In this example, we consider a standard type of unbounded mortality rate that is considered in literature. In order to test the efficacy of our numerical scheme, we assume that u_0, μ, and β are given by

$$u_0(x) = (1 - x)^5,\ \mu(x) = \tfrac{5}{1-x} + 18s^2,\ \beta(x, s) = 7(1 - x),\ \ x \in [0, 1),\ \ s \geq 0.$$

Note that, for these set of functions $u(x, t) = \frac{(1-x)^5}{\sqrt{1+t}}$ is a solution to (4.2). From

h	$\Vert \boldsymbol{U}^N - \boldsymbol{u}^N \Vert_\infty$	order(u)	$\Vert \boldsymbol{\Lambda}^N - \boldsymbol{\lambda}^N \Vert_\infty$	order(λ)
0.1/3	2.8225×10^{-4}	3.7548	2.2193×10^{-5}	2.6891
0.1/4	9.1319×10^{-5}	3.5184	1.0594×10^{-5}	2.8136
0.1/5	3.9448×10^{-5}	3.3576	5.7497×10^{-6}	2.8686
0.1/6	2.0908×10^{-5}	3.2845	3.4413×10^{-6}	2.8988
0.1/7	1.2419×10^{-5}	3.2370	2.2150×10^{-6}	2.9178
0.1/8	7.9692×10^{-6}	3.2014	1.5069×10^{-6}	2.9308

Table 4.3: The order of convergence for different choices of h with u_0, μ and β given in Example 4.6.2 using (4.36)–(4.47) and (4.10)–(4.11)

h	$\Vert \boldsymbol{U}^N - \boldsymbol{u}^N \Vert_\infty$	order(u)	$\Vert \boldsymbol{\Lambda}^N - \boldsymbol{\lambda}^N \Vert_\infty$	order(λ)
0.1/2	9.5184×10^{-4}	5.0938	2.7872×10^{-5}	5.0601
0.1/3	1.2293×10^{-4}	5.2508	4.6183×10^{-6}	5.2877
0.1/4	2.7872×10^{-5}	5.4257	1.0488×10^{-6}	5.4758
0.1/5	8.6093×10^{-6}	5.6448	3.2029×10^{-7}	5.6677
0.1/6	3.2285×10^{-6}	5.9418	1.1823×10^{-7}	5.9255

Table 4.4: The order of convergence for different choices of u_0, h with μ and β given in Example 4.6.2 using (4.132)–(4.138) and (4.10)–(4.11)

(4.4)–(4.5), we get that

$$\lambda(x,t) = \begin{cases} u(x,t)e^{\frac{-x+t}{2}}, & x \geq t, \\ u(x,t)\sqrt{1-x+t}, & x < t. \end{cases}$$

One can easily check that u_0, μ and β satisfy the hypotheses of Theorem 4.3.1. Hence (4.10) is a convergent numerical scheme.

In Table 4.3, we present the computational error and the experimental order of convergence using (4.36)–(4.47) and (4.10) for different choices of h. Similarly, we display the computational error and the experimental order of convergence using (4.132)–(4.138) and (4.10) for different choices of h in Table 4.4. In particular, we show the maximum error $\Vert \boldsymbol{U}^N - \boldsymbol{u}^N \Vert_\infty$ at $t = 1$ in the second column of the both tables. Besides this, the maximum error of $\Vert \boldsymbol{\Lambda}^N - \boldsymbol{\lambda}^N \Vert_\infty$ at $t = 1$ is presented in the fourth column of both the tables. From Tables 4.3 and 4.4, we can observe that the orders of convergence of proposed schemes (4.36)–(4.47) and (4.132)–(4.138) are three and four, respectively. The second and fourth columns of Tables 4.3 and 4.4 show that (U_i^n, Λ_i^n) indeed converges to (u_i^n, λ_i^n), as $h \to 0$.

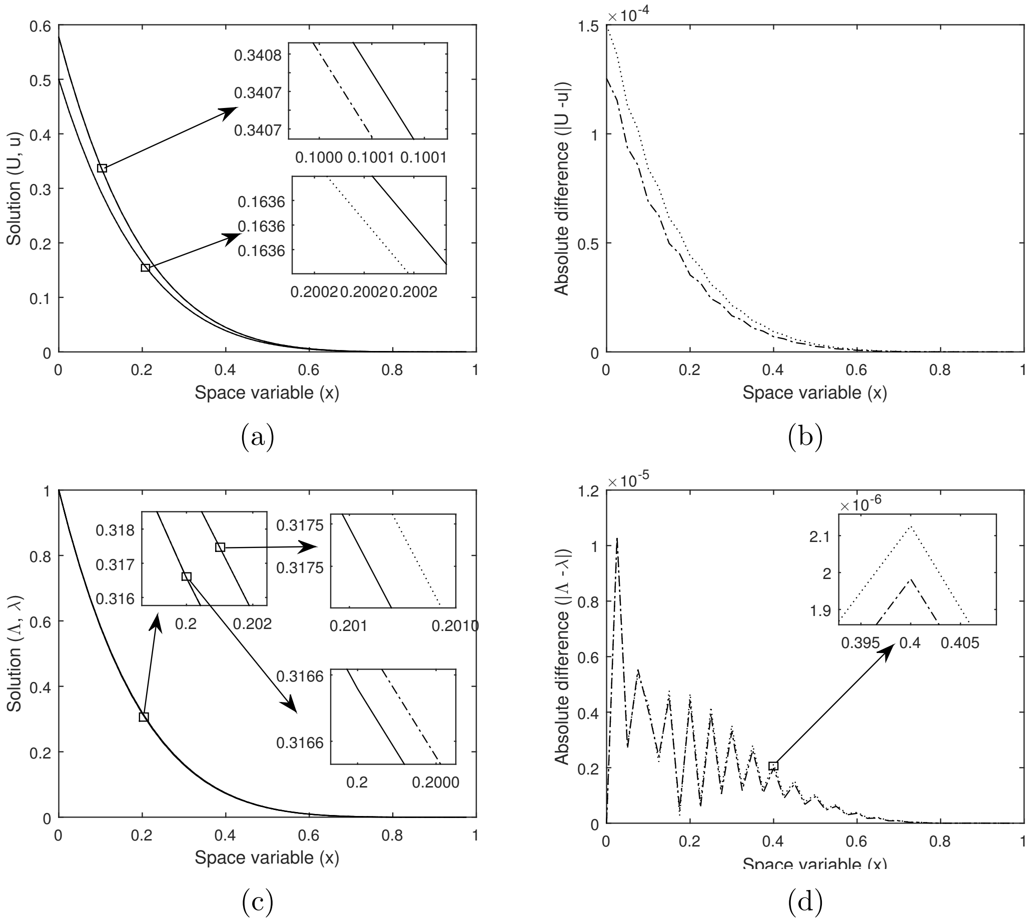

Figure 4.3: The exact solutions and the approximate solutions to (4.2) using (4.11) and the third order approximation of λ at $t = 2,\ 3$ for $0 \leq x < 1$ with $\mu(x,s)$, $\beta(x,s)$ given in Example 4.6.2; (a): $u(x,2), u(x,3)$ (solid line), $U(x,2)$ (dash-dotted line), $U(x,3)$ (dotted line), (b): $\mid u(x,2) - U(x,2) \mid$ (dash-dotted line), $\mid u(x,3) - U(x,3) \mid$ (dotted line), (c): $\lambda(x,2), \lambda(x,3)$ (solid line), $\Lambda(x,2)$ (dash-dotted line), $\Lambda(x,3)$ (dotted line), (d): $\mid \lambda(x,2) - \Lambda(x,2) \mid$ (dash-dotted line), $\mid \lambda(x,3) - \Lambda(x,3) \mid$ (dotted line).

In Figure 4.3, we present the exact and computed solutions to (4.2) and (4.5) and their absolute differences. To be more specific, we plot the exact solution and the computed solutions to (4.2) using (4.36)–(4.47) and (4.10) at different time levels with $h = 0.0.025$ in Figure 4.3(a), and the corresponding absolute error in Figure 4.3(b). We present λ and its approximation Λ using (4.36)–(4.47) at $t = 2, 3$ in Figure 4.3(c), and the corresponding $|\lambda - \Lambda|$ in Figure 4.3(d).
As before, the exact solutions to u and λ, and their approximated solutions using

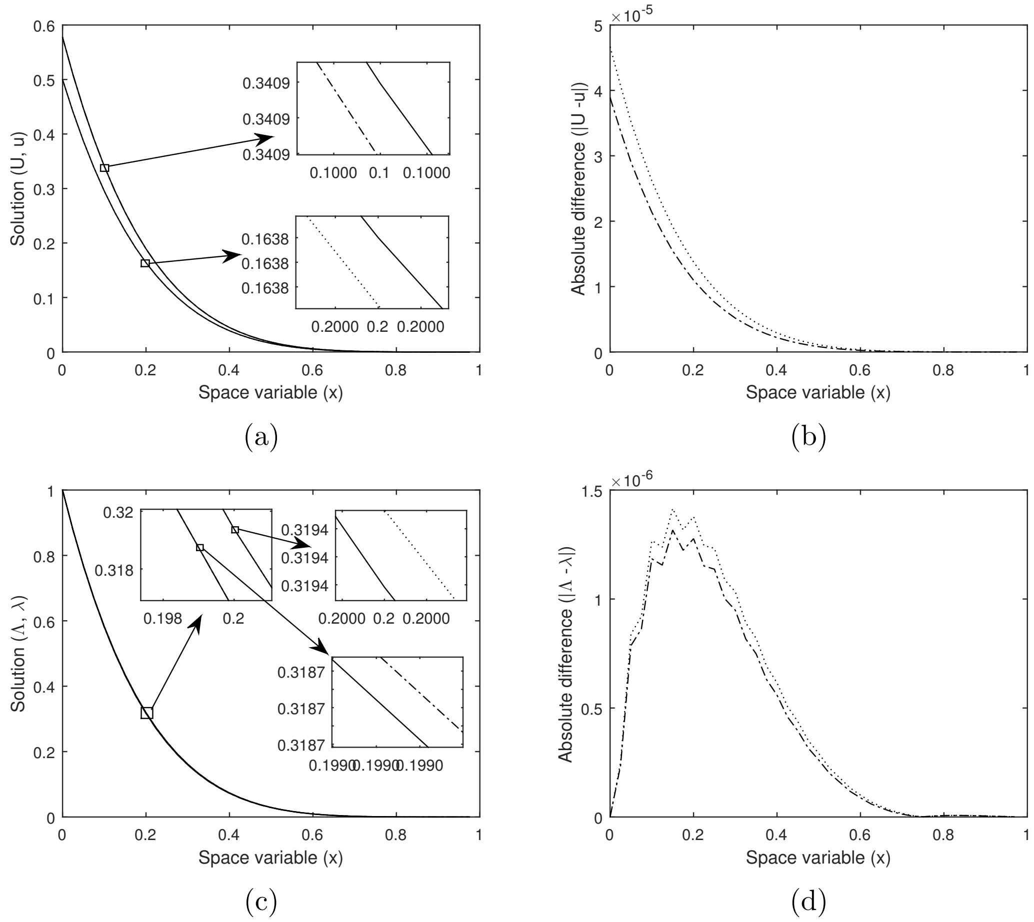

Figure 4.4: The exact solutions and the approximate solutions to (4.2) using (4.11) and the fourth order approximation of λ at $t = 2, 3$ for $0 \leq x < 1$ with $\mu(x, s)$, $\beta(x, s)$ given in Example 4.6.2; (a): $u(x, 2), u(x, 3)$ (solid line), $U(x, 2)$ (dash-dotted line), $U(x, 3)$ (dotted line), (b): $\mid u(x, 2) - U(x, 2) \mid$ (dash-dotted line), $\mid u(x, 3) - U(x, 3) \mid$ (dotted line), (c): $\lambda(x, 2), \lambda(x, 3)$ (solid line), $\Lambda(x, 2)$ (dash-dotted line), $\Lambda(x, 3)$ (dotted line), (d): $\mid \lambda(x, 2) - \Lambda(x, 2) \mid$ (dash-dotted line), $\mid \lambda(x, 3) - \Lambda(x, 3) \mid$ (dotted line).

(4.132)–(4.136) and (4.10) at $t = 2, 3$ with $h = 0.025$ are displayed in Figure 4.4(a) and Figure 4.4(c), respectively. We show the corresponding absolute differences $|u - U|$ and $|\lambda - \Lambda|$ in Figure 4.4(b) and Figure 4.4(d), respectively.

Example 4.6.3

Let the vital rates μ, β and the initial data u_0 be given by

$$u_0(x) = e^{-\int_0^x \left(\mu(y)-1\right) dy},\ \mu(x) = e^{\frac{1}{1-x}},\ \beta(x) = 3.9156e^{-x},\ \ x \in [0, 1).$$

One can easily check that $u(x, t) = e^{x-t-\int_0^x \mu(y)dy}$ is a solution to (4.2). From

h	$\|\boldsymbol{U}^N - \boldsymbol{u}^N\|_\infty$	order(u)	$\|\boldsymbol{\Lambda}_s - \boldsymbol{\lambda}_s\|_\infty$	order(λ_s)
0.1/2	2.5302×10^{-5}	5.5334	2.0396×10^{-6}	3.9304
0.1/3	2.5580×10^{-6}	5.2011	4.1738×10^{-7}	3.9677
0.1/4	5.4632×10^{-7}	4.8602	1.3378×10^{-7}	3.9816
0.1/5	1.7110×10^{-7}	4.5834	5.5131×10^{-8}	3.9882
0.1/6	6.9538×10^{-8}	4.4077	2.6676×10^{-8}	3.9918
0.1/8	1.8810×10^{-8}	4.2093	8.4686×10^{-9}	3.9953

Table 4.5: The order of convergence for different choices of h with u, μ and β given in Example 4.6.3 using (4.147) and (4.10)–(4.11)

(4.5), we get that $\lambda(x) = e^{-\int_0^x \mu(y)dy}$.

Since u_0, μ and β satisfy the hypotheses of Theorem 4.3.1, (4.10) is a convergent numerical scheme.

In Table 4.5, we show the magnitude of the computational error and the experimental order of convergence for different choices of h at $t = 1$. In the second and fourth columns, we present the maximum absolute error $\|\boldsymbol{U}^N - \boldsymbol{u}^N\|_\infty$ and $\|\boldsymbol{\Lambda}_s - \boldsymbol{\lambda}_s\|_\infty$, respectively at $t = 1$. The corresponding experimental orders of convergence are shown in the third and fifth column of the table, respectively. From Table 4.5, we can observe that the order of convergence of the proposed numerical scheme (4.10) and (4.146) is indeed four.

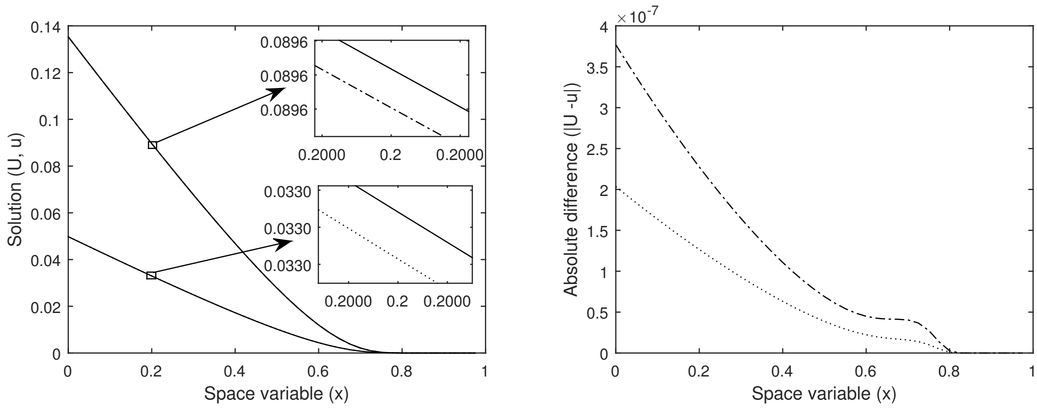

Figure 4.5: The exact solution to (4.1), and the approximate solutions using (4.11) and (4.147) with $\mu(x, s)$, $\beta(x, s)$ given in Example 4.6.3; Left: $u(x, 1)$ (solid line), $\boldsymbol{U}_{0.01}$ (dash-dotted line) for $0 \leq x < 1$, Right: $|\, u(x, 1) - \boldsymbol{U}_{0.01} \,|$ (solid line).

In Figure 4.5, we show the exact and computed solutions to (4.1) and their absolute differences with $h = 0.025$ at $t = 2, 3$. In particular, we display the exact

h	$\|\boldsymbol{U}^N - \boldsymbol{u}^N\|_\infty$	order(u)	$\|\boldsymbol{\Lambda}_s - \boldsymbol{\lambda}_s\|_\infty$	order(λ)	
0.1/4	1.8138×10^{-5}	5.4199	2.1744×10^{-9}	3.9990	
0.1/6	2.1157×10^{-6}	5.9903	4.2981×10^{-10}	3.9995	$\gamma = 5$
0.1/8	4.2368×10^{-7}	7.5077	1.3599×10^{-10}	3.9994	
0.1/4	4.4947×10^{-6}	5.9740	3.2233×10^{-9}	3.9914	
0.1/6	4.4745×10^{-7}	10.9143	6.3934×10^{-10}	3.9950	$\gamma = 4$
0.1/8	7.1506×10^{-8}	5.0687	2.0266×10^{-10}	3.9966	
0.1/4	1.3231×10^{-6}	5.9153	6.6043×10^{-8}	3.0000	
0.1/6	1.3355×10^{-7}	5.7828	1.9568×10^{-8}	3.0000	$\gamma = 3$
0.1/8	2.1924×10^{-8}	4.4181	8.2554×10^{-9}	3.0000	
0.1/4	1.0130×10^{-6}	4.0587	3.4820×10^{-7}	2.5000	
0.1/6	1.4755×10^{-7}	2.7357	1.2636×10^{-7}	2.5000	$\gamma = 2.5$
0.1/8	6.0789×10^{-8}	2.4910	6.1554×10^{-8}	2.5000	

Table 4.6: The order of convergence for different choices of h with u, μ and β given in Example 4.6.4 using (4.147) and (4.10)–(4.11)

solution and computed solutions to (4.1) using (4.10) and (4.146) at $t = 2, 3$ with $h = 0.025$ in Figure 4.5(left). In Figure 4.5(right), we present the absolute difference $|u - U|$ when $h = 0.025$.

Example 4.6.4

In this example, we consider a standard type of unbounded mortality rate that appears in the literature. In order to test the efficacy of the numerical scheme, we assume that u_0, μ, and β are given by

$$u_0(x) = (1-x)^\gamma e^x, \;\; \mu(x) = \tfrac{\gamma}{1-x}, \;\; \beta(x) = (\gamma+2)(1-x), \;\; x \in [0,1), \;\; s \geq 0.$$

For the given set of functions, one can observe that $u(x,t) = (1-x)^\gamma e^{x-t}$ is the solution to (4.1). From (4.145)–(4.146), we get that $\lambda(x) = (1-x)^\gamma$. It is easy to verify that μ satisfies the hypotheses of Theorem4.5.2 when $\gamma \geq 5$. Moreover, if $\gamma \in [3, 5)$, then μ satisfies the hypotheses of the main theorems of [3, 4]. In Table 4.6, we display the magnitude of the computational error and the experimental order of convergence for different choices of h and γ at $t = 1$. We show the maximum absolute error $\|\boldsymbol{U}^N - \boldsymbol{u}^N\|_\infty$ and $\|\boldsymbol{\Lambda}_s - \boldsymbol{\lambda}_s\|_\infty$ at $t = 1$ in the second and fourth columns of the table, respectively. In addition, the corresponding the experimental orders of convergence are presented in the third and fifth columns of the table, respectively. From Table 4.5, we can observe that the order of convergence of the proposed numerical scheme (4.10) and (4.146) is $\min\{\gamma, 4\}$. On the other hand, the order of the numerical scheme proposed in [3, 4] is at most 2. Though the hypotheses of Theorems 4.3.1 and 4.5.1 are not satisfied when $\gamma \in [3, 5)$, experimental results suggest that our method gives better order of convergence. Therefore from these calculations, it evident that proposed numerical scheme (4.10) and (4.146) is more efficient than the scheme proposed in [3, 4].

Conclusion

An implicit finite difference scheme is presented to approximate the solution to the McKendrick–Von Foerster equation with diffusion (M-V-D) (2.1) in which nonlocal nonlinear Robin boundary conditions is considered at both the end points. We have introduced the notion of upper and lower solutions and used effectively with the aid of the discrete maximum principle to study the wellposedness and stability of the numerical scheme. A relation between the numerical solutions to the M-V-D and the steady state problem is established. Moreover, we have proposed an implicit scheme to find an approximate the solution to the M-V-D with a special type of nonlinearity (see (2.41)). Using the similar technique, we have established a relation between the numerical solutions to (2.41) and its steady state problem.

We have proposed a finite difference numerical scheme to the M-V-D (3.1) in which the Robin condition is prescribed at the boundary point $x = 0$, and the Dirichlet condition is given at $x = a_\dagger$. Furthermore, we have proved that the proposed numerical scheme is stable restricted to the thresholds R_h. Moreover, we have established that the given scheme is indeed convergent using a result due to Stetter. The result is extended to the M-V-D with nonlocal nonlinear Robin boundary conditions at both the end points in a bounded domain (see (3.30)). Using the similar technique, one can easily obtain a convergent scheme when (3.1) has nonlinear, nonlocal Neumann boundary condition at $x = 0$. However, it is an interesting problem to design a convergent scheme for (3.1) in the unbounded domain $[0, \infty)$.

We presented higher-order numerical schemes to the McKendrick–Von Foerster equation (4.2) when the death rate has singularity at the maximum age. Using the method of characteristics (non-intersecting), we proposed the third, fourth-order schemes which are multi-step methods with appropriate corrections at each step. In fact, the convergence analysis of these schemes is discussed in detail in the thesis. Moreover, numerical experiments are provided to validate the orders of convergence of the proposed third-order and fourth-order schemes.

Bibliography

[1] L. M. Abia, O. Angulo, and J. C. López-Marcos. Age-structured population models and their numerical solution. *Ecological modelling*, 188(1):112–136, 2005. ↑91

[2] L. M. Abia, O. Angulo, J. C. López-Marcos, and M. A. López-Marcos. Numerical study on the proliferation cells fraction of a tumour cord model. *Math. Comput. Modelling*, 52(7-8):992–998, 2010. ↑63

[3] L. M. Abia, O. Angulo, J. C. López-Marcos, and M. A. López-Marcos. Approximating the survival probability in finite life-span population models. *J. Comput. Appl. Math.*, 330:783–793, 2018. ↑63, ↑91, ↑92, ↑93, ↑139, ↑140

[4] L. M. Abia, O. Angulo, J. C. López-Marcos, and M. Á. López-Marcos. Numerical approximation of finite life-span age-structured population models. *Mathematical Methods in the Applied Sciences*, 45(6):3272–3283, 2022. ↑91, ↑92, ↑93, ↑139, ↑140

[5] L. M. Abia and J. C. López Marcos. Runge-Kutta methods for age-structured population models. *Appl. Numer. Math.*, 17(1):1–17, 1995. ↑91

[6] O. Angulo, J. C. López-Marcos, M. A. López-Marcos, and F. A. Milner. A numerical method for nonlinear age-structured population models with finite maximum age. *Journal of mathematical analysis and applications*, 361(1):150–160, 2010. ↑90, ↑92, ↑93, ↑96

[7] O. Angulo, J. C. López-Marcos, and F. A. Milner. The application of an age-structured model with unbounded mortality to demography. *Math. Biosci.*, 208(2):495–520, 2007. ↑90

[8] T. Arbogast and F. A. Milner. A finite difference method for a two-sex model of population dynamics. *SIAM J. Numer. Anal.*, 26(6):1474–1486, 1989. ↑91

[9] K. E. Atkinson. *An introduction to numerical analysis.* John wiley & sons, 2008. ↑103, ↑104

[10] N. Bacaër. *A short history of mathematical population dynamics.* Springer-Verlag London, Ltd., London, 2011. ↑89

[11] C. Barril, À. Calsina, S. Cuadrado, and J. Ripoll. On the basic reproduction number in continuously structured populations. *Math. Methods Appl. Sci.*, 44(1):799–812, 2021. ↑64, ↑78

[12] B. Basse, B. C. Baguley, E. S. Marshall, W. R. Joseph, B. Van Brunt, G. Wake, and D. J. N. Wall. A mathematical model for analysis of the cell cycle in cell lines derived from human tumors. *Journal of Mathematical Biology*, 47(4):295–312, 2003. ↑3

[13] D. Breda, F. Florian, J. Ripoll, and R. Vermiglio. Efficient numerical computation of the basic reproduction number for structured populations. *J. Comput. Appl. Math.*, 384:Paper No. 113165, 15, 2021. ↑64

[14] D. Breda, T. Kuniya, J. Ripoll, and R. Vermiglio. Collocation of next-generation operators for computing the basic reproduction number of structured populations. *J. Sci. Comput.*, 85(2):Paper No. 40, 33, 2020. ↑64

[15] G. Choudury and P. Korman. On computation of solutions of fully nonlinear elliptic problems. *Journal of computational and applied mathematics*, 41(3):301–311, 1992. ↑25

[16] J. Coyle and N. Nigam. High-order discontinuous Galerkin methods for a class of transport equations with structured populations. *Comput. Math. Appl.*, 72(3):768–784, 2016. ↑90

[17] C. Cusulin and L. Gerardo-Giorda. A numerical method for spatial diffusion in age-structured populations. *Numer. Methods Partial Differential Equations*, 26(2):253–273, 2010. ↑91

[18] W. A. Day. Extensions of a property of the heat equation to linear thermoelasticity and other theories. *Quart. Appl. Math.*, 40(3):319–330, 1982. ↑4, ↑25, ↑63

[19] W. A. Day. *Heat conduction within linear thermoelasticity.* Springer, New York, 1985. ↑4, ↑6, ↑25, ↑29, ↑63

[20] K. Deng. Comparison principle for some nonlocal problems. *Quart. Appl. Math.*, 50(3):517–522, 1992. ↑25

[21] O. Diekmann and J. A. P. Heesterbeek. *Mathematical epidemiology of infectious diseases.* Wiley Series in Mathematical and Computational Biology. John Wiley & Sons, Ltd., Chichester, 2000. Model building, analysis and interpretation. ↑25, ↑63

[22] A. Friedman. Generalized heat transfer between solids and gases under nonlinear boundary conditions. *Journal of Mathematics and Mechanics*, 8:161–183, 1959. ↑25

[23] A. Friedman. Monotonic decay of solutions of parabolic equations with nonlocal boundary conditions. *Quart. Appl. Math.*, 44(3):401–407, 1986. ↑25

[24] D. Greenspan and S. V. Parter. Mildly nonlinear elliptic partial differential equations and their numerical solutoin. ii. *Numerische Mathematik*, 7(2):129–146, 1965. ↑25

[25] M. E. Gurtin. The galerkin method as applied to problems in viscoelasticity. *Internat. J. Solids Structures*, 10(9):933–943, 1974. ↑3

[26] M. E. Gurtin and R. C. MacCamy. Non-linear age-dependent population dynamics. *Arch. Rational Mech. Anal.*, 54:281–300, 1974. ↑90

[27] J. Halder and S. K. Tumuluri. A higher order numerical scheme to a nonlinear mckendrick–von foerster equation with singular mortality. *(communicated).* ↑18

[28] J. Halder and S. K. Tumuluri. A survey of age-structured population models in population dynamics. *The Proceedings of Telangana Academy of Sciences*, 1(1):156–168, 2020. ↑63, ↑89, ↑91

[29] J. Halder and S. K. Tumuluri. A numerical scheme for a diffusion equation with nonlocal nonlinear boundary condition. *Comput. Appl. Math.*, 42(2):article no: 84, 2023. ↑91

[30] J. Halder and S. K. Tumuluri. Numerical solution of a nonlinear mckendrick–von foerster equation with diffusion. *Numer. Algorithms*, 92(2):1007–1039, 2023. ↑64, ↑78, ↑91

[31] H. J. A. M. Heijmans. The dynamical behaviour of the age-size distribution of a cell population. In J. A. J. Metz and 0. Diekmann, editors, *Dynamics of Physiologically Structured Populations*, volume 68, pages 185–202. Springer, Singapore, 2nd edition, 1986. ↑2

[32] M. Iannelli. Mathematical theory of age-structured population dynamics. *Giardini editori e stampatori in Pisa*, 1995. ↑91, ↑96

[33] M. Iannelli and F. Milner. *The Basic Approach to Age-Structured Population Dynamics*. Springer, Dordrecht, 2017. ↑63, ↑89

[34] M. Iannelli and F. A. Milner. On the approximation of the lotka–mckendrick equation with finite life-span. *Journal of computational and applied mathematics*, 136(1-2):245–254, 2001. ↑90, ↑91

[35] Hisashi Inaba. *Age-structured population dynamics in demography and epidemiology*. Springer, 2017. ↑63, ↑89

[36] B. K. Kakumani and S. K. Tumuluri. On a nonlinear renewal equation with diffusion. *Math. MethodsAppl. Sci.*, 39(4):697–708, 2016. ↑4, ↑63, ↑64

[37] B. K. Kakumani and S. K. Tumuluri. Asymptotic behavior of the solution of a diffusion equation with nonlocal boundary conditions. *Discrete Contin. Dyn. Syst. Ser. B*, 22(2):407–419, 2017. ↑4, ↑6, ↑26, ↑29, ↑63, ↑64

[38] B. K. Kakumani and S. K. Tumuluri. A numerical scheme to the mckendrick–von foerster equation with diffusion in age. *Numer. Methods Partial Differential Equations*, 34(6):2113–2128, 2018. ↑26, ↑64

[39] B. Kawohl. Remarks on a paper by w.a.day on a maximum principle under nonlocal boundary conditions. *Quart. Appl. Math.*, 44(4):751–752, 1987. ↑25

[40] M. Kim. Long-time stability of numerical solutions to Gurtin-MacCamy equations by method of characteristics. *Appl. Math. Comput.*, 176(2):552–562, 2006. ↑91

[41] M. Kim. Discontinuous-continuous Galerkin methods for a structured model of a biological system. *SIAM J. Sci. Comput.*, 31(2):913–938, 2008/09. ↑90

[42] M. Kim and Y. Kwon. A collocation method for the gurtin–maccamy equation with finite life-span. *SIAM journal on numerical analysis*, 39(6):1914–1937, 2002. ↑90, ↑91, ↑92, ↑93, ↑96

[43] M. Kim and T. Selenge. Age-time continuous Galerkin method for a model of population dynamics. *J. Comput. Appl. Math.*, 223(2):659–671, 2009. ↑90, ↑93

[44] M. Kim and T. Selenge. Discontinuous-continuous Galerkin methods for population diffusion with finite life span. *Math. Popul. Stud.*, 23(1):17–36, 2016. ↑90

[45] Y. Kwon and C. Cho. Second-order accurate difference methods for a one-sex model of population dynamics. *SIAM J. Numer. Anal.*, 30(5):1385–1399, 1993. ↑91

[46] A. C. Lazer, A. W. Leung, and Murio D. A. Monotone scheme for finite difference equations concerning steady-state prey-predator interactions. *Journal of Computational and Applied Mathematics*, 8(4):243–252, 1982. ↑25

[47] M. C. A. Leite, B. Chen-Charpentier, and F. B. Agusto. A mathematical model of tree harvesting in age-structured forests subject to beetle infestations. *Comput. Appl. Math.*, 37(3):3365–3384, 2018. ↑63

[48] X. Li, J. Yang, and M. Martcheva. *Age structured epidemic modeling*, volume 52 of *Interdisciplinary Applied Mathematics*. Springer, Cham, [2020] ©2020. ↑89

[49] Y. Lin, S. Xu, and H. M. Yin. Finite difference approximations for a class of non-local parabolic equations. *Internat. J. Math. Math. Sci.*, 20(1):147–163, 1997. ↑25

[50] J. C. López Marcos. An upwind scheme for a nonlinear hyperbolic integro-differential equation with integral boundary condition. *Comput. Math. Appl.*, 22(11):15–28, 1991. ↑64, ↑68

[51] J. C. López Marcos and J. M. Sanz-Serna. A definition of stability for nonlinear problems. In *Numerical treatment of differential equations (Halle, 1987)*, volume 104 of *Teubner-Texte Math.*, pages 216–226. Teubner, Leipzig, 1988. ↑64, ↑69

[52] J. C. López-Marcos and J. M. Sanz-Serna. Stability and convergence in numerical analysis iii: Linear investigation of nonlinear stability. *IMA journal of numerical analysis*, 8(1):71–84, 1988. ↑64

[53] T. R. Malthus. *An essay on the principle of population.* J. Johnson, London, London, 1798. ↑1

[54] W. R. Mann and F. Wolf. Heat transfer between solids and gases under nonlinear boundary conditions. *Quarterly of Applied Mathematics*, 9(2):163–184, 1951. ↑25

[55] A. G. McKendrick. Applications of mathematics to medical problems. *Proceedings of the Edinburgh Mathematical Society*, 44:98–130, 1925. ↑2

[56] P. Michel and T. M. Touaoula. Asymptotic behavior for a class of the renewal nonlinear equation with diffusion. *Mathematical Methods in the Applied Sciences*, 36(3):323–335, 2012. ↑4

[57] P. Michel and T. M. Touaoula. Asymptotic behavior for a class of the renewal nonlinear equation with diffusion. *Mathematical Methods in the Applied Sciences*, 36(3):323–335, 2013. ↑4, ↑26, ↑63

[58] P. Michel and S. K. Tumuluri. A note on a neuron network model with diffusion. *Discrete Contin. Dyn. Syst. Ser. B*, 25(9):3659–3676, 2020. ↑4, ↑25, ↑63

[59] F. A. Milner and G. Rabbiolo. Rapidly converging numerical algorithms for models of population dynamics. *J. Math. Biol.*, 30(7):733–753, 1992. ↑91

[60] J. D. Murray. *Mathematical biology. I*, volume 17 of *Interdisciplinary Applied Mathematics*. Springer-Verlag, New York, third edition, 2002. An introduction. ↑25, ↑63

[61] J. D. Murray. *Mathematical biology. II*, volume 18 of *Interdisciplinary Applied Mathematics*. Springer-Verlag, New York, third edition, 2003. Spatial models and biomedical applications. ↑25, ↑63

[62] M. N. Özışık. *Boundary value problems of heat conduction*. courier Corporation, 1989. ↑25

[63] C. V. Pao. Asymptotic behavior of solutions for finite-difference equations of reaction-diffusion. *SIAM J. Numer. Anal.*, 24(1):24–35, 1987. ↑26

[64] C. V. Pao. Asymptotic behavior of solutions for finite-difference equations of reaction-diffusion. *J. Math. Anal. Appl.*, 144(1):206–225, 1989. ↑25, ↑26

[65] C. V. Pao. *Nonlinear parabolic and elliptic equations*. Plenum Press, New York, 1992. ↑25

[66] C. V. Pao. Dynamics of reaction-diffusion equations with nonlocal boundary conditions. *Quart. Appl. Math.*, 53(1):173–186, 1995. ↑25

[67] C. V. Pao. Finite difference reaction diffusion equations with nonlinear boundary conditions. *Numer. Methods Partial Differential Equations*, 11(4):355–374, 1995. ↑26, ↑28

[68] C. V. Pao. Asymptotic behavior of solutions of reaction-diffusion equations with nonlocal boundary conditions. *J. Comput. Appl. Math.*, 88(1):225–238, 1998. ↑25

[69] C. V. Pao. Numerical solutions of reaction-diffusion equations with nonlocal boundary conditions. *J. Comput. Appl. Math.*, 136(1-2):227–243, 2001. ↑26

[70] G. Pelovska. An improved explicit scheme for age-dependent population models with spatial diffusion. *Int. J. Numer. Anal. Model.*, 5(3):466–490, 2008. ↑91

[71] G. Pelovska and M. Iannelli. Numerical methods for the Lotka-McKendrick's equation. *J. Comput. Appl. Math.*, 197(2):534–557, 2006. ↑91

[72] B. Perthame. *Transport equations in biology*. Birkhäuser Verlag Basel, Berlin, 2007. ↑25, ↑63

[73] B. Perthame. *Parabolic equations in biology*. Lecture Notes on Mathematical Modelling in the Life Sciences. Springer, Cham, 2015. Growth, reaction, movement and diffusion. ↑25, ↑63

[74] L. W. Ross. Perturbation analysis of diffusion-coupled biochemical reaction kinetics. *SIAM Journal on Applied Mathematics*, 19(2):323–329, 1970. ↑25

[75] M. Rotenberg. Transport theory for growing cell populations. *J. Theoret. Biol.*, 103(2):181–199, 1983. ↑2

[76] R. D. Russell and L. F. Schampine. Numerical methods for singular boundary value problems. *SIAM J. Numer. Anal.*, 12:13–36, 1975. ↑25

[77] J. M. Sanz-Serna. Stability and convergence in numerical analysis. I. Linear problems—a simple, comprehensive account. In *Nonlinear differential equations (Granada, 1984)*, volume 132 of *Res. Notes in Math.*, pages 64–113. Pitman, Boston, MA, 1985. ↑64

[78] D. H. Sattinger. Monotone method in nonlinear elliptic and parabolic boundary value problem. *Indiana Univ. Math. J.*, 21:979–1000, 1972. ↑25

[79] H. J. Stetter. *Analysis of discretization methods for ordinary differential equations*. Springer-Verlag, New York-Heidelberg, 1973. Springer Tracts in Natural Philosophy, Vol. 23. ↑65, ↑69

[80] G. Q. Sun. Mathematical modeling of population dynamics with allee effect. *Nonlinear Dyn*, 85:1–12, 2016. ↑1

[81] H. R. Thieme. *Mathematics in population biology*. Princeton Series in Theoretical and Computational Biology. Princeton University Press, Princeton, NJ, 2003. ↑25, ↑63

[82] G. F. Webb. *Theory of nonlinear age-dependent population dynamics*, volume 89 of *Monographs and Textbooks in Pure and Applied Mathematics*. Marcel Dekker, Inc., New York, 1985. ↑2, ↑89

[83] R. White. A review of some mathematical models in cell kinetics. In M. Rotenberg, editor, *Biomarhematics und Cell Kinetics, Developments in Cell Biology*, volume 8, pages 243–261. Elsevier North-Holland Biomedical Press, 1981. ↑2

Numerical study of nonlinear McKendrick - von Foerster type equations

by Joydev Halder

Submission date: 27-Feb-2023 03:53PM (UTC+0530)
Submission ID: 2024201418
File name: Joydev_Halder.pdf (1.15M)
Word count: 42116
Character count: 153745

Numerical study of nonlinear McKendrick - von Foerster type equations

ORIGINALITY REPORT

46%	35%	44%	1%
SIMILARITY INDEX	INTERNET SOURCES	PUBLICATIONS	STUDENT PAPERS

PRIMARY SOURCES

1	Joydev Halder, Suman Kumar Tumuluri. "Numerical solution to a nonlinear McKendrick-Von Foerster equation with diffusion", Numerical Algorithms, 2022 Publication	20%
2	Joydev Halder, Suman Kumar Tumuluri. "A numerical scheme for a diffusion equation with nonlocal nonlinear boundary condition", Computational and Applied Mathematics, 2023 Publication	11%
3	arxiv.org Internet Source	5%
4	link.springer.com Internet Source	5%
5	www.tasc.org.in Internet Source	1%
6	deepai.org Internet Source	1%

Sources 1-6 are the publications of the student Joydev Halder. Thus they may be excluded in the plagiarism. allow the student to submit his thesis.

T. Suman Kumar 28/02/23

Dr. T. SUMAN KUMAR
सह प्रोफ़ेसर / Associate Professor
गणित और सांख्यिकी संकाय
School of Mathematics & Statistics
हैदराबाद विश्वविद्यालय / University of Hyderabad
हैदराबाद / Hyderabad-500 046. तेलंगाना, T.S.

7	Luis María Abia, Óscar Angulo, Juan Carlos López‐Marcos, Miguel Ángel López‐Marcos. "Numerical approximation of finite life‐span age‐structured population models", Mathematical Methods in the Applied Sciences, 2020 Publication	1%
8	ebin.pub Internet Source	<1%
9	archive.org Internet Source	<1%
10	Linß, Torsten (xx xx, Technische Universität Dresden, Institut für Numerische Mathematik and Technische Universität Dresden, Mathematik). "Layer-adapted meshes for convection-diffusion problems", Saechsische Landesbibliothek- Staats- und Universitaetsbibliothek Dresden, 2008. Publication	<1%
11	nozdr.ru Internet Source	<1%
12	Xue-Zhi Li, Junyuan Yang, Maia Martcheva. "Age Structured Epidemic Modeling", Springer Science and Business Media LLC, 2020 Publication	<1%
13	Angulo, O.. "Numerical integration of fully nonlinear size-structured population models",	<1%

Applied Numerical Mathematics, 200409
Publication

---

14 Bertil Gustafsson, Heinz-Otto Kreiss, Joseph Oliger. "Time-Dependent Problems and Difference Methods", Wiley, 2013
Publication
<1%

---

15 Zhi-Zhong Sun, Guang-hua Gao. "Fractional Differential Equations", Walter de Gruyter GmbH, 2020
Publication
<1%

---

16 vdoc.pub
Internet Source
<1%

---

17 C. V. Pao. "Nonlinear Parabolic and Elliptic Equations", Springer Science and Business Media LLC, 1993
Publication
<1%

---

18 Yifei Wang, Jin Huang, Ting Deng, Hu Li. "An efficient numerical approach for solving variable-order fractional partial integro-differential equations", Computational and Applied Mathematics, 2022
Publication
<1%

---

19 C.V. Pao. "Numerical solutions of reaction–diffusion equations with nonlocal boundary conditions", Journal of Computational and Applied Mathematics, 2001
Publication
<1%

20	silo.pub Internet Source	<1 %
21	dx.doi.org Internet Source	<1 %
22	mirror.jessie.ws Internet Source	<1 %
23	Representation and Control of Infinite Dimensional Systems, 2007. Publication	<1 %
24	Vangipuram Lakshmikantham, Srinivasa Leela, Anatoly A. Martynyuk. "Stability Analysis of Nonlinear Systems", Springer Science and Business Media LLC, 2015 Publication	<1 %
25	eprints.qut.edu.au Internet Source	<1 %
26	www.universalprint.org Internet Source	<1 %
27	Lopez-Marcos, J.C.. "An upwind scheme for a nonlinear hyperbolic integro-differential equation with integral boundary condition", Computers and Mathematics with Applications, 1991 Publication	<1 %
28	Banks, H.T.. "Monotone approximation for a nonlinear size and class age structured	<1 %

epidemic model", Nonlinear Analysis: Real World Applications, 200707
Publication

29 NAJMEDDINE ATTIA. "L'analyse En mathématiques Pour les élèves de prépa", Centre de publication universitaire <1%
Publication

30 denebola.if.usp.br <1%
Internet Source

31 pt.scribd.com <1%
Internet Source

32 refubium.fu-berlin.de <1%
Internet Source

33 Long, N.T.. "Existence and asymptotic expansion for a nonlinear wave equation associated with nonlinear boundary conditions", Nonlinear Analysis, 20070915 <1%
Publication

34 coek.info <1%
Internet Source

35 zombiedoc.com <1%
Internet Source

36 Bhargav Kumar Kakumani, Suman Kumar Tumuluri. "A numerical scheme to the McKendrick-von Foerster equation with <1%

diffusion in age", Numerical Methods for Partial Differential Equations, 2018
Publication

37	Submitted to National Institute of Technology, Rourkela Student Paper	<1%

Exclude quotes	On	Exclude matches	< 14 words
Exclude bibliography	On		